

**The development of dual signature, fluorescent-
magnetic sediment tracing technology**

Jack Poleykett BSc (Hons), MSc (Dist)

**This project was supported by the Centre for Global Eco-Innovation and
is part financed by the European Regional Development Fund.**

Centre for Global Eco-Innovation

This thesis is submitted in partial fulfilment of the requirements for the degree of Doctor of Philosophy

Jack Poleykett BSc Hons, MSc (dist)

The development of dual-signature, fluorescent-magnetic sediment tracing technology

For the degree of PhD

Submitted (08 / 2016)

Abstract

The erosion, transport and deposition of sediment create environmental problems and social issues worldwide. Due to these ecological, environmental and economic implications for society, the importance of protecting and managing the sediment and soil resource is increasingly recognised through legislation and government policy. These legislative drivers have inspired the development of new and innovative approaches towards applied sediment management research, to develop effective erosion and pollution control strategies and improve the understanding of sediment transport processes to inform management decisions. To implement real change and inspire a holistic view of coastal and catchment management, of which sediment is critical, it is necessary to fully understand how sediments, contaminants and microbes move around the planet and the environmental impact that this constant flux of material has on the wider environment and on specific ecosystems. As sediment and soil are a fundamental resource for humans appropriate management of these resources requires a full understanding of these issues. Crucial to this is the use of direct field techniques, practically able to identify the sediment sources, transport pathways and sink areas of different soil and sediment types.

Active sediment tracing is a field technique which uses materials designed to replicate the movement of sediment, whilst remaining identifiable within the native sediment load. Active sediment tracing techniques have been developed over the last century, yet despite extensive study, the 'perfect' sediment tracer and field methodology remains elusive. Sediment tracing provides a unique applied sediment and soil research and management tool able to provide information which can be used to protect ecological habitats,

inform sediment and soil management, and provide information and quantitative data to improve environmental modelling approaches. The development of a robust tool able to provide direct field information regarding sediment transport dynamics is important as sediment flux and deposited sediments and the associated contaminants and microbes negatively impact the environment and society as a whole. The development of informed management strategies is therefore crucial to maintain the sediment and soil resource for future generations.

Sediment tracing methodologies and tracer design has progressed significantly in the last century recovering from significant setbacks (i.e. the environmental ban on the use of irradiated grains) and fluctuations in popularity due to the somewhat resource intensive nature of a sediment tracing study. Recent technological developments have reinvigorated the technique and led to original application and commercial enterprise within the sector. A variety of sediment tracers are now available. Each tracer material has unique benefits and limitations. The search for the 'perfect' sediment tracer is ongoing. Here the evaluation and application of a novel dual signature sediment tracer are described. The tracer has two signatures: fluorescence and ferrimagnetism which is considered an advance on previously used mono-signature tracers. The tracer provided unique opportunities to employ a variety of techniques to monitor tracer within, and recover tracer from the environment. These techniques were applied within an informed methodological framework developed to provide consistency of methodological approach within all active sediment tracing studies across disciplines. The framework provides a clear and robust step by step guide to conducting a sediment tracing study. Further it has outlined a range of techniques useful to practitioners with a focus on the practical application of the technique to the field. Field trials were conducted to investigate real world sediment management problems, these being: soil erosion within an agricultural field; sand transport on a beach within a complex anthropogenically affected environment; and, the release of fine material as part of nearshore dredging activities.

The soil erosion study showed the tracer had the potential to be applied to trace multiple size classes and different soil types and explored the potential use of both passive and active sampling techniques to determine a soil erosion rate. The results indicated that the dual-signature tracer was an effective tracer of soil and showed strong potential as an applied soil management research tool. The beach face study demonstrated the utility of sediment tracing within the sediment and coastal management arena and again explored the use of passive and active sediment tracing approaches to optimise sediment monitoring and recovery from the field. The field trials successfully delineated the sediment transport pathways on the beach face in a complex environment. The study of the dispersion of fine material in the nearshore coastal zone demonstrated the critical role of tide and current in the near and far field transport of disposed dredged sediment. The spatio-temporal distribution and sedimentation pattern of the discharged particles was mapped over a tidal scale to determine the immediate, near and far field impact of disposed dredge material. The results highlighted the potential for significant redistribution of fine sediment through the nearshore coastal zone, with potentially significant environmental impacts. These three distinct field trials provide highlights the utility of active sediment tracing studies to further our understanding of sediment transport within different environments. These data are useful to manage and mitigate the associated impacts of eroded and transported sediment on the environment.

The dual signature tracer was found to be an improvement over previously used, mono-signature tracers. Throughout laboratory testing and field trials the tracer upheld the key fundamental assumptions of an active sediment tracer. The tracer imitated the hydraulic properties of natural sediments, whilst not disrupting the transport system and remaining identifiable within the native sediment load. For each field application a practical, multifaceted, sampling approach was developed which increased the quantity and quality of information garnered from each tracing study: an advance since sediment tracing studies fundamentally comprise an empirical evidence-based approach. Further, the development of an analytical procedure which reduced timescales and associated costs, has improved the

benefit-cost ratio of an active sediment tracing study. Continued development of the active tracing methodology can increase and enhance application of these techniques in both conventional and novel contexts. This thesis has provided baseline data for future studies utilising dual-signature tracer within laboratory or field research, or industry based studies.

Author Declaration

I hereby declare that I am the sole author of this thesis. This is a true copy of the thesis. I understand that my thesis may be made electronically available to the public.

Copyright Statement

The copyright of this thesis rests with the author. No quotation from it should be published without the author's prior written consent and information derived from it should be acknowledged.

Acknowledgments

Firstly, I would like to express my sincere gratitude to my supervisory team, Professor John Quinton, Dr. Alona Armstrong and Professor Barbara Maher for the continuous support of my PhD study, for their patience, motivation, and immense knowledge. Their guidance helped me throughout the research and writing of this thesis.

Besides my supervisory team, I would like to extend my sincere thanks to my sponsor company, Partrac Ltd, for supporting this collaborative research project, in particular Dr. Kevin Black and Dr. Matthew Wright for their support, comments and encouragement, but also for the opportunities made available to me throughout the period of study. Without this precious support it would not have been possible to conduct this research. In addition, I would like to thank the Centre for Global Eco-Innovation for support throughout and the funding of the European Regional Development Fund without which the project would cease to exist.

Thanks also go to my fellow researchers for the stimulating discussions, and help and support in the field, in particular Robert Hardy. I am grateful to Dr. Vassil Karloukovski and Mrs. Anne Wilkinson for providing training and support throughout.

Lastly, I would like to thank my family: my parents and to my sister for supporting me throughout the writing of this thesis and within my life in general, and my partner Jodie Rothwell, who has inspired, supported, and helped me through each stage of the process.

Table of Contents

Abstract	iii
Author Declaration	vii
Copyright Statement	viii
Acknowledgments	ix
Table of Figures.....	xv
Tables.....	xxvii
1. Project Rationale and Thesis Structure.....	1
2. Review of Relevant Literature	7
2.1. Thesis Aim.....	22
2.2. Objectives.....	22
3. Tracer Characterisation.....	24
3.1. Technology Description	24
3.2. Tracer Properties.....	24
3.2.1. Methods used to characterise the hydraulic properties of tracer and native sediment.....	25
3.2.1.1. <i>Particle size distribution</i>	25
3.2.1.2. <i>Particle density (specific gravity)</i>	25
3.2.2. Methods used to characterise the magnetic properties of the tracer	27
3.2.2.1. <i>Results of testing</i>	28
3.2.3. Methods used to characterise the fluorescent properties of the tracer	34
3.2.3.1. <i>Results of testing</i>	35
3.2.4. Methods used to assess the degradation / survivability of the tracer coating	39
3.2.4.1. <i>Results of testing</i>	40

3.3.	Tracer Characterisation: Discussion and Concluding Remarks.....	41
4.	Field Tracing Techniques: Method Development.....	44
4.1.	Tracer Recovery and Monitoring	44
4.1.1.	Active sampling.....	44
4.1.2.	Passive sampling	45
4.1.2.1.	<i>Magnetic susceptibility</i>	45
4.1.2.2.	<i>In situ fluorimeters</i>	48
4.1.2.3.	<i>Night-time fluorescence</i>	48
4.2.	Tracer Recovery: Magnetic Separation	50
4.3.	Tracer Enumeration: Spectrofluorometric Method.....	50
4.3.1.	Calibration curves	53
4.3.2.	The determination of dye concentration in samples containing one tracer colour	55
4.3.3.	The determination of dye concentration in samples containing two tracer colours	55
4.3.4.	Tracer dry mass enumeration	56
4.4.	Method Test	56
4.4.1.	Optimal elution duration	57
4.4.1.1.	<i>Results of testing</i>	57
4.4.2.	Instrument Test.....	58
4.4.2.1.	<i>Results of testing</i>	58
4.4.3.	The Influence of Background Material	61
4.4.3.1.	<i>Results of testing</i>	62
4.4.4.	Spiked environmental samples	66
4.4.4.1.	<i>Results of testing</i>	66
4.5.	Method Development: Discussion and Concluding Remarks	73
5.	Sediment Tracing Using Active Tracers: A Guide for Practitioners.	76
5.1.	Summary	76

5.2.	Introduction.....	76
5.3.	Approach	78
5.4.	A Methodological Framework	78
5.4.1.	Step 1: Background Survey	80
5.4.2.	Step 2: Tracer Design/Selection, Matching the Tracer to the Native Sediment and Quantity of tracer required.	82
5.4.3.	Step 3: Tracer Introduction.....	85
5.4.3.1.	<i>Marine, Coastal and Fluvial Environments</i>	86
5.4.3.2.	<i>Terrestrial</i>	88
	90
5.4.3.3.	<i>Step 4: Sampling</i>	90
5.4.3.4.	<i>Sampling Tools</i>	92
5.4.4.	Step 5: Tracer Enumeration.....	95
5.4.5.	Step 6: Analysis	97
5.5.	Discussion	99
5.6.	Conclusion.....	99
6.	The Evaluation and Application of a Dual Signature Tracer to Monitor Soil Erosion Events.	101
6.1.	Summary	101
6.2.	Introduction.....	101
6.3.	Methods.....	103
6.3.1.	Laboratory set-up	103
6.3.2.	Field set-up	106
6.3.3.	Soil loss calculations	110
6.3.4.	Statistical analyses.....	111
6.4.	Results	112
6.4.1.	Soil box experiments.....	112
6.4.2.	Field experiments.....	117

6.5. Discussion	121
6.6. Conclusion.....	124
7. Monitoring Wave-Driven Sediment Transport During High-Energy Events Using a Dual Signature Tracer – A Case Study from Scarborough, North Yorkshire UK.	126
7.1. Summary	126
7.2. Introduction.....	126
7.3. Site Description and Oceanographic Setting	128
7.4. Methodology	129
7.4.1. Statistical analyses	136
7.5. Results	136
7.6. Discussion	151
7.7. Conclusion.....	154
8. An Assessment of the Transport and Deposition of Sediments, Following a Simulated Disposal of Silt Sized Dredge Material Within a Near Shore Harbour Setting.	156
8.1. Summary	156
8.2. Introduction.....	156
8.3. Method	159
8.3.1. Tracer characterisation	159
8.3.2. Tracer deployment	159
8.3.3. Sampling	160
8.3.4. Tracer enumeration.....	165
8.3.5. Oceanographic monitoring	170
8.4. Results	171
8.4.1. Tracer characterisation, tide and current data.....	171
8.4.2. Sediment transport pathway	175
8.4.3. Sedimentation pattern	179

8.5. Discussion	182
8.6. Conclusion.....	185
9. Thesis summary.....	187
10. Thesis conclusion	198
11. References	200

Table of Figures

Figure 1: A flow chart which outlines the organisation of the thesis.....	3
Figure 2: A schematic diagram to illustrate the transport processes occurring during soil erosion due to water	10
Figure 3: A schematic diagram of wave and current driven longshore and cross – shore transport processes which occur in the breaker, surf and swash zone.....	11
Figure 4: A photomicrograph of chartreuse coloured, dual signature tracer. Image courtesy Partrac Ltd.....	24
Figure 5: The pycnometer calibration curve depicting the change in the mass of the pycnometer (filled with DI water) over a range of temperatures. The calibration curve is derived from equation 1	27
Figure 6: The anhysteretic remanent magnetisation (@ 100 uT dc, 80 uT ac) of different sized tracer particles subjected to stepwise alternating field demagnetization at 15, and 23 milliTesla. The markers show the mean response and the whiskers the standard error.....	32
Figure 7: The stepwise acquisition of isothermal remanent magnetisation (IRM) at 20, 50, 100, 300 and 1000 mT, of different sized tracer particles subsequently subjected to stepwise alternating field demagnetisation at 10 and 20 milliTesla. The IRM at 1000 mT is assumed to be the saturated isothermal remanent magnetisation (SIRM). The markers show the mean response and the whiskers the standard error.....	33
Figure 8: Low frequency magnetic susceptibility versus SIRM for different size fractions of dual signature tracer	34
Figure 9: These two images above show the same sample under white light (top) and ultraviolet light (UV-A – 400 nm) illumination (bottom). The image	

was captured using a 750D Digital SLR (Canon Ltd), fitted with a 50 mm lens. When captured under UV-A illumination the image was shot through a yellow dichroic filter 36

Figure 10: Silt sized tracer particles analysed under a fluorescence microscope. The image is captured under white light illumination (top) and under ultraviolet light (UV-A 400 nm) on an LSM 510 Meta laser scanning confocal fluorescence microscope used with Axio imager 2, imaging facilities (Zeiss Ltd)..... 37

Figure 11: Photograph of sand sized chartreuse tracer particles mixed with native beach sand at a density of 0.001 g cm^2 (top) and 0.185 g cm^2 (bottom) under blue light illumination (395 nm). The image was captured using a 750D Digital SLR (Canon Ltd), fitted with a 50 mm lens, shot through a yellow dichroic filter 38

Figure 12: The mean fluorometer response to samples stored outside, in the green house and the control sample over a period of 12 months. The markers show the mean response and the whiskers the standard error 41

Figure 13: Photo of a high field permanent magnet (11000 gauss) saturated with dual signature tracer. The magnet was positioned within the anticipated stream flow within a suspended sediment study. Image courtesy Partrac Ltd45

Figure 14: A plot of the dry tracer mass (g) recovered from a shallow soil core vs. the low frequency volume magnetic susceptibility of the core measured using an MS2K high resolution surface sensor. The operating frequency was 0.58 KhZ, the area of response was 25.4 mm full-width, half maximum, depth of response was 50 % at 3 mm, and 10 % at 8 mm, (Bartington Instruments Ltd, UK) 46

Figure 15: An example of the presentation of magnetic susceptibility (K_{LF}) data. The data represents the soil surface post tracer deployment, pre simulated rainfall event (left) and post simulated rainfall event (right) when a

coarse tracer (500 – 950 microns) was deployed in a soil box for typical experiments. The tracer deployment zone is centred on 17.5 cm. The magnetic susceptibility of the surface was measured using a MS2K high resolution surface sensor. The operating frequency was 0.58 KhZ, the area of response was 25.4 mm full-width, half maximum, depth of response was 50 % at 3 mm, and 10 % at 8 mm, (Bartington Instruments Ltd, UK) 47

Figure 16: An example of night time fluorescence. These photo mosaics show the soil surface of an erosion plot (2.75 m x 0.5 m) with a slope angle of 7 %. A 300 L water butt positioned directly above the plots, through hoses, supplied water to the plot. The water was delivered through poly-vinyl chloride pipe with 8 holes, located 6 cm apart. Finally, the water was passed through a plastic mesh to create droplets. The simulated overland flow event had a flow rate of 8 L/min and lasted 30 mins. The plot was photographed under blue light (395 nm) illumination, post tracer deployment, pre – overland flow event (left), and post overland flow event (right). The tracer deployment zone was centred on 2.5 m. Each image captured a 25 x 25 cm spatial area, defined by a quadrat placed on the soil surface using a 750D Digital SLR (Canon Ltd), fitted with a 50 mm lens shot through a yellow dichroic filter 49

Figure 17: The emission-excitation spectra for the chartreuse tracer pigment (top) and the pink tracer pigment (bottom). The peak excitation and emission wavelengths are noted..... 52

Figure 18: Dose response curves developed using the fluorescein probe to dye solutions derived from 0.1 g of *chartreuse* and *pink* tracer (60 - 100 microns in size). Each data point represents a dry mass of tracer, i.e. 0, 0.1, 0.2, 0.3, 0.4, 0.5, 0.6, 0.7, 0.8, 0.9, 1.0 g 54

Figure 19: Dose response curves of the rhodamine probe to dye solutions derived from 0.1 g of *chartreuse* and *pink* tracer (60 - 100 microns in size). Each data point represents a dry mass of tracer, i.e. 0, 0.1, 0.2, 0.3, 0.4, 0.5, 0.6, 0.7, 0.8, 0.9, 1.0 g 55

Figure 20: The response of the Rhodamine probe to dye solutions of P ₁₀₀ at low (0.2 g), intermediate (1 g) and high concentrations (5 g) over a period of 314 hours. The reference line indicates the end of the 7 day time period.....	58
Figure 21: The fluorescein probe response (V) to increasing quantities of CH ₁₀₀ (0.025, 0.1, 0.2, 0.5, 0.75, 1 g) during the testing of the device accuracy	59
Figure 22: The rhodamine probe response (v) to increasing tracer quantities of P ₁₀₀ (0.025, 0.1, 0.2, 0.5, 0.75, 1 g) during the testing of the device accuracy	60
Figure 23: The rhodamine probe response (v) to increasing tracer quantities of P ₃₀₀ (0.025, 0.1, 0.2, 0.5, 0.75, 1 g) during the testing of the device accuracy	61
Figure 24: dose response curves depicting the responses of P ₁₀₀ tracer particles of the same concentration with different levels of background material present i.e. none, low = 0.1 g, moderate = 1.0 g and high = 5.0 g. Each data point represents a dry mass of tracer, i.e. 0, 0.1, 0.2, 0.3, 0.4, 0.5, 0.6, 0.7, 0.8, 0.9, 1.0 g.....	64
Figure 25: dose response curves depicting the responses of P ₃₀₀ tracer particles of the same concentration with different levels of background material present i.e. none, low = 0.1 g, moderate = 1.0 g and high = 5.0 g. Each data point represents a dry mass of tracer, i.e. 0, 0.1, 0.2, 0.3, 0.4, 0.5, 0.6, 0.7, 0.8, 0.9, 1.0 g.....	65
Figure 26: Tracer mass Vs. calculated tracer mass for samples with one tracer colour, either pink or chartreuse, derived from the response of the rhodamine and fluorescein probes respectively	68

Figure 27: Tracer mass vs. calculated tracer mass for samples with two tracer colour in the sample, pink and green derived from the response of the rhodamine and fluorescein probes respectively..... 69

Figure 28: Tracer mass vs. calculated tracer mass for samples with one tracer colour in the sample, pink and green and mixed with: low (0.1 g); moderate (1 g); and high (5 g) background material derived from the response of the rhodamine and fluorescein probes respectively..... 70

Figure 29: Tracer mass vs. calculated tracer mass for samples with two tracer colours in the sample, pink and green and mixed with: low (0.1 g); moderate (1.0 g); and high (5.0 g) background material derived from the response of the rhodamine and fluorescein probes respectively..... 71

Figure 30: Proposed methodological framework for conducting a sediment tracing study using an active tracer 79

Figure 31: The percentage of studies that reported each step of the proposed methodological framework within peer reviewed articles. The green coloured slice represents studies that reported the results of each step and the red coloured slice represents studies that did not report the results of each step 80

Figure 32: The image captured under ultraviolet illumination shows a core of cohesive peat sediment mixed with a pink silt tracer. The tracer has been hydraulically matched to the cohesive peat sediment. The tracer has then been thoroughly mixed with the peat and left to settle. The image demonstrates that the hydraulically matched tracer and peat, due to the similar hydraulic characteristics of one or more of the constituent sediment particles have a similar settling rate, resulting in the tracer flocculating with, and becoming entangled with, peat material. Thus the peat flocs have been tagged with an identifiable 'signature' enabling cohesive sediment transport to be assessed. The tags will ensure that ensuing transport processes may be tracked and transport pathways delineated. Image provided by Partrac Ltd . 84

Figure 33: Green fluorescent tracer deployed on the beach face mixed 50:50 with native sand. Image provided by Partrac Ltd	87
Figure 34: Green fluorescent tracer deployed on the surface of an agricultural field. Image provided by Partrac Ltd	89
Figure 35: A decision making diagram to determine the most appropriate method of tracer introduction	90
Figure 36: A schematic diagram showing the laboratory setup of the soil box and rainfall simulator. The diagram is not to scale.....	105
Figure 37: The mean particle size distribution of the tracer – soil admixture and the native soil.....	108
Figure 38: The plots within the field at a slope of 4.6 %. Note the barriers positioned behind the plots	109
Figure 39: The tracer deployed to the soil surface.....	109
Figure 40: A comparison of the magnetic susceptibility (K_{LF}) of the tagged zone and non-tagged zone and the different tracer size fractions post deployment, pre rainfall, when tracer was used with a sandy loam, clay loam and silt loam soil. The box plot and whiskers represents the 5 th and 95 th percentile	112
Figure 41: The mass of tracer (g) recovered from the captured sediment during soil box experiments. The box plot and whiskers represents the 5 th and 95 th percentile	114
Figure 42: The measured soil loss vs soil loss estimated from the change in magnetic susceptibility values within the tagged zone converted to soil loss from equation 2 when tracer was used with the sandy loam soil. The markers	

indicate the mean of three replicates; the whiskers indicate the standard error 115

Figure 43: The measured soil loss vs soil loss estimated from the change in magnetic susceptibility values within the tagged zone converted to soil loss from equation 2 when tracer was used with the clay loam soil. The markers indicate the mean of three replicates; the whiskers indicate the standard error 116

Figure 44: The measured soil loss vs soil loss estimated from the change in magnetic susceptibility values within the tagged zone converted to soil loss from equation 2 when tracer was used with the silt loam soil. The markers indicate the mean of three replicates; the whiskers indicate the standard error 117

Figure 45: The mean soil loss for each deployment zone derived from tracer content values derived from equations 14-17. The markers indicate the mean of three replicates; the whiskers indicate the standard error..... 118

Figure 46: The mean soil loss for each deployment zone derived from changes in magnetic susceptibility pre and post rainfall event derived from equation 13. The markers indicate the mean of three replicates; the whiskers indicate the standard error 119

Figure 47: The mean soil depletion of each deployment zone derived from changes in magnetic susceptibility and tracer mass. A regression line for each deployment zone is added..... 120

Figure 48: Study area and location. The location of each tracer deployment zones (DZ 1-3) is marked. The locations of the core samples collected is also marked, the tracer content values determined at each of these locations were interpolated in figure 5 to provide a time step of tracer distribution across the beach face 129

Figure 49: Tracer deployed in a strip cross-shore on the beach face	131
Figure 50: Tracer deployed on the beach face	131
Figure 51: Blue light torch surveys conducted at night to qualitatively assess the spatial distribution of tracer on the beach face	133
Figure 52: Calibration (dose response) curves prepared for low, intermediate, and high material loads for samples collected from the beach face	135
Figure 53: A comparison of the mean particle size distribution of the native sand and tracer particles. The markers show the mean and the whiskers represent the standard error	138
Figure 54: Significant wave height and wave period captured at the Whitby wavenet site between 4th November 2010 to the 4th November 2011 across the study duration combined with the data derived from 30 minute interval spectral data from a wave buoy Directional WaveRider Mk III buoy (Datawell, BV, Netherlands) located at 54° 17.598' N, 00° 9.077' W managed by the North East Coastal Observatory during the study period. The data collected during the study period runs from day 33 – to day 87. This data is combined to apply context to the observed metocean data collected during the study period	139
Figure 55: Significant wave height and period derived from 30 minute interval spectral data from a wave buoy Directional WaveRider Mk III buoy (Datawell, BV, Netherlands) located at 54° 17.598' N, 00° 9.077' W managed by the North East Coastal Observatory during the study period.....	140
Figure 56: Wave direction (degrees re true north) frequency captured at the Whitby wavenet site from 4th November 2010 to the 4th November 2011 ..	141
Figure 57: Wave direction (degrees re true north) frequency captured across the study duration derived from 30 minute interval spectral data from a wave	

buoy Directional WaveRider Mk III buoy (Datawell, BV, Netherlands) located at 54° 17.598' N, 00° 9.077' W managed by the North East Coastal Observatory during the study period.....	142
Figure 58: A comparison of the magnetic susceptibility (K_{LF}) of each deployment zone prior to tracer injection, post tracer injection and following the first wave event. The markers represent the mean and the whiskers represent the standard error	143
Figure 59: Geospatial distribution of tracer dry mass (g m^2) 24 h after injection	147
Figure 60: Geospatial distribution of tracer dry mass (g m^2) 48 h after injection	147
Figure 61: Geospatial distribution of tracer dry mass (g m^2) 72 h after injection	148
Figure 62: Geospatial distribution of tracer dry mass (g m^2) 168 h days after injection	148
Figure 63: Geospatial distribution of tracer dry mass (g m^2) 336 h after injection	149
Figure 64: Geospatial distribution of tracer dry mass (g m^2) 54 days after injection	150
Figure 65: Tracer mass recovered (normalised to a unit area g m^2) from the upper and mid foreshore on the days following tracer deployment. The data graphically represented only reports the sampling campaigns where both the mid and upper foreshore were sampled at the same time, these being 2, 3, 7, 14 and 54 days following the first wave event	150

Figure 66: Total tracer mass recovered from the beach face during the sampling campaign.....	151
Figure 67: A schematic diagram to illustrate the deployment methodology and the transport processes of disposed sediment from a discharge vessel in the coastal zone. The boat is secured to the quay wall while tracer is being deployed subsurface from a pipe from the aft of the vessel. The diagram is not to scale	160
Figure 68: Schematic diagram showing how the magnets were deployed to sample tracer travelling in suspension.....	161
Figure 69: The magnets deployed <i>in situ</i> and recovered with tracer captured	162
Figure 70: The laboratory calibration of the field fluorometer. The calibration shows the fluorometer response to increasing tracer concentration ($\mu\text{g l}^{-1}$).	163
Figure 71: A schematic diagram showing the approximate near-shore and far-field sampling locations. The markers indicate the location of sample points where both the water column (1 m above the bed) and the sea bed were sampled. Each nearshore transect is marked (i.e. T1). The dashed red box indicates the discharge area and the red line indicate the approximate location of the fluorometer transects. The diagram is not to scale	164
Figure 72: Calibration (dose response) curves prepared for low material loads for samples collected using the magnet rigs (e.g. magnet – low) and and low material loads collected using a sea bed grab sampler (e.g. grab – low)	167
Figure 73: Calibration (dose response) curves prepared for high material loads for samples collected using the magnet rigs (i.e. magnet – high) and high material loads collected using a sea bed grab sampler (i.e.. grab – high) ...	168

Figure 74: The particle size distribution of the tracer. The markers show the mean and the whiskers represent the standard error	171
Figure 75: Tracer being deployed subsurface as a high concentration slurry. The plume of tracer dispersing is visible in the background	172
Figure 76: Observations of current magnitude derived from the data collected using the ADCP	173
Figure 77: Current velocities at flood tide derived from a hydrodynamic model of San Diego Harbour (Elawany, 2012). The location of the site is marked.	174
Figure 78: Observations of current direction degrees (re true north) derived from the data collected using the ADCP (the various colours indicate different depth intervals)	175
Figure 79: An interpolated map of the spatial distribution and relative tracer mass 1m above the bed post simulated discharge event. Data collected using <i>in situ</i> magnetic sampling. The discharge zone and North is marked.....	177
Figure 80: The fluorometer response during tracer deployment. The transport pathway is determined from the position of the fluorometer in relation to the discharge. The dashed red circle indicates initial transport to the south and the black circle indicates detection of significant tracer particles moving south, inferred to be a sediment laden plume	178
Figure 81: An interpolated map of the spatial distribution and relative tracer mass on the sea bed post simulated discharge event. Samples collected using a van veen sea bed grab sampler. The discharge zone and North is marked	179
Figure 82: The tracer concentration on the sea bed (g m^2) and in the water column (g l^3) Vs distance offshore from the quay wall. T_1 and T_2 are located to the north of the discharge zone, T_3 is directly offshore from the centre of the	

discharge zone and T_4 , T_5 and T_6 are located to the south of the discharge zone. Note: the offshore edge of the discharge zone is located at 60 m offshore from the quay wall..... 181

Figure 83: The threshold of incipient motion of deposited fine sediment at the site derived from the equation outlined by (Soulsby, 1997). 182

Tables

Table 1: The recent technological, and methodological, developments which have prompted a resurgence of interest in the sediment tracing technique... 14

Table 2: A table to show the difference ($p, 0.05$) between the measures and particle size derived from the one-way Anova test with a Tukey multiple comparison test. The dependant variables include ARM acquisition and AF demagnetisation at 15 and 23 millitesla..... 29

Table 3: A table to show the difference ($p = 0.05$) between the measures and particle size derived from the one-way ANOVA test with a Tukey multiple comparison test. The dependant variables include IRM acquisition at 20, 50, 100, 300 and 1000 millitesla and AF demagnetisation of SIRM at 10 and 20 militesla..... 30

Table 4: A table to show the difference ($p = 0.05$) between the measures and particle size derived from the one-way ANOVA test with a Tukey multiple comparison test. The dependant variables include low and high frequency mass specific magnetic susceptibility 31

Table 5: The mean percentage error (Equation 6) and standard deviation between the exact tracer content and measured tracer content for the rhodamine and fluorescein probe when measuring environmental samples containing one and two tracer colours with varying quantities of background material present. The significant difference between the fluorescent response of the exposed and control tracer batches were assessed using a two tailed paired t- test. The percentage error is derived from equation 6 72

Table 6: The passive sampling techniques available to monitor tracer particles in the environment for the most popular tracing materials 94

Table 7: The tracer enumeration methodologies available for the most popular tracing materials, fluorescent tracers, magnetic tracers and rare earth element tracers..... 95

Table 8: A summary of the physical characteristics of the tracer and native soil deployed as a tracer/soil admixture to the field.....	107
Table 9: Total soil loss and erosion rate per plot derived from the magnetic susceptibility values (equation 13) and tracer content values (equation 14-18)	121
Table 10: Summary of the calibration (dose response) curves produced....	135
Table 11: Summary of the physical – hydraulic characteristics of the tracer particles and the native sediment	137
Table 12: Surveyors diary notes following shore normal, night-time transects with blue light torches (395 nm) to assess the spatial distribution of tracer particles on the surface, utilising the spectral characteristics of the tracer ..	144
Table 13: Summary of the calibration (dose response) curves produced....	166

1. Project Rationale and Thesis Structure

Due to the ecological, environmental and economic implications for society, the protection of sediment and soil is increasingly recognised as an integral component of catchment and coastal management (Hamilton and Gehrke, 2005, Kay and Alder, 1999, Walker et al., 2001, White, 2006). Legislation such as: the Coastal Access Act (2009); the Water Framework Directive (Directive 2000/60/EC); the European Community Shellfish Waters Directive (2006/113/EC); the designation of Marine Protected Areas: the European Union Soil Thematic Strategy (COM (2006) 231); and proposed Soil Framework Directive (COM (2006) 232) has shifted the scope from local, to river basin and national scale sediment and soil management (Brills, 2008, Kothe, 2003). This demonstrates a change in priority away from industry and agricultural production, to environmental protection (Boardman et al., 2009, Page and Kaika, 2003, Ruhl, 2000). The development of new and innovative approaches towards sediment management and research (Black et al., 2007), would assist the development of effective erosion and pollution control strategies (Gibson et al., 2011, D'Arcy and Frost, 2001, Prato and Shi, 1990, Walling and Collins, 2008, Gallagher et al., 1991) and improve the understanding of sediment transport processes (Eidsvik, 2004, Cabrera and Alonso, 2010, Walling and Fang, 2003, Merritt et al., 2003).

Sediment tracing is a field tool which enables the user to investigate the impacts of sediment on ecological habitats, develop evidence based sediment and soil management strategies, and provides information and quantitative data to assess, and therefore improve, the performance of modelling approaches. Sediment tracing is best utilised to directly assess source-sink relationships and the transport rate through the environment. This is important as the movement of sediments, and the associated contaminants and microbes impact the environment and society in a variety of ways. The use of active sediment tracing studies furthers our understanding of sediment transport processes. Improving our understanding of these processes is crucial to maintaining (and potentially improving) the sediment and soil resource for future generations through the implementation of informed

management strategies. Fundamental to informing management strategies are robust field techniques.

Sediment tracing methodologies and tracer design has progressed significantly in the century following the study of Richardson (1902), recovering from significant setbacks (i.e. the environmental ban on the use of irradiated grains) and fluctuations in popularity. The resource intensive nature of a sediment tracing study has led both researchers and commercial organisations to strive to improve field and analytical methodologies. Recent developments have reinvigorated the technique and led to original application and commercial enterprise within the sector. A variety of tracers are now available to trace sediment in terrestrial, fluvial, marine and coastal environments. Each tracer has unique benefits and limitations. The most appropriate tracer is the tracer that can be effectively monitored within and recovered from the environment and which possesses the greatest similarity to the hydraulic properties of the native sediment. Tracer specific practical and analytical methodologies have unique benefits and limitations, which must be weighed against both methodologies relating to alternative tracer, and the appropriateness of the tracer as a tracer for the study of sediment dynamics. As such, a tracer is only as strong as its methodology and the methodology is only as robust as its tracer. Currently the 'perfect' sediment tracer does not exist.

This thesis describes the development of a novel sediment tracing approach utilising a commercially available dual signature sediment tracer. The tracer is fluorescent and magnetic providing unique opportunities to employ various techniques to monitor tracer within, and recover tracer from the environment. This collaborative research and development project was conducted in conjunction with Partrac Ltd, working as part of the Centre for Global Eco Innovation at Lancaster University. Partrac is a marine data acquisition company specialising in oceanographic, environmental and geoscience surveys. Partrac manufacture a dual signature, sediment tracer, which can be used to directly monitor the movement of mineral sediments, particulates, and the associated nutrients, contaminants and microbes, across space through time. The project explored the development of a fluorescent-

magnetic active sediment tracing methodology. These methods were then applied within a range of environments and study contexts to examine source-sink relationships, the nature and location of the transport pathway(s), and the rate of sediment transport through the environment. The thesis was based around examination of the tracer properties, original method development in the laboratory, and field application within a range of environments. Figure 1 outlines the thesis structure.

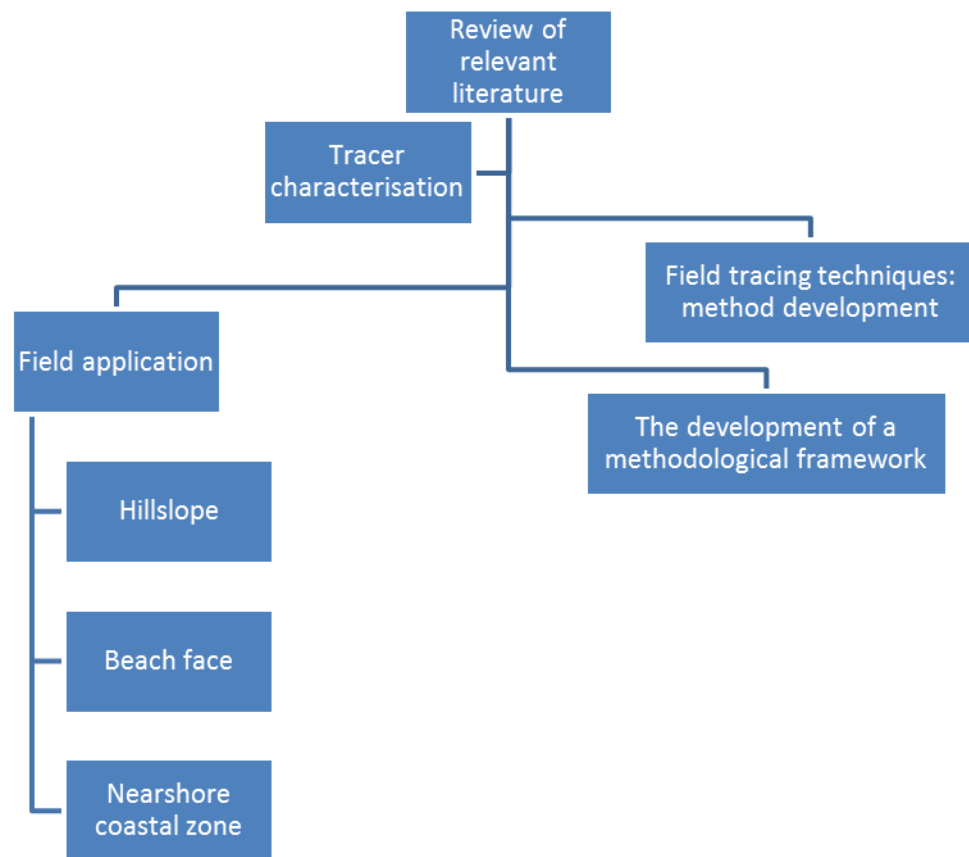


Figure 1. A flow chart which outlines the organisation of the thesis.

The following section provides a summary of each thesis chapter.

2. Review of Relevant Literature

This chapter provided a synthesis of the relevant literature. The review outlined the different sediment tracing approaches with a focus on active sediment tracing. The vast and differing range of materials used as active sediment tracers and approaches to monitor the movement of sediment, was

described. The chapter culminates by describing the thesis aims and objectives.

3. Tracer Characterisation

This chapter provided a description of the dual signature tracer technology, developed and owned by Partrac Ltd. The chapter then moves on to describing the methods used throughout the thesis to determine the hydraulic properties of both the native sediment and tracer. Following this, through a systematic series of tests, the tracer properties were characterised prior to application within the field. These tests were designed to assess the fluorescent and magnetic characteristics of the tracer, and the robustness / survivability of the tracer coating during exposure to simulated environmental conditions. The methods used and results of all testing conducted are described and a discussion of the results and concluding remarks are provided.

4. Field Tracing Techniques: Method Development

This chapter outlines the methodological development undertaken prior to application in the field. Both passive and active sampling techniques available to monitor and recover tracer from the environment were described. The development of the tracer enumeration process was outlined. The developed method was then tested prior to application, to: 1) evaluate the methodological bias; and, 2) determine best practice. The results of the testing are described. A discussion and concluding remarks are provided.

5. Sediment Tracing Using Active Tracers: A Guide for Practitioners.

This chapter explored the development of a methodological framework for the use of active sediment tracers. The framework can potentially be applied universally, regardless of study context, environment or tracer type. The framework aims to provide methodological consistency across academic and commercial disciplines to ensure robust active sediment tracing studies are being conducted. The recent technological advances in the field of active sediment tracing studies means now, more than ever, the technique is available to more practitioners with a broader experience and knowledge

base. The developed framework provides a step by step guide for practitioners to aid in conducting a robust sediment tracing study.

6. The Evaluation and Application of a Dual Signature Tracer to Monitor Soil Erosion Events.

This chapter described the evaluation, assessment and field application of dual signature sediment tracer, as a tracer of soil. A rigorous assessment of the tracer was conducted under controlled laboratory conditions. Following which, the tracer was applied to monitor soil erosion under natural rainfall conditions, at the plot scale, in a fallow agricultural field. These trials indicated that there is great potential for dual signature tracers to be used to monitor soil erosion events within terrestrial environments. The results were promising and a soil erosion rate was determined from both passive sampling and active sampling techniques leading to the development of a terrestrial fluorescent – magnetic sediment tracing methodology.

7. Monitoring Wave-Driven Sediment Transport During High-Energy Events Using a Dual Signature Tracer – A Case Study from Scarborough, North Yorkshire UK.

This chapter described the application of dual signature tracer to monitor wave driven sediment transport on the beach face, within a complex natural and anthropogenic setting. The tracer was deployed on the beach to delineate the sediment transport pathways. The tracer proved to be an appropriate tracer of native beach sand being unequivocally identifiable within the native sediment load and an excellent hydraulic match to the native beach mineral sediments. The tracer was successfully deployed and monitored through a period of wave activity at the site. The data generated indicated the existence of an area of sediment divergence on the beach which, depending on prevailing wave direction, was the source of beach material being delivered both South and North. Prior to this study this the sedimentary regime at the site was previously unknown.

8. An Assessment of the Transport and Deposition of Sediments, Following a Simulated Disposal of Silt Sized Dredge Material Within a Near Shore Harbour Setting.

The final application chapter evaluated the near and far field transport and deposition pattern of a silt-rich, near shore dredge disposal within a highly industrialised environment. This field trial evaluates the use of several technologies to monitor and sample tracer travelling in suspension within the water column. Tracking the movement of silt presents significant challenges when using active sediment tracers. The silt tracer was manufactured to replicate a silt sized sediment and deployed to the environment to simulate a nearshore dredge disposal. The immediate, near field and far field sediment transport pathways were investigated through the spring-neap tidal phase to evaluate the potential impacts of such a disposal on the near shore marine environment and local ecosystems.

9. Thesis Summary

A summary was provided to contextualise the results within the literature and summarise the findings of the thesis. At this stage the requirements for further research were identified and described.

10. Thesis Conclusion

A series of conclusions were drawn from the thesis. The key developments were identified and the requirement for future research and further development outlined.

2. Review of Relevant Literature

Change within environmental systems is an integral process that occurs naturally through time and can inspire system regeneration (Bauer et al., 2009) or where change exceeds systems resilience, can damage systems beyond repair (Tress and Tress, 2009). Since the industrial age began human intervention has increased the rate and magnitude of environmental change (Church et al., 2013, Devoy, 1992, Jevrejeva et al., 2014). The development of knowledge and technologies combined with increased concern regarding future uncertainties led to significant attempts to manage the environment through engineering solutions (Hamm et al., 2002, Hanson et al., 2002). Within dynamic environmental systems change is inherent. Two areas where environmental change directly impacts society occur within catchments (Gilvear et al., 2013) and at the coast (Sanchez-Arcilla et al., 2016). Within these environments a host of highly dynamic ecosystems reside. Critical to appropriate management of these systems is understanding change. The ability to predict change accurately must be based upon a complete understanding of the physical, chemical and biological processes occurring within the system (Falkowski et al., 2000, Christopher et al., 2006). Therefore, understanding all processes across instantaneous to decadal scale is of scientific importance to underpin future environmental management strategies, predictions and engineering solutions (Whitehouse et al., 2005). This requires an approach which incorporates a multitude of techniques working harmoniously across differing spatial and temporal scales to gather appropriate data (Tetzlaff and Laudon, 2010).

Sediment and soil are an integral and dynamic component of river catchments and coastal ecosystems (Forstner and Salomons, 2008, Costanza et al., 1990); form a variety of habitats (Venterink et al., 2006, Snelgrove, 1999, Covich et al., 1999, Sebens, 1991, Beekey et al., 2004, Hutchings, 1998, Schindler and Scheuerell, 2002, Gray, 1981); provide a source of life (Whitlatch, 1981, Palmer et al., 2000, Sherer et al., 1991, Newell et al., 1995); and have been a valuable resource for humans, for millennia (Brills, 2008, Owens, 2009, White, 2006). Sediment refers to organic and inorganic loose material (Masselink and Hughes, 2003, Droppo et al., 1997, Aspila et al.,

1976). Soil is a fundamentally important natural capital (Robinson et al., 2013) occurring on the surface of the earth, which is a medium for plant growth, and whose characteristics have resulted from the forces of climate and living organisms over a period of time (Donahue et al., 1971, White, 2006, Biswas and Mukherjee, 1994, Steila and Pond, 1989, Nortcliff et al., 2012). Sediment and soil are transported across the landscape and within fluvial, estuarine and coastal environments, through the forcing mechanisms created by rain, wind, flow, currents and gravity (Masselink and Hughes, 2003, Beasley, 1972, Reading, 1996, van Rijn, 1993, Dyer, 1995, Habersack and Kreisler, 2012)

The transport of sediment and associated nutrients, contaminants and microbes (Droppo, 2001, Gillan et al., 2005, Cordova-Kreylos et al., 2006), can create a range of environmental issues. These include: decreased agricultural production (Pimental et al., 1987, Pimental and Burgess, 2013); destruction of ecological habitats (Baxter and Hauer, 2000, Armstrong et al., 2003, Erftmeijer and Robin Lewis III, 2006, Erftemeijer et al., 2012); and a reduction of water quality in receiving water bodies (Boardman and Favis-Mortlock, 1992, Boardman et al., 2009, Billotta and Brazier, 2008).

The accelerated erosion and transport of soil and sediment is a significant environmental problem worldwide (Armstrong et al., 2012, Reganold et al., 1987, Pimental et al., 1987, Pimental and Sparks, 2000). Erosion of soil on agricultural land is a global environmental problem (Pimental and Sparks, 2000, Larssen et al., 2010, Ballantine et al., 2009, Beasley, 1972, Foley et al., 2005). Detrimental effects of soil erosion occur both within the field and within lotic and lentic ecosystems (Armstrong et al., 2012, Reganold et al., 1987). On site, erosion acts to reduce soil quality leading to a loss of productivity (Stevens and Quinton, 2008, Pimental et al., 1987, Pimental and Burgess, 2013). Off-site, soil that is eroded may be delivered to nearby watercourses (Collins et al., 2013, McHugh et al., 2002, Amore et al., 2006), and cause many environmental problems, including increased turbidity and sedimentation (Owens et al., 2005, Lane et al., 2007), which detrimentally impact wildlife (Baxter and Hauer, 2000, Armstrong et al., 2003). Moreover, the redistribution of nutrients (Haygarth and Jarvis, 1999, Catt et al., 1998) and contaminants (Wilcox et al., 1996, Cadwalader et al.,

2011), can lead to the eutrophication of water bodies (Quinton and Catt, 2007, Ullen et al., 2007, Balcerzak, 2006, Daniel et al., 1997). Understanding soil detachment, transport and depositional processes is therefore important in order to underpin numerical modelling of erosion, assess risk and develop effective mitigation strategies (Armstrong et al., 2011, Gobin et al., 2003). Critical to this is the development of approaches able to provide information on rates of soil loss (Clark et al., 1985, Walling, 1995, Poesen et al., 2003), applicable at the field scale (Gómez et al., 2008, Guzman et al., 2010).

Soil, on all but the lowest slopes, is moving downhill due to gravity (Allen, 1985, Heimsath et al., 2002). The principal forcing mechanism in the erosion (and subsequent transport) of soil is generated due to rainfall and water flow (Figure 2) (Beasley, 1972, Kinnell, 2010). Soil erosion due to water is based on two basic processes: 1) the detachment of particles due to raindrop impact; and 2) the transport of detached particles by raindrop splash and overland flow (Watson and Laflen, 1986, Kinnell, 2005, Morgan et al., 1998, Morgan, 2005, Lal, 2001). Environmental conditions and soil characteristics dictate the susceptibility of soil to erode. Factors include: rainfall intensity (Assouline and Ben-Hur, 2006, Defersha and Melesse, 2012, Sharma and Gupta, 1989, Sharma et al., 1991); soil type and surface conditions (Assouline and Ben-Hur, 2006, Rickson, 2014, Truman and Bradford, 1990, Le Bissonnais, 1990, Romkens et al., 1990); vegetation cover (Garcia- Ruiz, 2010, El Kateb et al., 2013, Thornes, 1990, Wainwright and Thornes, 2004, Kosmas et al., 1997); and slope (Fox et al., 1997, Fox and Bryan, 1999, Assouline and Ben-Hur, 2006, Defersha and Melesse, 2012). These factors directly affect, or are affected by, processes occurring at the micro scale, such as changes in micro topography (Morin et al., 1981, Jarvis, 2007, Horn et al., 1994, Parkin, 1993).

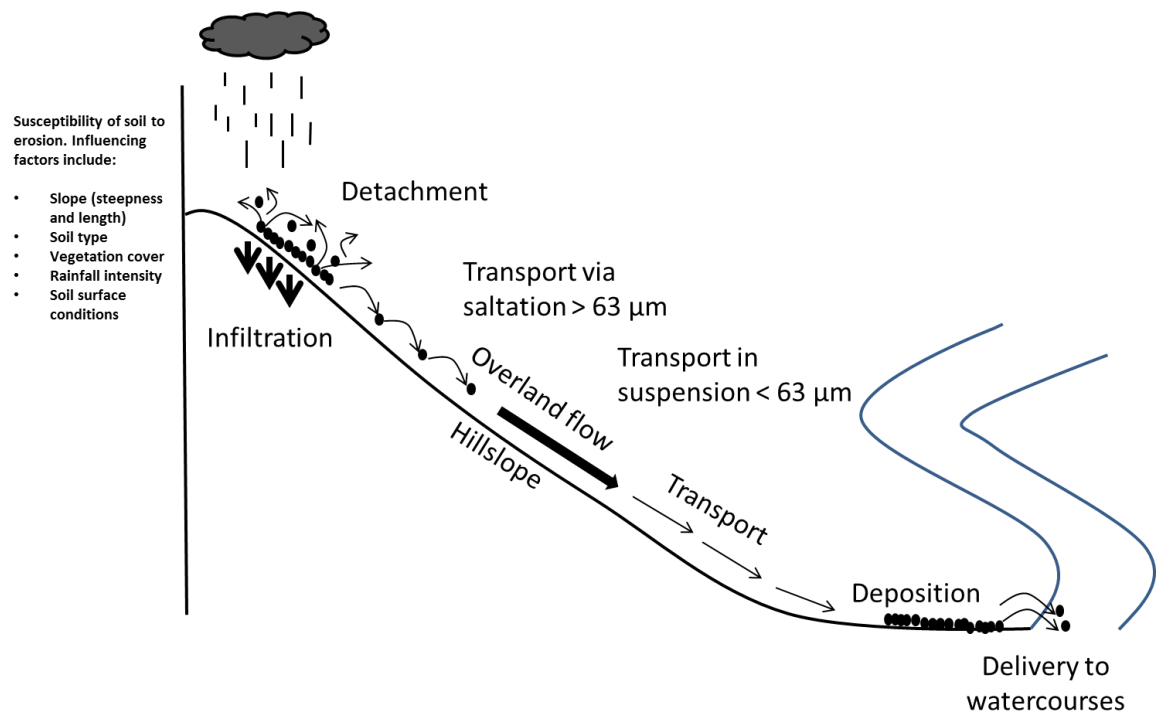


Figure 2. A schematic diagram to illustrate the transport processes occurring during soil erosion due to water.

Within coastal and marine environments, a range of industries (e.g. construction and maintenance dredging) act to suspend significant volumes of fine sediment (Carvalho, 1995, Wilber and Clarke, 2001, Gilmour, 1999, Smith and Friedrichs, 2011, Larcombe et al., 1995), inducing siltation of coastal areas (Al-Madany et al., 1991, Hossain et al., 2004, Eyre et al., 1998), negatively impacting upon marine habitats and coastal ecosystems (Erftmeijer and Robin Lewis III, 2006, Erftmeijer et al., 2012, Thrush et al., 2004, Kenneth et al., 2004, Thrush and Dayton, 2002). For sediment to move, the force of water flowing over it must be capable of overcoming both the force of gravity acting on the sediment grains, and the friction between the grains and the surface in which they are resting (Grabowski et al., 2011, Dey, 2014, Miller et al., 1977, van Rijn, 1984, Parchure and Mehta, 1985). Once mobilised, sediment transport processes depend on dynamic feedback interactions

between the hydrodynamics, bed forms and sediment properties (Nielsen, 2009, Soulsby, 1997). Several transport processes generated by a combination of waves and currents, move sediment in the along-shore and cross-shore direction (see Figure 3 modified from Brown et al. (1999) and Masselink and Puleo (2006)). Wave orbital action suspends sediment which is then transported in the direction of the prevailing currents. As waves approach the shore, an alongshore current is established which flows along the shoreline, transporting mobilised sediment (Brown et al., 1999, Masselink and Hughes, 2003). In addition, sediment is transported in the swash zone (Masselink and Puleo, 2006, Smith et al., 2003, Kamphuis, 1991, Puleo et al., 2000, Masselink and Hughes, 1998), through the processes of bed load, suspended load, sheet flow and single phase flow (Hughes et al., 1997, Masselink and Puleo, 2006).

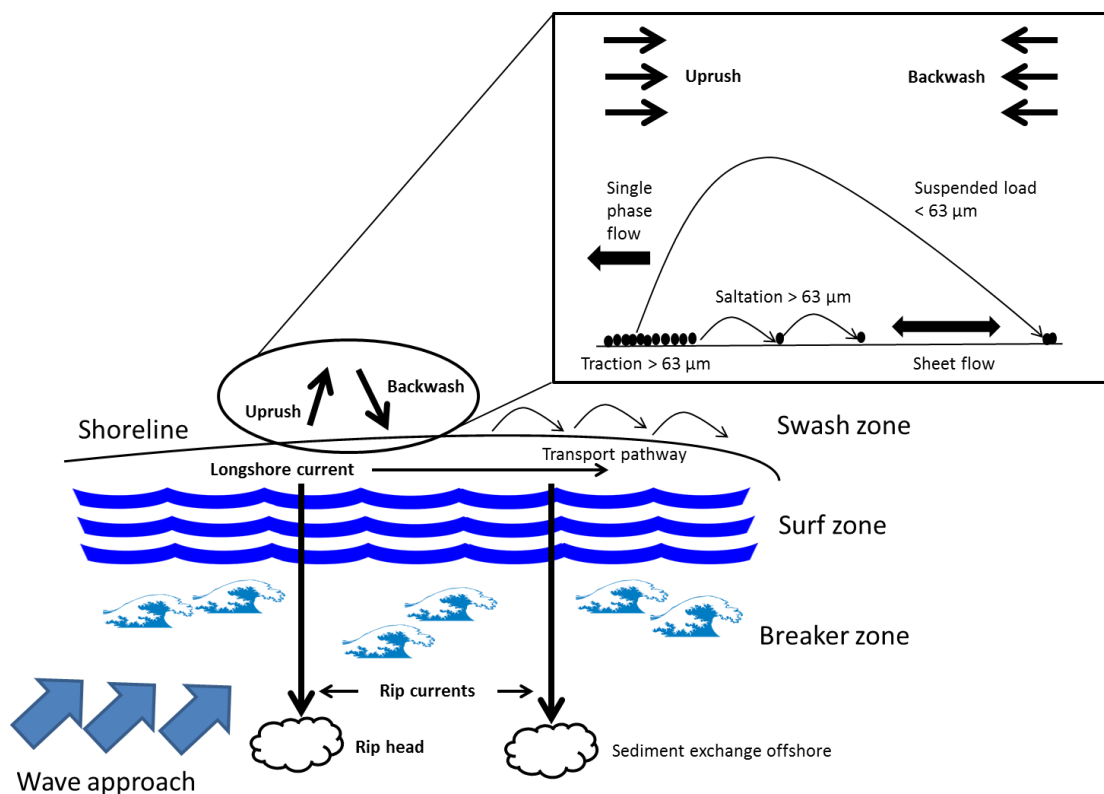


Figure 3. A schematic diagram of wave and current driven longshore and cross – shore transport processes which occur in the breaker, surf and swash zone.

Computational, physical and empirical modelling has been used extensively to evaluate coastal sediment processes (Carr et al., 2000, Catt et

al., 1998, Chen and Adams, 2007, Crabill et al., 1999, Kozerski and Leuschner, 1999), and erosive processes (Meybeck et al., 2003, Larssen et al., 2010, Lee et al., 2004, Lee et al., 2007, Digiacoimo et al., 2004). Modelling, though theoretically sound, often does not provide an accurate picture of what is occurring in reality (Athanasios et al., 2008, Gallaway, 2012, Cabrera and Alonso, 2010, Mehta, 2012, Araujo et al., 2002). The simplification of a process, although a precept in environmental modelling (Overton and Meadows, 1976, Simons and Simons, 1996, Dawdy and Vanoni, 1986) is of concern when strategic decisions are based solely upon modelling evidence (Black et al., 2007, Usseglio-Polatera and Cunge, 1985, Cromeey et al., 2002). Yet, modelling provides the strongest available tool to inform long term management plans and decision making (Gonenc and Wolflin, 2005). Therefore, it is crucial, that these models are as representative of real world processes as possible (Curtis et al., 1992). To ensure this, sediment transport models need to be validated using field techniques (Cromeey et al., 2002, Zobeck et al., 2003, Tazioli, 2009).

Field techniques used to investigate sediment transport primarily rely on point (Eulerian) measurement sampling approaches including, variously, sediment traps, turbidity sensors, acoustic sensors, erosion pins etc. (Vincent et al., 1991, Horn and Mason, 1994, Kraus and Dean, 1987, Kawata et al., 1990, Jimoh, 2001). At larger scales ($n \text{ km}^2$), remote sensing techniques can contribute to marine and coastal sediment transport studies e.g. the satellite-based CASI instrument (El-Asmar and White, 2002, Millington and Townshend, 1987), and terrestrial transport studies (King et al., 2005, Haboudane et al., 2002, Curzio and Magliulo, 2009, Vrieling, 2006) e.g. terrestrial LIDAR scanning (Castillo et al., 2012). In addition, computational, physical and empirical modelling have been developed to investigate coastal morphodynamic and sediment processes (Bertin et al., 2009, Lesser et al., 2004, Long et al., 2008, Picado et al., 2011, Suh, 2006), and hydrological and earth surface transport processes (Rushton et al., 2006, Batelaan and De Smedt, 2007, Lubczynski and Gurwin, 2005, Nearing et al., 1989). These techniques though useful provide limited information. Point measurement sampling techniques provide data on sediment movement in one position,

whereas sediment movement is predominately a geospatial phenomenon (Black et al., 2007, Hamylton et al., 2014, Karydas et al., 2014). Further, point measurement techniques struggle to monitor sediment transport on event based or short temporal scales (White, 1998, Lawler, 2005, Letcher et al., 2002, Peeters et al., 2008, Benaman et al., 2005). Remote sensing techniques enable changes to be viewed at a broader scale, providing a spatial context to evaluate the significance of field data (Campbell and Wynne, 2011). However, they are generally expensive, rarely set up for sediment studies, nor do they provide information on sediments other than in the very surface layer (Huntley et al., 1993, Brassington et al., 2003).

A judicious approach to assessing sediment transport dynamics would combine some (the most appropriate) of these methods, with a method which indicates specifically where sediment comes from, where it is transported to, and where it finally ends up: the technique available to do this is active sediment tracing (Foster, 2000, Black et al., 2007, Guzman et al., 2013). To garner information on the origin of the sediment, its associated transport pathway, and eventual fate, a sediment tracing approach (which is fundamentally Lagrangian in form) is required, since most commonly, it is not possible to differentiate the sediment in transport from the surrounding sediments (Black et al., 2007). Sediment tracing is the science associated with the use of tracers (Foster, 2000, Drapeau et al., 1991). Tracers are natural or synthetic materials which are identifiable from the native sediment load (Mahler et al., 1998, Crickmore, 1967, Spencer et al., 2011, Liu et al., 2004, Michaelides et al., 2010). Tracers are identifiable due to natural or applied “signatures”. This enables the spatio-temporal distribution of sediments, and anthropogenic derived particulates, to be monitored within the environment (Black et al., 2007, Drapeau et al., 1991). Sediment tracing can be used to identify point sources of sediment (Magal et al., 2008, Guymer et al., 2010, Inman and Chamberlain, 1959, Cromey et al., 2002), elucidate transport pathways (Collins et al., 1995, Mayes et al., 2003, Carrasco et al., 2013, Kimoto et al., 2006a, Polyakov and Nearing, 2004), and assess zones or areas of accumulation / deposition (Collins et al., 2013, Kimoto et al., 2006b). Furthermore, the methodology if applied correctly, can provide quantitative

data regarding the volume of sediment in transit (Ciavola et al., 1998), and the transport rate (Ingle, 1966, Ciavola et al., 1997, Ciavola et al., 1998, Carrasco et al., 2013, Ferreira et al., 2002, Vila-Concejo et al., 2004). Such data are considered essential benchmark data for numerical model development and validation (Athanasios et al., 2008, Merritt et al., 2003, Cromey et al., 2002).

Sediment tracing, using active tracers, has been a prevalent field technique for over a century. The first use of tracers in a scientific study investigated the long shore transport of shingle on Chesil beach, UK (Richardson, 1902). Early tracing studies e.g. Ingle (1966), Inman and Chamberlain (1959), Pantin (1961), Shinohara et al. (1958), King (1951), led to the development of methodologies and tracing principles which remain to this day. Though historically, studies often utilised tracing materials with disparate properties to the native sediment load e.g. pulverised coal (Shinohara et al., 1958), broken house bricks (West, 1949, Kidson and Carr, 1961), painted sediment (Dobbs, 1958, King, 1951, Luneberg, 1960), sediments wrapped in tin foil, (Lee et al., 2007), and fly ash mixed with cement (Hu et al., 2011, Dong et al., 2007, Dong et al., 2009). Due to the use of tracing materials with disparate properties, and resource intensive methodologies, the popularity of sediment tracing has fluctuated (White, 1998). Recent technological developments in tracer design and the tracing methodology (Table 1) combined with relevant environmental legislation (e.g. the water framework directive. Directive 2000/60/EC) have prompted a resurgence of interest in active sediment tracing (Black et al., 2007).

Table 1. The recent technological, and methodological, developments which have prompted a resurgence of interest in the sediment tracing technique.

Stage	Technological development	Impact
Tracer design	<i>Synthetic tracers</i>	The development of commercially available synthetic tracers has increased the application of the sediment tracing technique. Synthetic tracers provide a low cost sediment tracer e.g. Tauro et al.

Stage	Technological development	Impact
	<i>Improved labelling techniques</i>	<p>(2010), Ventura et al. (2001), Pedocchi et al. (2008), Angarita-Jaimes et al. (2008).</p> <p>Labelling or tagging natural sediment with an identifiable signature has led to the development of tracers which replicate the hydraulic properties of the native sediment load, remain stable through time and do not interfere with the transporting system e.g. Black et al. (2004), Guymer et al. (2010), Collins et al. (2013), Zhang et al. (2001), Armstrong et al. (2012), Van Der Post et al. (1995). This has increased the validity of the sediment tracing technique.</p>
Sampling advancements	<i>Passive sampling techniques</i>	<p>Passive sampling techniques are driving innovation within sediment tracing studies e.g. the use of <i>in situ</i> fluorimeters, imaging techniques and magnetic susceptibility. These techniques provide information regarding the spatio-temporal distribution of tracer particles, without direct sampling of the sediment or soil. This reduces both the interference with the system, and the requirement for resource intensive sampling campaigns and sample analysis.</p>
Analytical advancements	<i>Development of novel tracer enumeration</i>	<p>Tracing studies have regularly used resource intensive, sample analysis techniques. These techniques restrict sampling frequency in the field, due to the</p>

Stage	Technological development	Impact
	<i>techniques</i>	analytical timescales e.g. <i>Carrasco et al. (2013)</i> , <i>Cabrera and Alonso (2010)</i> , <i>Ferreira et al. (2002)</i> , <i>Benevente et al. (2005)</i> , <i>Cronin et al. (2011)</i> , and/or the related cost of samples analysis e.g. <i>Zhang et al. (2001)</i> , <i>Kimoto et al. (2006b)</i> , <i>Stevens and Quinton (2008)</i> , <i>Michaelides et al. (2010)</i> , <i>Zhang et al. (2003)</i> . Recent techniques have reduced the resource intensive nature of sample analysis techniques e.g. <i>Tauro et al. (2010)</i> , <i>Silva et al. (2007)</i> , <i>Yang et al. (2011)</i> , <i>Forsyth (2000)</i> , <i>Ventura et al. (2002)</i> .

Natural tracers use the signatures associated with native particles to trace the movement of sediment, termed sediment source ascription or sediment fingerprinting (Foster, 2000). The most popular technique utilises the fallout from nuclear weapons testing in the 1950's and 60's to study sediment transport at the catchment scale (Theuring et al., 2013, Smith et al., 2013, Porto et al., 2013, Belyaev et al., 2013, Bai et al., 2013). Popular radioisotope tracers include: Caesium-137 (^{137}Cs) (half-life, $t_{1/2} = 30.17$ years) (Pfitzner et al., 2004, Walling et al., 2000, Quine et al., 1999, Lu and Higgitt, 2000, Schuller et al., 2003); Thorium-234 (^{234}Th) ($t_{1/2} = 24.1$ days) (Bacon and Rutgers Van Der Loeff, 1989, Turnewitsch and Springer, 2001, Rutgers Van Der Loeff et al., 2002, Inthorn et al., 2006, Peine et al., 2009); lead-210 (^{210}Pb) ($t_{1/2} = 22.26$ years) (Porto et al., 2013); and Beryllium-7 (^7Be) ($t_{1/2} = 53.12$ days) (Walling, 2013).

Mineral magnetism has also been utilised as a tracer signature (Dearing, 1992, Yu and Oldfield, 1989, Oldfield et al., 1981) to determine the

relative sediment contribution of different river basins e.g. Royall (2001), Horng and Huh (2011), Dan (2001), Owens et al. (2000), Caitcheon (1993).

Sediment source ascription or sediment fingerprinting has significant application in catchment and river basin sediment studies (Collins et al., 1997, Walling et al., 2013). However, if specific data relating to the sediment source, transport pathway and sink areas is required an active sediment tracer must be utilised (Collins et al., 2013).

Sediment tracing using active tracers, involves the tagging or marking of natural or artificial sediments with an identifiable signature (Black et al., 2007). Active tracers are introduced to the environment providing a direct field method of monitoring the movement of sediment. The method is versatile with application in marine and coastal, (Vila-Concejo et al., 2004, Carrasco et al., 2013, Cronin et al., 2011, Benevente et al., 2005, Lee et al., 2007, Miller and Warrick, 2012); and terrestrial and fluvial environments (Stevens and Quinton, 2008, Ventura et al., 2002, Liu et al., 2004, Kimoto et al., 2006a, Tauro et al., 2010). The overriding strength of the technique is that it can delineate sediment transport pathways more effectively than other methods (Ingle, 1966, Mayes et al., 2003, Carrasco et al., 2013, Polyakov and Nearing, 2004). Further, it is a field method which if executed effectively, can provide an accurate picture of sediment transport trends (Ciavola et al., 1998, Ciavola et al., 1997, Ferreira et al., 2002, Vila-Concejo et al., 2004).

There are two principal types of active tracer that have been utilised in tracing studies; 1) labelled (coated) natural particles; and 2) labelled synthetic tracer (Black et al., 2007). Historically, the most popular tracer signatures have been applied radioactivity, fluorescence, magnetism and rare earth elements.

Following the advent of the nuclear age, the means were developed to irradiate sediment grains (White, 1998). These grains were used extensively as a sediment tracer (Crickmore and Lean, 1962, Inman and Chamberlain, 1959, Sarma and Iya, 1960, Davidson, 1958, Courtois and Monaco, 1968) due to the relative ease with which the irradiated grains could be monitored over a large spatial area, using hand held Geiger counters e.g. Inman and

Chamberlain (1959). However, irradiated tracers, are now not permitted in most environments on the basis of health and safety considerations, significantly limiting their use (Black et al., 2007, Sigbjornsson, 1994).

Applied fluorescent colour has proved a popular tracer signature. Fluorescent materials provide a unique visual tool which enables *in situ* non-invasive image analysis and visual inspection techniques to be utilised (Vila-Concejo et al., 2004, Ciavola et al., 1998, Carrasco et al., 2013, Russell, 1960, Solan et al., 2004). A fluorescent signature can be applied to a natural material via: the application of a fluorescent substance (Russell, 1960, Teleki, 1966); staining sediment with fluorescent dye (Ingle, 1966, Vila-Concejo et al., 2004, Ciavola et al., 1997, Ciavola et al., 1998, Carrasco et al., 2013); or the development of a fluorescent luminophore (Mahaut and Graf, 1987, Silva et al., 2007). The advantage of the luminophores is the long-lasting nature of the colorant and its fluorescent properties (Mahaut and Graf, 1987, Magal et al., 2008).

Rare Earth Elements (REE) have been applied to natural material as a tracing signature (Stevens and Quinton, 2008, Zhang et al., 2001, Zhang et al., 2003, Deasy and Quinton, 2010). Early studies used REE as a horizon marker (Knaus and Van Gent, 1989). Following this, natural particles tagged with a REE were used to investigate sediment transport trends (Tian et al., 1994, Olmez et al., 1994, Krezoski, 1985, Krezoski, 1989). In a pioneering study, Zhang et al. (2001) demonstrated that REE oxide powders, when directly mixed with soils, bound with silt sized soil particles and incorporated into soil aggregates of different sizes ($> 53 \mu\text{m}$) in uniform proportions (Zhang et al., 2001, Zhang et al., 2003). Due to the strong binding capability, low mobility and low natural background in soils, REE oxide powders were determined to be an effective tracer of soil (Kimoto et al., 2006b, Zhang et al., 2001). REE oxide powders have since been used to investigate soil erosion trends on agricultural land. (Deasy and Quinton, 2010, Stevens and Quinton, 2008, Zhang et al., 2003, Kimoto et al., 2006a). However, as the signal associated with REE tracers significantly reduces or fluctuates following dilution (Spencer et al., 2007), REE tracers have limited application within sub-aqueous environments (Spencer et al., 2011, Krezoski, 1985). In addition,

the related cost of sample analysis for REE tracers is high (Ventura et al., 2001), reducing the number of samples that can be collected from the field within a given resource budget. This limits the potential spatial and temporal resolution of a REE tracing study.

Alternatively, the magnetic signature of soils and sediments can be enhanced through heating (Oldfield et al., 1981, Armstrong et al., 2012, Van Der Post et al., 1995).

Technological progress in the development and manufacturing of polymers and synthetic materials has led to the use of entirely synthetic tracers (Tauro et al., 2010, Black et al., 2007, Guzman et al., 2013). In an analogous fashion to coated natural material, synthetic tracers are labelled with an identifiable signature. Synthetic tracing materials used historically include: fluorescent microspheres (Tauro et al., 2010, Angarita-Jaimes et al., 2008, Meselhe et al., 2004, Pedocchi et al., 2008); magnetic plastic beads (Ventura et al., 2001, Harvey et al., 1989, Tanaka et al., 1998); and REE tagged, glass particles (Riebe, 1995) and ceramic prills (Plante et al., 1999). However, synthetic particles are often unable to replicate the particle size distribution, particle density, shape, surface morphology, and surface reactivity of natural sediments (Zhang et al., 2003, Black et al., 2007). Also, concern has been raised over the deployment of entirely synthetic materials (e.g. plastic beads) to the environment, especially in ecologically sensitive areas (Thompson et al., 2004).

Active sediment tracers have had success in monitoring the transport trends of coarse sediments. However, tracing the movement of fine sediment has received far less scientific attention (Bruque et al., 1980, Adams, 1998). Recently, studies have labelled natural clays with: DNA (Mahler et al., 1998); iridium (Yin et al., 1993); and other REE oxides (Krezoski, 1985, Spencer et al., 2007, Spencer et al., 2011). Yet, despite these studies, tracking silt and clay sized particles remains a significant challenge (Black et al., 2007, Spencer et al., 2010). Consequently, the development of a tracer which is universally applicable, regardless of environment or study context, has the potential to enhance the field of active sediment tracing.

Tracking fine silts and cohesive sediment provides a significant challenge at every stage of the particle tracking methodology and due to this difficulty has received significantly less scientific attention. This is a surprise, as the silt fraction ($< 63 \mu\text{m}$) is of concern to agencies charged with providing catchment sediment management plans as the silt fraction increases turbidity in receiving water reaches and destroys ecologically sensitive aquatic habitats. The silt fraction is transported directly in suspension, and can be transported over great distances before being deposited again; this has implications for the feasibility of tracking studies. Some fine sediment is cohesive in character; cohesiveness results mainly from the presence of clay minerals in the sediment (Jordan and Valiela, 1983). The clay minerals form aggregates which are held together by electrostatic attraction and surface tension properties. This presents significant manufacturing challenges. The tracer must be transported in the same fashion as the native sediment; as cohesive sediment is transported primarily as flocs (Maltby, 1991); it is critical that any cohesive sediment tracer must flocculate (on its own or in conjunction with the natural sediment of study) and must have similar dynamic characteristics to naturally flocculated material (i.e. erosion, transport and settling rate) (Maltby, 2009). To do this, detailed matching of the tracer to the native sediment is vital to ensure the tracer is transported in the same fashion as the natural sediment.

Understanding the transport behaviour of fine and cohesive sediment is fundamental to the sustainable management of aquatic environments (Hutchinson et al., 1995). The collection of field data relating to cohesive sediment presents a range of technical and practical difficulties. Sediment tracing techniques, which have been widely used for measuring the transport pathways of sand-sized material in the field, need to be adapted, in terms of practical approach and technology, to be a viable technique that can provide direct field data relating to cohesive sediment processes. The development of tracers for tracking coarser material is relatively straight forward; the weight of the literature is based around sand, cobbles and shingle movement as it is considered easier to manufacture a suitable tracer for larger grain sizes. The development of a tracer suitable for tracking fine, cohesive sediment (> 63

um), including geo-chemically labelled clays has proved a significant challenge as coating of natural silts and clays with fluorescent dye significantly alters the hydrological properties of the individual particles (size and density) and hence transport characteristics (Eidsvik, 2004). Such tracers should have chemical signatures that can be easily detected following significant dilution in the field and should remain constant for the duration of the tracer study. Recently there has been considerable effort within the scientific community to develop a tracer for the fine sediment fraction. Fluorescent paint pigments have been used to track the dispersion of fine sediment from a marine sewer outfall (Maltby and Acreman, 2011), natural clays have been labelled with DNA (Milner et al., 2003), and iridium (Mitsch and Gosselink, 1983). Rare earth element oxides have also been used to engineer a suitable tracer for tracking silt (Moller, 2006, Mitsch et al., 1979, Olff et al., 1997) with limited success. The interaction of cohesive muds and injected cohesive tracer is vital to both the results and the viability of the technique. A cohesive tracer was tested by Maltby (2009) who concluded that even though the cohesive tracer flocculated and had similar hydrological properties as natural mud the tracer flocs have significantly different floc characteristics; this has implications for the use of cohesive tracer within particle tracking studies and could generate misrepresentative data. Following these findings Spencer et al. (2011) designed a rare earth element - labelled potassium depleted clay to track cohesive sediments in aquatic environments. The technique of labelling cohesive clays provides a tracer that has a number of significant advantages. REE's are non-toxic (Black et al., 2004) can be determined at low concentrations (Jarvis, 1989) and have strong binding capabilities with clays which provide a viable material that can be used for tracking cohesive sediments (Blake et al., 2006, Boardman, 1993). However, as discussed previously the use of REE's as a tracer in aquatic environments has a significant disadvantage, that the signal will reduce following dilution, making it difficult to distinguish the tracer from background native material. The commercial sector has developed synthetic, polymer based fluorescent tracers with the same size, density and surface charge characteristics as the silt fraction (Maltby, 2009).

This review has described a range of techniques available to investigate sediment transport dynamics with a focus on active sediment tracing methods. The recent resurgence of sediment tracing techniques within both the academic community and commercial sector has driven developments in tracer design and field methodologies. Sediment tracing has the potential to be a useful tool to investigate sediment transport dynamics within a range of environments and provide robust information to a range of real world sediment management problems. This thesis has assessed the use of a commercially available, dual signature tracer to investigate sediment transport trends in a range of environments e.g. Black et al. (2004), Guymer et al. (2010), Collins et al. (2013), Koch et al. (2013). This novel tracer has the potential to: 1) Improve the validity of active sediment tracing studies by increasing the quantity and quality of information to be garnered; 2) enable active sediment tracing approaches to be applied in a range of new environments in a range of study contexts by increasing the flexibility of the sediment tracing technique, enabling a range of sediment types (e.g. soils and mineral sediments) to be monitored; and, different sediment size fractions (from medium silts to cobbles).

2.1. Thesis Aim

The overarching aim of the thesis is to investigate active sediment tracing approaches and develop a novel, robust, fluorescent magnetic active sediment tracing methodology that can be applied to study sediment dynamics, regardless of environment or study context.

2.2. Objectives

The principal objectives were to:

1. Assess the utility and environmental significance of the active sediment tracing approach.
2. Evaluate the limitations of current active sediment tracing materials and assess the potential improvement to the active sediment tracing approach provided by a dual signature sediment tracer through an extensive review of the relevant literature.

3. Assess the efficacy of the active sediment tracing approach to the study of sediment transport dynamics in different environments and study contexts through a review of the relevant literature, extensive laboratory testing and method development and field trials in three distinct environments.
4. Evaluate and characterise the tracer properties to assess the effectiveness of the dual signature tracer to uphold the fundamental assumptions of a robust active sediment tracer.
5. Develop an analytical procedure suitably able to measure the tracer content of multiple tracer colours, within the same sample.
6. Reduce the timescales associated with the analytical procedure to enable the temporal and spatial resolution of tracing studies to increase.
7. Develop a methodological framework, within which, all tracing studies can be conducted.
8. Apply the technique to investigate real world, sediment management problems.
9. From the field trials assess and evaluate the field methodologies available to monitor and recover dual signature tracer from the environment.

3. Tracer Characterisation

3.1. Technology Description

Partrac Ltd (www.partrac.com) manufactures proprietary, dual-signature sediment tracers (Figure 4). The tracers possess highly similar hydraulic properties to natural mineral sediments (silts; sands; gravels) but are tagged, to enable unequivocal identification within the environment. Historically, tracers have relied on a single signature to identify them within the environment, dual-signature tracers are tracers which have two signatures, being fluorescence and ferrimagnetism. The fluorescent pigments are comprised of polymer nanospheres embedded within a water insoluble dye. The dye is loaded with a magnetic mineral oxide, resulting in each individual grain being fluorescent and ferromagnetic. There are four different coloured tracers available with a specific gravity (particle density) ranging from $1050 - 3800 \text{ kg/m}^3 \pm 115 \text{ kg/m}^3$.

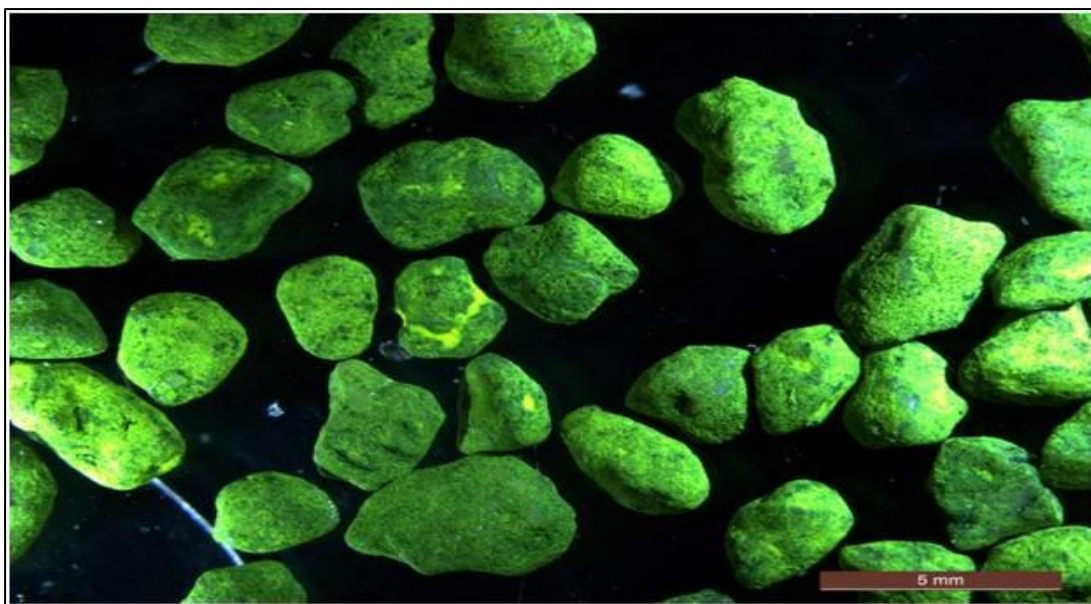


Figure 4. A photomicrograph of chartreuse coloured, dual signature tracer. Image courtesy Partrac Ltd.

3.2. Tracer Properties

The tracer properties were assessed in order to characterise the tracer prior to deployment to the environment. Firstly, the methods used to quantify the hydraulic properties of the tracer and native sediment throughout the thesis are described. Secondly, a series of tests were devised to assess: 1)

the fluorescent and magnetic characteristics of the tracer; and, 2) the degradation of the tracer coating over time.

SPSS statistics 20 software (IBM 2014) was used for all analysis. The significant differences between the responses of each tracer size fraction to the suite of magnetic measurements were assessed using a one-way ANOVA test with a Tukey multiple comparison test. The difference between the fluorescent emission of tracer, following exposure, and the fluorescent emission of the tracer control batch, was assessed using a paired T test.

3.2.1. Methods used to characterise the hydraulic properties of tracer and native sediment

The hydraulic properties of the tracer should strongly match those of the native (or target) sediment (Black et al., 2007a, Dyer, 1986). The key hydraulic properties that effect sediment transport are the particle size distribution and the particle density (specific gravity). The methods used to determine these properties are outlined below.

3.2.1.1. Particle size distribution

The particle size distribution of each tracer used and native sediment (where the tracer is designed to replicate the native sediment), was determined using a *Mastersizer 2000* laser diffraction particle size analyser device. A sub-sample of tracer or native sediment was analysed in triplicate. The methodology followed the standard operating procedure and best practice outlined in ISO 13320:2009, and the device's handbook (Ltd, 2015) Where organic material was present, analysis was conducted following acid digestion (Laubel et al., 2003).

3.2.1.2. Particle density (specific gravity)

The specific gravity of each tracer and native sediment (where the tracer is designed to replicate the native sediment) was determined empirically, utilising a standard pycnometer procedure (Germaine and Germaine, 2009). Prior to testing, the pycnometer was calibrated to account for temperature change during the experiment (Figure 5). To calibrate the pycnometer it was cleaned, dried and weighed with and without distilled water. These measurements were then applied to the following equation:

$$M_{B+W_T} = M_B + V_{B_{T_C}} \{1 + (T - T_C) \epsilon_g\} (P_{W_T} - P_{a_T}) \quad (1)$$

Where, M_{B+W_T} is the mass of the pycnometer and water at temperature T (g), M_B is the mass of the pycnometer, $V_{B_{T_C}}$ is the volume of the pycnometer at temperature T_C (cm³), T is the temperature of the pycnometer during individual measurement (°C), T_C is the temperature of the bottle at calibration condition (°C), ϵ_g is the coefficient of the cubical expansion of glass (0.1 x 10⁻⁴ / °C), P_{W_T} is the mass density of water at temperature T (g / cm³) and P_{a_T} is the mass density of air (0.001 g / cm³).

To calculate the specific gravity of the tracer, a subsample of tracer (~ 10 g) was weighed to three decimal places. The sample was then carefully transferred to the pycnometer, half filled with DI water, and left to rest for 24 hours. Following this time period the entrapped air was removed by placing the pycnometer in a beaker of gently boiling water. The pycnometer and contents were then left to cool to room temperature. The pycnometer was filled completely with DI water, and the stopper placed in the top. The outside of the pycnometer was cleaned and dried, and the pycnometer and its contents weighed to three decimal places. Finally, the temperature of the contents of the pycnometer was obtained using a mercury thermometer. The specific gravity of the tracer was determined using the following equation:

$$G_{S_T} = \frac{M_S}{(M_{B+W_T} + M_S) - M_{B+W+S_T}} \quad (2)$$

Where M_{B+W+S_T} is the mass of the pycnometer filled with DI water, and sediment, at temperature T . M_S is the mass of dry sediment (g).

Specific gravity values were reported at 20 °C. Thus, the value must be corrected to account for the change in water density using equation 3:

$$G_S = G_{S_T} \frac{P_{W_T}}{P_{W_{20}}} \quad (3)$$

Where P_{W_T} is the mass density of water.

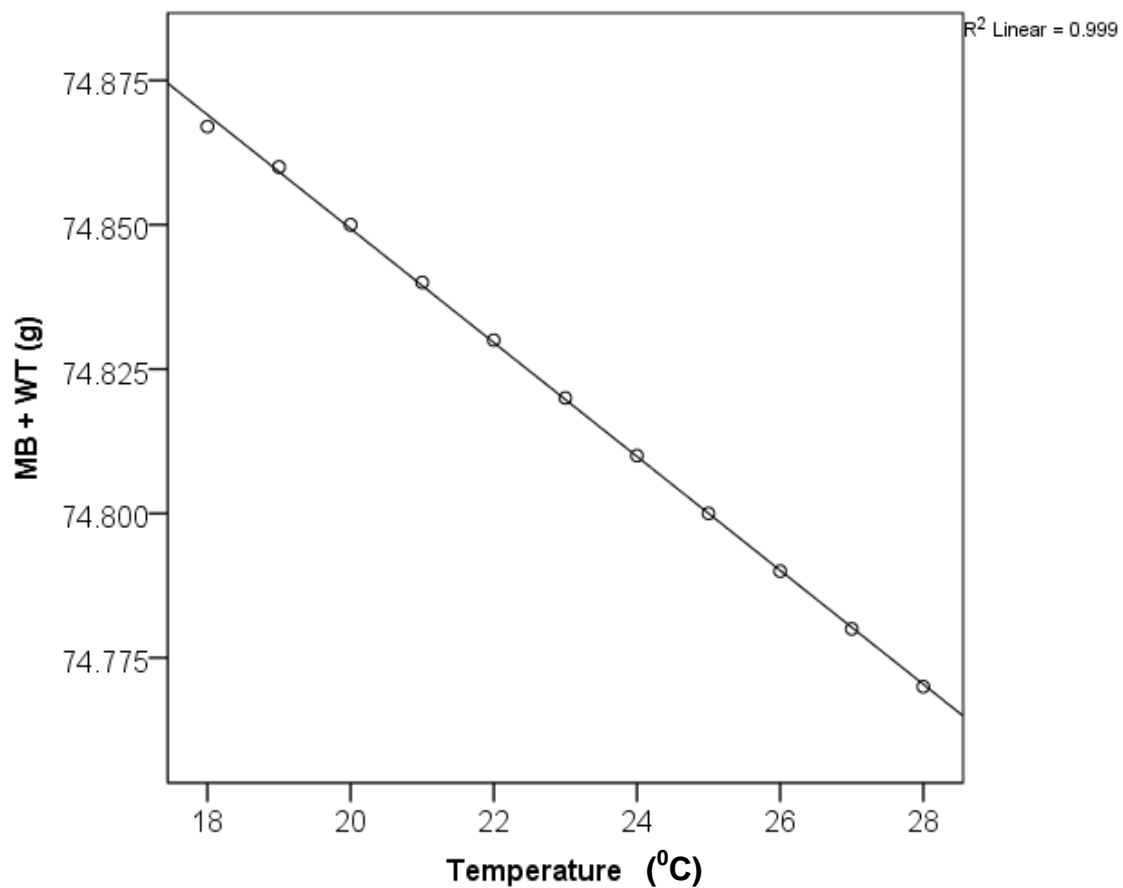


Figure 5. The pycnometer calibration curve depicting the change in the mass of the pycnometer (filled with DI water) over a range of temperatures. The calibration curve is derived from equation 1.

3.2.2. Methods used to characterise the magnetic properties of the tracer

In order to evaluate the magnetic properties of the dual signature sediment tracer a suite of magnetic tests were conducted to characterise the magnetic properties of the tracer. These tests were designed to assess the relative ease at which the tracer is able to ‘acquire’ magnetisation when exposed to an incrementally increasing magnetic field, and correspondingly, the relative ease at which the tracer is ‘demagnetised’ from a ‘magnetised’ state. To do this, a tracer was dry sieved into five different size fractions, < 63, 63-125, 125-250, 250-500 and > 500 microns. Triplicate samples of each size fraction were weighed and wrapped in cling film ready for analysis of the magnetic parameters. A set of magnetic measurements were performed based on the methodology described by Armstrong et al. (2012).

Measurements were collected at room-temperature, in the following sequence: low frequency magnetic susceptibility (K_{LF}); high frequency magnetic susceptibility (K_{HF}); anhysteretic remanent magnetisation (ARM, subsequently subjected to stepwise alternating field demagnetization at 15, and 23 milliTesla, mT) and stepwise acquisition of isothermal remanent magnetisation (IRM) at 20, 50, 100, 300 and 1000 mT (subsequently subjected to stepwise alternating field demagnetisation at 10 and 20 milliTesla, mT). The IRM at 1000 mT is assumed to be the saturated isothermal remanent magnetisation (SIRM). Low and high frequency magnetic susceptibility were measured using a MS2B susceptibility sensor, and all remanence measurements were made on a mini spin fluxgate magnetometer (noise level $2.5 \times 10^{-5} \text{ Am}^{-1}$). A demagnetizer with an ARM attachment was used for the ARM (up to a peak alternating field, AF, of 80 mT with a small steady field, 0.08 mT, superimposed) and for all AF demagnetizations. For the IRM acquisition experiments, a pulse magnetizer was used to generate direct current (d.c.) fields up to 300 mT and a Newport electromagnet for fields of 1000 mT. All instruments detailed (Bartington Instruments Ltd).

3.2.2.1. Results of testing

Tracers of all size fractions were attracted to an introduced magnetic field. The mean magnetic susceptibility of the tracer was $598 \times 10^{-8} \text{ m}^3 \text{ Kg}^{-1}$. Each tracer size fraction, when exposed to an alternating electromagnetic field showed high magnetic remanence (Figure 6, 7 and 8). Tracer, < 63 microns in size, showed a significantly higher magnetic remanence than the coarser sized fractions ($n = 14$, $p < 0.05$) and a significantly lower magnetic susceptibility than each of the other tracer size fractions ($n = 14$, $p < 0.05$) (Table 4). The highest susceptibility was observed with tracer of a size 63-125 microns, which displayed a significantly higher susceptibility, in comparison to the other size fractions ($n = 14$, $p < 0.05$) (Table 4). Throughout each measurement where tracer was exposed to an incrementally increasing magnetic field (ARM and IRM), significant differences between the remanent magnetisation were observed between tracer particles sized, < 63 microns, and 63-125 microns, and the coarser particles ($n = 14$, $p < 0.05$) (Table 2 and 3). However, no significant difference was observed between the different size fractions

following de magnetisation of ARM at 23 mT and demagnetisation of SIRM at 20 mT (n 14, $p > 0.05$) (Table 2 and 3). Each tracer size fraction tested, is discernible from each other (Figure 6, 7 and 8).

Table 2. A table to show the difference ($p, 0.05$) between the measures and particle size derived from the one-way Anova test with a Tukey multiple comparison test. The dependant variables include ARM acquisition and AF demagnetisation at 15 and 23 millitesla.

	Significant difference ($p = 0.05$)		
Particle size (micron)	ARM ($\text{Am}^2 \times 10^{-8}$)	AF demag of ARM @ 15 mT ($\text{Am}^2 \times 10^{-8}$)	AF demag of ARM @ 23 mT ($\text{Am}^2 \times 10^{-8}$)
(1) < 63	2, 3, 4, 5	4, 5	No sig diff
(2) 63-125	1, 3, 4, 5	No sig diff	No sig diff
(3) 125 -250	1, 2	No sig diff	No sig diff
(4) 250 – 500	1, 2	No sig diff	No sig diff
(5) 500 – 950	1, 2	No sig diff	No sig diff

Table 3. A table to show the difference ($p = 0.05$) between the measures and particle size derived from the one-way ANOVA test with a Tukey multiple comparison test. The dependant variables include IRM acquisition at 20, 50, 100, 300 and 1000 millitesla and AF demagnetisation of SIRM at 10 and 20 militesla.

	Significant difference ($p = 0.05$)						
	IRM acquisition ($\text{Am}^2 \times 10^{-8}$)					AF demagnetisation of SIRM ($\text{Am}^2 \times 10^{-8}$)	
Particle size (micron)	20 mT	50 mT	100 mT	300 mT	1000 mT	10 mT	20 mT
< 63 (1)	2, 3, 4, 5	2, 3, 4, 5	2, 3, 4, 5	2, 3, 4, 5	2, 3, 4, 5	2, 3, 4, 5	No sig diff
63-125 (2)	1, 3, 4, 5	1, 3, 4, 5	1, 3, 4, 5	1, 3, 4, 5	1, 3, 4, 5	1, 3, 4, 5	No sig diff
125 -250 (3)	1, 2	1, 2	1, 2	1, 2	1, 2	1, 2	No sig diff
250 – 500 (4)	1, 2	1, 2	1, 2	1, 2	1, 2	1, 2	No sig diff
500 – 950 (5)	1, 2	1, 2	1, 2	1, 2	1, 2	1, 2	No sig diff

Table 4.. A table to show the difference ($p = 0.05$) between the measures and particle size derived from the one-way ANOVA test with a Tukey multiple comparison test. The dependant variables include low and high frequency mass specific magnetic susceptibility.

	Significant difference ($p = 0.05$)	
	Mass specific magnetic susceptibility ($\times 10^{-8} \text{ m}^3 \text{ kg}^{-1}$)	
Particle size (micron)	Low frequency	High frequency
< 63 (1)	2, 3, 4, 5	2, 3, 4, 5
63-125 (2)	1, 3, 4, 5	1, 3, 4, 5
125 -250 (3)	1, 2	1, 2
250 – 500 (4)	1, 2	1, 2
500 – 950 (5)	1, 2	1, 2

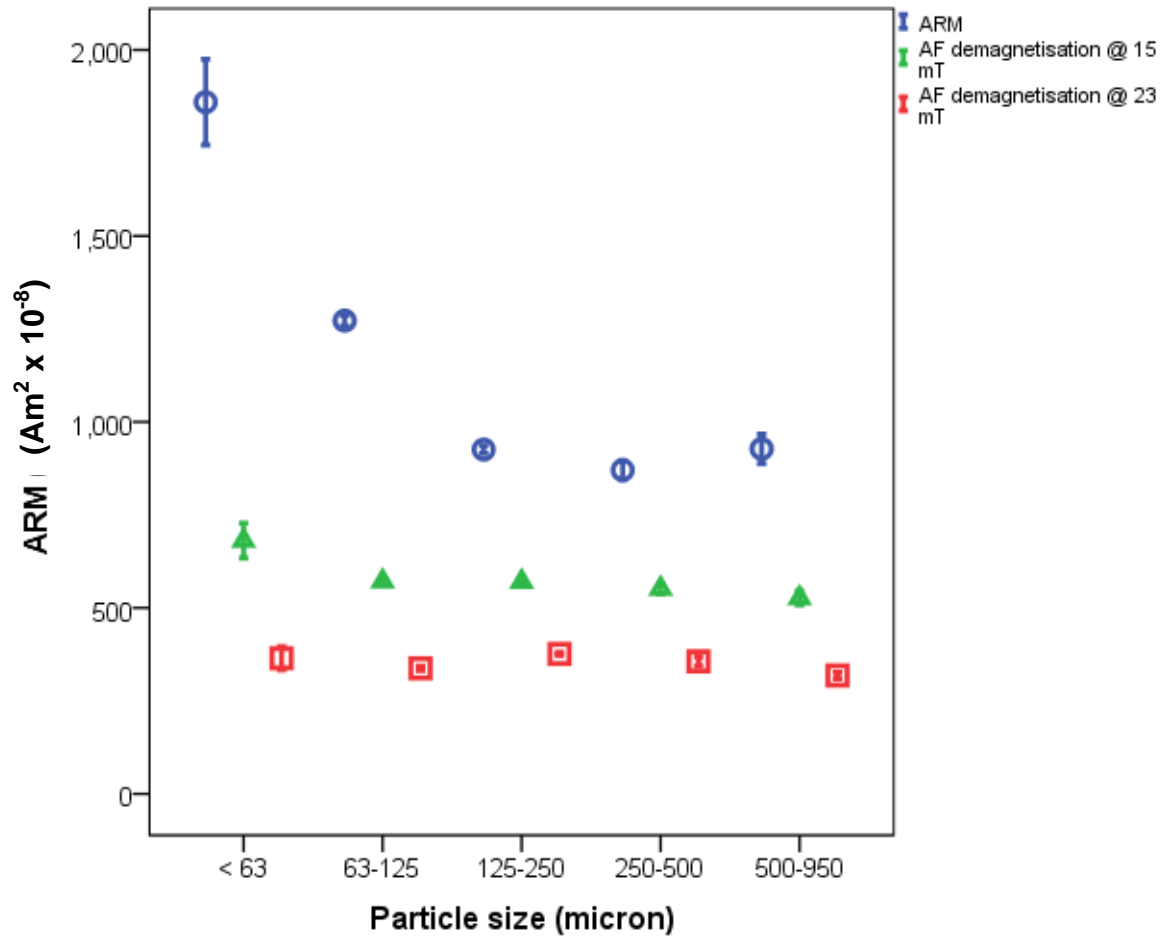


Figure 6. The anhysteretic remanent magnetisation (@ 100 uT dc, 80 uT ac) of different sized tracer particles subjected to stepwise alternating field demagnetization at 15, and 23 milliTesla. The markers show the mean response and the whiskers the standard error.

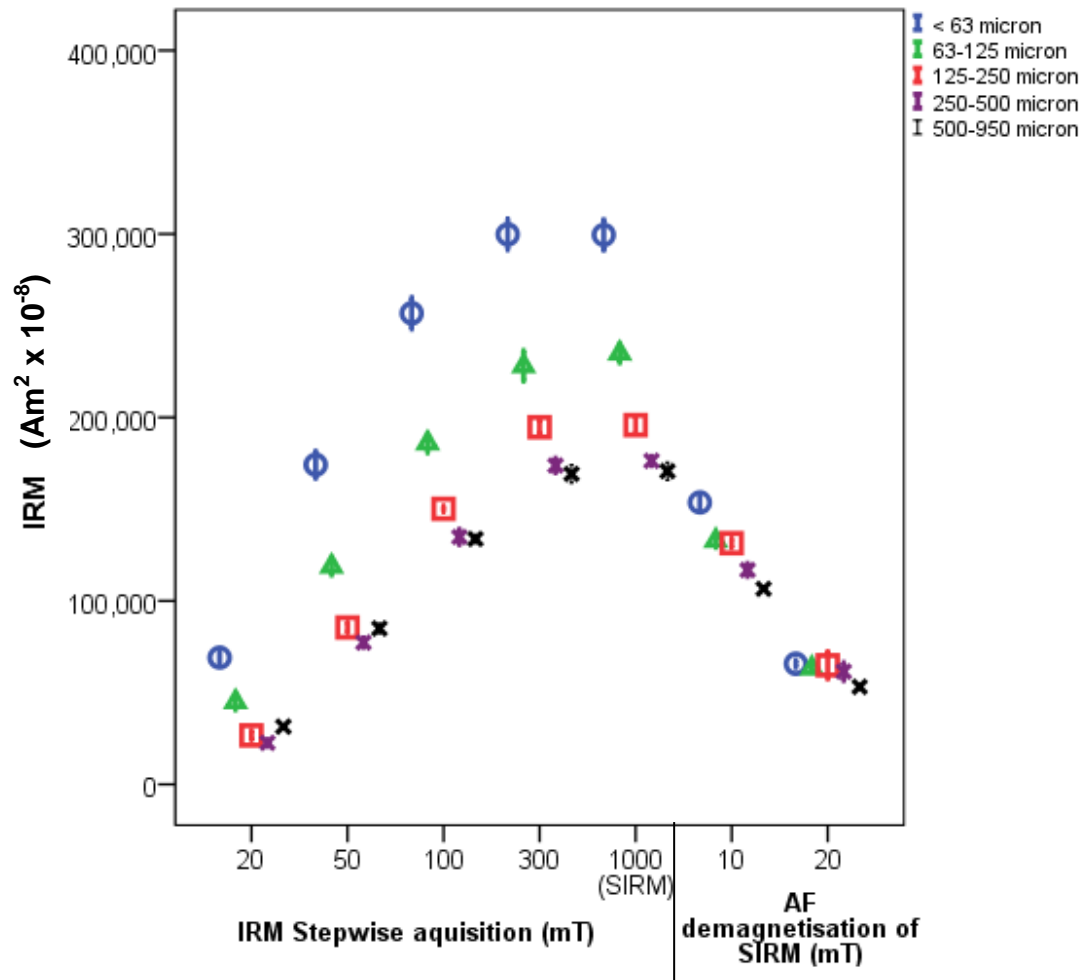


Figure 7. The stepwise acquisition of isothermal remanent magnetisation (IRM) at 20, 50, 100, 300 and 1000 mT, of different sized tracer particles subsequently subjected to stepwise alternating field demagnetisation at 10 and 20 milliTesla. The IRM at 1000 mT is assumed to be the saturated isothermal remanent magnetisation (SIRM). The markers show the mean response and the whiskers the standard error.

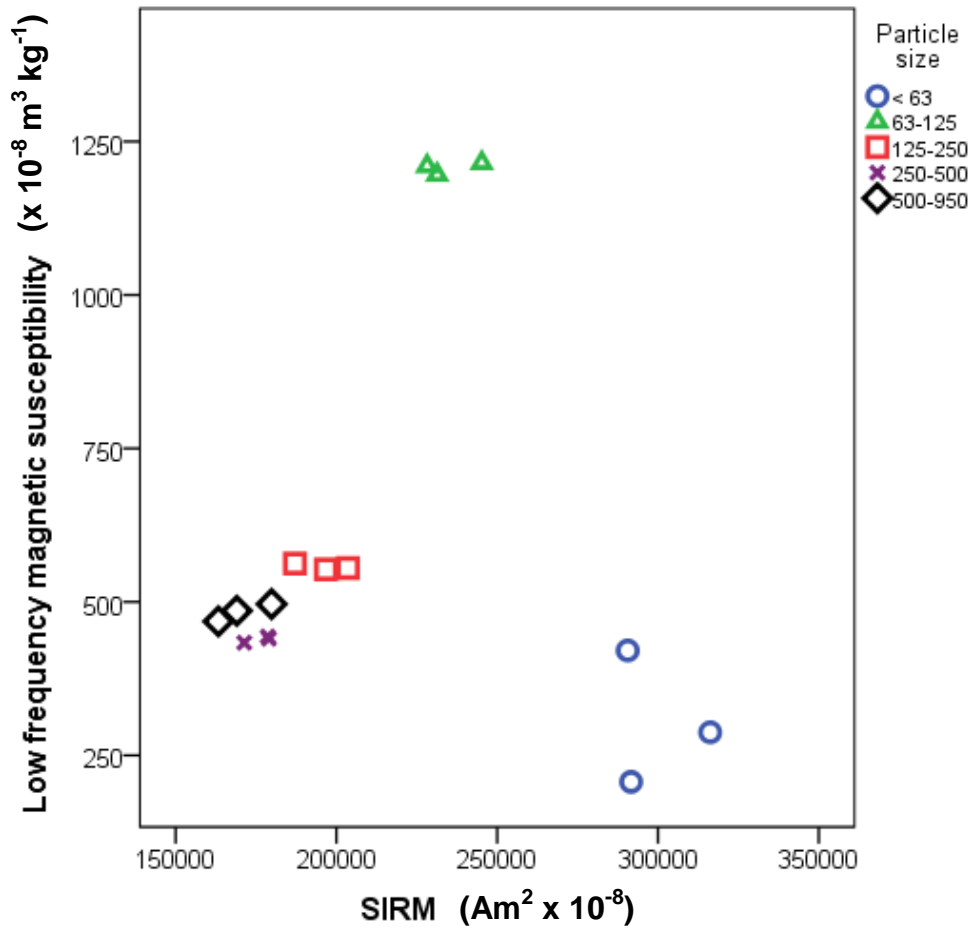


Figure 8. Low frequency magnetic susceptibility versus SIRM for different size fractions of dual signature tracer.

3.2.3. Methods used to characterise the fluorescent properties of the tracer

The fluorescent emission of a range of different sized (silts; sands and gravels) and different coloured tracers (pink and chartreuse), were qualitatively assessed under white light and ultra violet (400 nm) or blue light illumination (395 nm). Tracer particles were assessed at microscopic and non-microscopic scales. A LSM 510 Meta laser scanning confocal fluorescence microscope (Zeiss Ltd) combined with Axio imager 2; imaging facilities (Zeiss Ltd) was used to capture an image under white light and UV-A illumination. At non-microscopic scale, under white light illumination, an image was captured using a 750D Digital SLR camera (Canon Ltd), fitted with a 50 mm lens. To capture an image under blue light or UV-A illumination a yellow dichroic filter was fitted to the lens.

3.2.3.1. *Results of testing*

Each tracer analysed was consistently reactive upon exposure to UV-A or blue light. The fluorescent emission was clearly visible to the human eye (Figure 9, 10 and 11). Consequently, the tracer is unequivocally identifiable from the native sediment load, due to the fluorescent signature.

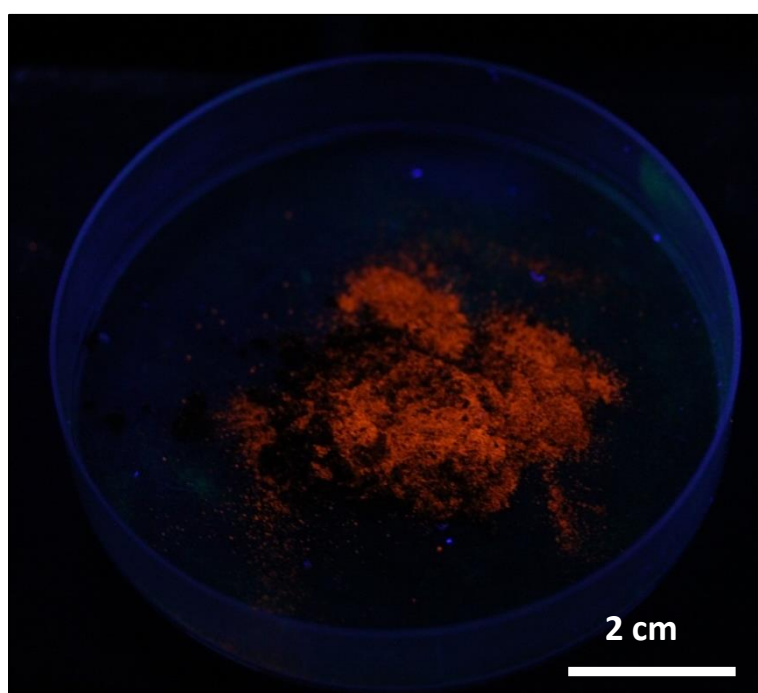
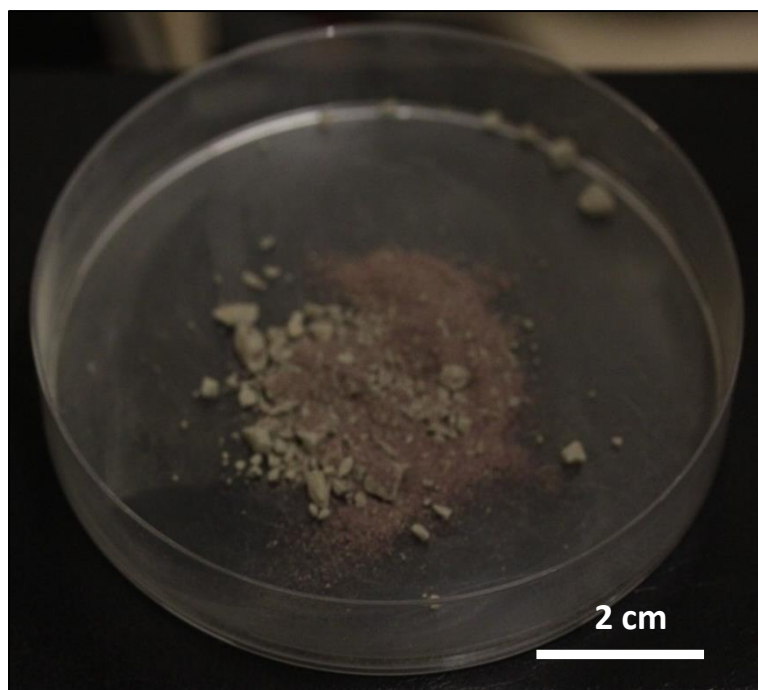


Figure 9. These two images above show the same sample under white light (top) and ultraviolet light (UV-A – 400 nm) illumination (bottom). The image was captured using a 750D Digital SLR (Canon Ltd), fitted with a 50 mm lens. When captured under UV-A illumination the image was shot through a yellow dichroic filter.

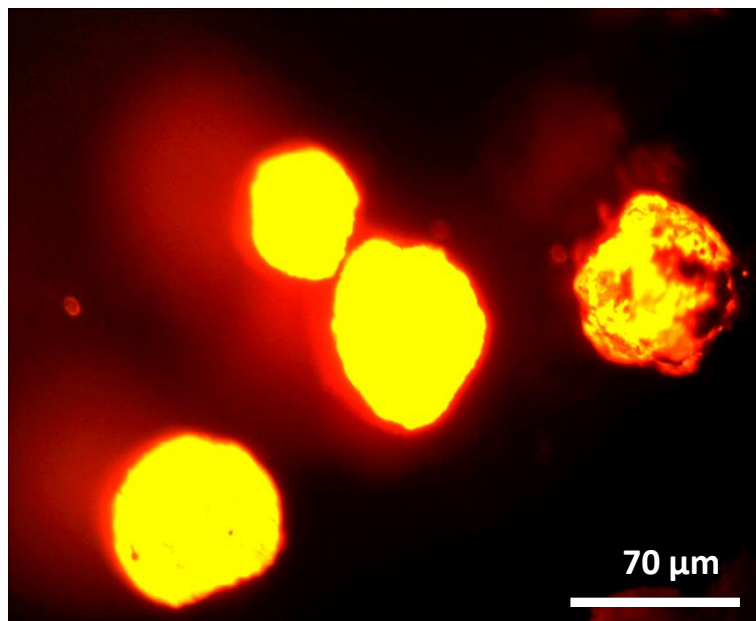
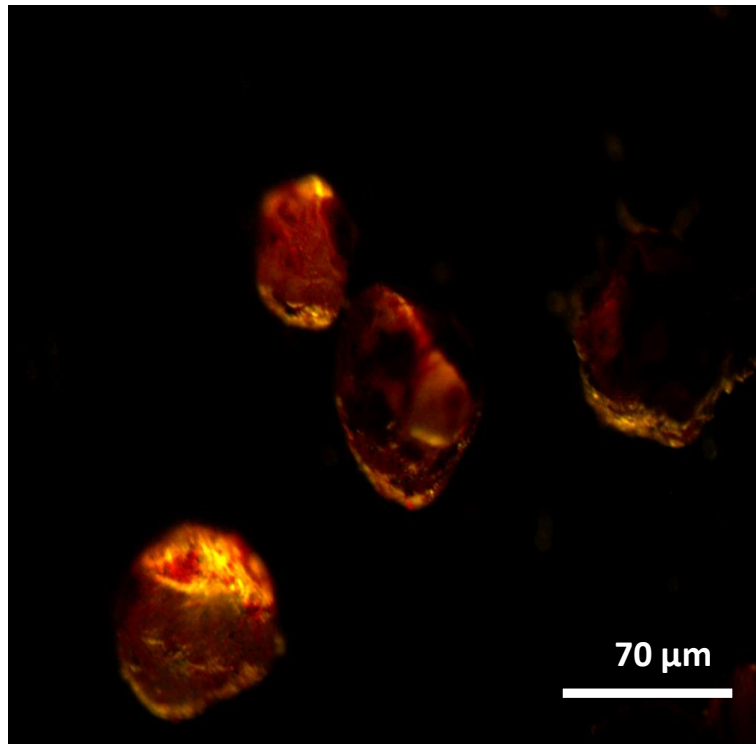


Figure 10. Silt sized tracer particles analysed under a fluorescence microscope. The image is captured under white light illumination (top) and under ultraviolet light (UV-A 400 nm) on an LSM 510 Meta laser scanning confocal fluorescence microscope used with Axio imager 2, imaging facilities (Zeiss Ltd).

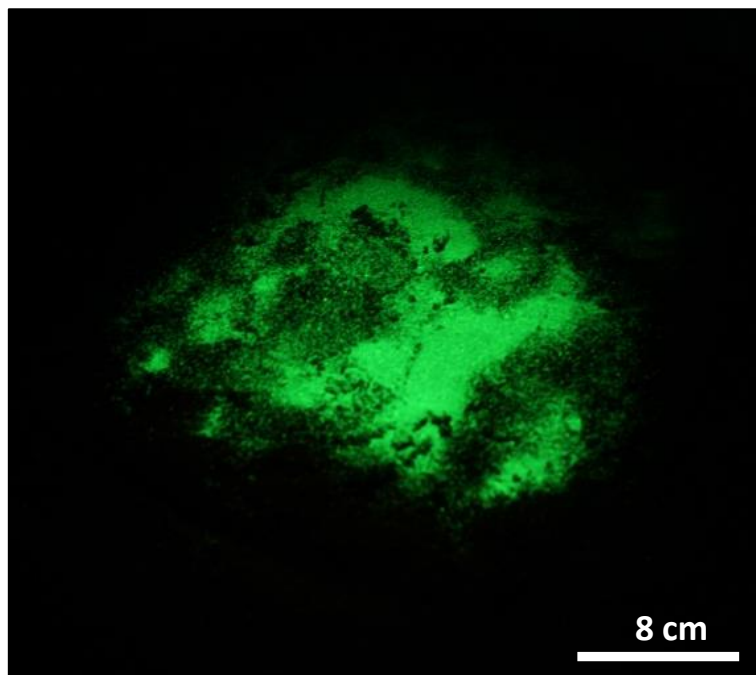
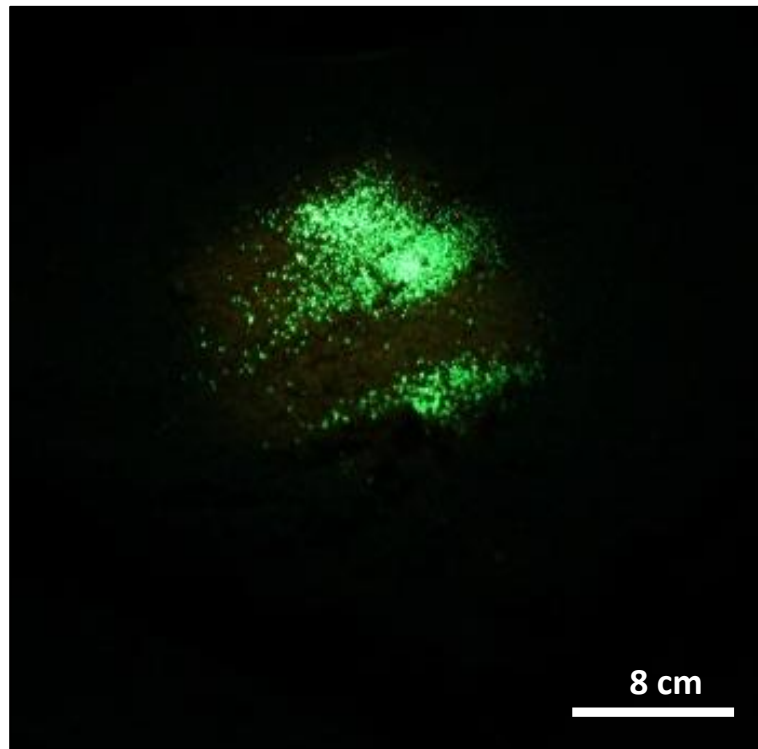


Figure 11. Photograph of sand sized chartreuse tracer particles mixed with native beach sand at a density of 0.001 g cm^2 (top) and 0.185 g cm^2 (bottom) under blue light illumination (395 nm). The image was captured using a 750D Digital SLR (Canon Ltd), fitted with a 50 mm lens, shot through a yellow dichroic filter.

3.2.4. Methods used to assess the degradation / survivability of the tracer coating

It is important that the applied tracer signals (fluorescence and ferrimagnetism) are not significantly altered once introduced to different environments (Foster, 2000, Black et al., 2007b). Therefore the degradation of the tracer coating through time, due to exposure to a range of environmental conditions, was investigated. Due to the makeup of the tracer coating, a reduction in the fluorescent emission would indicate a reduction in both tracer signals. Therefore degradation of the tracer coating was assessed by statistically comparing the fluorescent emission of exposed tracer particles, to the fluorescent emission of a control sample. A chartreuse sand tracer ($D_{50} = 125$ microns) was used for all testing. A systematic series of tests were devised to evaluate the degradation of the tracer coating during exposure to: 1) an abrasive environment; 2) a sub-aqueous environment; and, 3) weathering.

To simulate an abrasive environment, 10 samples of 10 g of tracer mixed with 10 g of natural mineral sand were submerged in distilled (DI) water in 50 ml sample tubes. These sample tubes were then placed in an end over end shaker and continuously run at 20 rpm, for 60 days. Each sample was sub-sampled and analysed at the end of the time period to assess coating degradation.

To simulate submersion in a subaqueous environment, 10 samples of 10 g of tracer were submerged within 40 ml of fresh and sea water in 50 ml sample tubes, respectively. These samples were stored in a fridge for 60 days prior to analysis. Each sample was sub-sampled and analysed at the end of the time period to assess coating degradation.

To simulate the effect of weathering two different soil types were split between 12 separate pots (a clay loam soil of the Wick 1 association, and a sandy loam soil of the Oak 2 association). Within each pot 10 g of tracer was deployed to the soil surface as a mono-granular layer, by hand. In total, 6 pots were positioned outside and six pots were positioned in a greenhouse facility. The pots positioned in the greenhouse were exposed to controlled

environmental conditions. These were: dry conditions under artificial light exposure for 14 hours per day, day temperature of 18 °C and a night temperature of 14 °C. A random sampling technique was used to collect samples in triplicate, from pots positioned outside, and in the green house. Sampling was conducted every four months over a 12 month period. Each sample was sub-sampled and analysed using the methodology outlined below.

Following collection, all samples were oven dried at 105 °C. The magnetic fraction (tracer) was separated using a high-field permanent magnet (11000 Gauss) e.g. Ventura et al. (2002) (method described in full in section 4.2). The fluorescent emission of the exposed tracer sample and control batch was accurately measured using a fluorimeter (Chelsea Technologies Group, UK). This enabled sensitive changes in the fluorescent emission to be determined. To measure the fluorescent emission of the tracer, a dye solution was prepared by adding a known dry mass of tracer particles (0.2 g) to 10 ml of solvent in an eppendorf tube, mixing and then allowing the solution to equilibrate for 7 days in the refrigerator (a series of prior tests indicated this was the optimal time period for dissolution of the dye coating). Following this, 200 µl of the eluted dye solution was then mixed with 2 ml of HPLC analytical grade solvent (a dilution of 1 in 10) to create a stock solution (optically dilute solution). Approximately, 20 seconds worth of raw fluorescent intensity data (volts) was recorded for each measurement using a 1 second (1 Hz) sampling rate. The fluorescent response of the exposed sample was then statistically compared to the control batch. The magnetic properties of the sample were not compared as all tracer particles remained attracted to an applied magnetic field following exposure.

3.2.4.1. Results of testing

Exposure to an abrasive environment (n 9, p > 0.05), and submersion within a sub-aqueous environment, within fresh (n 9, p > 0.05), and sea (n 9, p > 0.05) water had no significant effect on tracer signal. Comparatively, a significant effect was observed (n 17, p < 0.05) when the tracer was exposed to weathering. The tracer signal reduced by 3 - 5% over a period of 12 months (Figure 12). The reduction in fluorescent emission is attributed to photo-

degradation of the tracer particles by sunlight (Rabek, 2012). This result should be considered, and mitigated for, if conducting tracing studies over significant temporal scales where extended periods of sunshine are likely. Further, this result has implications for shallow aqueous and abrasive environments where photo degradation of the tracer particles is likely to occur. It is of note, though no degradation occurred within the simulation of an abrasive environment or sub-aqueous environment, these tests were conducted indoors.

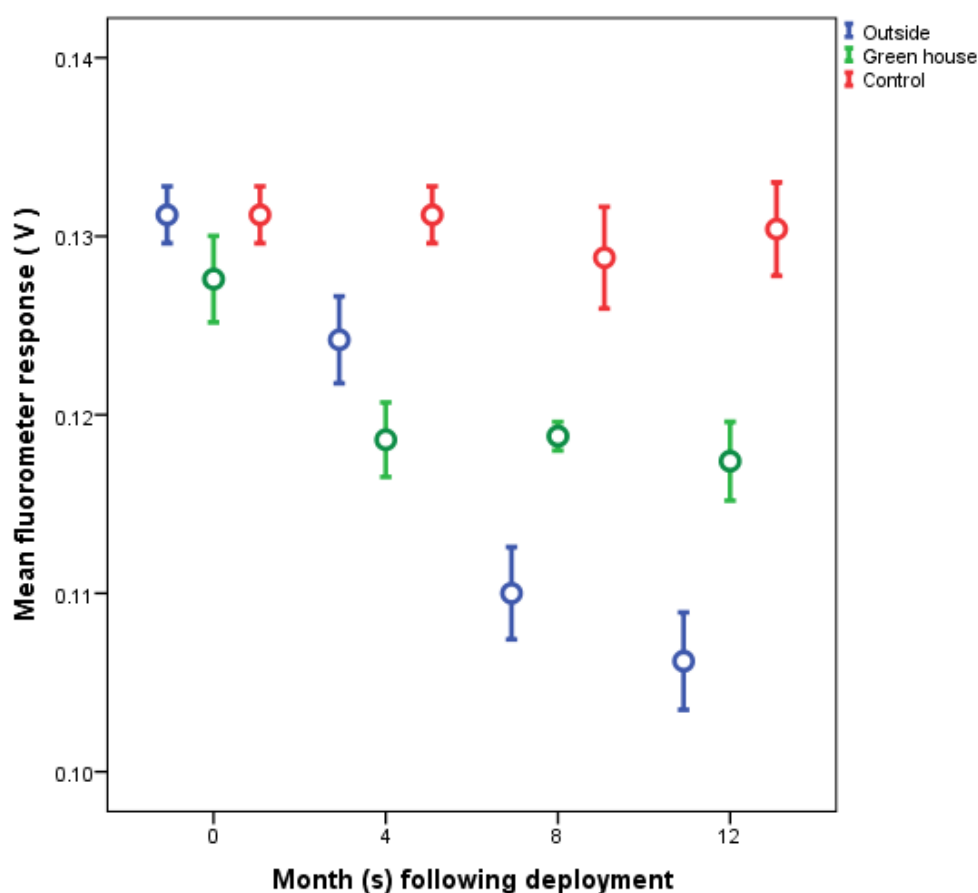


Figure 12. The mean fluorometer response to samples stored outside, in the green house and the control sample over a period of 12 months. The markers show the mean response and the whiskers the standard error.

3.3. Tracer Characterisation: Discussion and Concluding Remarks

Prior to application the tracer was characterised to determine the suitability of dual signature tracer, as a tracing material. A suite of testing was conducted to assess the fluorescent and magnetic properties of the tracer and the robustness/survivability of the tracer coating. The results demonstrated the

fluorescent and magnetic signal would enable silt, sand and gravel sized tracers to be identified within the environment, a fundamental precept of sediment tracing studies. The tracer is highly magnetic (Figure 5). The variance observed in the magnetic signature of tracer particles of different size fractions (silts and sands) has implications for studies that: 1) utilise magnetic susceptibility to monitor the spatio-temporal distribution of tracer particles; 2) where tracers with a multimodal size distribution are deployed; or, 3) a specific particle size fraction is of interest. The variance between the responses of different size fractions to a range of magnetic tests is due to the increased surface area of finer particles. This inherently increases the volume of dye, and thus, the quantity of magnetic mineral oxides per unit mass of tracer. This increases the degree of magnetisation of the sample (Oldfield et al., 1981). It is of note that during the manufacturing process a dust fraction is created (which consists of coated, partially coated and uncoated sediment mixed with dye and mineral oxide fragments). Further, the manufacturing process is unable to effectively label fine silt sized particles (< 10 microns in size). Material sized < 10 microns is present in each tracer batch, but this sized material consists of uncoated particles, shards of dye pigment and / or magnetic oxide powder etc. These materials are not able to be reliably traced.

The testing of the fluorescent properties indicated the fluorescent particles were reactive when exposed to blue (395 nm) or UV-A light (400 nm). The tracer is highly fluorescent (Figure 6 – 8). Fluorescent marking techniques combine a fluorescent compound with a natural mineral kernel by physical or chemical action (Ciavola et al., 1997, Mahaut and Graf, 1987). The specific manufacturing process used to develop the dual-signature tracer is protected as a trade secret. Thus, the specific physical and chemical make-up of the tracer is unknown. Degradation of tracer, through time, will inevitably lead to the breakdown of the fluorescent complex, introducing fluorescent dye to the environment. The toxicity of fluorescent dyes used within water tracing studies such as fluorescein, rhodamine B and rhodamine WT have been assessed in terms of their effects on aquatic organisms and marine life (Smart and Laidlaw, 1977). At low concentrations, no deleterious effects on ecology were recorded (Bandt, 1957, Sowards, 1958). However, as organisms were

exposed to greater dye concentrations, over longer periods of time, deleterious effects (Akamatsu and Matsuo, 1973, Keplinger et al., 1974, Sturn and Williams, 1975, Ganz and Stensby, 1975), and mortality (Marking, 1969, Parker, 1973) were observed. The toxicity of these dyes can be assumed to be similar to other fluorescent dyes available (Smart and Laidlaw, 1977).

The results of the survivability/degradation testing indicated the tracer should remain identifiable when deployed to terrestrial, marine, estuarine and fluvial environments. The data appears to show the tracer is robust enough to withstand exposure, across research and industry relevant, temporal scales.

The toxicity data of regularly used fluorescent dyes and the robustness / survivability of the dual-signature tracer coating indicates that following the culmination of a tracing study, the environmental impact of the dual-signature tracer remaining in the environment will be negligible. As the tracer is able to withstand extensive exposure without significant degradation and loss of fluorescent dye, at the stage where fluorescent dye is released, the particulate tracer is likely to be sufficiently dispersed and diluted. At this point, dye concentrations should be reduced to less than that of dye tracing studies, which input a dye solution directly into the environment at a concentration of ten-parts per 1000 (Stern et al., 2001) which is insufficient to create deleterious effects on the environment, ecology and human population (Smart and Laidlaw, 1977).

The results of the tracer characterisation testing indicate the tracer should uphold the fundamental characteristics of an effective active sediment tracer as outlined by Foster (2000). This demonstrates the tracer is suitable for each application proposed.

4. Field Tracing Techniques: Method Development

4.1. Tracer Recovery and Monitoring

Active sampling techniques directly sample native sediment with the aim being to determine the tracer content within the sample. Within the thesis active sampling techniques were used to sample deposited tracer from the sea bed, beach face and field. Additionally, within the suspended sediment transport application, active sampling techniques were used to sample tracer directly from the water column or water flow. Comparatively, passive sampling techniques enabled the spatial distribution or concentration of tracer to be assessed, without the requirement for active sampling techniques.

4.1.1. Active sampling

The active sampling techniques utilised throughout the thesis, included: the collection of shallow sediment cores and sediment grab (Van Veen) samples; and *in situ* magnetic sampling (Pantin, 1961b, Ventura et al., 2002, Guymer et al., 2010, Collins et al., 2013a). *In situ* magnetic sampling only samples iron or Fe-bearing materials. Within the suspended sediment transport study, high-field permanent bar magnets (11000 gauss) were deployed directly in the water column on float moorings, and attached to infrastructure to capture passing tracer (Koch et al., 2013, Black et al., 2013) (Figure 13). The magnets were deployed with a slim fitting sheath which is removable, enabling material captured by the magnet to be sampled, *in situ* (Black, 2012).



Figure 13. Photo of a high field permanent magnet (11000 gauss) saturated with dual signature tracer. The magnet was positioned within the anticipated stream flow within a suspended sediment study. Image courtesy Partrac Ltd.

4.1.2. Passive sampling

A range of passive sampling techniques were utilised throughout the thesis to gather evidence regarding the tracer content within the native sediment and spatio-temporal distribution of tracer on the sediment surface. The following sections described the techniques used.

4.1.2.1. *Magnetic susceptibility*

Magnetic susceptibility is a comparative measure of the relative ease with which a material can acquire a magnetic field, when exposed to a low or high frequency alternating magnetic field (Oldfield et al., 1981). Fe - bearing or

iron-rich particles acquire a magnetic field far more easily than non Fe-bearing particles (Oldfield et al., 1999). Susceptibility is measured using a magnetic susceptibility sensor (e.g. Bartington Instruments Ltd). Figure 14 shows a positive correlation between tracer mass (g) and low frequency susceptibility. This semi-quantitative method for measuring tracer concentration in sediments and soils (Van Der Post et al., 1995) enables the rapid determination of the spatial distribution of tracer (Guzman et al., 2013) (Figure 15).

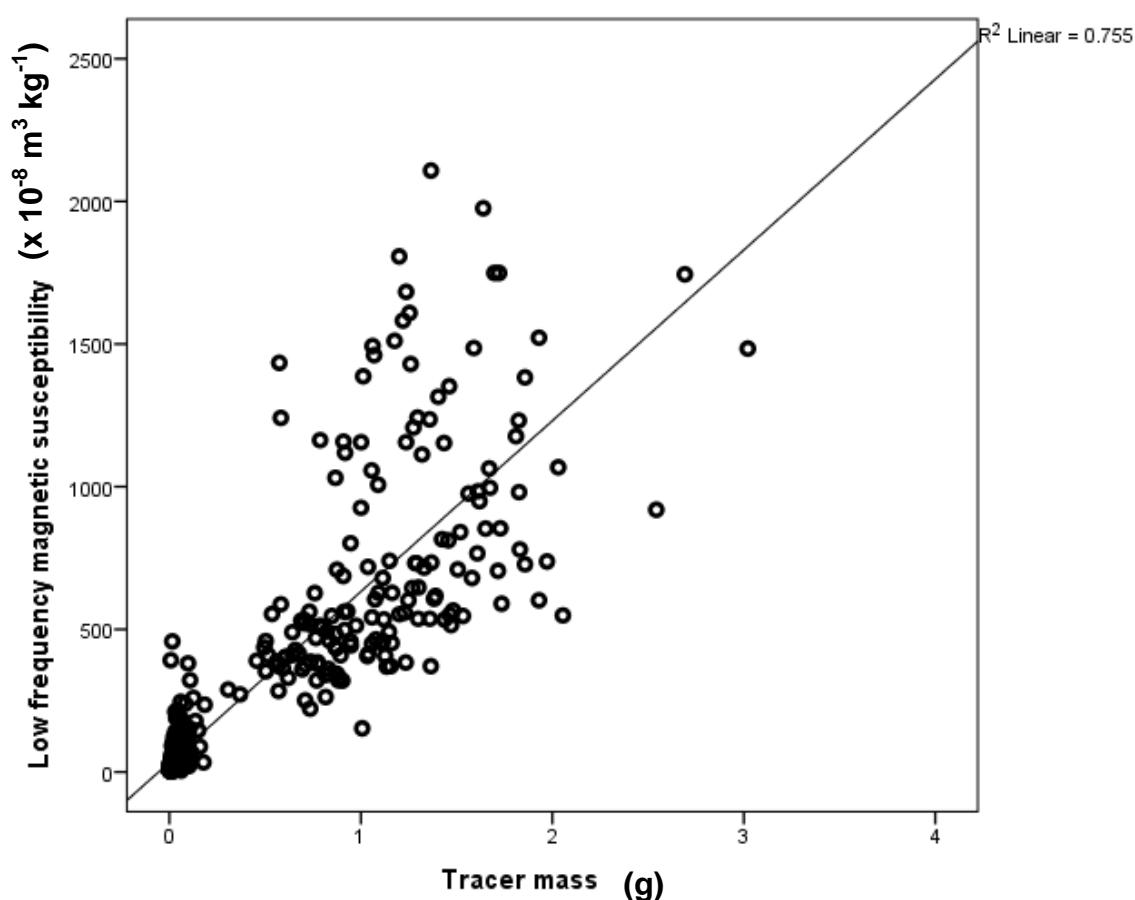


Figure 14. A plot of the dry tracer mass (g) recovered from a shallow soil core vs. the low frequency volume magnetic susceptibility of the core measured using an MS2K high resolution surface sensor. The operating frequency was 0.58 KHz, the area of response was 25.4 mm full-width, half maximum, depth of response was 50 % at 3 mm, and 10 % at 8 mm, (Bartington Instruments Ltd, UK).

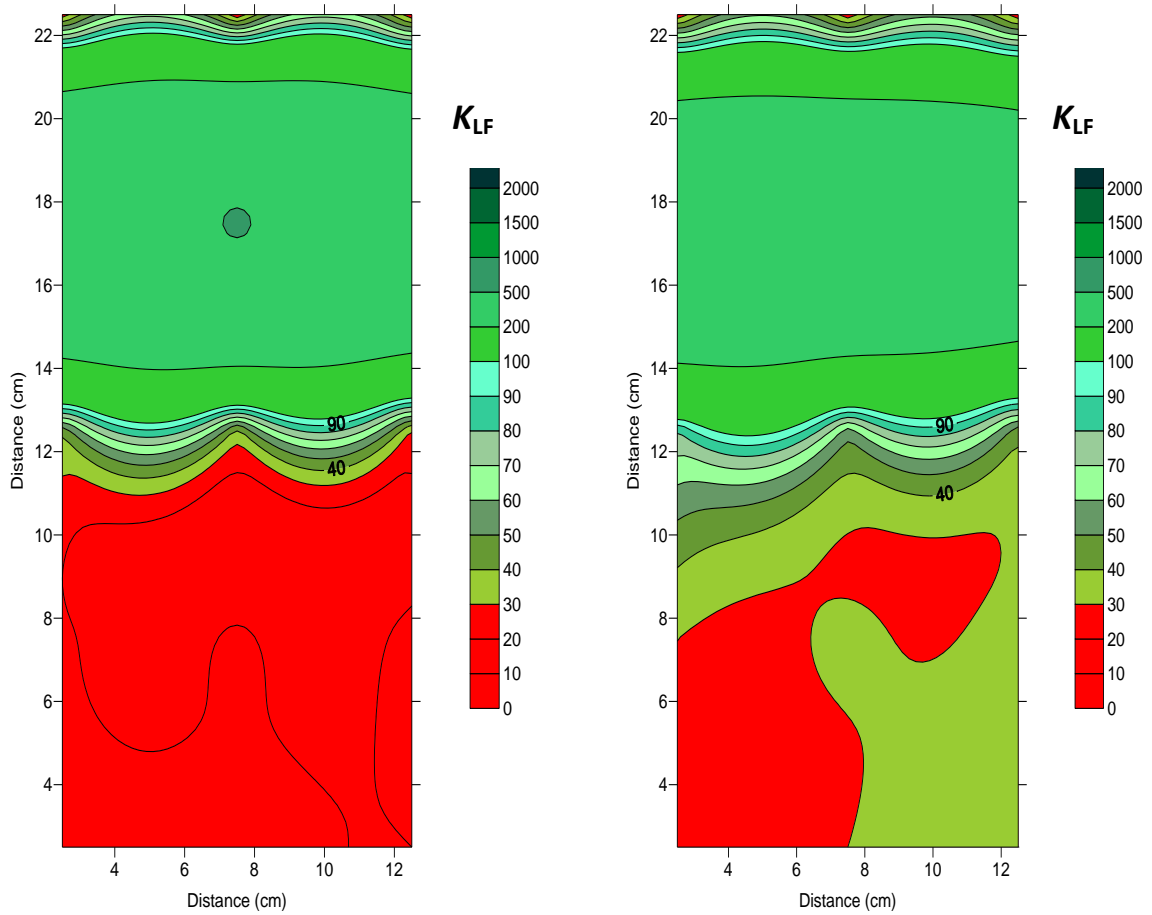


Figure 15. An example of the presentation of magnetic susceptibility (K_{LF}) data. The data represents the soil surface post tracer deployment, pre simulated rainfall event (left) and post simulated rainfall event (right) when a coarse tracer (500 – 950 microns) was deployed in a soil box for typical experiments. The tracer deployment zone is centred on 17.5 cm. The magnetic susceptibility of the surface was measured using a MS2K high resolution surface sensor. The operating frequency was 0.58 KhZ, the area of response was 25.4 mm full-width, half maximum, depth of response was 50 % at 3 mm, and 10 % at 8 mm, (Bartington Instruments Ltd, UK).

4.1.2.2. *In situ* fluorimeters

Within the suspended sediment transport study, an *in situ* fluorimeter was used to detect the fluorescent emission of the cloud of suspended tracer particles as they pass the sensor e.g. Guymer et al. (2010). Following calibration of the instrument in the laboratory, the estimated tracer concentration ($\mu\text{g} / \text{l}$) beneath the fluorimeter was determined.

4.1.2.3. *Night-time fluorescence*

The spectral characteristics of the tracer enabled identification of the tracer particles within the environment using a blue light torch (emitting wavelength 395 nm). Using these torches, at night, the spatial distribution of tracer on the sediment surface was visually assessed e.g. Ciavola et al. (1998), Russell (1960a), Silva et al. (2007), Carrasco et al. (2013), Vila-Concejo et al. (2004a), and an image captured e.g. Tauro et al. (2010), Solan et al. (2004) (Figure 16). During each tracing study where night time fluorescence inspections were utilised, a sampling diary was kept. Each diary entry provided a qualitative description of the observed spatial distribution of tracer particles on the sediment surface.

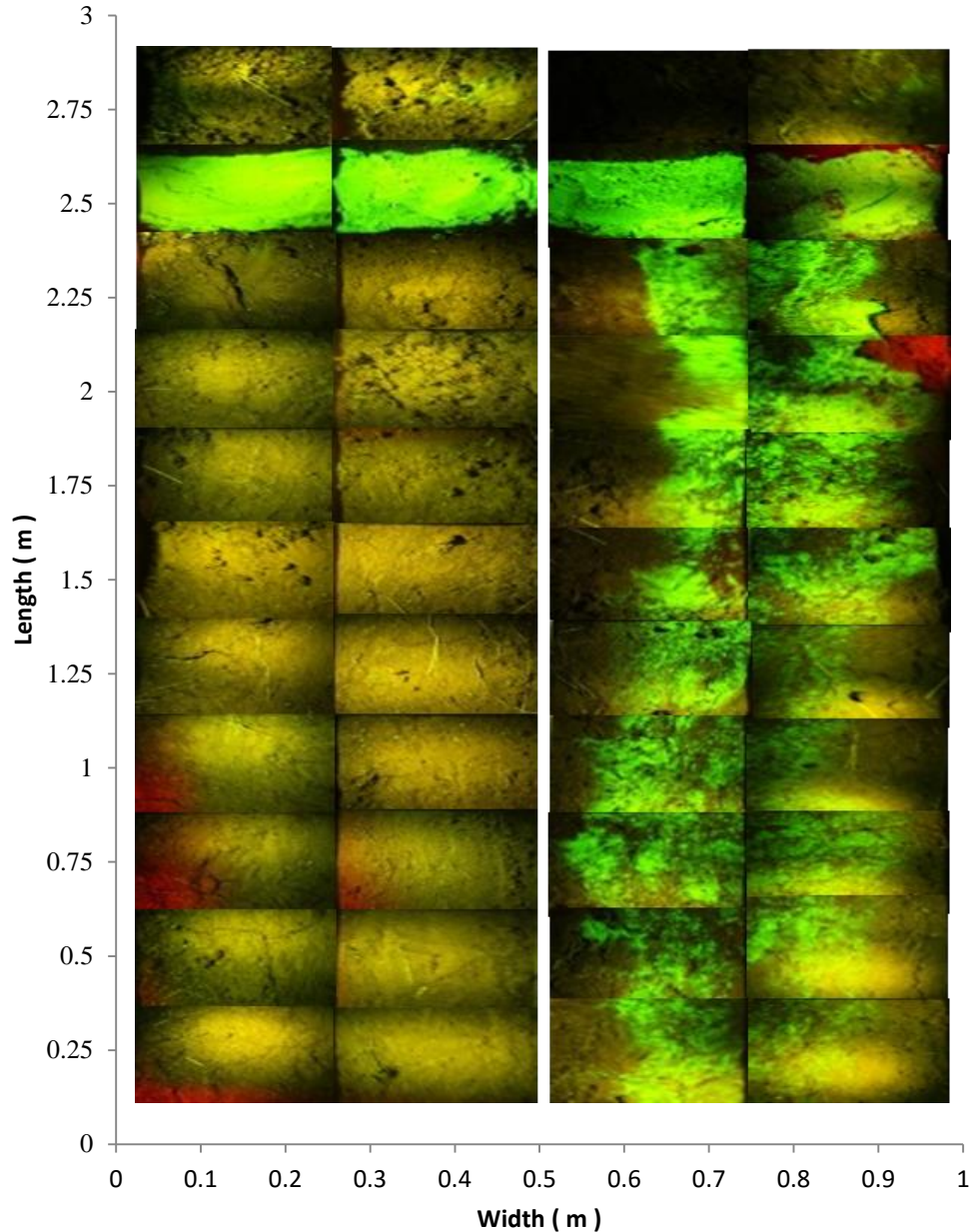


Figure 16. An example of night time fluorescence. These photo mosaics show the soil surface of an erosion plot (2.75 m x 0.5 m) with a slope angle of 7 %. A 300 L water butt positioned directly above the plots, through hoses, supplied water to the plot. The water was delivered through poly-vinyl chloride pipe with 8 holes, located 6 cm apart. Finally, the water was passed through a plastic mesh to create droplets. The simulated overland flow event had a flow rate of 8 L/min and lasted 30 mins. The plot was photographed under blue light (395 nm) illumination, post tracer deployment, pre – overland flow event (left), and post overland flow event (right). The tracer deployment zone was centred on 2.5 m. Each image captured a 25 x 25 cm spatial area, defined by a quadrat placed on the soil surface using a 750D Digital SLR (Canon Ltd), fitted with a 50 mm lens shot through a yellow dichroic filter.

4.2. Tracer Recovery: Magnetic Separation

Within each tracing application, environmental samples were collected and analysed to determine tracer content. To determine tracer content a magnetic separation method was used (Pantin, 1961b, Black et al., 2013, Ventura et al., 2002). Each sample was dried in an oven at 105 °C for 24 hours, then transferred to a pestle and mortar and gently disaggregated. The sample was then spread to an approximately granular monolayer on a large piece of white card board and a permanent, 11,000 Gauss magnet, was scanned across the sample at a distance of 2-3 mm, facilitating separation of magnetic particles from the native (non-magnetic sediment load). This procedure was repeated, with intermittent cleaning, until no further magnetic particles were extracted. Magnetic particles were recovered by simply removing the plastic sheath from the surface of the magnet. The magnetic particles were then weighed. It is critical to determine empirically the tracer extraction efficiency for each application. Where background, non-fluorescent, magnetic material was present within the sample, the tracer dry mass content could not be determined by simply weighing the recovered magnetic particles. In this scenario a spectrofluorometric method was used to determine tracer content.

4.3. Tracer Enumeration: Spectrofluorometric Method

The ultimate aim of any study is to locate, and enumerate, the dry mass (M , g) of tracer in each sample. The method chosen is a modification of a spectrofluorometric method (Carey, 1989, Farinato and Kraus, 1980). The dye pigment of coated mineral (and polymeric) fluorescent tracers can be extracted from the particles using a solvent. Consequently, if fluorescent particles and native (non-fluorescent) sediment is mixed within a sample, the dye pigment of the tracer can be extracted from the particles and measured. Carey (1989) found that analysis of the fluorescent intensity of the eluted (extracted) solution at certain wavelengths is proportional to the number of particles and thus also to the concentration of fluorescent pigments within the sample. Under certain circumstances the relationship between concentration and intensity is linear (Gunn, 1963), and the fluorescence intensity can be

proportioned to dry mass (M , g) of fluorescent tracer particles within the sample.

The analytical method utilised a fluorimeter to measure the intensity and wavelength distribution of emitted radiation after excitation by a certain spectrum (wavelength) of light. It is hypothesised that this methodology, has the potential to increase the utility of tracing studies by reducing analytical timescales and the associated costs (and hence allowing for a greater number of samples to be analysed within a given budget). Further, it has the potential to increase the flexibility of the fluorescent tracing technique by measuring two different tracer colours in one sample.

The enumeration technique to determine the dry mass of tracer within an environmental sample containing either one or two colour tracer particles was developed using *chartreuse* and *pink* tracer colours. The two colours were selected, as although their respective absorption (excitation) spectra overlap, importantly, there is no spectral overlap between the peaks of the respective emission spectra, within the electromagnetic radiation frequency spectrum (Figure 17). To measure the fluorescent emission of the sample, two fluorimeters, were used (Chelsea Technologies Group, UK). The fluorescein probe, employed to detect *Chartreuse* tracer particles was configured to excite fluorescence at 470 nm and collect emission at 530 nm. The rhodamine probe employed to detect the *Pink* tracer particles is configured to excite fluorescence at 530 nm and collect emission at 625 nm (Figure 17).

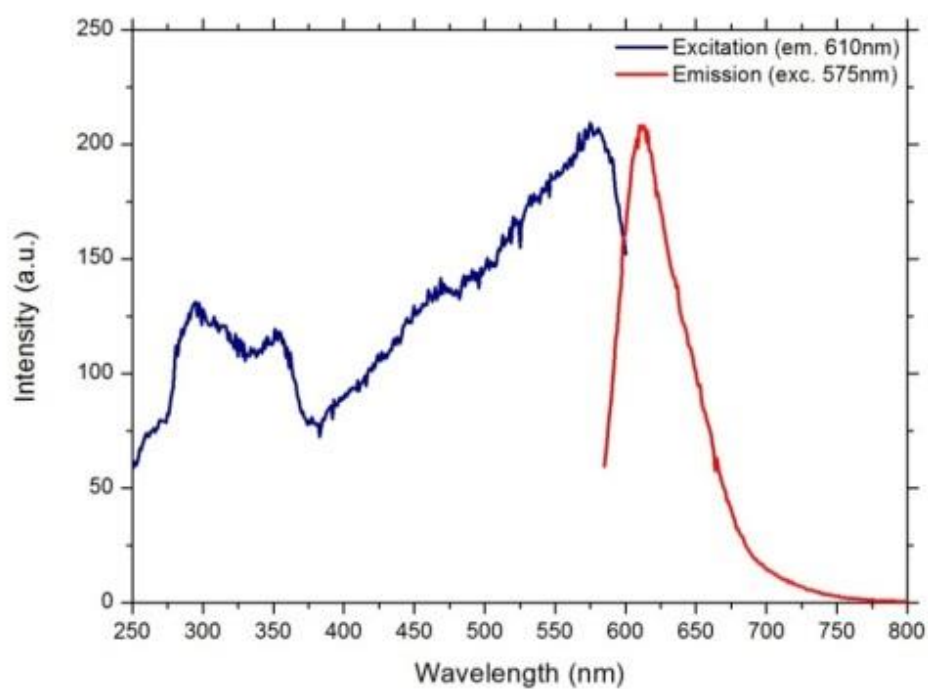
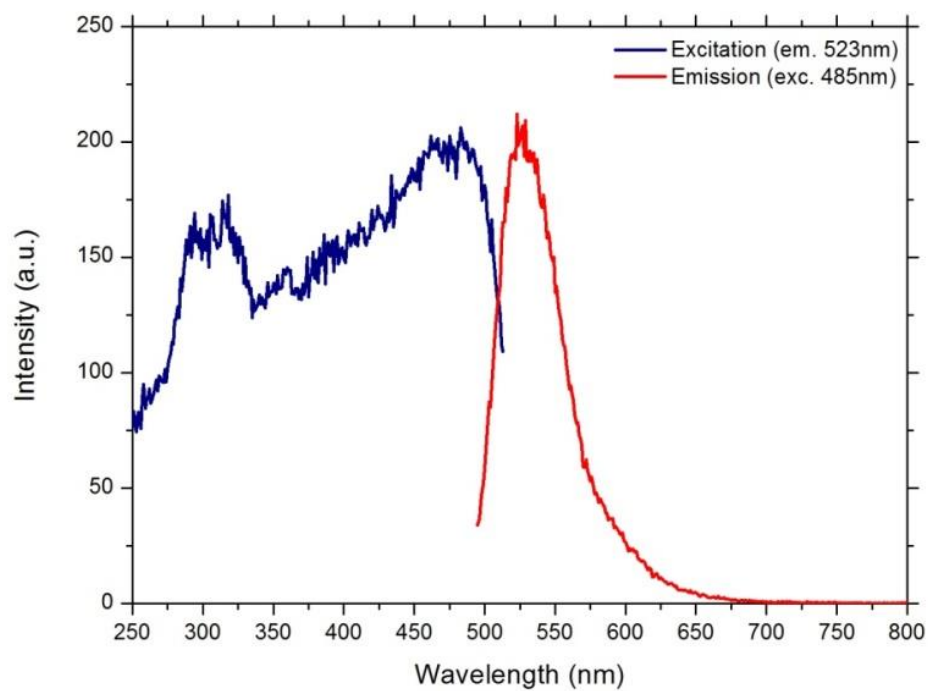


Figure 17. The emission-excitation spectra for the chartreuse tracer pigment (top) and the pink tracer pigment (bottom). The peak excitation and emission wavelengths are noted.

4.3.1. Calibration curves

Three dose response curves, otherwise known as calibration curves, consisting of plots of fluorescence intensity vs. assumed dye concentration were developed (Figure 18 and 19). These calibration curves were developed to empirically relate fluorimetric measurements (probe reading in volts) to tracer dye concentration (i.e. the concentration of dye following solvent elution) over the range of dry masses (0 – 1 g). These graphs depict the response of two colours of the same size fraction (60-100 microns in size). These calibration curves were created from a single dye solution prepared by adding a known dry mass of tracer particles (0.1 g) to 10 ml of solvent in an Eppendorf tube, mixing and then allowing the solution to equilibrate for 7 days in the refrigerator. Following this, 200 μ l of the eluted dye solution was then mixed with 2 ml of HPLC analytical grade solvent (a dilution of 1 in 10) to create a stock solution (optically dilute solution). Dose response curves were obtained by filling the measurement vial of the fluorimeter with 75 ml of analytical grade solvent and recording a baseline, or dye zero concentration reading. To determine the baseline reading a blank was tested; blanks are solutions made up in entirely the same manner as samples but without inclusion of a sediment / tracer sample. In total, 10 sequential 20 μ l aliquots of the stock solution was then added, the sample was mixed and a reading taken. This procedure creates 10 samples of monotonically increasing dye concentration (up to 2600 mg L), which correspond to discrete tracer dry masses of 0.1, 0.2, 0.3, 0.4, 0.5, 0.6, 0.7, 0.8, 0.9 and 1.0 g (Figure 18 and 19). Approximately 20 seconds worth of raw fluorescent intensity data (volts) was recorded for each measurement using a 1 second (1 Hz) sampling rate and average and standard deviation values computed. Least-squares regression analysis (Fowler et al., 1998) was performed on the data to generate calibration functions. These graphs can be considered reference standards for each dye colour. Site and tracer specific calibration curves were determined empirically for each different application of the tracer to reduce potential sources of error.

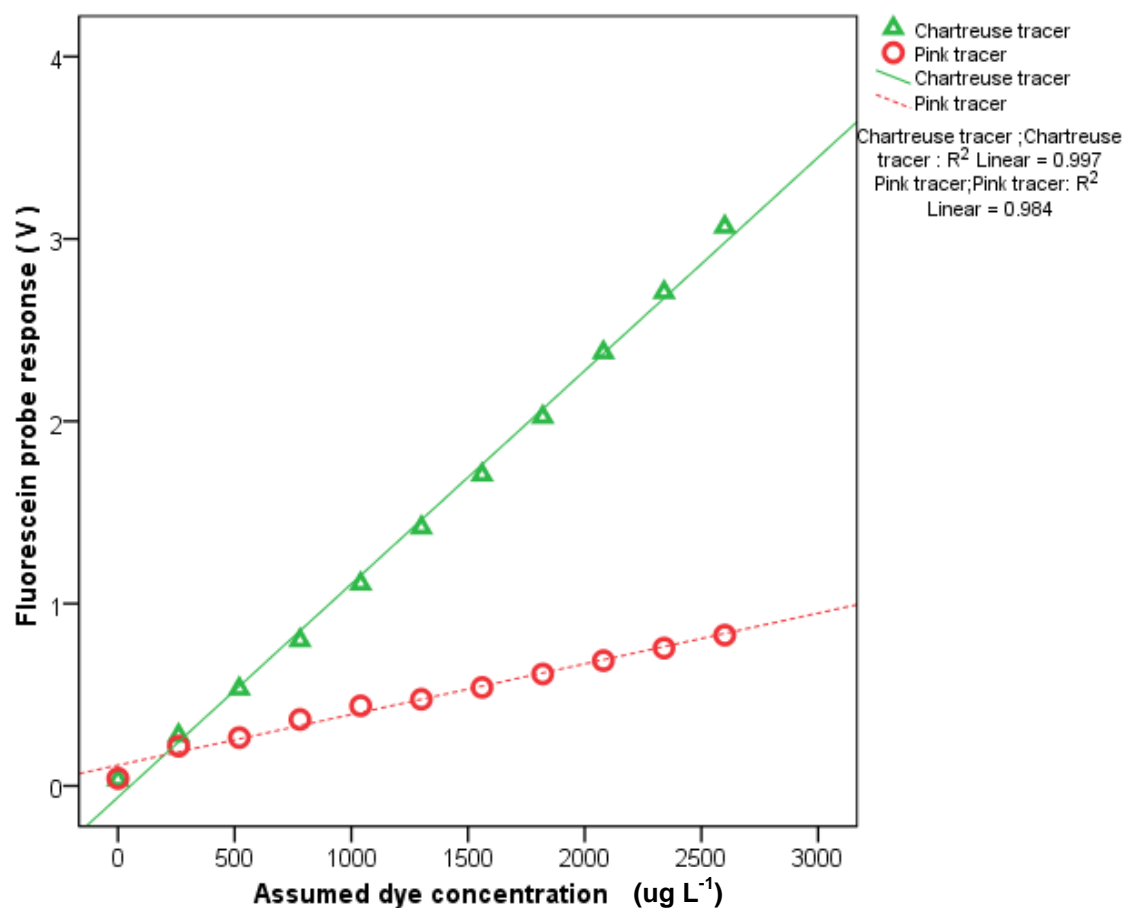


Figure 18. Dose response curves developed using the fluorescein probe to dye solutions derived from 0.1 g of *chartreuse* and *pink* tracer (60 - 100 microns in size). Each data point represents a dry mass of tracer, i.e. 0, 0.1, 0.2, 0.3, 0.4, 0.5, 0.6, 0.7, 0.8, 0.9, 1.0 g.

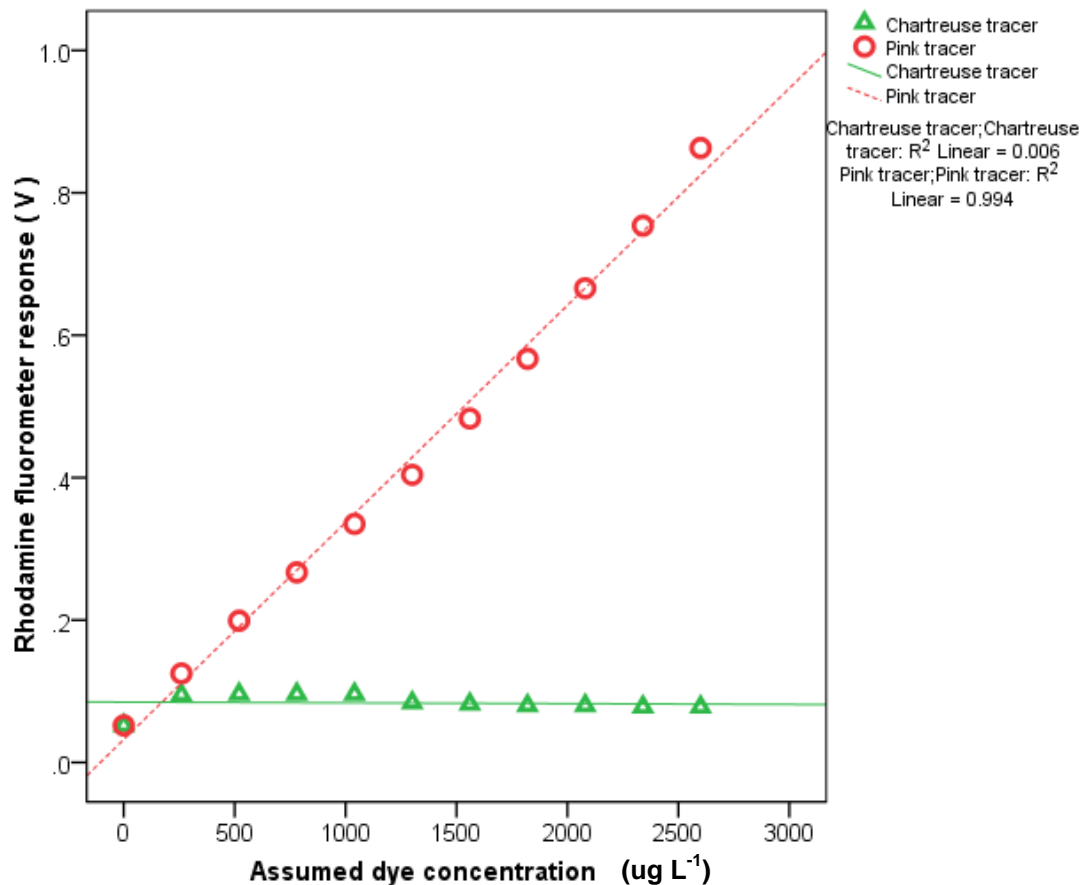


Figure 19. Dose response curves of the rhodamine probe to dye solutions derived from 0.1 g of *chartreuse* and *pink* tracer (60 - 100 microns in size). Each data point represents a dry mass of tracer, i.e. 0, 0.1, 0.2, 0.3, 0.4, 0.5, 0.6, 0.7, 0.8, 0.9, 1.0 g.

4.3.2. The determination of dye concentration in samples containing one tracer colour

To determine dye concentration (DC) in a sample containing one tracer colour, the respective regression equation was used.

4.3.3. The determination of dye concentration in samples containing two tracer colours

By using the data obtained from the dose response curves for each fluorimeter, exposed to both coloured dyes (Figure 18 and 19), it is possible to determine the respective tracer DC for two different tracer colours within one sample. Within this approach there are two simultaneous equations with two unknowns (Equation 4). These two simultaneous equations, solved algebraically generate the two unknown concentrations for both dyes:

$$S_F = SL_{FC} \times (Ch_r) + SL_{FP} \times (P_r) + O_F$$

And

$$S_R = SL_{RC} \times (Ch_r) + SL_{RP} \times (P_r) + O_R \quad (4)$$

Where, S_F is the sample signal from the fluorescein UniLux. SL_{FC} is the slope of the chartreuse dye response on the fluorescein UniLux. SL_{RC} is the slope of the chartreuse dye response on the Rhodamine UniLux. S_R is the sample signal from the rhodamine UniLux. SL_{FP} is the slope of the pink dye response on the fluorescein UniLux. SL_{RP} is the pink dye response on the rhodamine UniLux. O_F is the offset (the solvent blank signal) for the fluorescein UniLux and O_R is the offset for the rhodamine UniLux. Ch_r and P_r is the response of each probe to the sample.

4.3.4. Tracer dry mass enumeration

Once dye concentration is derived for one or two tracer colours within a sample the tracer dry mass (TDM) can then be calculated using the following equation:

$$TDM = \left(\frac{DC}{DC_{max}} \right) \times TDM_{max} \quad (5)$$

Where, DC_{max} is the maximum assumed dye concentration and TDM_{max} is the equivalent tracer dry mass value.

4.4. Method Test

A systematic series of tests were devised to assess the spectrofluorimetric technique in a logical manner and to fully characterise the methodology. Three tracers were used:

1. Chartreuse tracer, 60-100 micron size fraction (Ch_{100})
2. Pink tracer, 60-100 micron size fraction (P_{100})
3. Pink tracer, 300 micron size fraction (P_{300})

SPSS statistics 20 software (IBM 2014) was used for all analysis. The significant difference between the probe response with no background material and with the addition of background material was assessed using a

two tailed paired t- test. The percentage error (P_E) between the measured and exact tracer content value of the spiked samples was determined using the following equation:

$$P_E = \frac{M_v - E_v}{E_v} 100 \quad (6)$$

Where, M_v is the measured value and E_v is the exact value.

4.4.1. Optimal elution duration

Dissolution of dye into the solvent was hypothesised to be a time dependent, cumulative process i.e. the longer a sample was left then the greater quantity of dye would be found in the solvent. To investigate the optimal elution time of the dye pigment, from the surface of the tracer into the solvent, three samples of tracer (P_{100}) were carefully prepared at various concentrations (0.2 g, 1 g and 5 g), and the fluorescent intensity (probe response) measured 10 times over a period of 314 hours.

4.4.1.1. Results of testing

The elution of dye from the surface of tracer particles by the solvent displayed a consistent asymptotic profile through time (Figure 20) regardless of the quantity of tracer used. A steep initial increase in fluorescent emission (corresponding to greater elution rates) was observed up to ~ 100 hours, following which the elution process slows and comes to a (relative) equilibrium wherein further time does not significantly increase fluorescent emission. The time at which the fluorescent intensity is observed at > 90 % of the final fluorescent emission was determined for each concentration. This was observed at: 68 hours for 0.2 g; 95 hours for 1 g; and 220 hours for 5 g. These data indicated a minimum 7 day elution period is required to ensure sufficient time for the dye pigment to be eluted from the surface of the tracer particles.

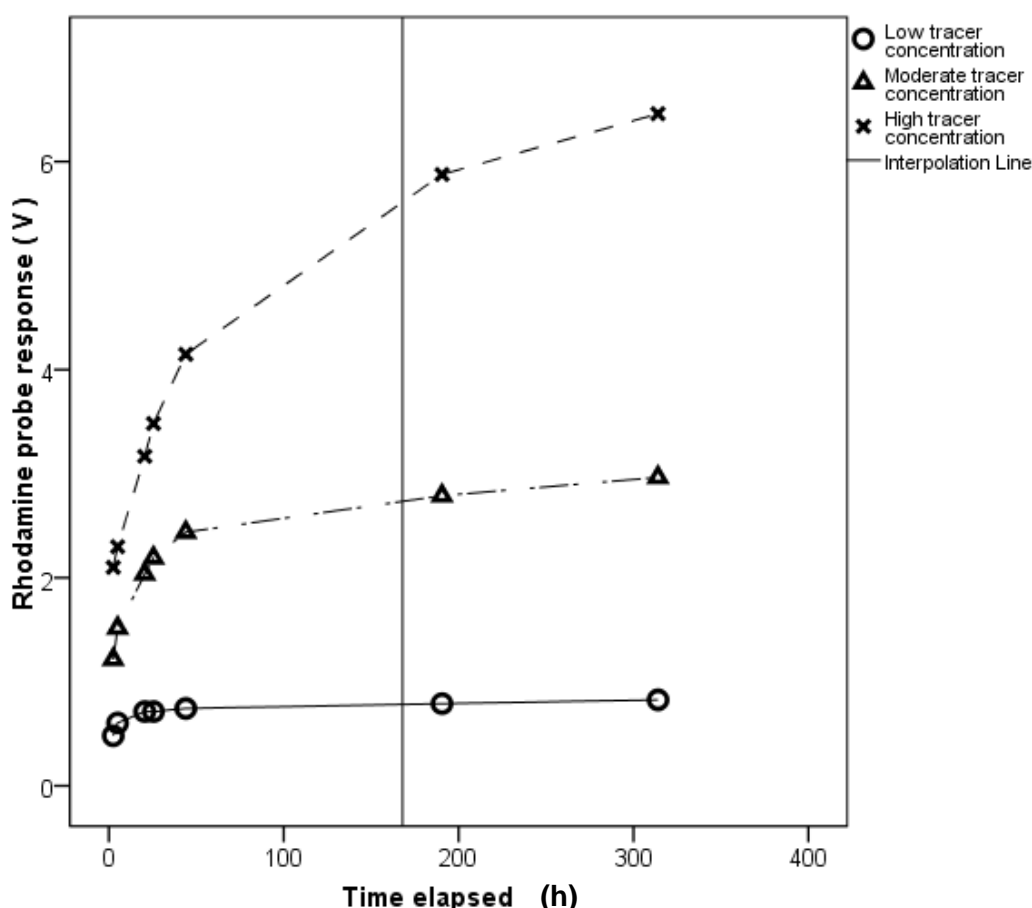


Figure 20. The response of the Rhodamine probe to dye solutions of P_{100} at low (0.2 g), intermediate (1 g) and high concentrations (5 g) over a period of 314 hours. The reference line indicates the end of the 7 day time period.

4.4.2. Instrument Test

The accuracy of the two fluorimeters was assessed. This was achieved by recording the fluorimeters response to all tracers (Ch_{100} , P_{100} and P_{300}) across a range of dye concentrations. The instrument was tested by carefully preparing 10 samples, each, of a known dry mass of tracer particles (0.025, 0.1, 0.2, 0.5, 0.75, 1 g). The fluorimeter response was then measured under controlled laboratory conditions. High accuracy was indicated by a stable value and an associated low standard deviation.

4.4.2.1. Results of testing

The testing of the accuracy of the instrument shows strong reproducibility across a range of concentrations for both the rhodamine and

fluorescein probe (Figure 21, 22 and 23). The results indicate there is a relationship between increased concentration and increased variance. Overall, high accuracy is observed, indicated by a relatively low deviation from the mean. The deviation represents the systematic error related to the use of the UniLux fluorimeters, determined at 3 - 12%.

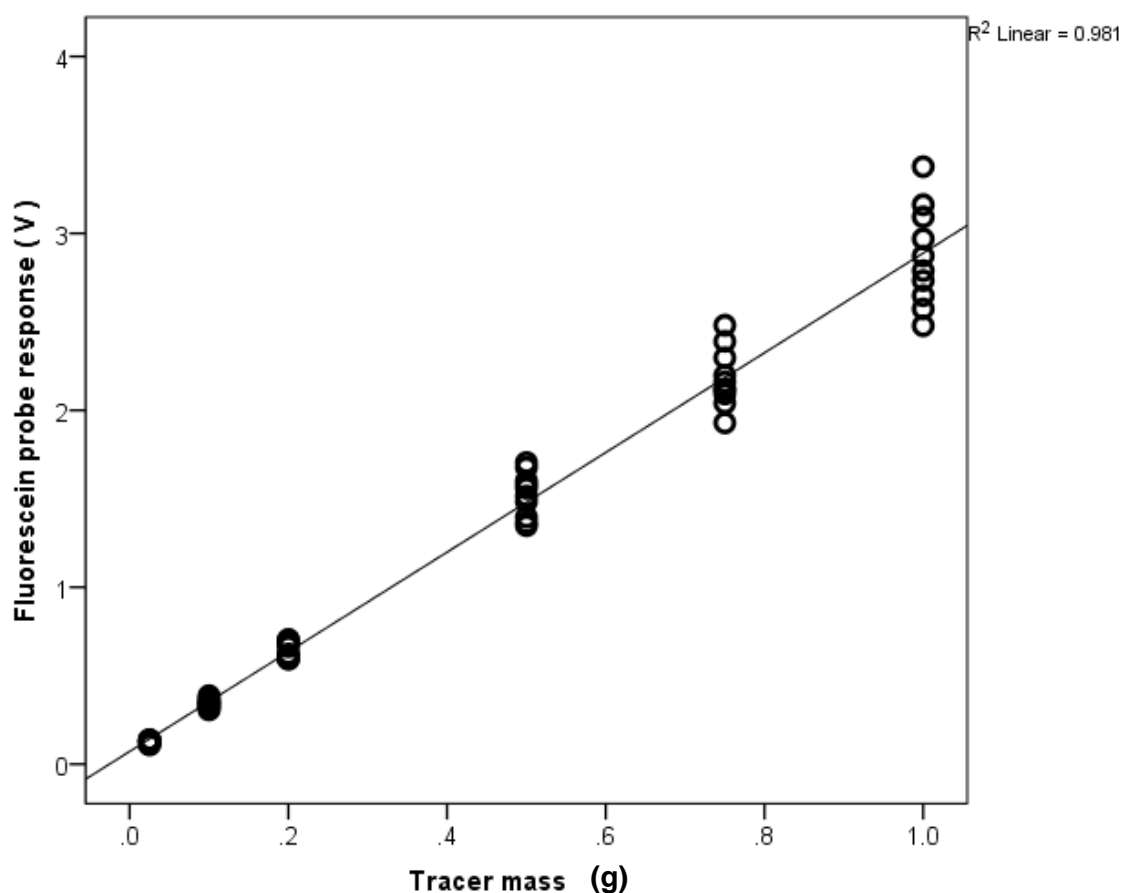


Figure 21. The fluorescein probe response (V) to increasing quantities of CH_{100} (0.025, 0.1, 0.2, 0.5, 0.75, 1 g) during the testing of the device accuracy.

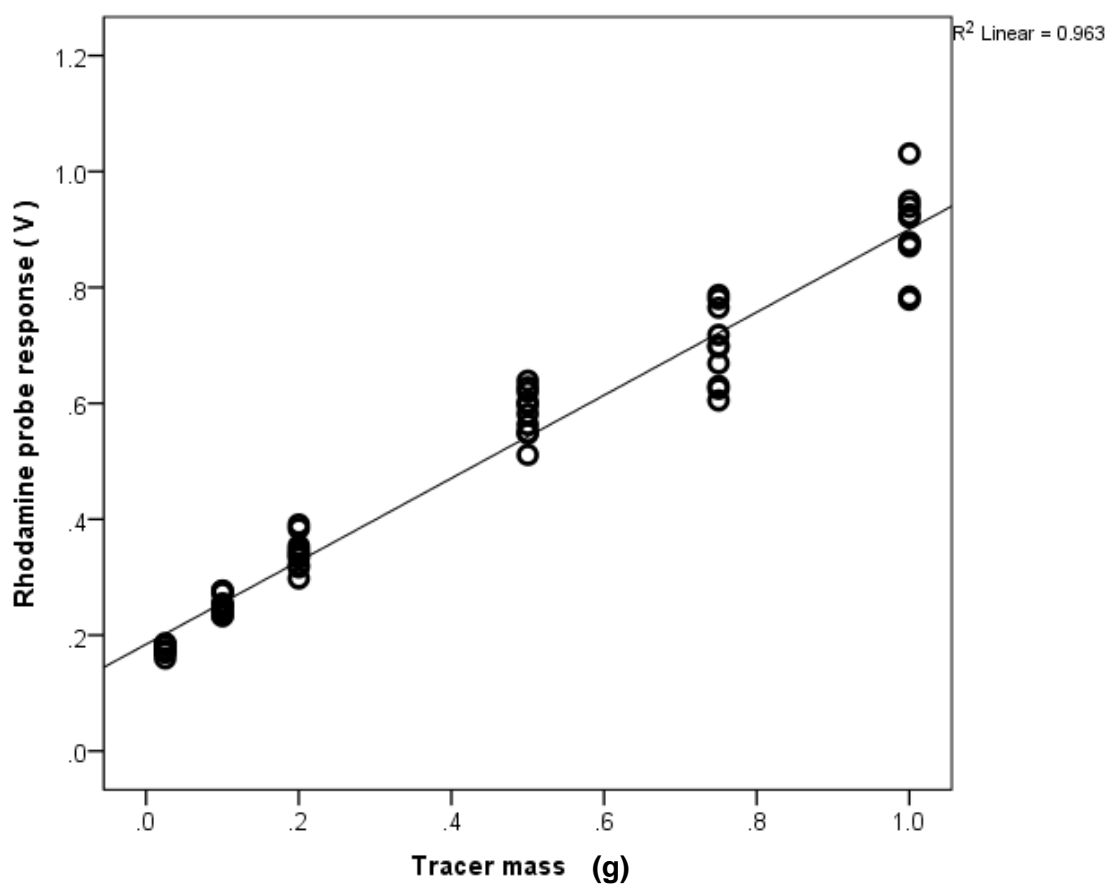


Figure 22. The rhodamine probe response (v) to increasing tracer quantities of P₁₀₀ (0.025, 0.1, 0.2, 0.5, 0.75, 1 g) during the testing of the device accuracy.

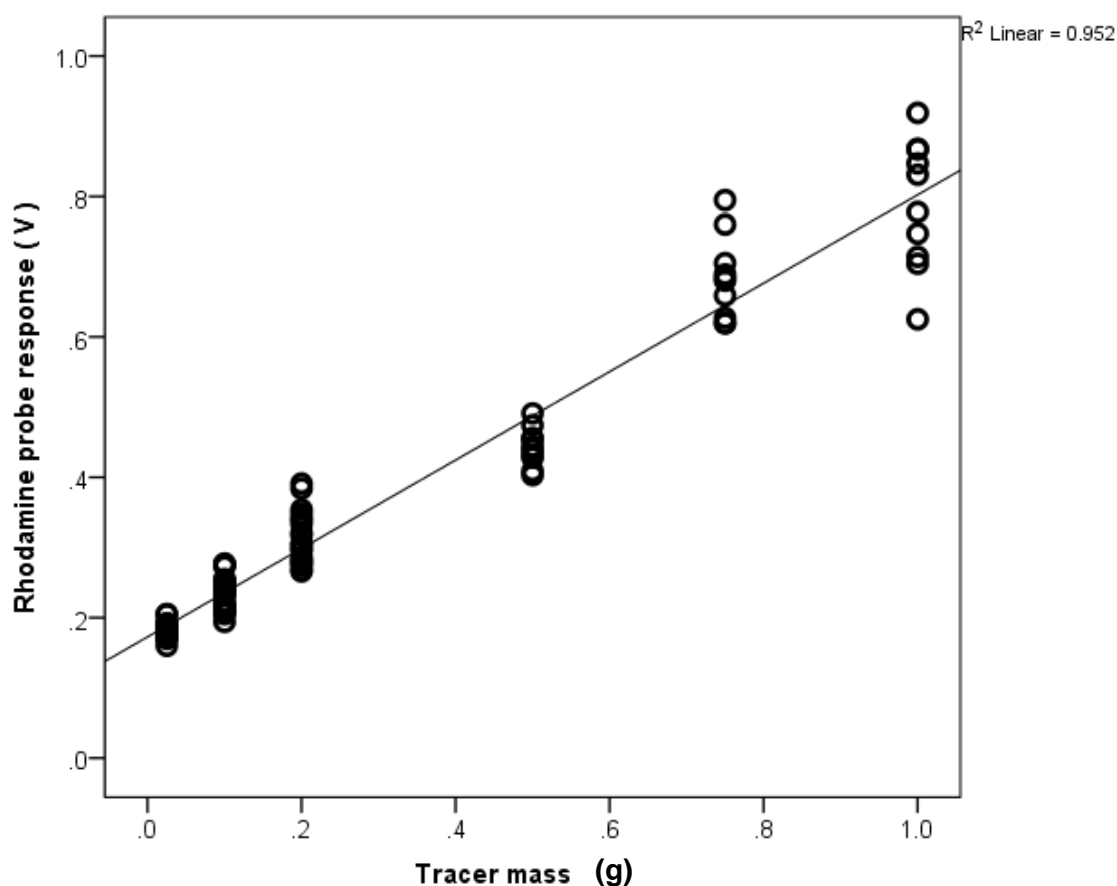


Figure 23. The rhodamine probe response (v) to increasing tracer quantities of P_{300} (0.025, 0.1, 0.2, 0.5, 0.75, 1 g) during the testing of the device accuracy.

4.4.3. The Influence of Background Material

In many environments (e.g. industrialised environments) non-fluorescent but magnetic, background material are present (Mead et al., 2013, Pearce et al., 2014). In terms of a fluorescent-magnetic tracing study, this constitutes noise, and forms undesired additional mass in samples (Black, 2012). The presence of non-fluorescent, magnetic material within the sample reduces the fluorescent emission of the tracer particles via a radiation quenching process (Lakowicz, 2006, Albani, 2008). Quenching is any process that decreases the fluorescent intensity of a sample (Lakowicz, 2006, Albani, 2008). Where non-fluorescent molecules are present within a sample, a number of external decay pathways competitively contribute to the decay of the molecules excited state, reducing the fluorescent intensity of the molecule (Eftinka and Ghiron, 1981, Ihalainen et al., 2005). Fluorescence quenching typically occurs through the mechanisms of dynamic (Wyatt et al., 1987, Eftink and Ghiron, 1976, Huber et al., 1999) or static quenching (Malliaris, 1987,

Tong et al., 2012). Dynamic quenching is observed when a fluorophore in an excited state collides with another molecule in the solution, resulting in a deactivation of the fluorophore and a return to the ground state (Lakowicz, 2006). In static quenching, complexation occurs in the ground state between the quenching molecules and the fluorophores (Geddes, 2001, Gehlen and De Schryver, 1993, Valeur and Berberan-Santos, 2012, Arik et al., 2005), resulting in the absorbed energy being dissipated by heat and only a small amount of energy being emitted by light (Lakowicz, 2006, Tyagi et al., 1998, Bernacchi and Mely, 2001). The emission of the sample is reduced as the quenching molecules reduce the number of fluorophores which can emit fluorescence (Lakowicz, 2006). This must be accounted for if accurate tracer mass values are to be established. To investigate the potential effect of background material on the fluorescent emission intensity of the eluted fluorescent dye, dose response curves were produced with different known masses of background material present (Figure 24 and 25). To simulate the effect of background material, representative environmental samples were prepared using (non-fluorescent) quarried sand (300 μm), and magnetite powder (~ 10 microns, 99.99 % purity). Dose response curves were prepared with tracer (P_{100} and P_{300}) mixed with 4 levels of background material: 1) no background material; 2) low background material (0.2 g); 3) moderate background material (2 g); and, 4) high background material (5 g),

4.4.3.1. Results of testing

Figures 24 and 25 show the presence of additional non-fluorescent mass significantly reduced ($n = 10$, $p = < 0.05$) the fluorescent emission of the sample, except when 'low' background material was added to a sample of P_{100} tracer particles ($n = 10$, $p = > 0.05$). The rhodamine probe response at the maximum dye concentration (2600 $\mu\text{g} / \text{l}$) reduced by 0% and 1%, 66% and 29% and 67% and 46% when low, moderate and high background material were added to samples of P_{300} and P_{100} tracer particles, respectively. The reduction in fluorescent emission is due to static quenching demonstrated by the linear result observed (Figure 24 and 25). A non-fluorescent complex is being formed by the dye solution and the non-fluorescent native material (Steiner and Kubota, 1983, Papadopoulou et al.,

2005) due to hydrophobic and electrostatic effects causing the dye and quencher molecules to stack together (Johansson, 2006). These unique properties were able to be effectively calibrated. This technique of creating the calibration curves using the native background material effectively obviates the problems associated with fluorimetric analysis where significant background material is present. This was tested and the results confirmed the use of this as a suitable methodology to generate revised calibration curves. Due to the broad application of fluorescent tracing studies significant variation in the make-up of background material is highly likely e.g. the background material in an estuary will differ to that found on a sandy beach or within an agricultural field (Droppo, 2001). Thus, it is important the empirical coefficient is determined using material native to the site, study area or area of interest.

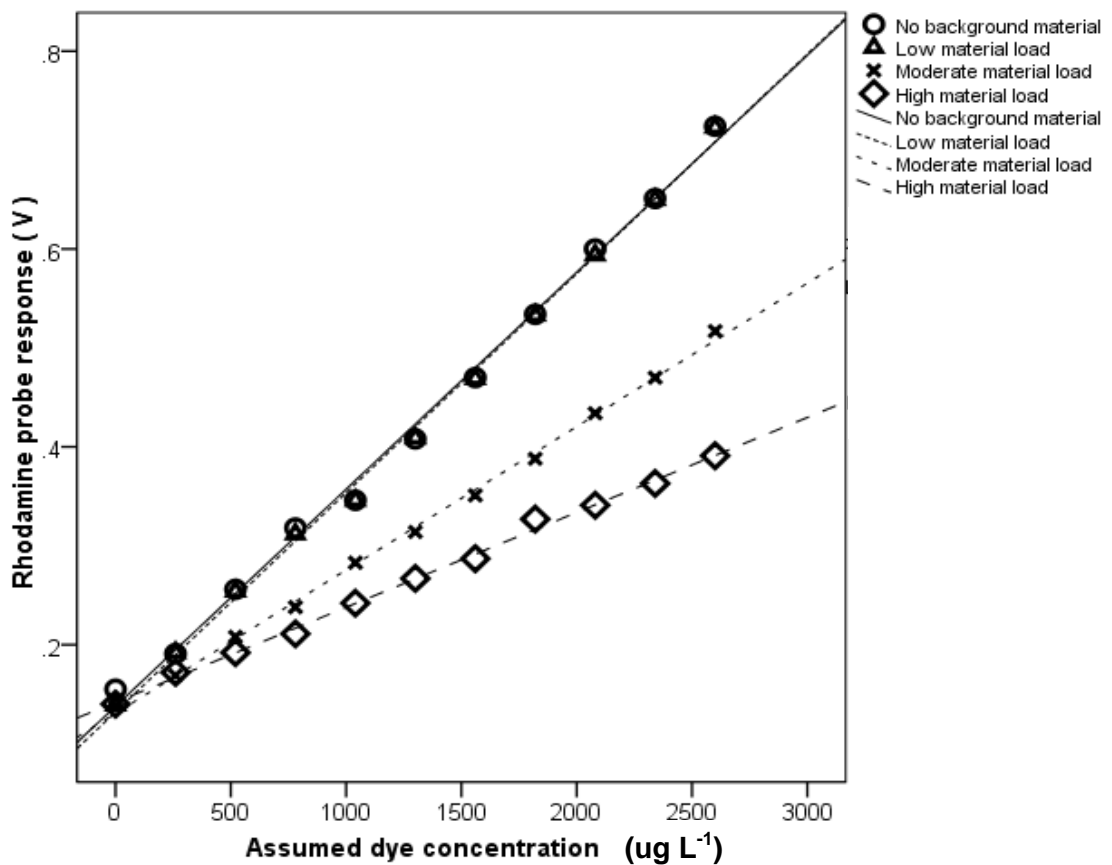


Figure 24. dose response curves depicting the responses of P_{100} tracer particles of the same concentration with different levels of background material present i.e. none, low = 0.1 g, moderate = 1.0 g and high = 5.0 g. Each data point represents a dry mass of tracer, i.e. 0, 0.1, 0.2, 0.3, 0.4, 0.5, 0.6, 0.7, 0.8, 0.9, 1.0 g.

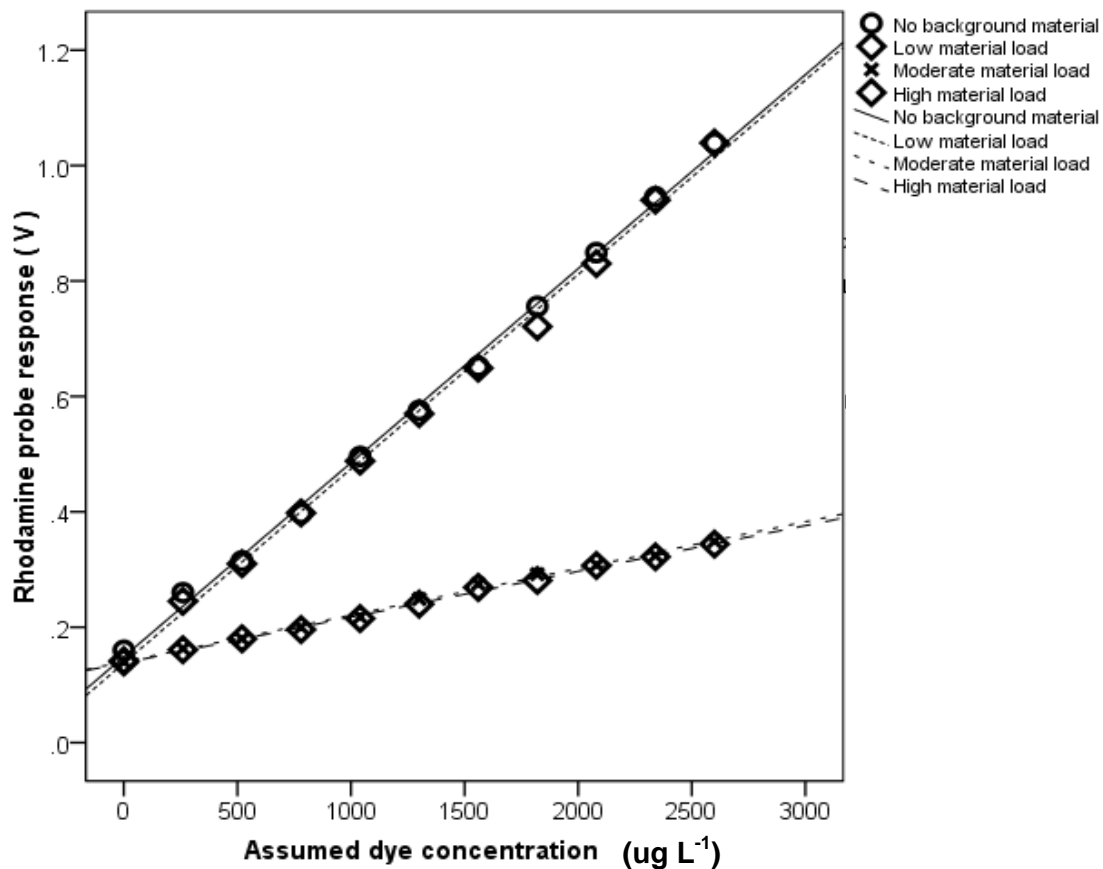


Figure 25. dose response curves depicting the responses of P_{300} tracer particles of the same concentration with different levels of background material present i.e. none, low = 0.1 g, moderate = 1.0 g and high = 5.0 g. Each data point represents a dry mass of tracer, i.e. 0, 0.1, 0.2, 0.3, 0.4, 0.5, 0.6, 0.7, 0.8, 0.9, 1.0 g.

4.4.4. Spiked environmental samples

Environmental samples spiked with varying quantities of both one and two tracer colours were prepared to investigate the methodological accuracy (i.e. the difference between measured tracer content and known tracer content). To do this, 64 samples were prepared, 40 without background material present and 24 with background material present, variously mixed with single or two tracer colours (P_{100} and Ch_{100}). Each set of samples that were mixed with background material were separated into triplicates of 4 and mixed with low background material (0.2 g), moderate background material (2 g) and high background material (5 g). The tracer content values of each spiked sample were unknown to the person who undertook the measurements and analysis. Calibration curves were developed empirically to account for the experimental and environmental conditions at the time of testing. The calculated value of the sample was statistically compared to the measured value using a two tailed paired t test, and the percentage error and standard deviation determined.

4.4.4.1. Results of testing

A significant difference was observed between the known and measured value of spiked samples containing one and two tracer colours. Where samples had no additional background material added, the mean percentage error between the known and measured value where one tracer colour was present within the sample was $19 \pm 13 \%$ ($n = 19$, $p = < 0.05$), and $6 \pm 5 \%$ ($n = 19$, $p < 0.05$) for the rhodamine and fluorescein probes respectively (Figure 26). The mean percentage error where two tracer colours were present within the sample was $26 \pm 9 \%$ ($n = 19$, $p < 0.05$), and $29 \pm 8 \%$ ($n = 19$, $p < 0.05$) for the rhodamine probe and fluorescein probe respectively (Figure 27).

Where samples had various quantities of background material present within the sample a significant difference was observed between the known and measured value of spiked samples containing one tracer colour, with background material present when using the rhodamine probe. No significant difference was observed when using the fluorescein probe. The mean percentage error between the known and measured value was $16 \pm 12 \%$ (n

11, $p < 0.05$), and $11 \pm 6 \%$ ($n = 11$, $p > 0.05$) for the rhodamine probe and fluorescein probe respectively (Figure 28). A significant difference was observed between the known and measured value of spiked samples containing two tracer colours with background material present in the sample. The mean percentage error was $25 \pm 15 \%$ ($n = 11$, $p < 0.05$), and $19 \pm 11 \%$ ($n = 11$, $p < 0.05$) for the rhodamine probe and fluorescein probe respectively (Figure 29). Table 5 provides an overview of the results of the spiked sample analysis of both samples with no background material present and samples with background material present, containing one and two tracer colours.

A methodological bias of $\pm 20 \%$ for single colour sample analysis and $\pm 30 \%$ for two colour sample analysis has been quantified from the percentage error and standard deviation. An experienced technician is able to analyse 150 - 200 mono colour samples and 75 - 150 dual colour samples per day (8 hours). This analytical method can be used in combination with a variety of fluorescent marking and labelling techniques (including polymers), and adapted to a range of fluorescence sensing technologies.

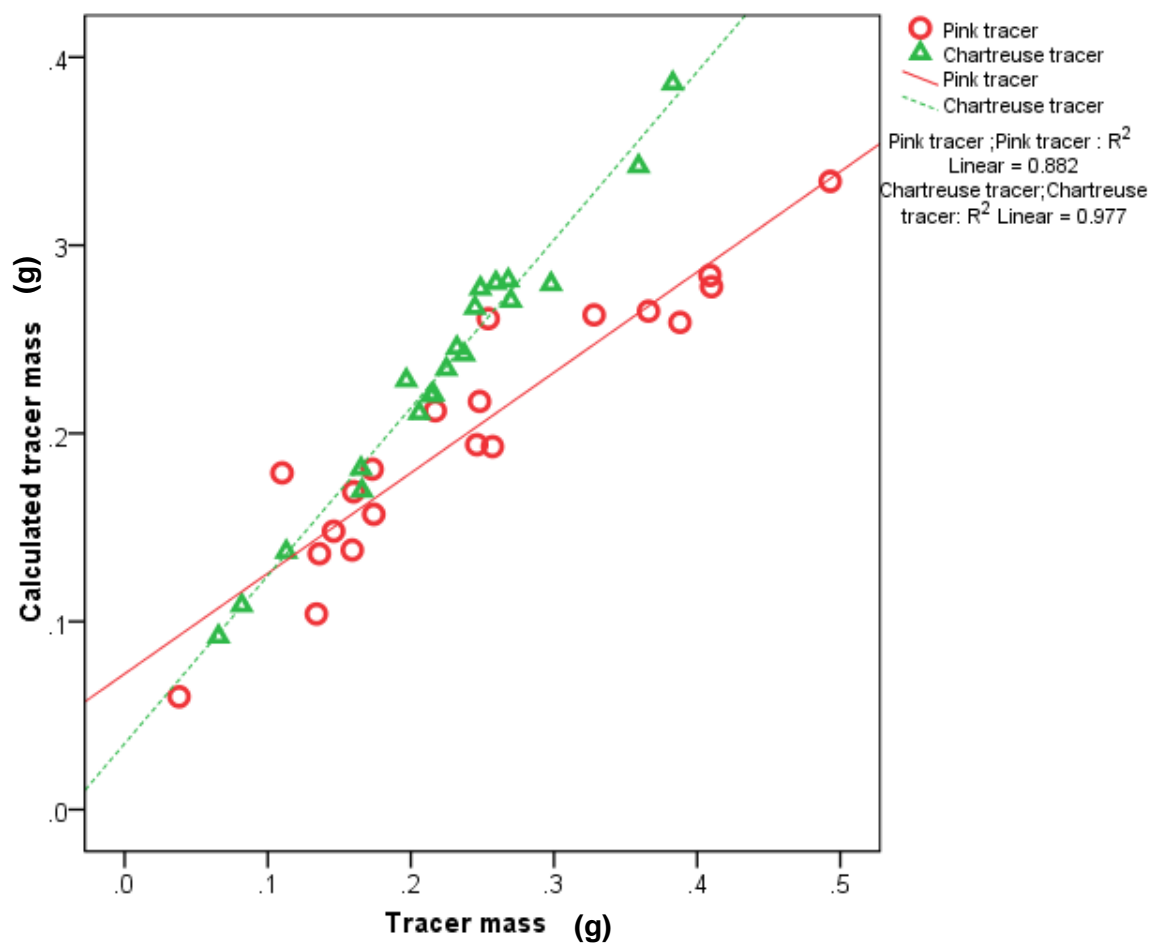


Figure 26. Tracer mass Vs. calculated tracer mass for samples with one tracer colour, either pink or chartreuse, derived from the response of the rhodamine and fluorescein probes respectively.

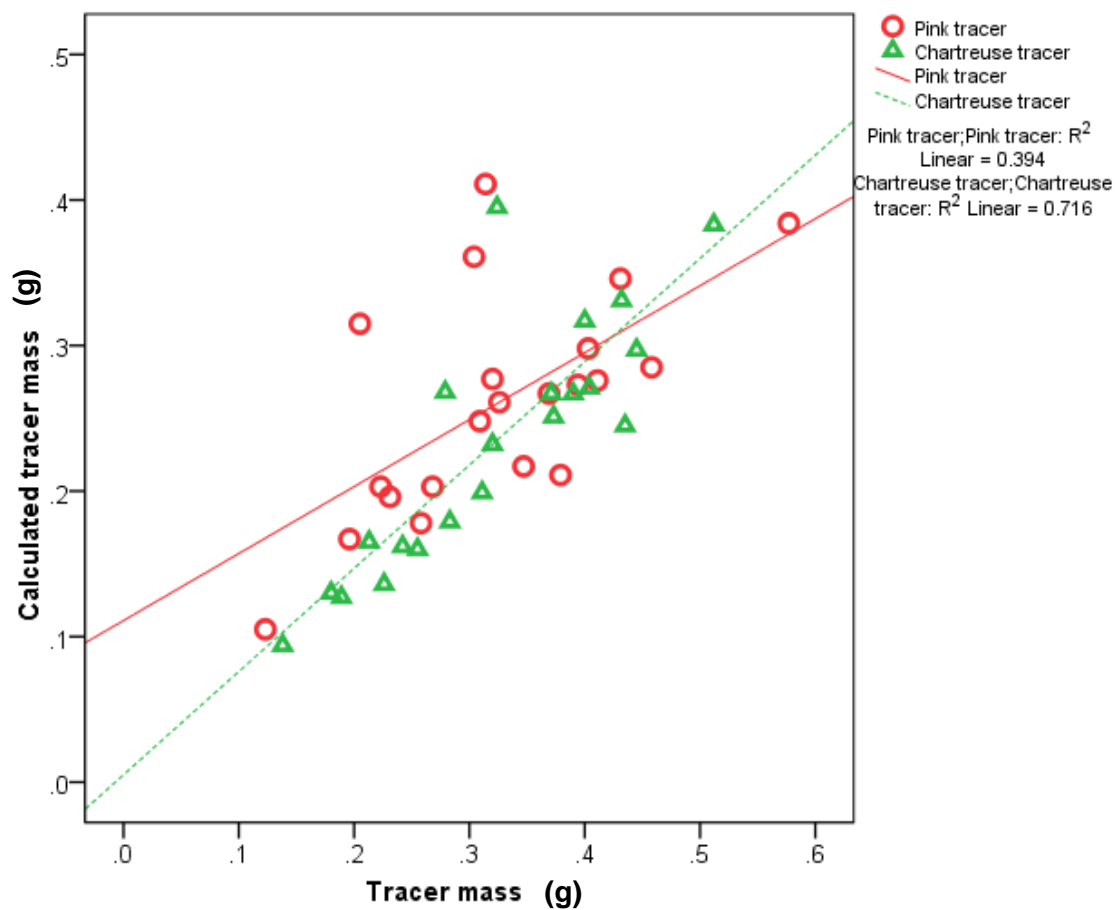


Figure 27. Tracer mass vs. calculated tracer mass for samples with two tracer colour in the sample, pink and green derived from the response of the rhodamine and fluorescein probes respectively.

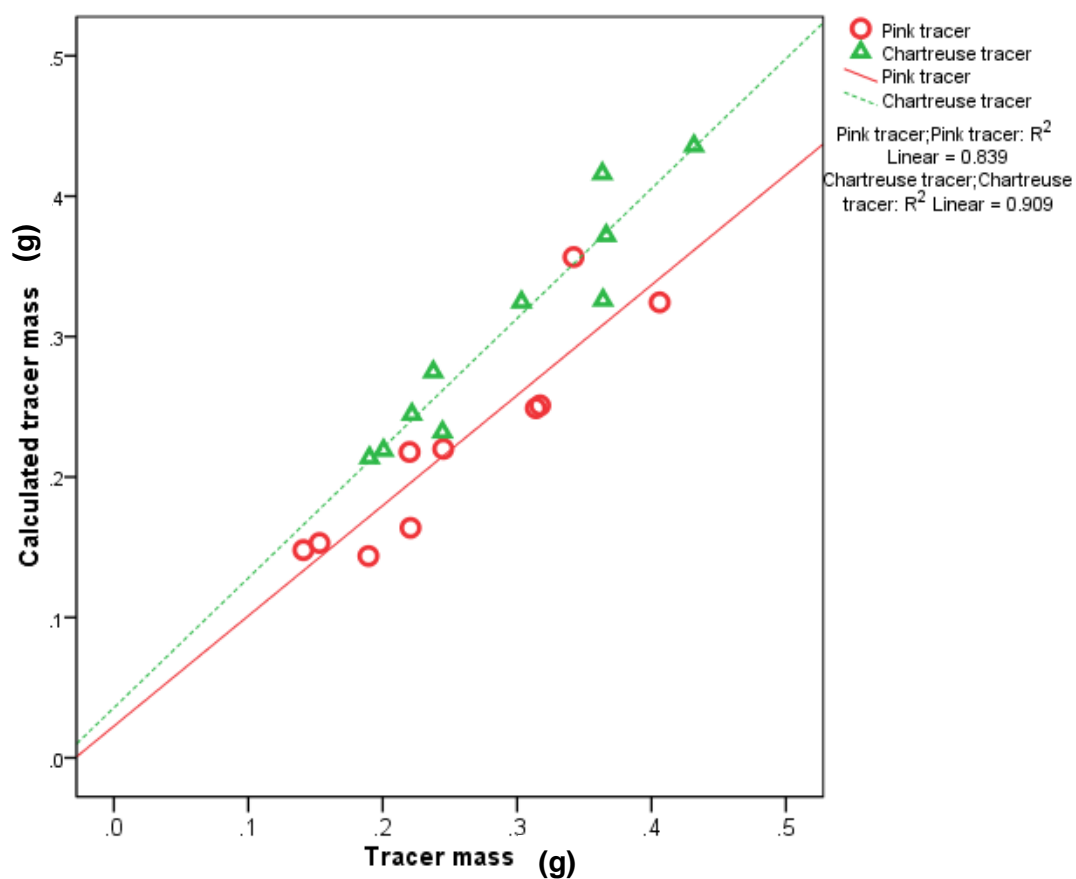


Figure 28. Tracer mass vs. calculated tracer mass for samples with one tracer colour in the sample, pink and green and mixed with: low (0.1 g); moderate (1 g); and high (5 g) background material derived from the response of the rhodamine and fluorescein probes respectively.

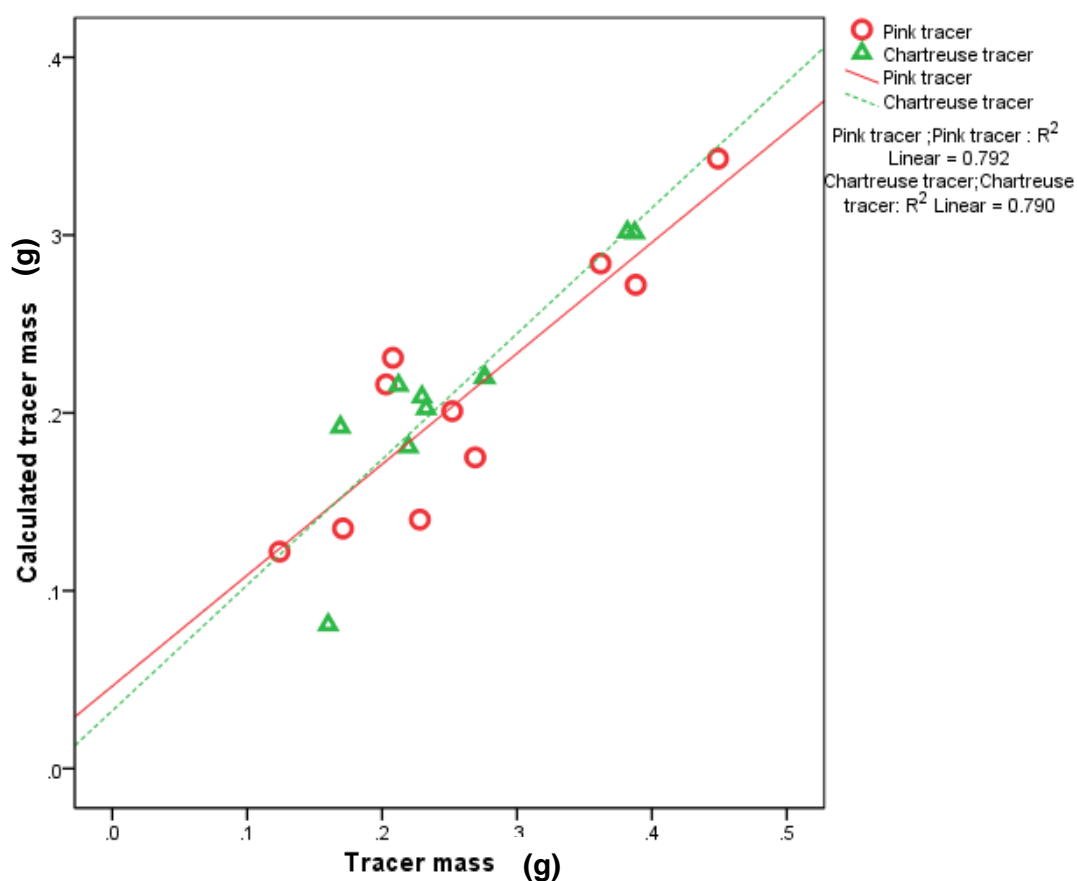


Figure 29. Tracer mass vs. calculated tracer mass for samples with two tracer colours in the sample, pink and green and mixed with: low (0.1 g); moderate (1.0 g); and high (5.0 g) background material derived from the response of the rhodamine and fluorescein probes respectively.

Table 5. The mean percentage error (Equation 6) and standard deviation between the exact tracer content and measured tracer content for the rhodamine and fluorescein probe when measuring environmental samples containing one and two tracer colours with varying quantities of background material present. The significant difference between the fluorescent response of the exposed and control tracer batches were assessed using a two tailed paired t- test. The percentage error is derived from equation 6.

Mean percentage error and standard deviation between the known mass and measured mass within an environmental sample			
<i>Single colour sample</i>			
Sample	No of samples	Fluorescein	Rhodamine
No background material	20	6% ± 5% (n 19, p < 0.05)	19% ± 13% (n 19, p < 0.05)
Background material present	12	11% ± 6% (n 11, p > 0.05)	16% ± 12% (n 11, p < 0.05)
<i>Two colour sample</i>			
No background material	20	29% ± 8% (n 19, p < 0.05)	26% ± 9% (n 19, p < 0.05)
Background material present	12	19% ± 11% (n 11, p < 0.05)	25% ± 15% (n 11, p < 0.05)

4.5. Method Development: Discussion and Concluding Remarks

The passive and active sampling techniques described, detail a range of techniques available to monitor and recover silt and coarse sized tracer particles once deployed to the environment. Having two signatures (fluorescence and ferrimagnetism) proved beneficial during the analytical process. Magnetic separation provides a quick and simple technique to determine the tracer dry mass content (mass per unit mass) within environmental samples. However, in the majority of environments naturally occurring magnetic material is present (Pearce et al., 2014). This undesired additional mass means that magnetic separation is unable to be used to determine tracer dry mass content. Despite this, where additional magnetic material is present, magnetic separation remains useful practically, as it reduces sample volume.

The spectrofluorometric analytical procedure was adapted and developed to exploit the fluorescent attribute of the tracer particles, to provide directly, the dry tracer mass (M , g). The technique has sufficient spectral resolution to distinguish low concentrations (< 0.01 g) of two spectrally unique tracer colours. The fluorescent excitation and emission wavelengths of fluorescent derivative were located at 470 nm, and 530 nm respectively for chartreuse tracer particles, and 530 nm, and 625 nm respectively for pink tracer particles. The fluorescent excitation of these derivatives are not common to materials commonly found in water (Stern et al., 2001, Wilson et al., 1986). The dye concentration was proportioned to dry mass (M , g) of fluorescent tracer particles through the use of colour specific reference standards. A methodological bias of $\pm 20\%$ for single colour sample analysis, and $\pm 30\%$ for two tracer colour sample analysis, was quantified. The observed increased error associated with the analysis of two colour spiked samples in comparison to single coloured spiked samples, indicated where high precision is required, the use of a single tracer colour is preferable. Also, the data indicates there is a greater methodological bias related to the use of the rhodamine probe in comparison to the fluorescein probe. This is attributed to the greater probe response of the fluorescein probe (fluorescein probe response @ dye concentration of $2600 \text{ ug} / \text{l} = 3.066 \text{ v}$) to the corresponding

dye concentration of the rhodamine probe (rhodamine probe response @ dye concentration of 2600 ug / l = 0.863 v). The methodological bias is considered tolerable within the sediment tracing methodology, due to the error associated with other enumeration techniques e.g. an error of 5 - 10 % was attributed by Carrasco et al. (2013) to counting fluorescent tracer grains by eye. Further, the error related to models of sediment transport are judged to be of the order of a factor of 10 (Eidsvik, 2004), reduced to a factor of 5 or better once validated (Soulsby, 1997).

The fluorometric method was validated and applied to the determination of representative environmental samples spiked with various quantities of one or two tracer colours. The representative environmental samples indicated that background material (native environmental particulates of the sample) reduced the fluorescent emission of derived dye solution due to static quenching effects by up to 67%, dependant on the quantity of background material within the sample. This was accounted for empirically by determining colour specific reference standards with known masses of representative native material. This methodology provided a relatively simple, fast and non-resource intensive approach to tracer enumeration within fluorescent tracing studies, which will potentially contribute to improvement of the general utility of the technique.

Within the spectrofluorometric technique a range of factors affect the specific coefficient of fluorescence intensity vs. tracer dry mass. Potential sources of error include: 1) human error, which can be obviated by using an experienced technician with a practical and theoretical understanding of spectrofluorimetry (Gunn, 1963); and, 2) the empirical relationship between the assumed concentrations of a sample to tracer dry mass; the homogenous mixing of the particles and the native sediment; particle size distribution and surface area of the particles; the dye loading on the surface of the individual tracer particles; and the properties of the solvent and dye pigment. These potential sources of error can be significantly reduced if the coefficient is determined empirically for each combination of conditions (Carey, 1989, Gunn, 1963).

The spectrofluorometric analytical methodology can be utilised to determine the dry mass of fluorescent tracer samples of different size fractions, and two different tracer colours separately, or concurrently. In comparison to other methods of determining the mass of fluorescent tracer particles within a sample, this is a relatively fast, reliable and low cost technique. The linear calibration lines, small variance of experimental points, and consistently high coefficients of determination (R^2) indicate the potential for high accuracy of tracer enumeration.

5. Sediment Tracing Using Active Tracers: A Guide for Practitioners.

5.1. Summary

Determining the source, pathway and fate of sediment, soil and associated contaminants, nutrients and microbes is desirable as a result of the growing environmental concern and economic consequences surrounding the movement of sediment and soil. Sediment tracing, or as it is sometimes termed 'sediment tracking', can provide qualitative and quantitative data detailing the spatial and temporal dynamics of sediment and soil particles. To date, research has predominantly focused on the effectiveness of various types of tracers, with little emphasis on how they are deployed, monitored, and recovered, and yet study outcomes are highly dependent on these factors. A generic six step methodological framework is presented for robust sediment and soil tracing developed from the analysis of existing studies. The inextricable link between tracers and the applied methodology identifies that a holistic view of the tracing methodology is required at the planning stage, to improve method development and crucially, tracer material selection. It is anticipated that this framework will be a valuable guide for practitioners and researchers interested in the practical application of sediment tracing techniques to sediment transport problems, and that it may promote the uptake or adoption of a robust, universal methodology across academic (and commercial) fields.

5.2. Introduction

Sediment tracing techniques progressed significantly in the century following the first tracing study of Richardson (1902). The technique has recovered from significant setbacks e.g. the environmental ban on the use of irradiated grains (Black et al., 2007, Sigbjornsson, 1994) and fluctuations in popularity, primarily due to the resource intensive nature of the method (White, 1998). Recent developments in tracer design and methodological approach have revived the technique. This has led to novel application and commercial enterprise within the sector (Black et al., 2013, Black, 2012, Smith et al., 2007). A number of tracers are now available to perform tracing studies. These tracers provide robust information regarding sediment dynamics in both terrestrial and fluvial (see Guzman et al. (2013) for a synthesis of the subject),

and marine and coastal environments (see Black et al. (2007) for a synthesis of the subject). Each tracer has its own benefits and limitations (Guzman et al., 2013, Black et al., 2007). Similarly, tracer-specific practical and analytical methodologies each have their own benefits and limitations. These benefits and limitations must be weighed against other tracer materials, and the appropriateness of the specific tracer for the study area (Liu et al., 2004). As tracers are now more readily available, a unified methodological approach is needed to provide consistency, given increasing application of the tracing technique to real world, sediment management problems. A robust methodological framework should provide an effective sequence of events that can be considered, regardless of choice of tracer material.

An optimal tracer is one that can be tracked, recovered from environmental samples and enumerated successfully, and which has similar properties to the native sediment (, Zhang et al., 2001, Mahler et al., 1998, Liu et al., 2004). Key assumptions that commonly introduce error into tracing studies include:

- I. The tracer's hydraulic and bio-organic properties closely match those of the native sediment such that the tracer is transported in the same manner as the native sediment.
- II. The tracer properties are stable and do not change through time.
- III. Introduction of the tracer does not disrupt the transporting system.

It is essential that these assumptions are acknowledged, tested and the results considered in the light of potential effects on sediment transport dynamics (Foster, 2000).

Historically, tracing studies were somewhat crude in nature, utilising tracer that violated the three key assumptions outlined above (Pantin, 1961, Lee et al., 2007b, Shinohara et al., 1958, Kidson and Carr, 1961, Dobbs, 1958). Modern technological advances have resulted in the development of tracers which do not violate the above precepts. This has led to an increase in the validity of the technique. However, such tracers still need to be applied using a clear, defined methodological framework.

The aim of this article is to develop a generic sediment tracing methodological framework, applicable regardless of environment and context. The framework is focused on 'active' tracers (i.e. where a tracer is actively introduced or injected into an environment) and not on approaches that use the natural 'signature' of native particles, such as 'sediment source ascription' or 'sediment fingerprinting' e.g. Foster (2000), nor those which utilise the presence of anthropogenic radioactive fallout e.g. Walling (1999) Herein, the most appropriate steps and sequence of active tracing methods are proposed. The crucial elements of each step are identified from previous approaches that are particularly applicable to oceanographic, geological, geomorphological, and hydrological and soil science research.

5.3. Approach

Altogether, 51 peer-reviewed journal papers were identified from literature searches conducted through Web of Science (Thomson Reuters, 2014). The following keywords and search terms were investigated: tracing, tracers, sediment, soil, fluorescent, magnetic, rare earth element. The paper was considered relevant if an artificial tracer had been introduced to the environment. From a review of the methodologies used within these studies, six logical and consistent steps required to conduct a successful tracer study were identified. Following identification, each paper was reviewed to establish which study type conducted (and reported) each step (Figure 31).

5.4. A Methodological Framework

Any tracing study begins with an assessment of the problem or issue that needs to be addressed. Once the aim and objective(s) of the study have been decided, there are six methodological steps to ensure a robust, practical tracing study is conducted (Black, 2012). The six key steps identified (Figure 30) are: 1) perform a background survey; 2) design / select tracer by matching the tracer properties to those of the native sediment and determine the quantity of tracer required; 3) introduce the tracer to the environment; 4) sampling; 5) tracer enumeration; and 6) analysis of results. The requirements of each step are outlined below.

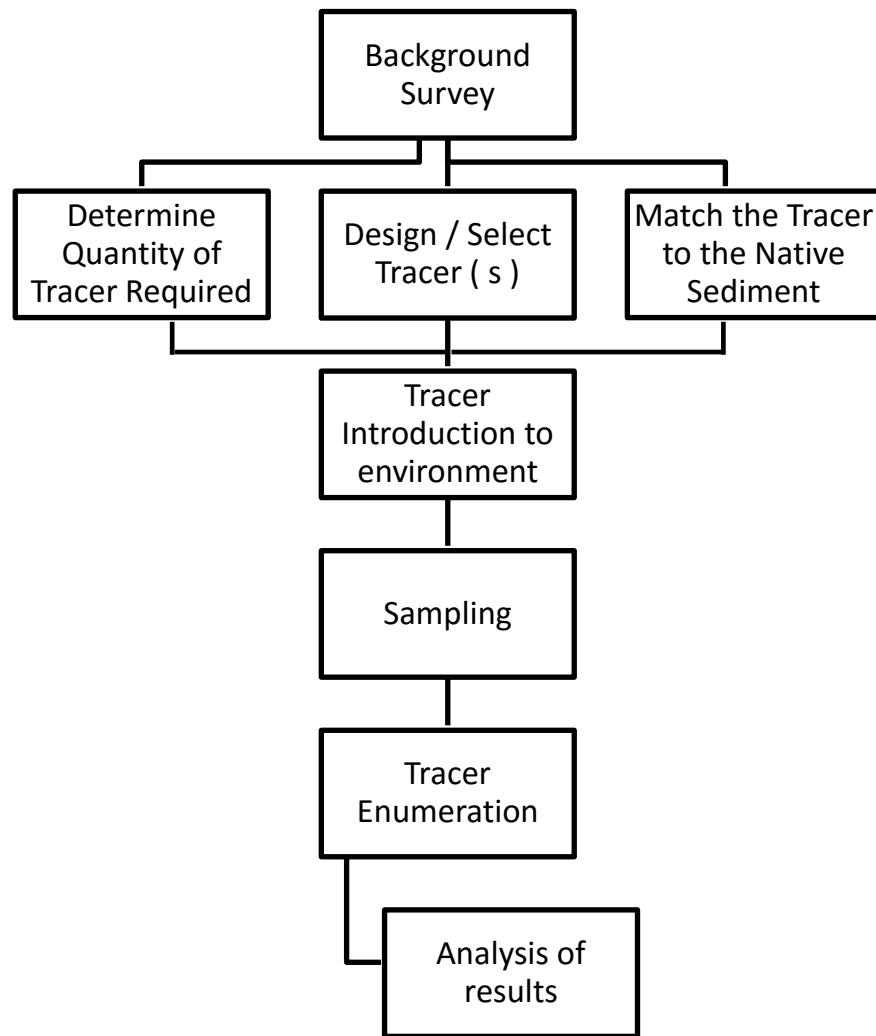


Figure 30: Proposed methodological framework for conducting a sediment tracing study using an active tracer.

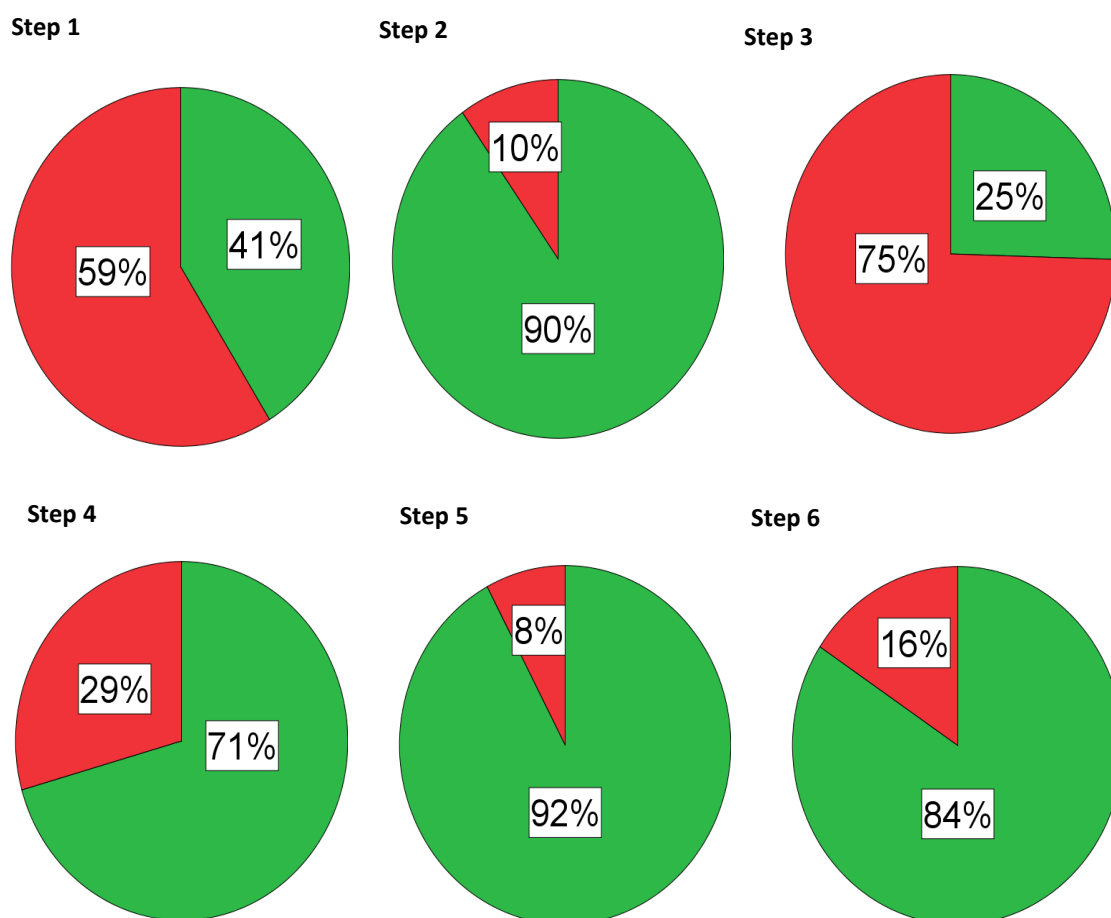


Figure 31: The percentage of studies that reported each step of the proposed methodological framework within peer reviewed articles. The green coloured slice represents studies that reported the results of each step and the red coloured slice represents studies that did not report the results of each step.

5.4.1. Step 1: Background Survey

The purpose of a background survey is manifold. It is to: 1) determine the presence / absence of particulates within the study region with the same or similar characteristics as the proposed tracer of use; 2) provide a comprehensive assessment of the properties of the native sediment on which tracer design can be based; and 3) evaluate environmental baseline readings by testing any sampling techniques proposed, to ensure no false positives are recorded.

Only 41 % of the studies identified in the literature survey reported the findings of a background survey (Figure 31). This was unexpected, as it is crucial to know that the tracer to be used has a unique signature in the environment of use (Crickmore, 1967, Spencer et al., 2011, Liu et al., 2004, Benevente et al., 2005, Michaelides et al., 2010). This can only be assessed through sampling (and testing) of the environmental sediments (Vila-Concejo et al., 2004, Inman et al., 1980, Miller and Warrick, 2012, Polyakov and Nearing, 2004, Ferreira et al., 2002). Determining if the sediment (or other native material) has similar properties to the tracer material is critical, as this constitutes noise within a tracing study (Stevens and Quinton, 2008, Mahaut and Graf, 1987, Cronin et al., 2011, Russell, 1960). To achieve this, sediment samples (cores, grabs etc.) should be collected throughout the study area / area of interest, focusing on potential source areas, transport pathways and deposition zones (Inman et al., 1980, Stevens and Quinton, 2008, Mahaut and Graf, 1987, Krezoski, 1989, Collins et al., 2013). Within the literature some studies collected just one bulk sample (Vila-Concejo et al., 2004, Ciavola et al., 1998, Lee et al., 2007, Carrasco et al., 2013, Ferreira et al., 2002). This risks incomplete capture of the sediment characteristics of the site and their spatial variation. From experience it is recommended that a minimum of five core samples are collected from each (potential) - distinct sediment zone per km² within the study area (e.g. upper and lower foreshore, and disturbed and undisturbed soils). Each sample should be analysed for the characteristics critical to sediment transport such as, the particle size distribution and specific gravity (particle density) (Dyer, 1986). This allows a tracer to be designed - based upon, the physical characteristics of the native sediment. Further, the bulk density of the native sediment should be determined, to quantify the appropriate mass of tracer required. If heterogeneous sediment characteristics are found (or known) throughout the area of interest, it is possible to reduce the volume of samples collected whilst still maintaining statistical significance using a random sampling technique (Wang et al., 2012).

The background survey should also be used to collect relevant data regarding the forcing mechanisms at the site (e.g. the collection of current velocity data, quantification of flow rates, slope and topography etc.) (Smith et

al., 2007, Cabrera and Alonso, 2010, Miller and Warrick, 2012, Carrasco et al., 2013, Cronin et al., 2011). Also a qualitative site assessment should be made (e.g. evidence of erosion, beach profiles, land use and management), as this may provide extra information regarding possible sediment transport rates and pathway(s) within the study area (Deasy and Quinton, 2010, Stevens and Quinton, 2008, Silva et al., 2007, Lee et al., 2007, Guymer et al., 2010, Collins et al., 2013). Fully understanding the study area prior to introduction of the tracer enables an informed methodological strategy to be developed.

5.4.2. Step 2: Tracer Design/Selection, Matching the Tracer to the Native Sediment and Quantity of tracer required.

A tracer that matches the native sediment in terms of its hydraulic attributes should be selected and / or designed. Little or no recognition has been given to the importance of matching the tracer to the native sediment in historic studies (Richardson, 1902, Joliffe, 1963, Kidson and Carr, 1961). Only 25 % of the papers identified in the literature survey reported the findings of matching (Figure 2) (termed 'hydraulic matching') and as such the accuracy of the reported results is uncertain (Caldwell, 1981). The tracer should ideally match the native sediment, in terms of its physical, biological and electrochemical properties (Madsen, 1987, White, 1998, Black et al., 2007, Foster, 2000, Ambulatov and Patrikeiev, 1963). Whether this is ever achieved in reality is debatable. However, ensuring the tracer is *hydraulically matched* to the native sediment *is* a methodological necessity which must be achieved, and should be prioritised over other characteristics (Black et al., 2007). Two hydraulically matched, or hydraulically equivalent, sediments will be cycled (eroded, transported, deposited) in the same way by a fluid flow (Black, 2012, Dyer, 1986). On a practical level matching the tracer hydraulic properties to the native sediment is straight-forward; samples collected within the background survey and the tracer are tested for characteristics that influence transport, namely size distribution and density (and within silt tracing studies occasionally settling velocity), and the results statistically compared (Ciavola et al., 1997, Tauro et al., 2010, Stevens and Quinton, 2008, Silva et al., 2007, Miller and Warrick, 2012, Cronin et al., 2011).

Commonly the results of this similarity matching are expressed as a similarity ratio (e.g. $d_{50 \text{ tracer}} / d_{50 \text{ native}}$). Tracing materials are designed to be unique within the environment; therefore it is unlikely that a perfect hydraulic match will be achieved. Permissible differences between the hydraulic characteristics of the native sediment and tracer have been outlined in the literature (Black et al., 2007). The median grain size (modal grain diameter) of the tracer should be within $\pm 10 \%$ of the native sediment (White and Inman, 1989), and the specific gravity (particle density) should be within $\pm 6 \%$ (Black et al., 2007) to limit the effects on field observations.

Matching is particularly critical when tracking the finer fractions (Louisse et al., 1986). It is also more challenging given its cohesive nature (Brown et al., 1999), and the hydraulic matching process may be based upon different precepts to those of coarse sediments. Unlike sand and gravel particles, cohesive sediment is transported primarily as flocs (Droppo, 2001). Thus it is critical that any tracer mimicking cohesive sediment must be able to flocculate (on its own), and thereby resemble a natural floc aggregate (Spencer et al., 2011), an approach which can be commonly called *direct floc mimicking*. This approach is preferable as it accounts for the mineral sediments and the organic and inorganic floc constituents (Droppo et al., 1997, Droppo, 2001). Unfortunately, tracers able to directly mimic a floc are not widely available, not least because within the direct floc mimicking approach it is difficult to establish that the tracer flocs, behave the same as native flocs, in terms of temporal aggregation and disaggregation processes (Louisse et al., 1986, Spencer et al., 2007, Spencer et al., 2010, Spencer et al., 2011). Significant theoretical and practical challenges remain in the development of effective clay sized tracers. Therefore, outlined below is an alternative approach, termed *floc tagging* e.g. Koch et al. (2013). In this approach the tracer particles must have similar hydraulic characteristics (i.e. size, density and settling rate) to one or more of those *constituent* sediment particles found within naturally flocculated material (Spencer et al., 2010). This approach facilitates tracking of the flocs by directly labelling the flocs (Figure 30). For this approach, the key information is the particle size distribution (following acid digestion e.g. (Laubel et al., 2003) of the native floc.

As silts are by definition $< 63 \mu\text{m}$ in size, a tracer of size e.g. $25\text{-}55 \mu\text{m}$ would be suitable for the majority of projects (Black et al., 2013). Figure 32 illustrates the principle of floc tagging.

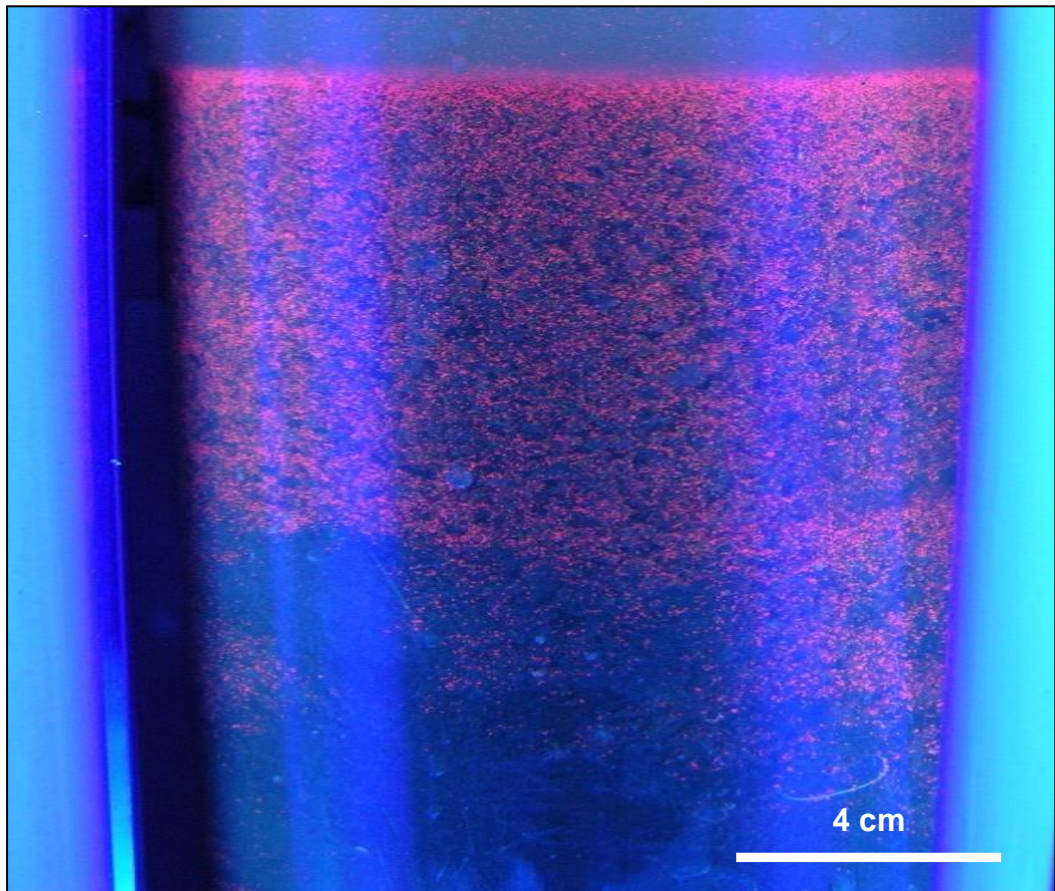


Figure 32: The image captured under ultraviolet illumination shows a core of cohesive peat sediment mixed with a pink silt tracer. The tracer has been hydraulically matched to the cohesive peat sediment. The tracer has then been thoroughly mixed with the peat and left to settle. The image demonstrates that the hydraulically matched tracer and peat, due to the similar hydraulic characteristics of one or more of the constituent sediment particles have a similar settling rate, resulting in the tracer flocculating with, and becoming entangled with, peat material. Thus the peat flocs have been tagged with an identifiable ‘signature’ enabling cohesive sediment transport to be assessed. The tags will ensure that ensuing transport processes may be tracked and transport pathways delineated. Image provided by Partrac Ltd.

Within the literature survey the quantity of tracer deployed is driven by environment (Lee et al., 2007). Studies conducted within the marine and coastal environment predominately deploy a significantly greater mass than

studies conducted within terrestrial environments. Tracer mass deployed regularly exceeds 100 kg e.g. Silva et al. (2007) and 1 tonne e.g. Collins et al. (1995), Smith et al. (2007). Studies conducted in the terrestrial environment have focused less on the mass of tracer deployed and more on desired tracer concentration post deployment (Stevens and Quinton, 2008, Deasy and Quinton, 2010, Michaelides et al., 2010, Kimoto et al., 2006b, Ventura et al., 2002). The amount of tracer introduced is critical – if too much material is deployed to the environment sediment transport processes may be unduly affected (Foster, 2000). Yet, if too little is deployed recovery of tracer is compromised (Ciavola et al., 1998, Courtois and Monaco, 1968). This may result in insufficient amounts of tracer being recovered, limiting the conclusions that can be drawn from the data set. A further consideration is the environmental impacts of the tracer following the study as the majority of tracer will remain within the system. Concern has been raised regarding the toxicity of fluorescent dyes (Smart and Laidlaw, 1977) and the use of entirely synthetic (plastic) tracing materials (Thompson et al., 2004).

Pragmatically, for many studies the quantity of tracer that can be used is dictated primarily by the project budget. Due to large uncertainties many studies do not attempt to define a sediment budget. Consideration of environment and project restrictions, choice of tracer, the sampling and analysis methodology, and desired precision is required. In general, the more dynamic the environment and the less controlled the study, the greater tracer mass is required, as the resolution of the data obtained is dependent upon the measuring technique employed (Guymer et al., 2010, Liu et al., 2004). At this stage, the extent of the source area (e.g. where the tracer is introduced to the field), and a site boundary (sample limit) should be clearly defined. The quantity of tracer required is then determined by multiplying the bulk density of the native sediment within the source area by the spatial extent of the study area (Kimoto et al., 2006b, Polyakov and Nearing, 2004, Liu et al., 2004, Ventura et al., 2002, Zhang et al., 2003).

5.4.3. Step 3: Tracer Introduction

Tracer introduction methodologies are project and environment specific, but for all applications it is extremely important that the tracer

particles are introduced into, or onto the area, of interest with minimal loss and redistribution of tracer. To ensure representative data are obtained it is critical that the tracer is introduced to at least the base of the active transport layer (Inman and Chamberlain, 1959). There are two primary methods of tracer introduction; 1) The foregoing introduction method (FIM) where tracer is introduced to the environment at one point in time (Ferguson, 2002, Miller and Warrick, 2012, Ingle, 1966, Ciavola et al., 1997); and 2) the continuous introduction method (CIM) which involves continuously introducing tracer to a point at a steady rate and measuring downstream (Spencer et al., 2011a, Luhmann et al., 2012, Magal et al., 2008, Stern et al., 2001, Cromey et al., 2002). Figure 35 presents a decision making flow diagram which summarises the options related to tracer introduction. The following sections details the methods specific to each environment and study type.

5.4.3.1. *Marine, Coastal and Fluvial Environments*

Traditional beach face studies require the tracer to be raked into the surface sediment layer (Inman and Chamberlain, 1959, Inman et al., 1980, Mahaut and Graf, 1987, Russell, 1960a), or introduced into a shallow trench (< 10 cm deep) (Silva et al., 2007, Corbau et al., 1994, Dolphin et al., 1995, Miller and Warrick, 2012, Bertin et al., 2007). It is recommended that where possible, tracer is introduced to the environment combined with native sediment in a 50:50 ratio (Figure 33), to aid incorporation (Crickmore and Lean, 1962, Krezoski, 1989), particularly for cohesive sediment projects (Cronin et al., 2011, Spencer et al., 2011). The tracer should be mixed with a small amount of seawater prior to introduction on the surface, or to a trench, to ensure that no redistribution of the tracer particles by aeolian transport occurs e.g. Ciavola et al. (1998). Adding a small amount of detergent (< 5 %) to the tracer / seawater admixture reduces the surface tension properties of the particles (Vila-Concejo et al., 2004), a factor which is generally helpful practically to stop tracer being transported on the water surface due to surface tension.

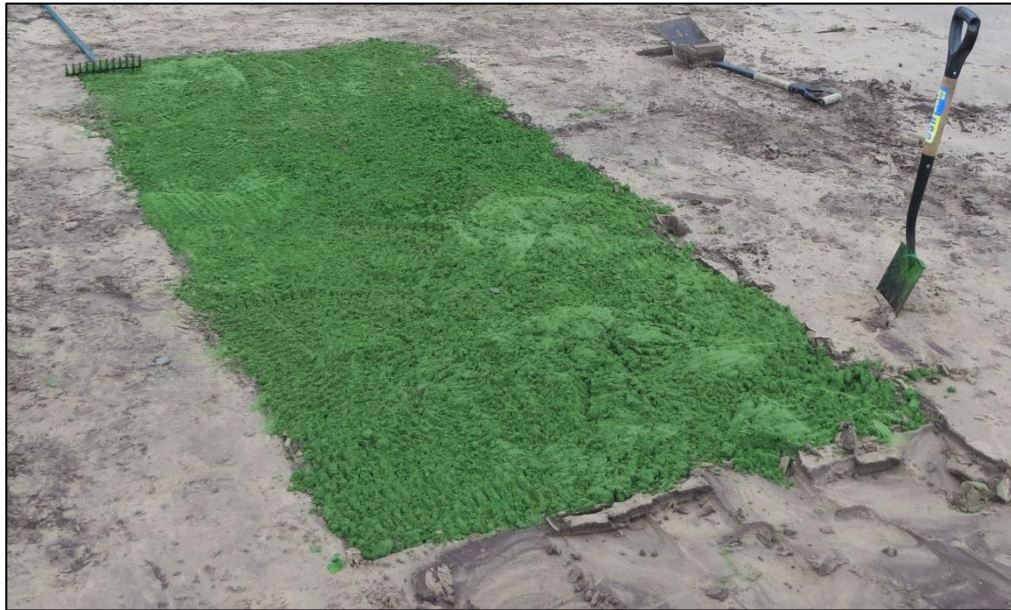


Figure 33: Green fluorescent tracer deployed on the beach face mixed 50:50 with native sand. Image provided by Partrac Ltd.

Introducing tracer into deeper water is more challenging. Novel and ambitious methods have been utilised to deploy tracer to the bed. These include: the use of water soluble bags that dissolve (Smith et al., 2007); and remotely operated chambers lowered from a ship (Courtois and Monaco, 1968, Ingle, 1966, White, 1987). Other specially designed or purpose built devices have been utilised (Van den Eynde, 2004, Cheong et al., 1993, Tudhorpe and Scoffin, 1987, Collins et al., 1995); e.g.- a weighted knife blade that rips open a bag of tracer upon contact with the sea bed (Vernon, 1963); or the use of a tube running from the ship to the sea floor (Joliffe, 1963a, Crickmore, 1967). Ideally, in deep water studies, the use of diver emplacement (SCUBA) is preferable due to the wealth of extra information provided by the divers (Mcomb and Black, 2005, Ingle, 1966, Ciavola et al., 1998, Solan et al., 2004, Inman and Chamberlain, 1959). Where possible *in situ* underwater videography or photography should be utilised to monitor and assess the success of the deployment (Cromey et al., 2002). From the review of the literature, it is recommended, that a coarse sand tracer should be deployed through a subsurface pipe within shallow water studies (Joliffe, 1963, Crickmore, 1967, Ferreira et al., 2002) and using dissolvable bags within deep water studies (Smith et al., 2007).

Silt tracers, applied to assess the entrainment and transport processes of deposited silts, presents specific issues. It is necessary to introduce the tracer onto the bed without loss of material to the water column. One way to introduce silt tracer to the sea bed is to encapsulate the tracer in ballasted ice, as this provides a secure, robust vehicle able to deliver tracer to the bed. This approach was pioneered by Krezoski (1989), who deployed a frozen pellet consisting of tracer and natural fine grained sediment to the bed. Recent adaptations of this technique have seen frozen plates consisting of 50 % tracer mixed with 50 % natural sediment, deployed to the mouth of an estuary at low tide (Cronin et al., 2011), and pre-made deep frozen tracer blocks deployed from the side of a vessel (Black, 2012). The colder the blocks can be made generally the better they perform as this increases the timeframes for encapsulation, enabling tracer introduction to greater depths (Black et al., 2007b).

Where studies are solely investigating suspended sediment transport there is often no requirement for the tracer to be deployed to the bed. The tracer can be deployed to simulate a floc or plume of suspended sediment directly by flushing tracer down a tube in suspension, subsurface (Black et al., 2013, Guymer et al., 2010, Cromeey et al., 2002). It is recommended that the tracer is pre-mixed with salt or fresh water, to create a high concentration tracer slurry which can be manoeuvred easily with trowels or shovels (Black et al., 2013). High flow water pumps, able to create a turbulent field are required to ensure complete disaggregation of the tracer particles within the slurry, as the slurry is deployed to the receiving water (Black et al., 2013).

5.4.3.2. *Terrestrial*

Terrestrial deployments require careful thought to ensure preferential transport of tracer does not occur. Preferential transport of tracer may occur: if the tracer does not bind with soil particles; where the tracer is not integrated into the soil matrix; or where the hydraulic characteristics of the tracer do not match the native soil particles (Zhang et al., 2001). Again, it is critical to deploy the tracer in a manner so as not to disturb the natural system. The tracer can be deployed on the surface (Cabrera and Alonso, 2010, Stevens and Quinton, 2008, Liu et al., 2004, Zhang et al., 2001, Collins et al., 2013)

(Figure 34). This is preferable when deploying tracer to a large spatial area ($> 5 \text{ m}^2$), and can be achieved simply and accurately using an adapted agricultural seed disperser (Stevens and Quinton, 2008, Collins et al., 2013, Polyakov and Nearing, 2004) or a knapsack sprayer (Deasy and Quinton, 2010) - although again avoidance of aeolian transport at the time of deployment is essential. To avoid aeolian transport, the tracer can be lightly wetted and deployed on a calm day. Where tracer is deployed at smaller scales ($< 5 \text{ m}^2$) it is preferable to pre-mix the tracer and native soil in a 50:50 ratio to aid incorporation e.g. Guzmán et al. (2010), Ventura et al. (2002), Michaelides et al. (2010). Introduce the tracer / soil admixture in the form of a shallow trench (1 – 3 cm deep), where the surface is flush with the surrounding soil surface (Armstrong et al., 2012, Liu et al., 2004, Ventura et al., 2002, Michaelides et al., 2010).



Figure 34: Green fluorescent tracer deployed on the surface of an agricultural field. Image provided by Partrac Ltd.

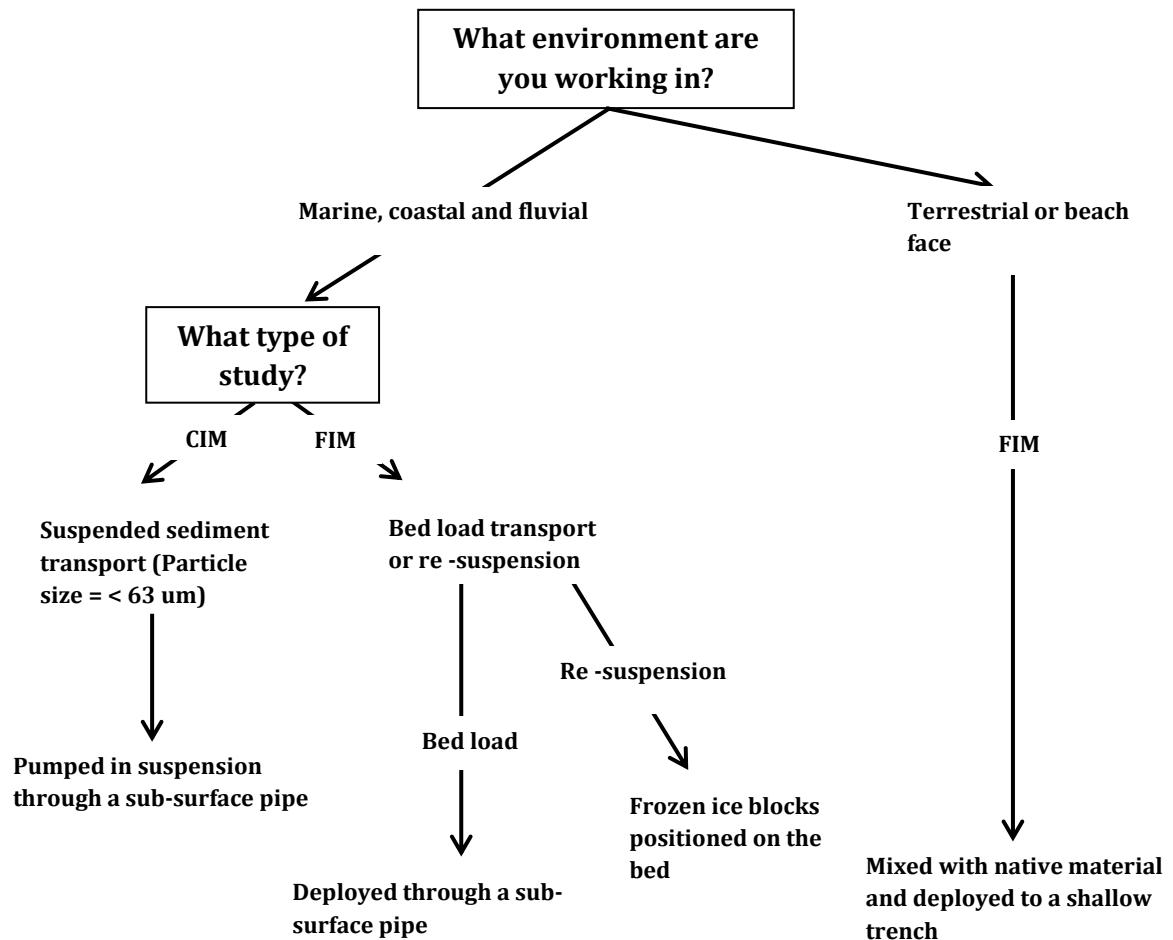


Figure 35: A decision making diagram to determine the most appropriate method of tracer introduction.

5.4.3.3. Step 4: Sampling

Recovering tracer for enumeration, or determining the presence of tracer *in situ*, requires spatial and temporal sampling (Black et al., 2007). Due to the dynamic nature of sediment transport within all environments, dilution and dispersal of the tracer to beyond / below the detection limit can occur. Therefore an adaptive sampling regime which considers sampling in the entire near field, mid-field and far field-relative to the tracer injection locality, and incorporates a strategy for recurrent sampling (through time), is required. Poor sampling strategies can lead to flawed conclusions, the most common being the conclusion that tracer is not present, whereas it might simply be that it cannot be detected (Ferguson, 2002, Collins et al., 1995). Sampling approach, as expected is referred to in the majority of literature sources

(Figure 29) demonstrating the sampling step is an inherent and highly important part of the sediment tracing methodology.

The two basic methods of sampling identified from the literature are the spatial integration method (SIM) (also referred to as Lagrangian sampling), where identified sample locations are sampled once (Ciavola et al., 1997, Ciavola et al., 1998, Bertin et al., 2007, Carrasco et al., 2013, Ferreira et al., 2002), and the temporal integration method (TIM) where identified sample locations are sampled repeatedly over time, via recurrent surveys (White, 1998, Crickmore, 1967). Predominately the SIM is used when sampling coarse sediments transported as bed load (often associated with beach face, longshore transport type studies), whereas TIM is used to sample sediments transported in suspension (Black et al., 2007).

A combination of random and systematic sampling techniques are recommended within tracing studies, which draw sampling units independently from each other with equal probability (Wang et al., 2012). In both systematic and random sampling it is assumed that the target population (tracer) is independent and identically distributed. Where no information is available regarding the direction of transport, practice dictates that a systematic sampling grid is used, and is usually arranged in two directions either side of the point of tracer injection (Black et al., 2007). The samples are collected in a given order relative to the first collection point, requiring the use of systematic sampling zones (Wang et al., 2012). However, where transport direction is known *a priori*, the use of systematic grids have the potential to introduce bias (Webster, 1999), and a more complex approach which uses both random and stratified sampling may be more appropriate. In practical terms sampling grid layout and size are often dictated by landscape features, man-made structures, morphology and budgetary and time constraints (Vila-Concejo et al., 2004). Due to this, and that within the majority of studies the dispersion rates of tracer are unknown prior to deployment, the collection of measurements at intermediate locations along the transport pathway, in addition to the target receptor is required (Ciavola et al., 1997, Komar, 1969, Ingle (1966), Vila-Concejo et al., 2004, Inman et al., 1980). To improve any tracing study, simply increasing the sample scope in terms of spatial and

temporal resolution, provides greater information regarding the distribution of tracer particles throughout the study area. This provides a greater evidence base from which conclusions can be drawn (Guzman et al., 2013, Kimoto et al., 2006b). As a simple rule, as much information as possible should be sought, within the resources of the study.

5.4.3.4. Sampling Tools

Tools commonly used to sample sediment in the marine, coastal and fluvial environments include core and grab samplers (Cronin et al., 2011, Gibson et al., 2011, Horng and Huh, 2011, Silva et al., 2007, Spencer et al., 2011), sediment traps (Peine et al., 2009, Solan et al., 2004), water samplers (Guymer et al., 2010, Martínez-Carreras et al., 2010), and *in situ* magnetic sampling (Guymer et al., 2010, Black et al., 2013, Collins et al., 2013). More recently, sensor based systems (e.g. fluorimeters) have found practical application of the *in situ* measurement of tracer e.g. Guymer et al. (2010). Within the terrestrial field, core samples and the collection of runoff samples are universally used (Ventura et al., 2002, Armstrong et al., 2012, Hu et al., 2011, Zhang et al., 2001, Michaelides et al., 2010). The use of a collection pool (Liu et al., 2004), and / or covered drains (Stevens and Quinton, 2008, Deasy and Quinton, 2010) to capture run-off samples enables time-integrated samples to be collected.

By far the most popular sampling tool within tracing studies is the collection of sediment cores. When collecting a core sample it is critical to sample through to the base of the active sediment layer, to maximise the chance of tracer recovery (following mixing), and to determine the mass (volume) of sediment in transport, investigate burial trends and calculate sediment transport rates through the environment (Ciavola et al., 1998, Bertin et al., 2007). If the thickness of the active layer is unknown, a visually identifiable tracer, can be used as a horizon marker to ensure the sample has been collected through the active layer (King, 1951, Inman and Chamberlain, 1959a, Komar, 1969, Inman et al., 1980), alternatively, where tracer content is known, the following equation can be used (White and Inman, 1989):

$$K_0 = \frac{\sum N(z) \Delta z(z)}{N_{\max}} \quad (7)$$

Where K_0 is transport thickness, Δ_z is the vertical thickness of the horizontal slice, N is the sediment volume concentration and N_{max} is the maximum tracer concentration in the core. Due to the surface disturbance created during active sampling, cores should only be taken post transport event.

Sampling strategies should strive to be flexible and adaptive to changes in environmental conditions that occur during the study, consequently a tracer that is able to be monitored effectively without using intrusive sampling techniques is advantageous (Guzman et al., 2013). Semi quantitative qualitative sampling techniques (such as submersible fluorescence imaging e.g. Solan et al. (2004), and night time, blue light torch surveys e.g. Russell (1960), Ciavola et al. (1998), Silva et al. (2007), Carrasco et al. (2013), Vila-Concejo et al. (2004) are driving innovation within tracing studies. These techniques should be used to monitor the spatial distribution of tracer particles in a non-intrusive manner, prior to using intrusive sampling techniques to quantify tracer content within the sampling grid. Table 6 summarises the passive sampling techniques available to monitor the most popular tracing materials, being fluorescent tracers, magnetic tracers and rare earth element tracers.

Table 6: The passive sampling techniques available to monitor tracer particles in the environment for the most popular tracing materials.

Tracer Material	Passive sampling techniques	Information
Fluorescent Tracers	<p><i>In situ fluorimeters</i></p> <p><i>Visual inspection under blue light or ultraviolet (UV) illumination</i></p>	<p><i>In situ</i> fluorimeters monitor the fluorescent emission of particulates (or dyes) directly beneath the sensor, through time. This enables the detection of fluorescent tracer as a cloud of suspended tracer particles passes the sensor (e.g. Guymer et al. (2010)). The sensor can be adapted to assess tracer on the sea bed or hill slope.</p> <p>The spectral characteristics of fluorescent tracer enable unequivocal identification of the tracer particles within the environment using a blue light or ultraviolet (UVA) lamps (emitting wavelength 395 nm – 400 nm). Using these torches or lamps allows the spatial distribution of tracer to be assessed. Further, there is the potential for <i>in situ</i> photography and image analysis e.g. Darvishan et al. (2014).</p>
Magnetic Tracers	<i>Magnetic susceptibility</i>	<p>Mass-based magnetic susceptibility is a comparative measure of the relative ease with which a material can acquire a magnetic field when exposed to a low frequency alternating magnetic field. Ferrous or iron-rich particles acquire a magnetic field far more easily than non-ferrous particles. The magnetic susceptibility of a granular material is measured using a magnetic susceptibility sensor (e.g. Bartington Instruments Ltd). The technique is especially useful as it provides rapid determination of tracer concentration in sediments and soils e.g. Van Der Post et al. (1995), (Ventura et al., 2002).</p>
Rare Earth Element Tracers	<i>None available</i>	

5.4.4. Step 5: Tracer Enumeration

The ultimate aim of any tracing study is to determine the tracer concentration (mass per unit volume), or dry mass of tracer from within each sampling location or time step. The preferred enumeration method should be able to accurately analyse a large number of samples within a short period of time. This allows for many more samples to be collected from the field and analysed within a given resource budget, a facet which substantially improves many tracing studies (Guzman et al., 2013). Tracer enumeration techniques are wholly dependent on the type of tracer utilised. The benefits and limitations of the analysis techniques associated with each tracer illustrate the importance of taking a holistic view of the entire methodology, at the study planning stage, to inform tracer material selection decisions. Table 7 summarises the methodologies used to enumerate tracer mass or tracer content within environmental samples associated with the most popular tracing materials.

Table 7: The tracer enumeration methodologies available for the most popular tracing materials, fluorescent tracers, magnetic tracers and rare earth element tracers.

Tracer Material	Enumeration techniques	Information
Fluorescent Tracers	Counting by eye <i>(Carrasco et al., 2013, Cabrera and Alonso, 2010, Ferreira et al., 2002, Benevente et al., 2005, Cronin et al., 2011, Collins et al., 1995)</i>	The spectral characteristics of fluorescent tracer enable unequivocal identification of the tracer particles within environmental samples using a blue light or ultraviolet lamps (UV) (emitting wavelength 395 nm). The sample is thinly spread and the tracer particles counted. This technique is not viable when using silt tracers.
	Filtration/sedimentation followed by digital image analysis <i>(Solan et al., 2004, Tauro et al., 2010, Silva et al., 2007, Yang et</i>	A similar methodology as described above except an image of the sample is captured under ultraviolet (UV) illumination and a digital image analysis system is used to count the fluorescent particles within the image.

Tracer Material	Enumeration techniques	Information
	<p><i>al., 2011)</i></p> <p><i>Dissolution of the fluorescent coating, centrifugation and spectrofluorometric analysis</i></p> <p><i>(Carey, 1989, Farinato and Kraus, 1980)</i></p> <p><i>Flow cytometry</i></p> <p><i>(Forsyth, 2000)</i></p>	<p>Measuring the fluorescence intensity of an environmental sample via spectrofluorimetric analysis allows the tracer content within an environmental sample to be determined and enables the determination of tracer content when using both silt and sand sized tracers.</p> <p>At the interrogation point of a flow cytometer the fluorescence intensity is measured. This technique enables silt sized particles to be analysed yet is unable to analyse sand sized particles. In addition the sample size able to be analysed is restricted requiring sub-sampling.</p>
Magnetic Tracers	<p><i>Magnetic Separation</i></p> <p><i>(Pantin, 1961, Black et al., 2004, Black et al., 2013, Ventura et al., 2002)</i></p>	<p>Magnetic tracers mean that an entire sample can be flushed through a magnetic separator (Frantz Isodynamic Separator) to recover tracer by separating the non-magnetic and magnetic fractions from the sample. Use of all sample material obviates any necessity for sub-sampling, which avoids sub-sampling errors and means the probability of finding tracer is far greater.</p>
Rare Earth Element Tracers	<p><i>Neutron activation analysis</i></p> <p><i>(Orvini et al., 2000, Liu et al., 2004)</i></p> <p><i>Inductively coupled plasma-</i></p>	<p>Rare Earth Elements can be extracted from environmental samples and detected at very low concentrations. The cost of this analytical procedure often restricts the number of samples that can be analysed.</p>

Tracer Material	Enumeration techniques	Information
	<p>mass spectrometry (ICP – MS)</p> <p>(Zhang et al., 2001, Kimoto et al., 2006b, Stevens and Quinton, 2008, Polyakov and Nearing, 2004, Michaelides et al., 2010)</p>	

5.4.5. Step 6: Analysis

Tracer enumeration provides point specific tracer mass/concentration data at a single instant in time. The data should be generated to provide an overview of the study as a time step (e.g. at each sampling stage), and across the extent of the spatial area. Computer software such as Geographical Information System (GIS) (Esri, 2015), Surfer (Golden Software, 2015) and MATLAB (Mathworks, 2015) are useful tools to do this (Polyakov and Nearing, 2004).

The direction of transport is determined via the quantity of tracer recovered from the sampling grid, best described as a percentage of the total tracer mass recovered, not the total tracer mass deployed (e.g. > 50 % of tracer recovered was found to the south of position X). As transport of sediment is often multidirectional, the dominant transport pathway, and receptor area, is determined by the presence of the greatest quantity of tracer. However care must be exercised, as these results only reflect the conditions observed within the study. Within terrestrial studies of erosion on hill slopes where direction of transport is known *a priori* (downslope), the objective is often to determine the quantity of tracer lost, rather than the transport direction of the soil. Thus, data are often presented as a cumulative soil loss, depletion or erosion rate ($\text{kg}^{-1} \text{m}^{-2}$) e.g. Deasy and Quinton (2010), Stevens and Quinton (2008), Zhang et al. (2003).

A precept of tracing studies is normalisation of the data to represent tracer concentration within the surrounding area (White, 1998, Black et al., 2007, Vila-Concejo et al., 2004). This was first described by Inman and Chamberlain (1959) who concluded that the mass of tracer recovered from a

sample point (S_x) is representative of the mass of tracer in a rectangular shape around the point of the sample, with the boundaries of the rectangle being midway between sample points. To compute the tracer content within each area of the sample grid, the volume (V_{ri}) of the area (A_{ri}) represented by each core sample can be calculated:

$$V_{ri} = A_{ri}h \quad (8)$$

Where h is the height of the tagged layer.

A multiplying factor (T_{mi}) used to extrapolate the tracer concentration of the core (C) to the entire represented area can then be calculated by dividing C by the volume of the core (C_{vol}).

$$T_{mi} = \frac{C}{C_{vol}} \quad (9)$$

The tracer concentration of the represented area (M_i) is then calculated by multiplying the T_{mi} by the representative volume.

$$M_i = T_{mi} V_{ri} \quad (10)$$

Extrapolation must be used with caution and the sampling frequency (i.e. distance between sample points) must be appropriate (Black et al., 2007b).

The transport rate of tracer through the environment can be described through the advance of the tracer front (Madsen, 1987, Black et al., 2007) and determination and tracking of the mass centre of tracer distribution e.g. Vila-Concejo et al. (2004), (Cabrera and Alonso, 2010, Silva et al., 2007, Lee et al., 2007, Ferreira et al., 2002). The average transport velocity is calculated from the distance moved by the mass centroid of tracer divided by the time between injection and sampling (White, 1998). Assuming that all samples collected have been sampled throughout the active transport layer, following the enumeration of tracer content from each sampling point, the location (Y) of the mass centre of the tracer distribution can be determined:

$$y = \sum M_i D_i / \sum M_i \quad (11)$$

Where M_i is the mass of tracer at each grid node and the average grain mass (usually obtained using mean grain size values from the area of interest), and D_i is the distance from the introduction point.

5.5. Discussion

This review has identified 6 key steps formed into a methodological framework critical to successfully conducting a practical sediment tracing study. The methodological framework aids decision making and project planning and provides a guide as to how to conduct a tracing study, from inception to delivery. Critical to the success of a study is identifying the most suitable tracer type, as subsequent decisions regarding sampling strategy, sample numbers and analytical techniques are driven by tracer choice (Black et al., 2007, Guzman et al., 2013, Liu et al., 2004). Different tracers may also have differing basic costs and thus tracer choice may be dictated by project budgets. Sediment tracing requires an empirical evidence-based approach, subsequently a multistage sampling campaign is preferable and as such, tracers that allow this are considered advantageous (Zhang et al., 2001, Guzmán et al., 2010).

Active sediment tracing is a useful tool able to provide information which aids in the protection of ecological habitats, supports the development of sediment management plans, and is able to provide baseline data to inform sediment transport models (Athanasios et al., 2008), important for long term planning and development at the catchment and coastal scale (Gibson et al., 2011, Gallagher et al., 1991). Continued development of sediment tracing techniques, and the methodology, will increase application in traditional, original and novel or emerging fields. This combined with the availability of commercially available tracers (Black et al., 2007), is increasing the use of active sediment tracers to assess sediment transport pathways and sediment dynamics. Non-specialist users require a methodological framework to work within.

5.6. Conclusion

A methodological framework has been presented which applies to all studies which utilise an active sediment tracer, regardless of study context or

environment. The framework provides a clear and robust step by step guide to conducting a sediment tracing study. Further it has outlined a range of techniques useful to practitioners with a focus on the practical application of the technique to the field. As the application of the technique increases and is applied to increasingly varied sediment management problems, a broader range of scientists, researchers and practitioners are likely to use sediment tracing techniques. As such, the development of the methodological framework enables a broader range of practitioners to use tracers effectively, in a robust manner, with confidence.

6. The Evaluation and Application of a Dual Signature Tracer to Monitor Soil Erosion Events.

6.1. Summary

Erosion of soil on agricultural land is internationally recognised as a significant environmental issue. Erosion creates problems both on-and-off site; reducing agricultural production, and contributing to the degradation of receiving waters. Understanding soil transport processes is critical both to assess the risk of erosion, and develop and implement effective mitigation strategies. Soil tracing potentially comprises a field technique for monitoring the spatio-temporal distribution of soil, without the requirement of extensive infrastructure. Yet, despite significant research, the 'perfect' soil tracer does not currently exist. Here we evaluate and apply a commercially-available, dual-signature (fluorescent and ferrimagnetic) tracer for the study of soil erosion. The tracer's properties and behaviour were rigorously assessed through soil box experiments in the laboratory, prior to application in the field to monitor soil loss at the plot scale. The tracer replicated soil transport processes at different size fractions, within different soil types. The magnetic signature enabled rapid determination of tracer content in the field through measurement of magnetic susceptibility; the mean magnetic susceptibility of the tracer particles, $\sim 600 \times 10^{-8} \text{ m}^3 \text{ kg}^{-1}$ was found to be 50 x's higher than that of the native soils. Soil loss in the field, due to rainfall, ranged from 0.02 to 0.07 kg m². The tracer appears to provide an effective tool to monitor soil movement both in the laboratory and at field/plot scale. Further, the methods described enabled rapid collection of a high-volume of robust data - a factor critical to the success of any tracing study.

6.2. Introduction

Traditional approaches of studying water erosion in the field utilise equipment such as Gerlach troughs (Koulouri and Giourga, 2007, Francis, 1990, Gerlach, 1967, Novara et al., 2011), run-off tanks (Wendt et al., 1986, Bagarello and Ferro, 1998, Ghidey and Alberts, 1998), and water flow meters (Isensee and Sadeghi, 1993, Meyer et al., 2000). All require infrastructure that often is expensive to maintain and does not provide information on the spatial distribution of eroded soils (Lal, 1994). An alternative to the collection of

eroded sediment is the use of sediment tracers, able to trace the spatial distribution of soil within the landscape and/or determine net losses of soil without the requirement of infrastructure (Guzman et al., 2010).

Soil erosion tracers have been used to identify sediment sources (Collins et al., 1997, Collins et al., 2012, Walling and Collins, 2005, Stevens and Quinton, 2008, Deasy and Quinton, 2010), elucidate sediment transport pathways (Wallbrink and Murray, 1996, Wallbrink et al., 2002), and determine erosion rates (Walling and He, 1999, Blake and Walling, 1999, Hao et al., 1998). By far the most popular soil tracer has been the anthropogenically derived radioisotope, caesium-137 (^{137}Cs) (Guzman et al., 2013), which has been used extensively within agricultural catchments (Owens et al., 2000, Walling et al., 2006, Gruszowski et al., 2003, Quine et al., 1999, Walling and He, 1999). However, uncertainties surrounding variable deposition (Owens and Walling, 1996, Sutherland, 1996, Walling and Quine, 2006, Mabit et al., 2008, Wallbrink et al., 1994), and the use of un-validated calibration models (Walling and He, 1999), have raised concerns over the findings of many studies (Porto et al., 2001, Smith and Blake, 2014).

Thus, the need exists for a means of tracing soil with all the advantages of this methodology but with substantially reduced uncertainties. The use of active tracers reduce the uncertainties as the tracer is applied to the field in a known quantity, simplifying determination of a sediment budget (Kondolf and Piegay, 2003). Active tracing materials used historically within agricultural catchments have been diverse, and include rare earth elements (Deasy and Quinton, 2010, Polyakov and Nearing, 2004, Michaelides et al., 2010, Tian et al., 1994, Zhang et al., 2003), fluorescent glass particles (McDowell and Wilcock, 2004), DNA-labelled particles (Mahler et al., 1998) and steel nuts (Petticrew et al., 2006).

Due to their ease of sampling, and relatively low cost, magnetic tracing materials have proved popular (Guzmán et al., 2010, Guzman et al., 2013). These have included magnetically-coated plastic (Ventura et al., 2002); and various magnetic iron oxides (Guzmán et al., 2010, Parsons et al., 1993), including fly ash (Olson et al., 2013), magnetic powder and fly ash mixed with

cement or bentonite (Hu et al., 2011, Dong et al., 2007, Dong et al., 2009), and magnetically-enhanced soil (Armstrong et al., 2012).

In order to assess and monitor the spatio-temporal dynamics of soil erosion, rigorous testing is required of any tracer (Zhang et al., 2001, Ventura et al., 2001, Spencer et al., 2007, Guzman et al., 2010). The ‘perfect’ soil tracer should be able to bind strongly with soil particles and/or be easily incorporated into soil aggregates; possess a high analytical sensitivity; afford easy, inexpensive measurements; have low background concentrations in soil; not interfere with sediment transport; be able to trace different particle size fractions; have a low biological uptake; be environmentally benign; and have availability of multiple tracer signals (Zhang et al., 2001, Guzmán et al., 2010). No tracer used so far meets all of these criteria (Guzman et al., 2010).

Here, this problem has been approached by using a tracer comprising particles with two signatures, fluorescent colour and ferrimagnetism. This chapter evaluates the effectiveness of this dual-signature tracer as a tracer of soil, both at the laboratory scale, and at field-plot scale, in order to quantify soil loss due to rainfall. The main objectives were to:

1. Assess tracer behaviour through soil box experiments in the laboratory.
2. Evaluate the dual-signature tracer as a soil erosion tracer within a range of soil types.
3. Develop a robust methodology to monitor the spatio-temporal distribution of tracer within an agricultural field.
4. Apply the tracer in the field to quantify soil loss from erosion plots.

6.3. Methods

6.3.1. Laboratory set-up

The studied tracer consists of a chartreuse-coloured, dual-signature tracer (Partrac Ltd, UK) derived of natural mineral kernels coated with two applied tracer signals, fluorescence and ferrimagnetism. The Gaussian size

distribution of the original tracer (as supplied) allowed the tracer to be dry-sieved into five discrete size fractions (1-63, 63 - 125, 125 – 250, 250 – 500, and 500-950 microns), and a composite tracer made with equal amounts of each size fraction, forming six tracers in total. Bulk soil samples were collected from three sites: a clay loam soil of the Wick 1 association from Lancaster, Lancashire (54.0082° N, 2.7805° W); a sandy loam soil of the Oak 2 association from Calthwaite, Cumbria (54.7544° N, 2.8281° W); and a silt loam soil of the Brickfield 2 association collected from Preston, Lancashire (53.8531° N, 2.7631° W). All three soil samples were air-dried and screened to < 4 millimetres.

Triplicate soil box experiments were conducted for each of the tracer particle size fractions applied to each of the bulk soil samples, resulting in 54 experiments. Soil box design and preparation were based upon the methodology of Armstrong et al. (2012). The sieved, air-dried bulk soil sample was carefully packed onto a sand base in the soil box in 1 cm layers to a density of 1.5 g cm^{-3} . Five centimetres from the top of the soil box, a trough of soil (- 3 cm deep and 5 cm wide) was removed, thoroughly mixed with 7 g of the separated tracer size fraction or composite tracer and then carefully re-packed into the trough (hereafter referred to as the tagged zone). The tagged zone made up 20 % of the soil surface area, with 0.5 % of the bulk soil sample consisting of tracer particles. The soil box was positioned at a slope of 10 % under rainfall generated using a gravity-fed rainfall simulator with an intensity of 31 mm h^{-1} for one hour. To ensure consistent water quality, de-ionized water was used throughout (Figure 36).

Prior to and after the simulated rainfall, the magnetic susceptibility of the soil surface was mapped using a MS2K high resolution surface sensor. The operating frequency was 0.58 KhZ, the area of response was 25.4 mm full-width, half maximum, depth of response was 50 % at 3 mm, and 10 % at 8 mm, (Bartington Instruments Ltd, UK). Measurements were made using a grid with 4 cm spacing with the second grid row centred on the tagged zone. Shallow surface core samples were collected post rainfall at a depth of 1 cm using a plastic soil coring tool (radius – 1.4 cm), on the same grid spacing as the magnetic susceptibility measurements. Following each run the soil box

and surrounding area was inspected under blue light illumination (395 nm) in the dark to qualitatively assess the loss of tracer due to splash erosion.

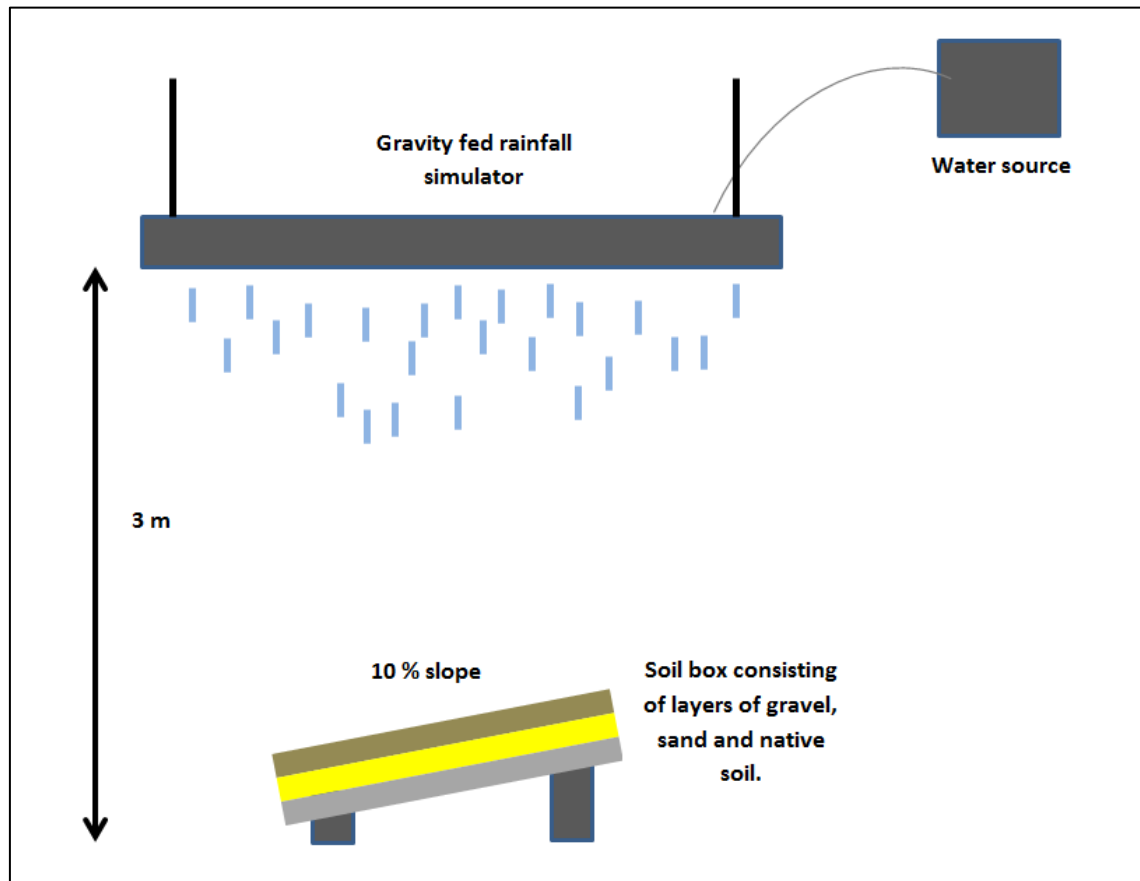


Figure 36: A schematic diagram showing the laboratory setup of the soil box and rainfall simulator. The diagram is not to scale.

The surface run-off during the one-hour period was collected and all samples were analysed for tracer content (tracer dry mass) by separating the magnetic fraction from the non-magnetic fraction. Briefly, the sample was oven dried (105⁰C) for 24 h, then transferred to a pestle and mortar and gently disaggregated. The sample was then smoothed to an approximately granular monolayer on a large piece of white cardboard and a permanent, 11,000 Gauss magnet was scanned across the sample at a distance of 2-3 mm, facilitating separation of magnetic particles. This procedure was repeated, with intermittent cleaning and recovery of the particles from the surface of the magnet, until no further magnetic particles were extracted and the magnetic particles weighed. The extraction efficiency of the methodology was 106 % (determined through testing of spiked samples and a comparison of the known tracer mass and extracted tracer mass). To determine tracer content values (*C*) the mass of magnetic material (*M*) is divided by the extraction efficiency (*E*).

$$C = \left(\frac{M}{E} \right) 100 \quad (12)$$

6.3.2. Field set-up

The field experiments were conducted on a fallow agricultural field at Winton Hill Farmstead, Cumbria (54.743851° N -2.816782° W). The soil is a silt loam. A topographic survey was undertaken and three, 1 m² plots (hereafter referred to as the deployment zones), were constructed on slopes of 4.6 %, 6.3 % and 7.6 %. 10 m upslope from the plots, 2 m-long, 30 cm-high barriers were installed to minimise the difference in run-on between plots. A standard tipping bucket rain gauge with a CR800S measurement and control data logger (Campbell Scientific Ltd, UK) was deployed to monitor rainfall (mm) at the site.

A bulk soil sample (for mixing with tracer to create a tracer/soil admixture) and 10 shallow cores were collected from the field. From the deployment zones 5 cores were collected using a stratified random sampling technique. Away from the deployment zones 5 cores were collected using a random sampling technique. For each of the cores the bulk density, specific gravity and particle size were determined. The specific gravity was determined

using an adapted pycnometer technique (Germaine and Germaine, 2009), and the particle size distribution with a Mastersizer 2000 laser diffraction particle sizer (Malvern Instruments Ltd, UK), following acid digestion, as described in Laubel et al. (2003). The tracer (Partrac Ltd, UK), which replicated the specific gravity of the native soil, was dry sieved to develop a composite tracer that mimicked the particle size distribution of the native soil (Table 8, Figure 37) and mixed 1:1 with native soil before application to the site.

Table 8: A summary of the physical characteristics of the tracer and native soil deployed as a tracer/soil admixture to the field.

Material	Colour	Quantity (Kg)	Size (microns) D50	Specific gravity Kg/ m ³ @20 ⁰ C	Particles ferrimagnetic (%)	Particles fluorescent (%)
Tracer	Chartreuse	40.5	12-15	2343	100	100
Native soil	none	40.5	7-10	2482	0	0

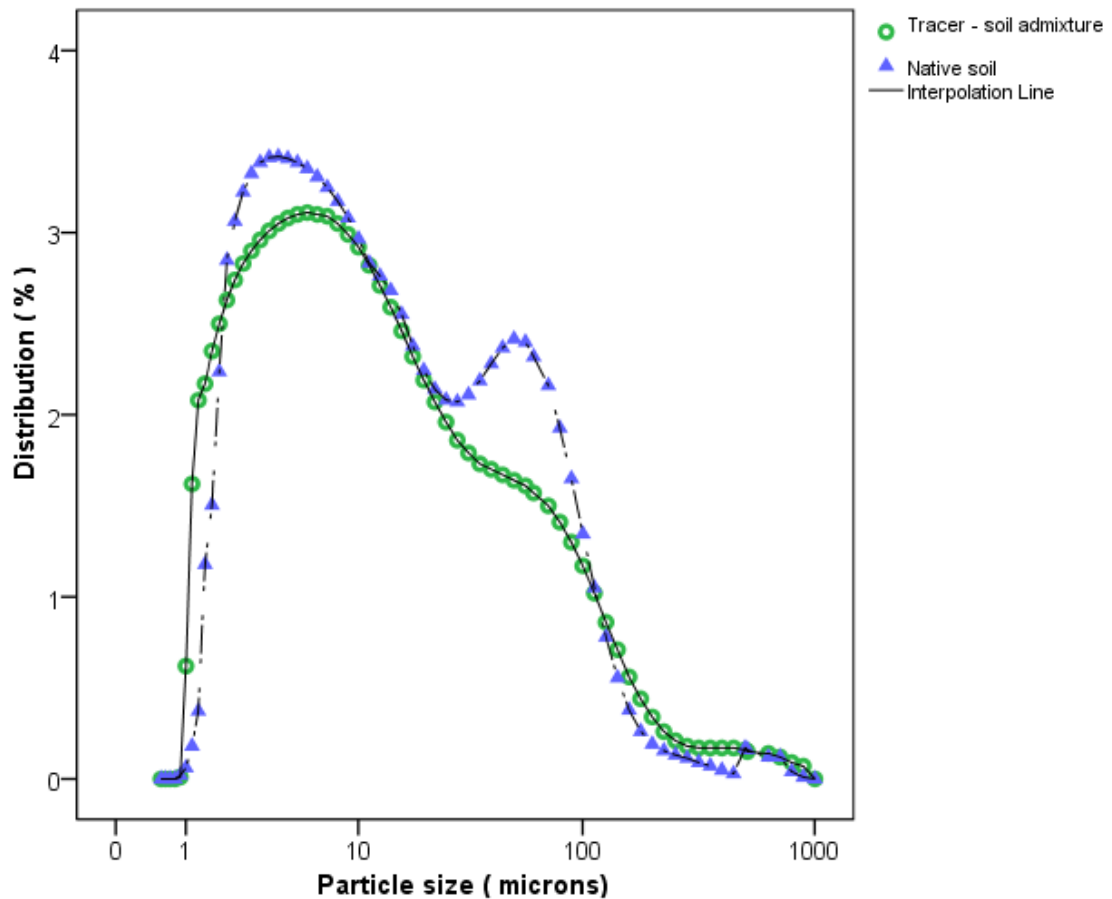


Figure 37: The mean particle size distribution of the tracer – soil admixture and the native soil.

The tracer/soil admixture (50:50) was deployed by hand using a trowel. The admixture was deployed to each grid spacing within the plot in turn, at a density of $0.9 \text{ g per cm}^{-3}$ to a depth of 1 cm, resulting in an assumed tracer concentration of $0.45 \text{ g per cm}^{-3}$. A total of 9 kg of tracer/soil admixture was deployed at each plot. To facilitate application prior to deployment the admixture was mixed with 200 ml of distilled water and thoroughly mixed (Figure 38 and 39).



Figure 38: The plots within the field at a slope of 4.6 %. Note the barriers positioned behind the plots.



Figure 39: The tracer deployed to the soil surface.

Sampling was conducted following rainfall events > 1 mm over 8 hours. The rainfall events occurred over a 33-day period and amounted to 4, 3.2, 2.9, 27.1, and 18.9 mm, respectively. Within each 1 m² plot, magnetic susceptibility measurements were taken using a grid with 25 cm spacing, resulting in the collection of 1440 surface susceptibility readings. At each grid node within each plot, one 4 cm-deep core sample was collected using a plastic coring tool (diameter 5.5 cm). A sampling frame (25 cm²) was used to standardise the collection of core samples within the grid and ensure that repeat sampling did not occur. So as to not affect subsequent transport processes, the hole left by the removal of a core sample was backfilled using native soil. A measurement of low frequency magnetic susceptibility was made before a soil core was collected (and after the hole was backfilled) using an MS2 magnetic susceptibility meter with an MS2D surface scanning probe (operating frequency 0.958 kHz, depth of response 50% at 15mm, 10% at 60mm) used with a MS2 probe handle (Bartington Instruments Ltd, UK). In addition to the *in situ* magnetic measurements, the tracer content in all collected cores was measured using the magnetic separation method described above (Black et al., 2013, Pantin, 1961b, Ventura et al., 2002). Run-off from the plots was qualitatively assessed during night time inspections using blue light torches (395 nm)

6.3.3. Soil loss calculations

Total soil loss from each plot was determined in two ways in order to assess the optimum field methodology. First, the measured changes in magnetic susceptibility, pre and post-rainfall, were used, via an adapted version of a conversion model described in Guzman et al. (2013);

$$L = \frac{m}{a} \Delta x \quad (13)$$

Where L is soil loss, m is the mass of tracer deployed, a is the tagged area and x is the difference in magnetic susceptibility pre - and post – rainfall.

Second, to calculate total soil loss from each plot, the tracer dry mass values are extrapolated to each grid section, based on the assumption that tracer mass within a sample is representative of tracer concentration within

the surrounding area (White, 1998, Black et al., 2007b). To compute the tracer content within each area of the sample grid, the volume (V_{ri}) of the area (A_{ri}) represented by each core sample can be calculated.

$$V_{ri} = A_{ri}h \quad (14)$$

Where h is the height of the tagged layer.

A multiplying factor (T_{mi}) used to extrapolate the tracer content of the core (C) to the entire represented area can then be calculated by dividing C by the volume of the core (C_{vol}).

$$T_{mi} = \frac{C}{C_{vol}} \quad (15)$$

The tracer content of the represented area (M_i) is then calculated by multiplying T_{mi} by the representative volume.

$$M_i = T_{mi} V_{ri} \quad (16)$$

The mass of tracer remaining in each plot (M_{TOT}) is then calculated by summing of all the M_i obtained for each plot at the end of the sampling campaign.

$$M_{TOT} = \sum M_i \quad (17)$$

Assuming loss of tracer represents soil loss from the plot, total soil loss (T_{SL}) is then calculated by subtracting M_{TOT} from the mass of tracer deployed (m) to each plot.

$$T_{sl} = m - M_{TOT} \quad (18)$$

6.3.4. Statistical analyses

SPSS Statistics 20 (IBM, 2014) was used for all analysis. For the soil box experiments, a paired t test was used to assess for: significant differences between the magnetic susceptibility of the tracer and native soil; estimated and measured soil loss within the soil box; and mass of soil and tracer captured in the run-off sediment. In the field experiment, a paired t test was used to assess the difference between soil losses calculated from magnetic susceptibility values and tracer mass.

6.4. Results

6.4.1. Soil box experiments

The tagged zone had a mean magnetic susceptibility ~ 50 times that of the native soil ($n = 161$, $p < 0.05$), resulting in the tracer being unequivocally identifiable within the native sediment load. Further, the tracer was reactive under exposure to blue light (395 nm) resulting in the tracer being identifiable due to the fluorescent signature. This enabled the movement of fine ($< 125 \mu\text{m}$) and coarse size fractions ($> 125 \mu\text{m}$) to be traced. Across all three soil types, the greatest initial difference in magnetic susceptibility between the tagged zone and non-tagged zone was observed during the deployment of the fine fraction (1-63 microns) (Figure 40).

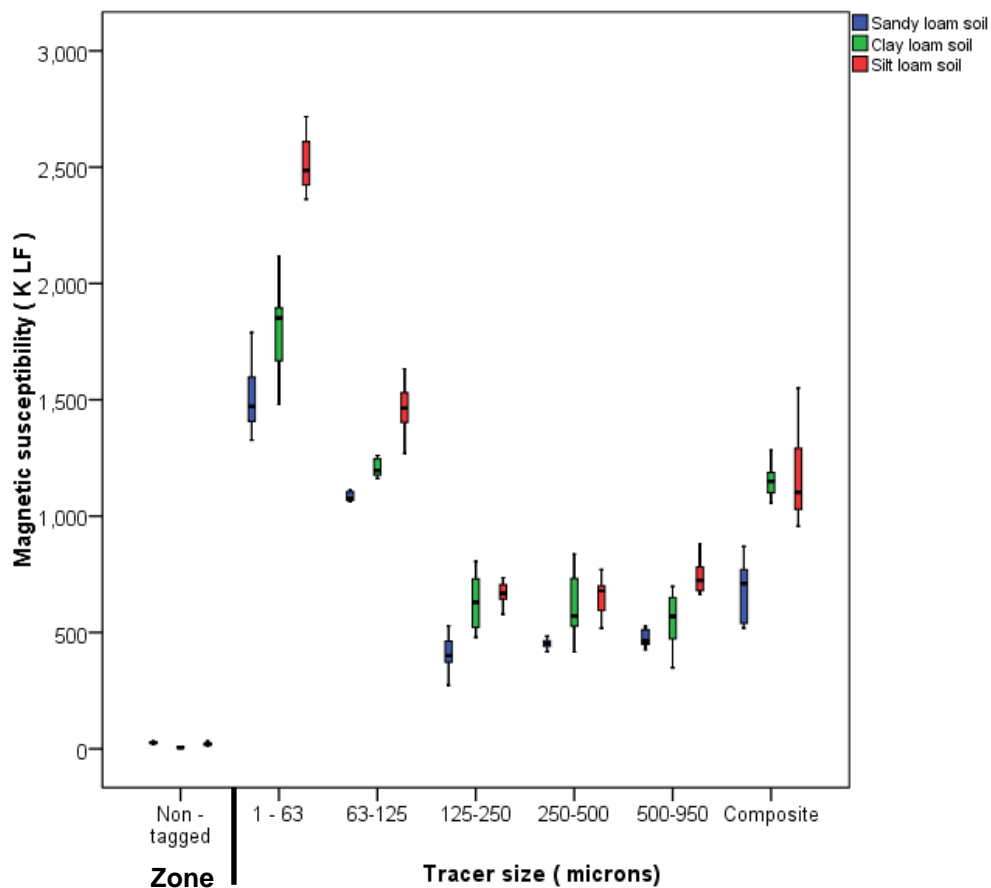


Figure 40: A comparison of the magnetic susceptibility (K_{LF}) of the tagged zone and non-tagged zone and the different tracer size fractions post deployment, pre rainfall, when tracer was used with a sandy loam, clay loam and silt loam soil. The box plot and whiskers represents the 5th and 95th percentile.

After the simulated rainfall, the mean magnetic susceptibility of the tagged zone had decreased in all soils, and across all tracer size fractions, by between 8 and 45 %. The observed increase in magnetic susceptibility downslope from the tagged zone was between 6 and 2121 %, with the exception of the top box section in the sandy loam soil which recorded a mean decrease of 4 %. The fine tracer fractions appear more erodible than the coarse tracer fractions (Figure 41).

The contribution of the tagged zone to the run-off was determined by separating the tracer particles from the collected sediment. When the tracer was used with the sandy loam and silt loam soil, the contribution of the tagged zone increased as the particle size reduced. This was not observed when the tracer was used with the clay loam soil (Figure 41). When the tracer was used with the clay loam soil the contribution of the tagged zone to the run-off was low (< 0.1 g). Further, the contribution of the tracer to the run-off sediment slightly increased as particle size increased. The mean contribution of the tagged zone to the sediment was 0.8 ± 0.4 %, 0.1 ± 0.2 % and 3.2 ± 2.3 % for the sandy loam, clay loam and silt loam soils respectively. The percentage of the material within the soil box which is tracer is 0.5 %.

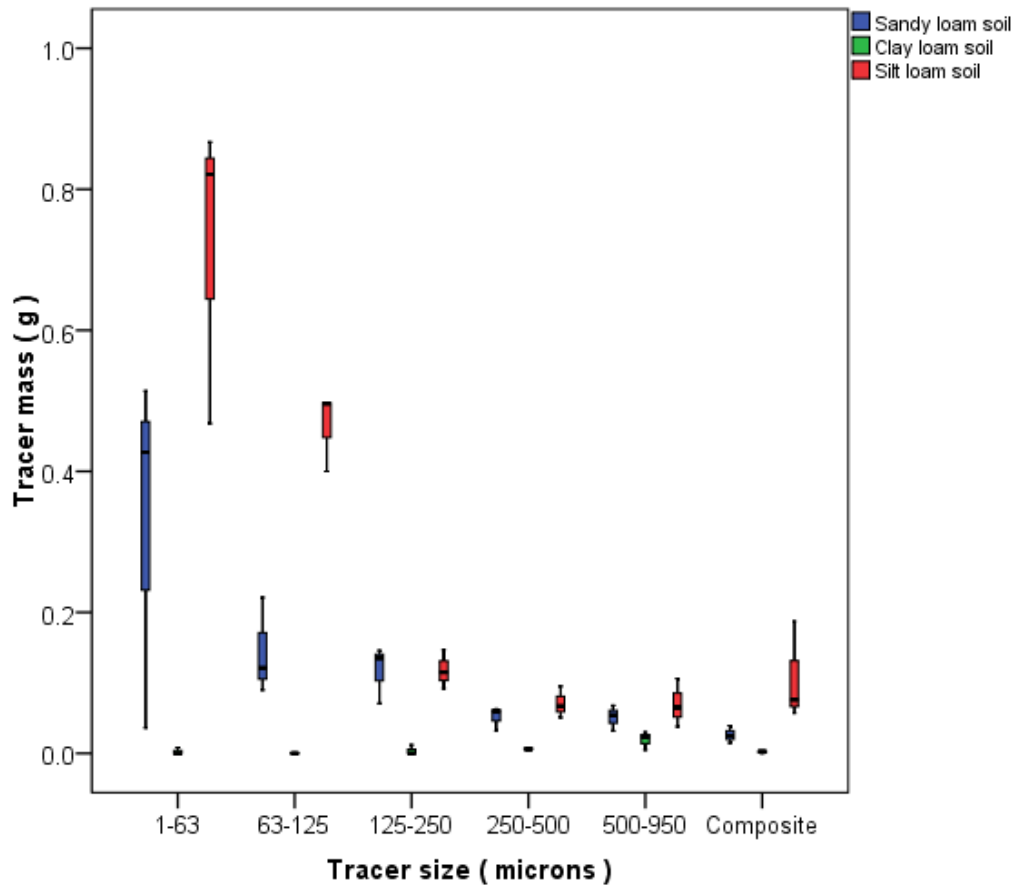


Figure 41: The mass of tracer (g) recovered from the captured sediment during soil box experiments. The box plot and whiskers represents the 5th and 95th percentile.

The use of magnetic susceptibility to estimate soil loss was evaluated (equation 13). The estimated soil loss was compared with the measured soil loss captured in the run-off at the bottom of the soil box (Figure 42, 43 and 44). It was anticipated that variance between the estimated soil loss, and measured soil loss, would be observed. This was hypothesised due to the logarithmic scale of the response to depth and the variance of the magnetic susceptibility of different tracer size fractions and the different soil types. The mean soil loss observed during rainfall simulations was 14.1 ± 9.1 g, 6.2 ± 3.5 g and 7.7 ± 4.6 g for the sandy loam, clay loam and silt loam soil respectively. This compared with the mean estimated soil loss was 4.7 ± 5.0 g, 12.3 ± 4.8 g and 11.0 ± 8.7 g for the sandy loam, clay loam and silt loam soil respectively. Figure 42, 43 and 44 illustrate the relationship between soil losses derived from changes in magnetic susceptibility and measured soil loss. These data indicate changes in magnetic susceptibility can be used to

provide an estimation of soil loss, but tracer content data are required to quantify soil loss.

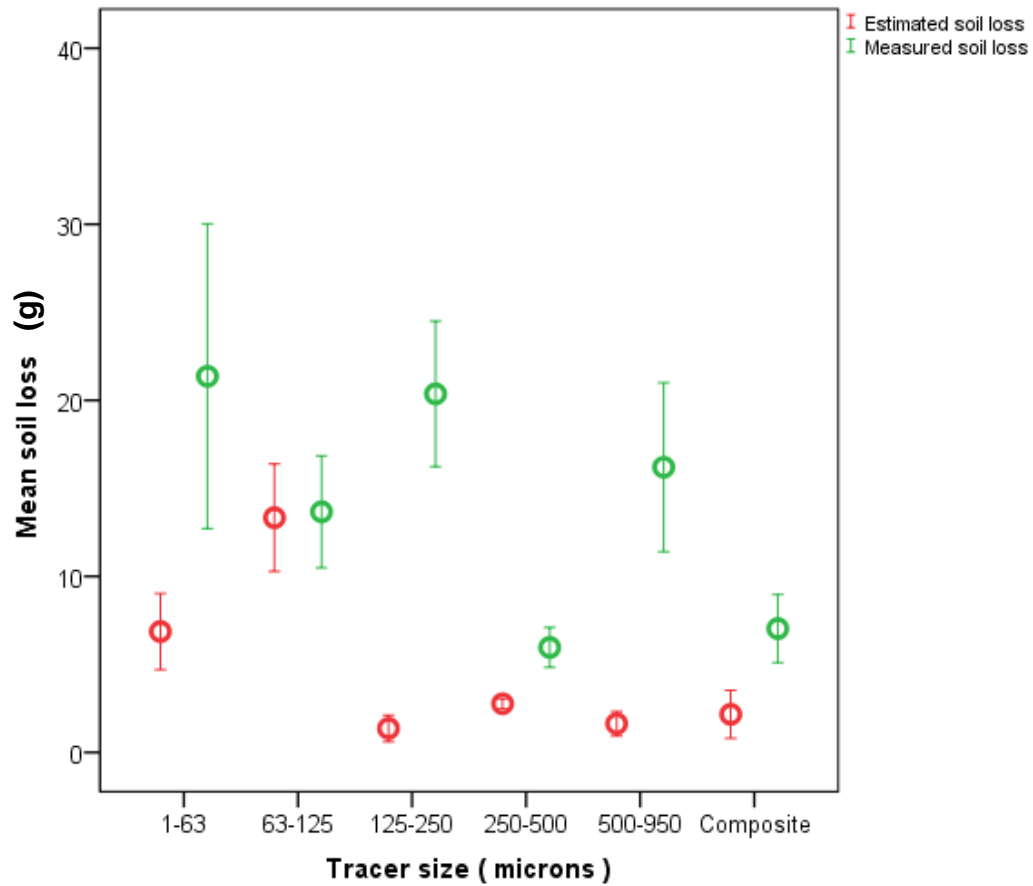


Figure 42: The measured soil loss vs soil loss estimated from the change in magnetic susceptibility values within the tagged zone converted to soil loss from equation 2 when tracer was used with the sandy loam soil. The markers indicate the mean of three replicates; the whiskers indicate the standard error.

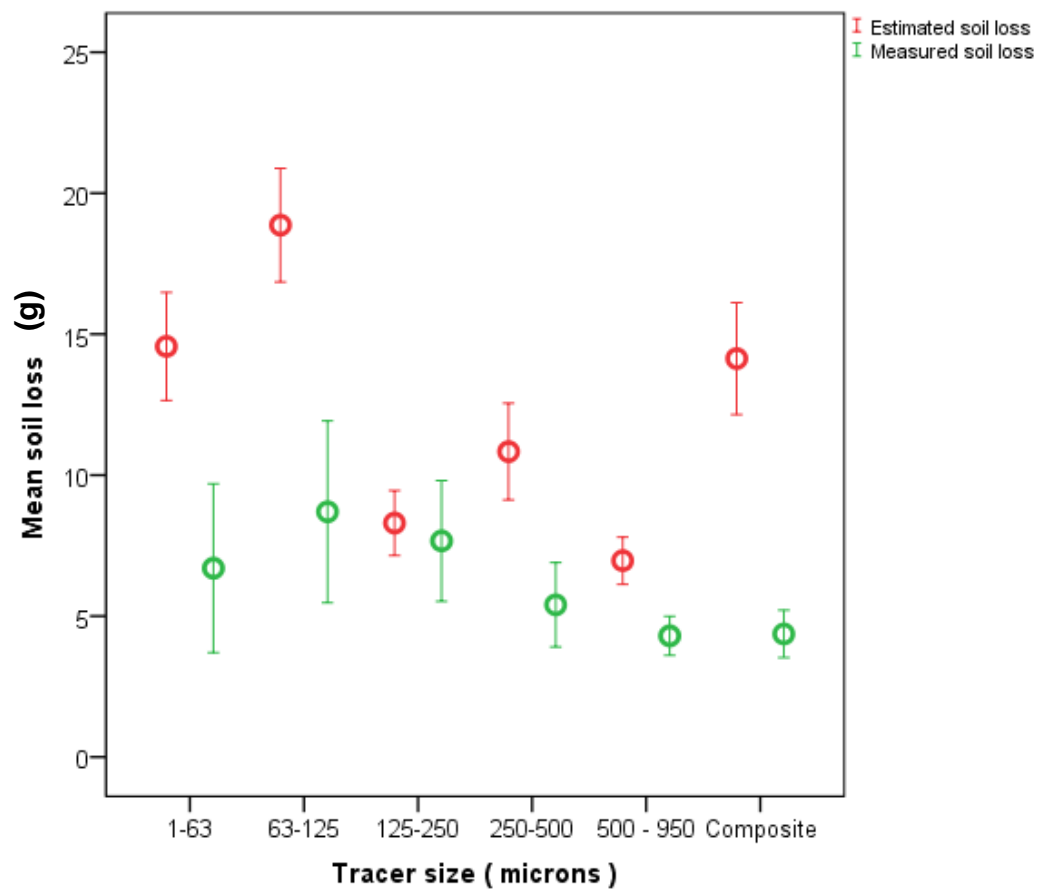


Figure 43: The measured soil loss vs soil loss estimated from the change in magnetic susceptibility values within the tagged zone converted to soil loss from equation 2 when tracer was used with the clay loam soil. The markers indicate the mean of three replicates; the whiskers indicate the standard error.

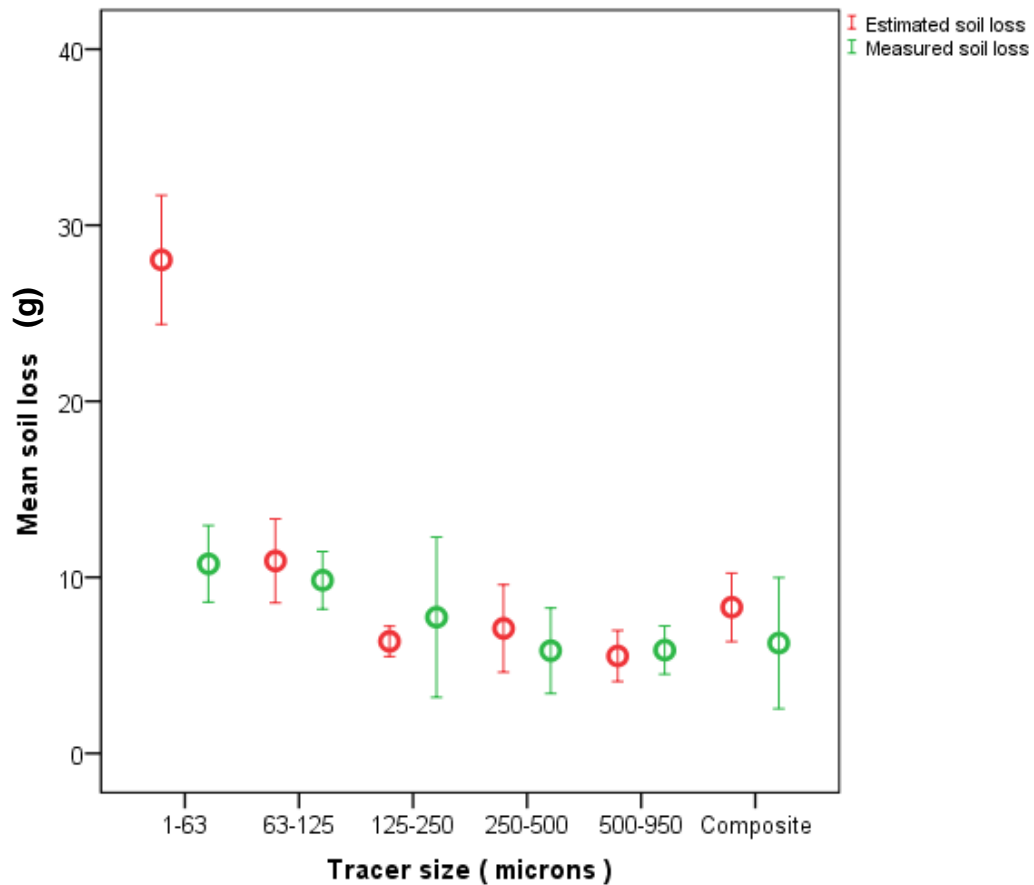


Figure 44: The measured soil loss vs soil loss estimated from the change in magnetic susceptibility values within the tagged zone converted to soil loss from equation 2 when tracer was used with the silt loam soil. The markers indicate the mean of three replicates; the whiskers indicate the standard error.

6.4.2. Field experiments

The total rainfall recorded at Winton Hill Farmstead, Cumbria, during deployment of tracer was 56.1 mm with a peak rainfall intensity of 6.8 mm hr, occurring between the third and fourth sampling campaign. Determination of soil loss derived from the tracer mass data (equation 14-17) (Figure 45) and magnetic susceptibility data (equation 13) (Figure 46) showed depletion through time via erosion at each deployment zone. No significant difference in soil loss was observed between values derived from magnetic susceptibility data and tracer mass data ($n = 8$, $p > 0.05$). The regression plot indicates approximately $> 10,000$ mm of rainfall would be required to erode all tracer deployed at the tracer plots from the hillslope (Figure 47).

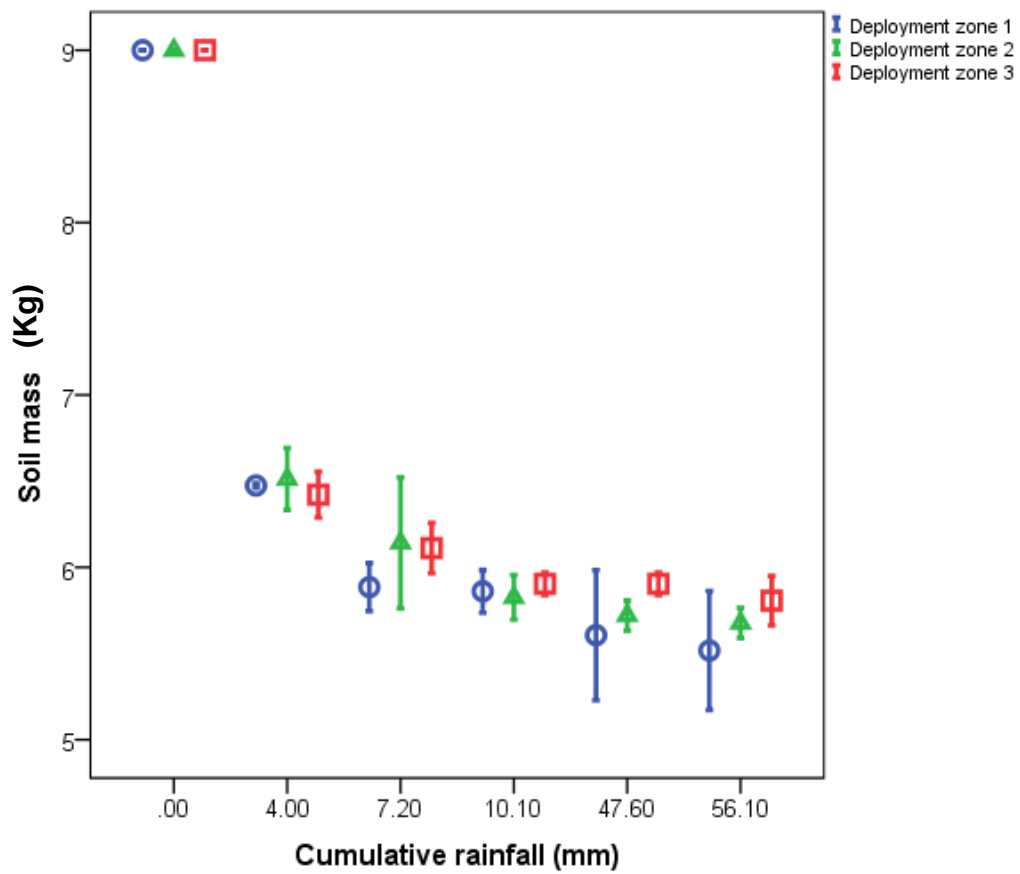


Figure 45: The mean soil loss for each deployment zone derived from tracer content values derived from equations 14-17. The markers indicate the mean of three replicates; the whiskers indicate the standard error.

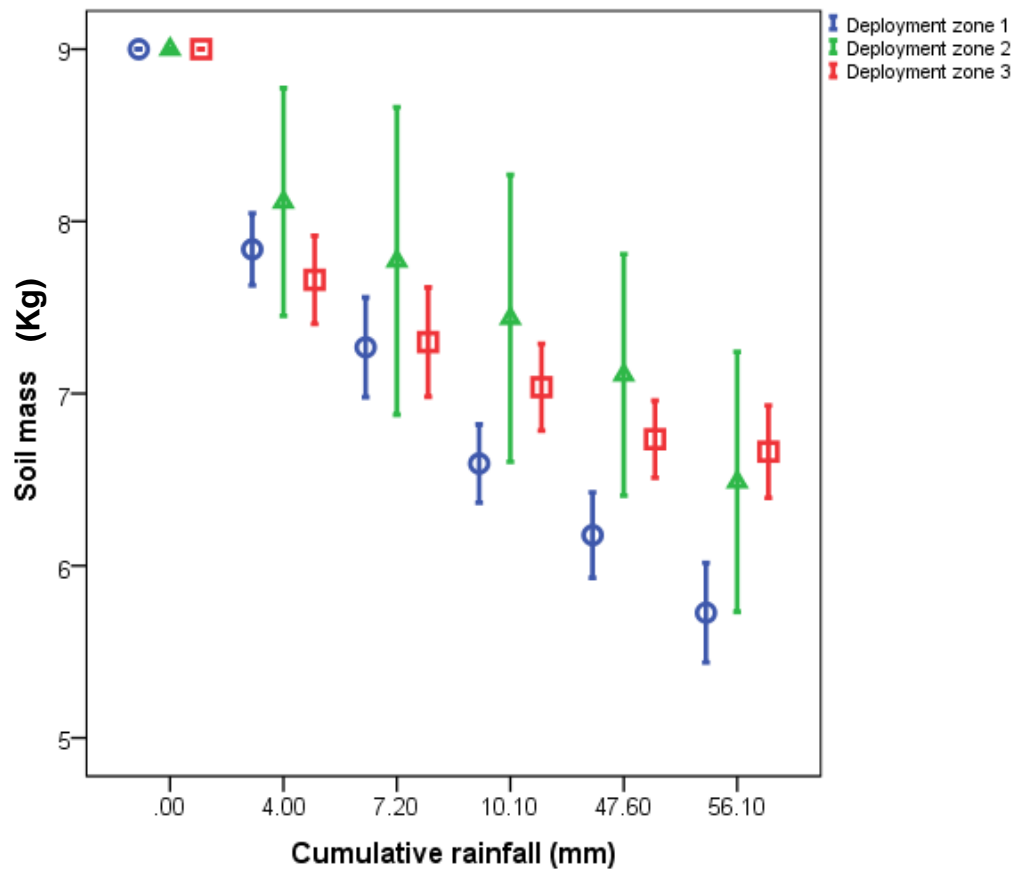


Figure 46: The mean soil loss for each deployment zone derived from changes in magnetic susceptibility pre and post rainfall event derived from equation 13. The markers indicate the mean of three replicates; the whiskers indicate the standard error.

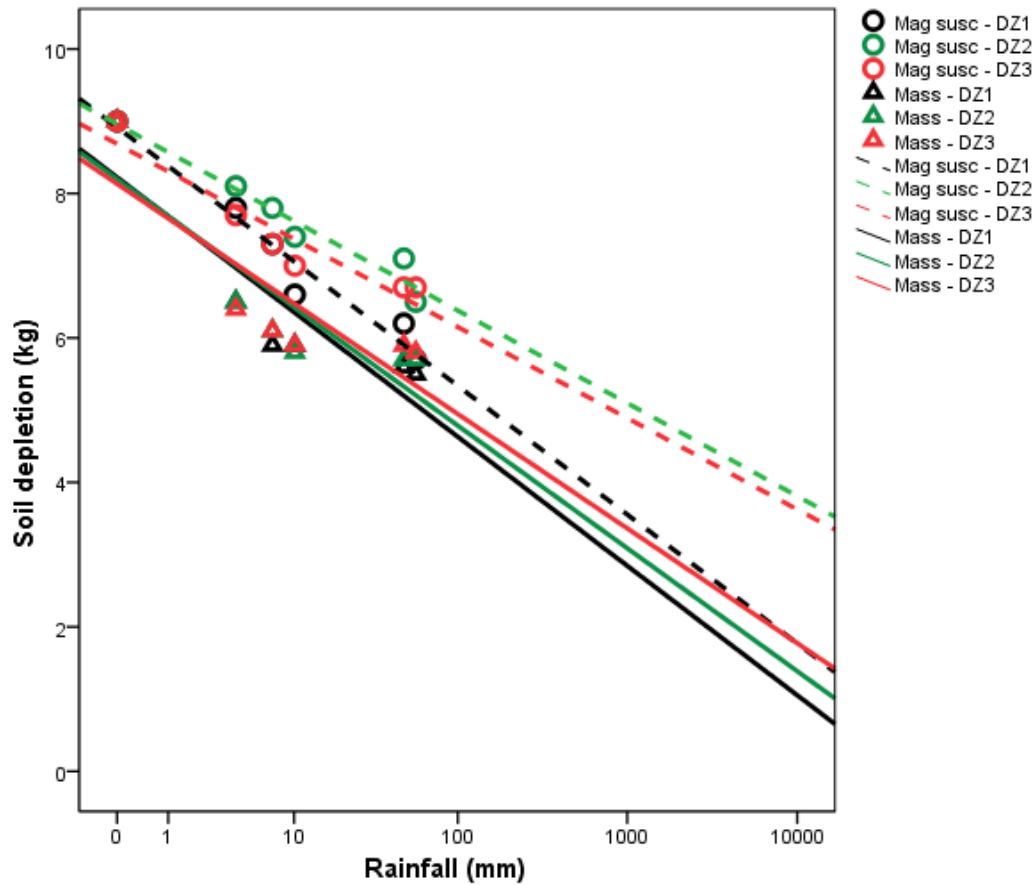


Figure 47: The mean soil depletion of each deployment zone derived from changes in magnetic susceptibility and tracer mass. A regression line for each deployment zone is added.

The mean soil loss derived from changes in magnetic susceptibility was 3.3 ± 0.5 kg, 2.5 ± 1.3 kg and 2.3 ± 0.5 kg¹. The mean soil loss derived from tracer mass was 3.5 ± 0.6 kg, 3.3 ± 0.2 kg and 3.2 ± 0.2 kg, from deployment zone 1, 2 and 3 respectively (Table 9). The mean soil loss from each plot ranged from 27 – 42 %, resulting in a mean erosion rate of 0.05 ± 0.01 kg m².

Table 9: Total soil loss and erosion rate per plot derived from the magnetic susceptibility values (equation 13) and tracer content values (equation 14-18).

Soil loss (Kg)									
Plot (n)	Plot 1	Plot 2	Plot 3	Plot 4	Plot 5	Plot 6	Plot 7	Plot 8	Plot 9
Slope angle (%)	4.6	4.6	4.6	6.3	6.3	6.3	7.6	7.6	7.6
Derived from magnetic susceptibility	2.7	3.7	3.3	1.2	2.5	3.8	2.7	2.5	1.8
Derived from tracer content	3.3	3.0	4.1	3.4	3.2	3.4	3.5	3.2	3.0
Difference	0.6	0.7	0.8	2.2	0.7	0.4	0.8	0.7	1.2
Erosion rate (Kg m ² per mm of rainfall)									
Derived from magnetic susceptibility	0.05	0.07	0.06	0.02	0.05	0.07	0.05	0.04	0.03
Derived from tracer content	0.06	0.05	0.07	0.06	0.06	0.06	0.06	0.06	0.05
Difference	0.01	0.02	0.01	0.04	0.01	0.01	0.01	0.02	0.02

6.5. Discussion

The data generated from the laboratory experiments indicated that the dual-signature tracer is able to replicate the hydraulic properties of different particle size fractions. This enabled a range of particle size fractions to be traced within a range of soil types. The field study demonstrated that the dual

signature tracer can be monitored, within the field, across a time series of rainfall/erosion events. Therefore, dual-signature tracer shows potential in quantifying short-term, event-driven, soil loss within the field. The described methodology utilised multiple sampling techniques to provide a large-volume of robust empirical data which can improve our understanding of erosion rates and processes.

The tracer: afforded easy, inexpensive measurements; was distinct within soil; did not interfere with sediment transport; was able to trace different particle size fractions; and provided two tracer signals; meeting the criteria proposed by Zhang et al. (2001). The magnetic signature enabled rapid determination of tracer content data using magnetic susceptibility (Guzman et al., 2013), as the mean magnetic susceptibility of the tracer particles, $\sim 600 \times 10^{-8} \text{ m}^3 \text{ kg}^{-1}$ was found to be ~ 50 times higher than that of the native soils. The closely matched hydraulic properties of the tracer and native soil combined with the results of the paired laboratory and field testing of the tracer, provided confidence that tracer movement replicated size specific transport processes within a range of soil types, thus tracer loss can be considered to represent soil loss. Fine and coarse tracer size fractions were successfully deployed, monitored and recovered from the soil. This is important as transport regimes are linked strongly to particle size, reflecting size-specific erosion processes (Armstrong et al., 2012). Size-selective tracers for a given particle or aggregate size, and size-selective transport by erosion, are two recurrent issues in sediment tracing studies (Guzman et al., 2010), and non-selective transport is often assumed, rather than tested (Zhang et al., 1998). Within the soil box, a decrease in tracer content within the run-off sediment was observed for two soils as particle size increased. This replicated known transport processes where different tracer size fractions are preferentially eroded (Rickson, 2014). When the tracer was used with the clay loam soil, the tracer was transported from the tagged zone, yet only small quantities reached the end of the box ($< 0.1 \text{ g}$). The tracer content in the run-off sediment slightly increased, as particle size increased, indicating that erosion and transport occurred primarily by splash and creep/rolling (Kinnell,

2009). These data demonstrated the requirement for effective clay sized tracers to be developed (Armstrong et al., 2012, Spencer et al., 2010).

Further, the data gathered from the soil box experiments suggests that when tracer is used with different soil types the tracer particles are more or less erodible. The erodibility of tracer when deployed to different soil types replicated the erodibility of the host soil i.e. the greatest tracer loss was recorded when tracer was used with the highly erodible silt loam soil; tracer loss reduced when used with the sandy loam, and reduced further in the clay loam soil. This is indicative of the tracer mimicking the behaviour of the host soil. The contribution of the tagged zone to the run-off sediment, ranged from 0.1 - 3.2 %, where the tagged zone made up 0.5 % of the total soil content within the box. This suggests the different tracer size fractions were incorporated within each soil type.

Within the field, a multi-stage sampling campaign enabled monitoring of erosion plots both spatially and temporally, critical given the highly variable nature of soil erosion (Armstrong et al., 2012, Bryan, 2000, Wood and Armitage, 1997). Also, the field sampling and analytical process was non-resource intensive enabling a large volume of data to be collected, a factor important to the success of any tracing study (Guzman et al., 2013, Black et al., 2007b). No significant difference was observed between soil loss in the field determined from magnetic susceptibility, and tracer content data. Tracer depletion values determined from magnetic susceptibility appear to underestimate soil loss per event. The depletion curves also indicated a soil erosion pattern, where depletion (mean rate of $0.05 \pm 0.01 \text{ kg m}^{-2}$) peaked after the initial event and then decreased in subsequent events of greater rainfall intensity. This is attributed to changes in surface soil cohesion (potentially a consequence of the tracer deployment methodology) resulting in the loose and fine particles being flushed from the soil surface (Fox and Bryan, 1999). This phenomenon was also observed by Haiyan et al. (2015) and could indicate a transport-limited sediment regime (Kinnell, 2005). The estimated erosion rate of between $0.042 \text{ kg}^{-1} \text{ m}^2$ and $0.062 \text{ kg}^{-1} \text{ m}^2$ when extrapolated to the hectare scale appear relatively high in comparison to average annual UK erosion rates reported in the literature (600 kg ha^{-1} for

clay soils, 1500 kg ha⁻¹ for silt soils, and 2500 kg ha⁻¹ for sandy soils (Evans, 1996). However, the regression plot indicates, from the data captured at site ~ 10000 mm of rainfall would be required to erode all tracer deployed within a single plot. The evidence suggests that increased erosion observed post deployment is likely due to the limited period of consolidation time afforded to each plot prior to rainfall. This led to increased erosion during the first event. This should be considered in future studies. In addition, it is highly likely that differences in erosion rate would be observed due to the spatial and temporal resolution of the two datasets. The study would have been improved by the addition of a Gerlach trough to compare measured and actual soil loss.

To better understand soil loss, and thus erosion rates, within an agricultural setting, data at greater spatial resolution, accounting for changes in land use, topography and soil characteristics are required (Renschler and Harbor, 2002, Renschler et al., 1999). It is recommended that, when using dual-signature tracer, detailed sampling is performed over both spatial and temporal scales (e.g. spatial scales of 1 to 1000 m, temporal scales of 1 to 365 days) dependant on study objectives. Monitoring should be undertaken using a magnetic susceptibility sensor, prior to intrusive samples being collected at the penultimate stage of the sampling campaign. This would reduce interference with the system, and related sample analysis costs, further improving the methodology. This methodology has the potential to be adapted in future studies to delineate sediment transport pathways, assess mitigation measures and determine source-sink areas.

6.6. Conclusion

This study has tested a dual signature tracer within controlled laboratory experiments and applied it within the field. The soil box experiments showed that a range of particle sizes can be traced within a variety of soil types, and that the erodibility of the tracer simulated that of the host soil. The soil box data demonstrated the requirement for effective clay sized tracers to be developed. During the soil box experiments variance between the measured soil loss, and estimated soil loss, derived from changes in magnetic susceptibility, was observed. However, at the field scale no significant difference between the soil loss derived from changes in magnetic

susceptibility and tracer content data was observed. This suggests that from changes in magnetic susceptibility, soil loss can be estimated. However, further work is required to understand the effect of multimodal particle size distributions on magnetic susceptibility in the field, to enable the quantification of an erosion rate, solely from magnetic susceptibility data. The methodology outlined enabled a large-volume of data to be collected. This potentially could enable future studies to work at a greater spatial and temporal resolution, a factor important to improving our understanding of soil erosion rates across the landscape. Overall, the results suggest that dual signature tracer shows great potential as a tracer of soil. This study provides baseline data for future academic or industry-based soil tracing studies.

7. Monitoring Wave-Driven Sediment Transport During High-Energy Events Using a Dual Signature Tracer – A Case Study from Scarborough, North Yorkshire UK.

7.1. Summary

Shoreline management decisions relating to the transport of sediment are often based solely upon physical and empirical modelling, yet there is a dearth of calibration data. Without effective model calibration, through field data collection, uncertainties remain surrounding these transport models. Here, the transport pathway of wave-driven sediment in a complex shoreline setting (affected both by natural and anthropogenic influences) is investigated using a dual-signature tracer. The tracer comprises coated natural mineral kernels with two tracer signals – fluorescence and ferrimagnetism. The mass of sediment mobilised during the first wave event was substantial mobilising and dispersing an estimated 21 – 108 kg of sediment from the three deployment zones (each of 10 m²). Further, sediment transport at the site was found to be extensive spatially, with multidirectional transport both in the alongshore and cross-shore directions observed, highlighting the unpredictable nature of sediment transport. The results demonstrated the effectiveness of active sediment tracing to provide field data that could be used for sediment transport model calibration. Further, this study identified a robust field methodology associated with the dual-signature tracer, which enabled the geospatial movement of sediment to be monitored.

7.2. Introduction

Within the United Kingdom (UK), a strategic planning framework for coastal management has been developed to progress solutions (Pontee and Parsons, 2009) to manage beaches in a sustainable fashion (Jennings, 2004). Shoreline management is critical to this (Leafe et al., 1998), and must be based on an understanding of coastal processes, including sediment transport (Mason and Coates, 2001).

Numerous methods are used to monitor sediment transport on the beach face, and within the coastal zone, including point measurement sampling, using sediment traps (Komar, 1969, Mahaut and Graf, 1987, Maher

et al., 2009., Bianchi, 2007, Bertrand-Krajewski et al., 1998); micro scale remote sensing techniques, using optical back scatter (OBS) sensors (Downing et al., 1981), and/or acoustical back scatter (ABS) sensors (Vincent et al., 1991); and x scale remote sensing techniques such as bathymetric, topographic and LIDAR surveys (Hesham M. El-Asmar 2002, Montgomery, 2007). In general these techniques struggle to define sediment transport trends, as sediment transport is highly variable, both spatially (Anderson et al., 2014), and temporally (White, 1998).

In the absence of measurements, sediment management decisions are based on empirical formulae, analytical theories and engineering judgement (Nearing et al., 1989, Wang et al., 1995, Nino and Garcia, 1996, Ogawa and Shuto, 1981) which can be unreliable (Nearing et al., 1989, Wang et al., 1995, Nino and Garcia, 1996, Ogawa and Shuto, 1981). Computational, physical and empirical modelling of sediment transport has been conducted extensively (Booth and Jackson, 1997, Carr et al., 2000, Chen and Adams, 2007, Crabill et al., 1999, Kozerski and Leuschner, 1999), and is considered the most effective tool to inform long term management plans (Winn et al., 2003). However, to ensure that the models provide an accurate representation of sediment transport processes, they must be evaluated against field data (Ciavola et al., 1998, Szmytkiewicz et al., 2000, Davies et al., 2002). Given the poor spatio-temporal resolution of point measurement and remote sensing techniques, sediment tracing can provide a field tool for monitoring of the spatio-temporal distribution of sediment on the beach face e.g. Ciavola et al. (1997), Ciavola et al. (1998), Carrasco et al. (2013), Ingle (1966), Russell (1960a).

Sand tracers delineate sediment transport pathways effectively (Black et al., 2007b). A range of sand tracers primarily derived of natural sand or synthetic tracers with identifiable signals added, has been used (Black et al., 2007b). Fluorescent sand tracers are most commonly used to evaluate littoral drift (White, 1998, Cochran, 1977, Teleki, 1966, Carrasco et al., 2013, Vila-Concejo et al., 2004). Magnetic (Van Der Post et al., 1995), and irradiated tracers have also been successfully used (Drapeau et al., 1991, Cheong et al., 1993).

Sand tracing studies often suffer from excessive dilution, resulting in insufficient tracer being recovered for analysis (Black, 2012). Excessive dilution is especially a problem in studies examining sediment transport over greater spatial and temporal scales and during high-energy transport events e.g. Ciavola et al. (1998), Courtois and Monaco (1968), Collins et al. (1995). Also, when working within complex industrialised settings the presence of pollutant particulate material within the system (Sharma and Sharma, 1994, Eisma, 1993) is, considered ‘noise’ when conducting a sediment tracing study (Black et al., 2013). This has limited the application of active tracers within industrialised settings. Yet, data collected from these environments are crucial to developing robust sediment transport models (Schoones and Theron, 1995). Thus, there is a need for a tracing methodology that is able to monitor tracer particles over extended spatial and temporal scales, in order to resolve beach sediment transport in high-energy, complex environments. Such resolution of sediment movement will also enable validation of existing transport models.

This study aims to test the use of a dual-signature sediment tracer. The objectives are: 1) evaluate the utility of a dual-signature tracer to investigate the sediment transport pathways on the beach face, during real wave conditions; 2) validate the numerical and physical models of sediment transport at the site.

7.3. Site Description and Oceanographic Setting

This study was undertaken in Scarborough South Bay, Yorkshire, UK. South Bay is a 1.8 km bay, with a wide sandy foreshore (~150 m at the widest point at mean low water) in the north which progressively lowers and narrows, ending in a rock shore platform in the south (Figure 48). In general, the wind in the North Sea is restricted by the land masses of Western Europe and the east coast of the UK. Storm tracks are predominantly from west to east (Lamb and Frydendahl, 1991), generating fetch-limited waves of short (< 9 s) and long period (> 9 s), from a dominant wave approach from the north and north east, with significant but reduced frequency of exposure from directions south of east (Haskoning, 2007). A natural headland, commercial harbour and local bathymetry (through diffraction) all tend to re-align wave approach to a shore-

parallel orientation. Additionally, the headland and harbour provide shelter from the dominant north easterly wave direction, reducing inter-tidal longshore transport (Haskoning, 2007). However, through both diffraction of the incoming waves and wave approach from a southerly aspect, net transport of sediment is observed contrary to the general sediment drift within the region. Within the study area, numerical (Wallingford, 2001) and physical modelling (Wallingford, 2002) have identified that sediment transport is bi-directional (Haskoning, 2007).



Figure 48: Study area and location. The location of each tracer deployment zones (DZ 1-3) is marked. The locations of the core samples collected is also marked, the tracer content values determined at each of these locations were interpolated in figure 5 to provide a time step of tracer distribution across the beach face.

7.4. Methodology

Three bulk sediment samples were collected from the upper, mid and lower beach face at low water using a random sampling technique. For each

of the samples collected a subsample was analysed to determine the specific gravity using an adapted pycnometer technique (Germaine and Germaine, 2009), and the particle size distribution determined using a Mastersizer 2000 laser diffraction particle sizer (Malvern Instruments Ltd, UK). The samples were also tested to determine the mass fraction of naturally occurring magnetic particles and for the proportion (%) of fluorescent particles. In total, 750 kg of chartreuse coloured (visually green-yellow); dual signature tracer comprising a coated natural mineral (sand) kernel with two applied tracer signals (fluorescence and ferrimagnetism) was manufactured (Partrac Ltd, UK) that strongly matched the properties of the native sediment (Table 11). Tracer was deployed in three batches of 250 kg at three locations on the beach face, hereafter referred to as deployment zones, *DZ1*, *DZ2* and, *DZ3*, over three consecutive days during a period of low wave action (mean wave height: 0.9 m, wave period: 4 s, wave direction 210 degrees re true north), in order to assess wave driven sand transport across the beach face. *DZ1* was positioned at 54° 27.906 N, 00° 39.753 W; *DZ2* at 54° 27.926 N, 00° 39.741 W, and; *DZ3* at 54° 28.070 N, 00° 39.665 W. At each location a trench, 0.04 m deep, 1 m wide and 10 m long was dug in the upper beach face ~5 m below the neap high water mark. Approximately, 50 % of the native sand removed during the excavation of the trench was admixed with tracer in a cement mixer on site (50/50 ratio), and 3 - 5 L of seawater added. The tracer/native sand admixture was then carefully introduced to the trench using a shovel. The admixture was then raked flush with the sediment surface (Figure 49 and 50). The tracer was deployed at a density of $\sim 1.46 \text{ g cm}^3$ determined through the collection of random cores post - deployment.



Figure 50: Tracer deployed in a strip cross-shore on the beach face.



Figure 49: Tracer deployed on the beach face.

Measurements and sampling were conducted over a 54-day period, 1, 2, 3, 7, 14 and 54 days following the first wave event, using surface magnetic susceptibility measurements, qualitative assessment for tracer presence using blue light lamp inspections, and direct retrieval of sediment samples, to provide independent and complementary data and optimise tracer recovery and enumeration.

To assess the mass of sediment mobilised from each deployment zone during the first event, surface measurements of magnetic susceptibility were made. Magnetic susceptibility is defined as the degree of magnetisation of a material in response to an applied magnetic field (Oldfield et al., 1999). Measurements were taken across the deployment zones using a grid with spacing of 1 m². A measurement was taken at the centre of each grid node, positioned using a Differential Global Positioning System (Trimble Ltd, UK). All measurements were taken using a MS2 magnetic susceptibility meter with a MS2D surface scanning probe (operating frequency 0.958 kHz, depth of response 50% at 15mm, 10% at 60mm) and a MS2 probe handle (Bartington Instruments Ltd, UK). One measurement was made at each grid node, across each deployment zone, prior to, and following tracer introduction. Following the first wave event measurements were re-measured at the same location and the difference in magnetic susceptibility determined (Figure 49). To calculate sediment loss (L) from the change in magnetic susceptibility an adapted version of a conversion model described in Guzman et al. (2013) was used:

$$L = \frac{m}{a} \Delta x \quad (19)$$

Where m is the mass of tracer deployed, a is the tagged area and x is the difference in magnetic susceptibility.

Blue light (395 nm) torch inspections were used to qualitatively assess the spatial distribution of tracer on the beach face. Night-time, shore-normal transects were conducted at low tide, following one tidal inundation, after tracer introduction to each deployment zone. This technique was employed to monitor sediment transport during a period of low wave action and to assess

the spatial distribution of tracer particles following the spring – neap tidal cycle (Figure 51).



Figure 51: Blue light torch surveys conducted at night to qualitatively assess the spatial distribution of tracer on the beach face.

Sand was sampled from the upper, mid and lower beach face along shore-normal transects, at 30-50 m spacing, resulting in the collection of 526 shallow core samples. Sand samples were collected by placing a survey quadrat (10 cm²) on the sediment surface and manually excavating to the mixing depth determined from an exploratory trench cut into each deployment zone, following the first wave event. The tracer acts as a horizon marker (King, 1951, Inman and Chamberlain, 1959a, Komar, 1969). The mixing depth was identified at 5 cm; all samples were excavated to a depth of 6 cm.

Positions were determined using a Differential Global Positioning System (Trimble Ltd, UK and Garmin Ltd, UK). Wave height (m), period (s), and direction (degrees re true North), were derived from 30 minute interval spectral data from a wave buoy Directional WaveRider Mk III buoy (Datawell, BV, Netherlands) located at 54° 17.598' N, 00° 9.077' W managed by the North East Coastal Observatory.

The tracer content of each sand sample was determined using an adapted spectrofluorimetric technique (Carey, 1989). Four 'dose response', calibration curves of fluorescence intensity versus assumed dye concentration were developed (Figure 52). These calibration curves enable measurements of fluorescence (probe reading in volts) to be empirically related first, to tracer dye concentration and then to tracer dry mass (g). It is important, to account for the 'quenching effects of any native material which acts to reduce the fluorescent intensity of the sample (Lakowicz, 2006). Due to the significant non-fluorescent magnetic background (from naturally - occurring magnetic minerals present at the site). Dose response curves were thus prepared with tracer and native material, collectively (Table 10). The magnitude of any quenching effect is related to the dry mass of the native material. Thus three individually tailored dose response curves were prepared in order to enumerate the tracer mass from the samples collected. One dose response curve represented samples of 'high' native material load: one of 'intermediate'; and one of 'low' native material load (Table 10). During analysis, the appropriate calibration curve was selected dependant on the mass of background/native material present. Least-squares regression analysis

(Fowler et al., 1998) was performed on the data to generate calibration functions (Figure 52).

Table 10: Summary of the calibration (dose response) curves produced.

Description	Spiked dry tracer mass (g)	Native material mass (g)	Peak (assumed) dye concentration ($\mu\text{g l}^{-1}$)
Low material load	0.01	1.5	16.66
Intermediate material load	0.1	3.0	166.66
High material load	1.5	15	2500

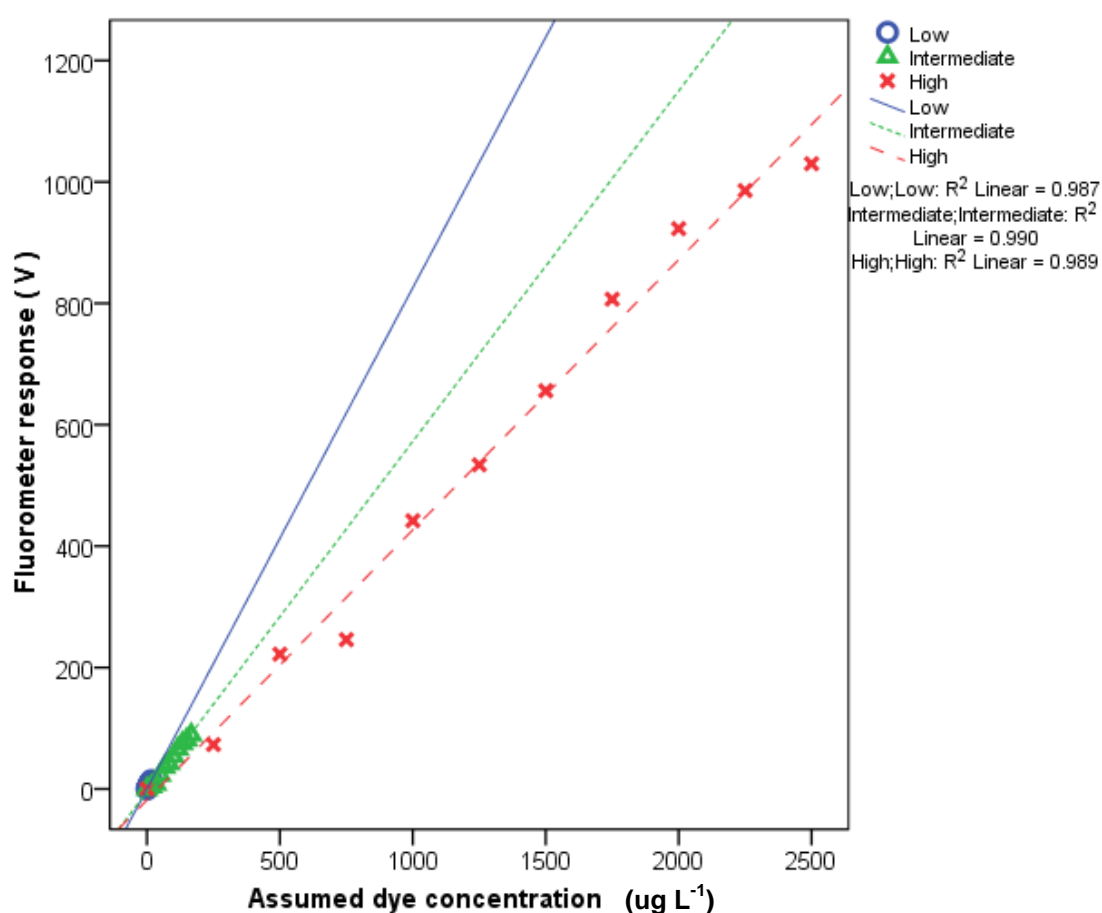


Figure 52: Calibration (dose response) curves prepared for low, intermediate, and high material loads for samples collected from the beach face.

The analyses were carried out using a Fluorosens fluorometer (Gilden Photonics Ltd, UK). An emission scan was conducted at the tracer's peak excitation wavelength (485 nm) and the response recorded at the peak

emission wavelength (530 nm). Each sample was run in triplicate and the mean value determined. To enumerate the dry mass (M , g) of tracer the respective regression equation is used to determine dye concentration (D_C) from probe response. Tracer dry mass (T_{DM}) is then calculated using the following equation:

$$T_{DM} = \left(\frac{D_C}{C_{max}} \right) T_{DMmax} \quad (20)$$

Where C_{max} is the maximum assumed dye concentration (ug L) and T_{DMmax} is the equivalent tracer dry mass value. Tracer dry mass (T_{DMmax}) values were normalised to relate to a unit area and hence reported as g m² based on the assumption that tracer content from a shallow core sample is representative of tracer concentration within the surrounding area (White, 1998, Black et al., 2007b).

Prior to analysis, the ferromagnetic tracer was recovered from its host sand using a simple magnetic extraction technique (Pantin, 1961b, Ventura et al., 2002), thereby reducing sample volume, a factor helpful practically. Briefly, the sample was oven dried at 105 °C for 24 h, then transferred to a pestle and mortar and gently disaggregated. The sample was then smoothed to an approximately granular monolayer on a large piece of white cardboard and a permanent, 11,000 Gauss magnet was scanned across the sample at a distance of 2-3 mm, facilitating separation of magnetic particles. This procedure was repeated, with intermittent cleaning and recovery of the particles from the magnet surface, until no further magnetic particles were extracted.

7.4.1. Statistical analyses

SPSS Statistics 20 (IBM, 2014) was used for all analysis. A paired t test was used to assess for significant differences between the hydraulic properties of the tracer, and native sediment, and the magnetic susceptibility of the deployment zones following tracer deployment.

7.5. Results

The tracer's hydraulic characteristics were not significantly different from those of the native sediment ($n = 3$, $p = > 0.05$) (Table 11, Figure 53).

The tests for the magnetic and fluorescent attributes of the native sediment indicated the presence of background magnetic material, but no naturally occurring fluorescent particles. These data demonstrated that the tracer strongly matched the native sediment and the tracer was identifiable within the environment, due to the tracer signals, fluorescence and ferrimagnetism.

Table 11: Summary of the physical – hydraulic characteristics of the tracer particles and the native sediment.

Material	D10 micron	D50 micron	D90 micron	Specific gravity (kg m ³)	Significant difference	Particles magnetic (%)	Particles fluorescent (%)
Tracer	163	244	379	2436	No	100	100
Native material	165	260	431	2709		1.2	0

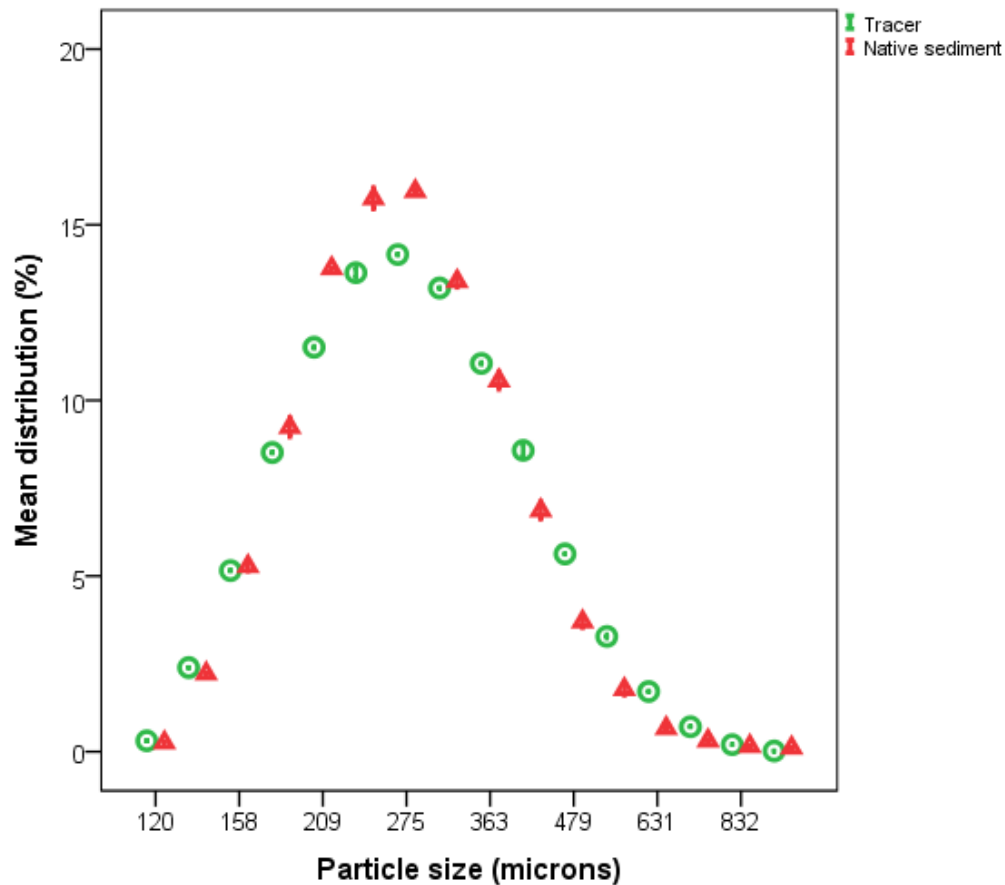


Figure 53: A comparison of the mean particle size distribution of the native sand and tracer particles. The markers show the mean and the whiskers represent the standard error.

During the study period the tidal range was 4.5 m, increasing to 6 m. High energy wave conditions were observed throughout, with a mean wave height during the study period of 1.1 ± 0.5 m, with wave heights reaching 3.1 m and not dropping below 0.3 m. The mean wave period observed was 5 ± 1 s (Figure 55). A mean wave direction of 103 ± 129 degrees re true north, was observed, with 79 % of frequency data showing waves from the N or NE quadrant (Figure 57). A yearlong summation of Metocean data captured from the directional WaveRider Mk III buoy located off the coast at Scarborough was sourced to provide comparative values from which it is possible to assess whether the wave climate observed during the observation period could be considered typical (Figure 54 and 56). The data shows that the wave climate observed during the study period could be considered ‘typical’ of significant

wave height, wave period and direction. No significant storm events occurred during the study period.

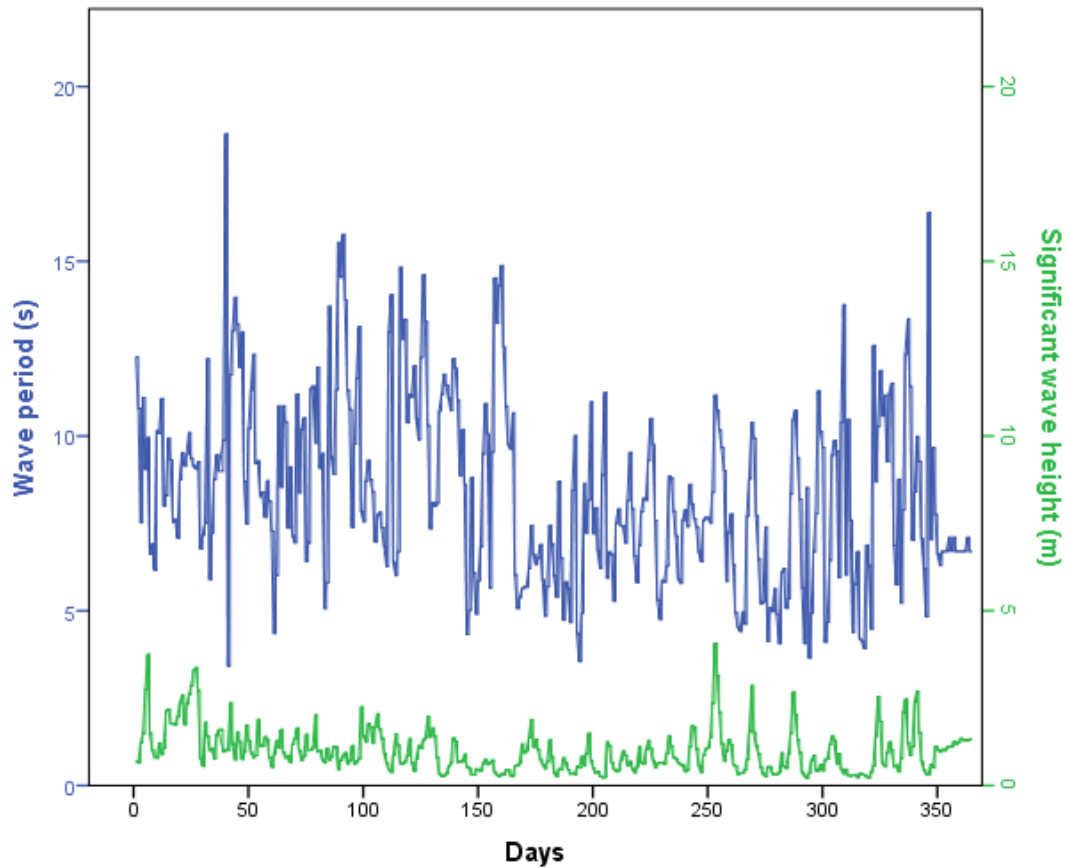


Figure 54: Significant wave height and wave period captured at the Whitby wavenet site between 4th November 2010 to the 4th November 2011 across the study duration combined with the data derived from 30 minute interval spectral data from a wave buoy Directional WaveRider Mk III buoy (Datawell, BV, Netherlands) located at 54° 17.598' N, 00° 9.077' W managed by the North East Coastal Observatory during the study period. The data collected during the study period runs from day 33 – to day 87. This data is combined to apply context to the observed metocean data collected during the study period.

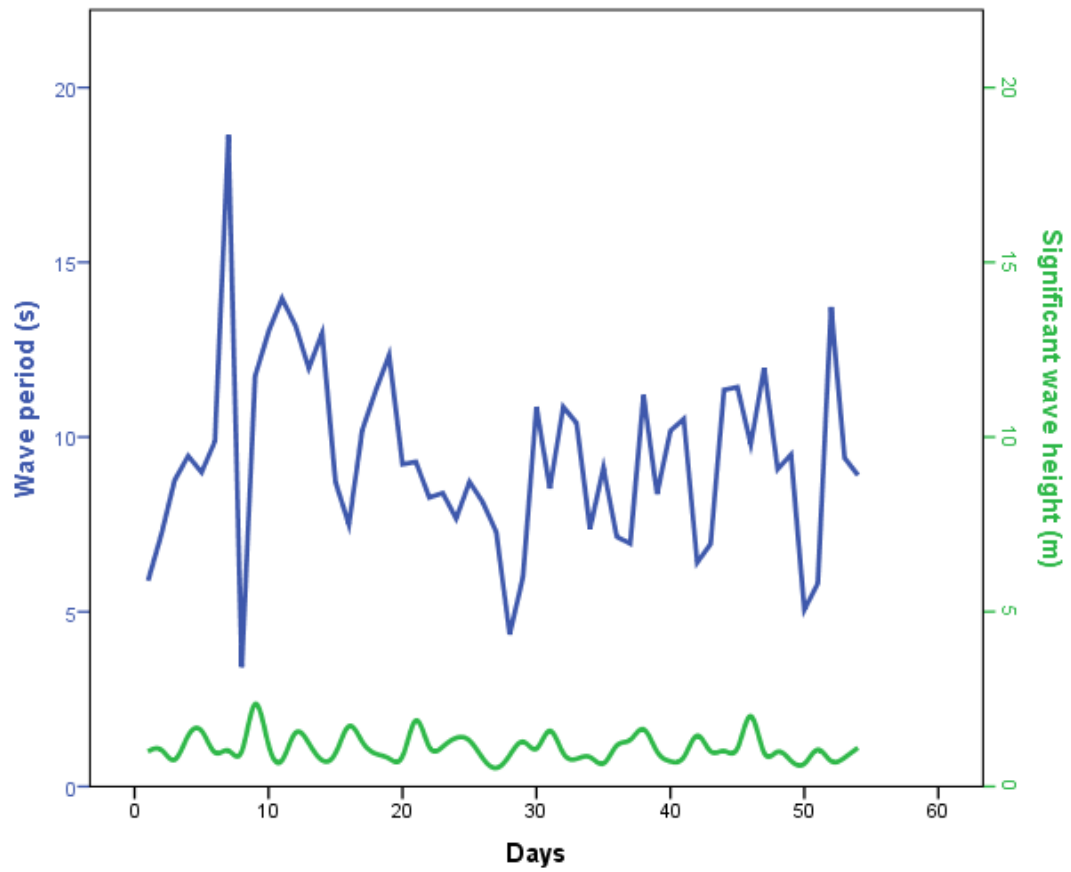


Figure 55: Significant wave height and period derived from 30 minute interval spectral data from a wave buoy Directional WaveRider Mk III buoy (Datawell, BV, Netherlands) located at 54° 17.598' N, 00° 9.077' W managed by the North East Coastal Observatory during the study period.

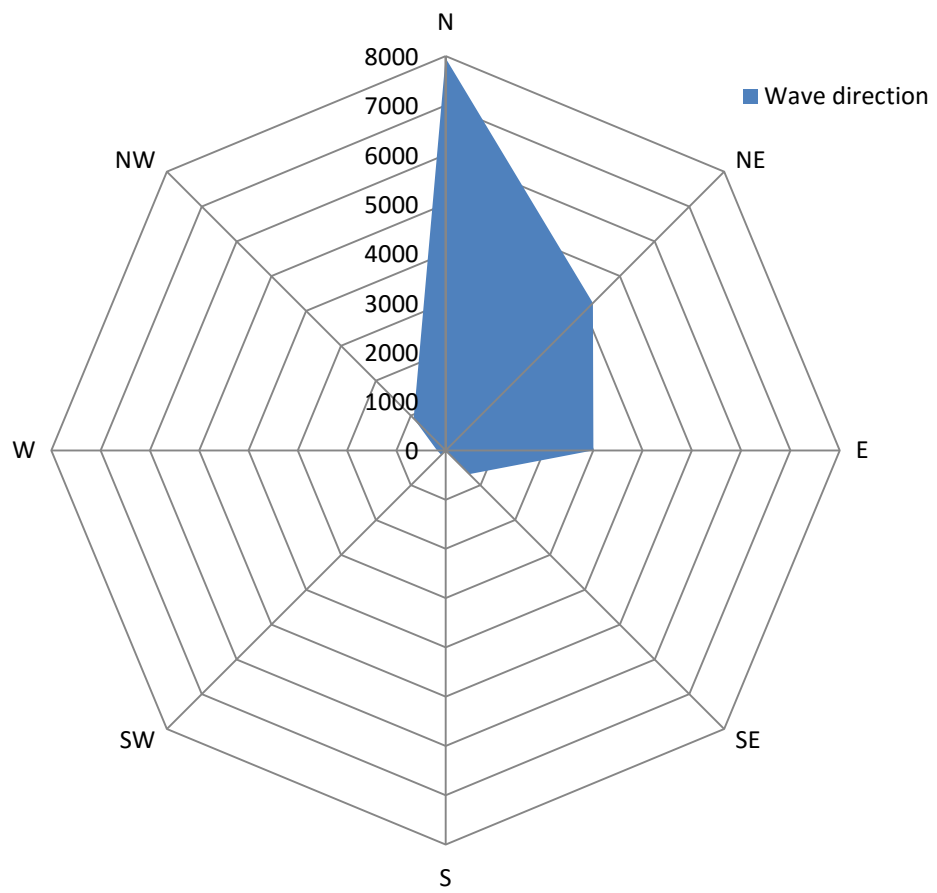


Figure 56: Wave direction (degrees re true north) frequency captured at the Whitby wavenet site from 4th November 2010 to the 4th November 2011.

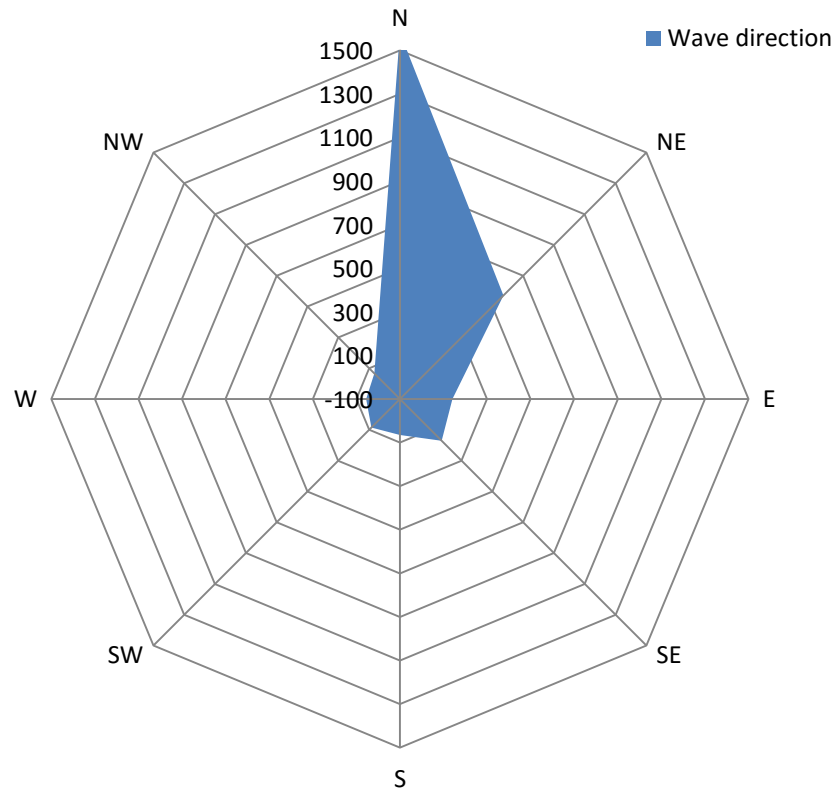


Figure 57: Wave direction (degrees re true north) frequency captured across the study duration derived from 30 minute interval spectral data from a wave buoy Directional WaveRider Mk III buoy (Datawell, BV, Netherlands) located at 54° 17.598' N, 00° 9.077' W managed by the North East Coastal Observatory during the study period.

Following deployment of tracer in each deployment zone, the mean magnetic susceptibility of the DZ's were seven times greater than that of the native sand, increasing from a mean value of $144 \pm 92 K_{LF}$ to $1004 \pm 290 K_{LF}$ ($n= 29$, $p = < 0.05$) (Figure 58).

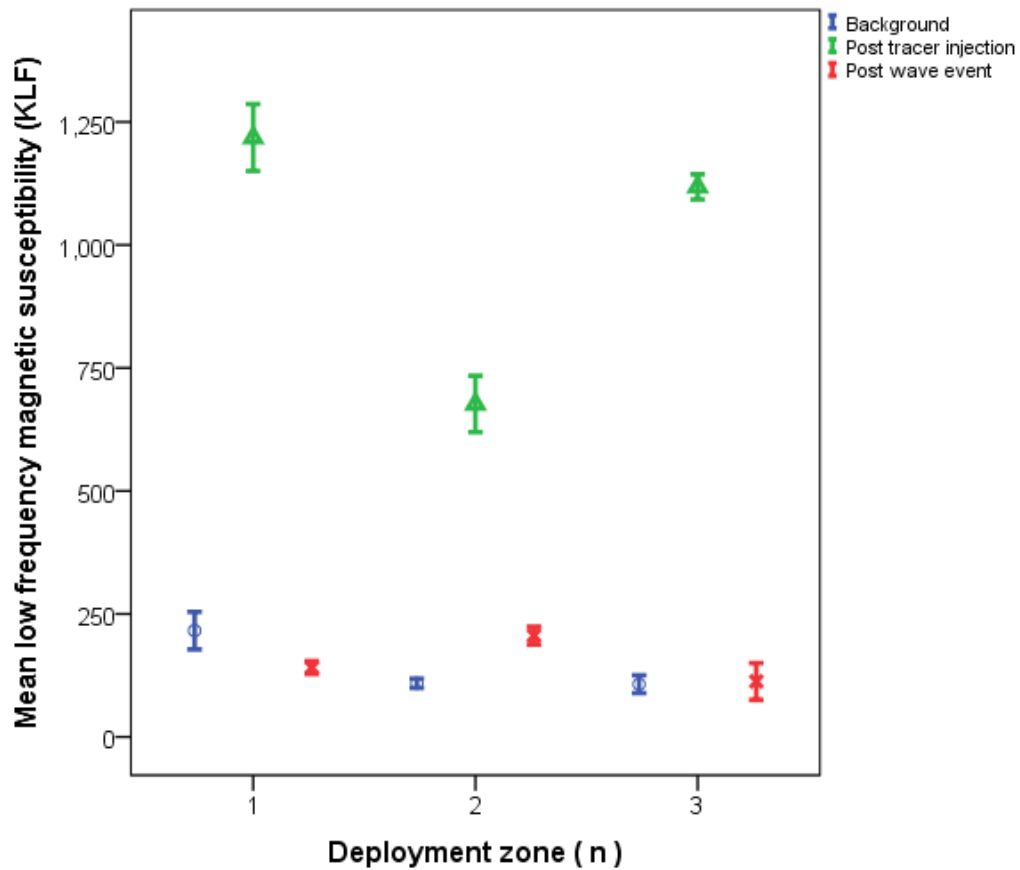


Figure 58: A comparison of the magnetic susceptibility (K_{LF}) of each deployment zone prior to tracer injection, post tracer injection and following the first wave event. The markers represent the mean and the whiskers represent the standard error.

Night - time transects with blue light torches, conducted following the first tidal inundation after, deployment of the tracer, indicated that during a period of low wave action (prior to the first wave event), net longshore transport over ~ 100m was observed in the direction of the general sediment drift found within the region (Table 12). In general, transport was localised to the source (i.e. each deployment zone). A qualitative assessment indicated that a substantial load of tracer remained *in situ* at each DZ prior to the first wave event.

Table 12: Surveyors diary notes following shore normal, night-time transects with blue light torches (395 nm) to assess the spatial distribution of tracer particles on the surface, utilising the spectral characteristics of the tracer.

Survey Description	Diary notes (approximate distance values)
Post deployment of tracer at DZ1	<p>Tracer visible on beach face, 100 m to the south, 30 m to the north and to the water's edge (70 m). A reduction in tracer concentration is observed as distance away from source increased.</p> <p>An exploratory trench within DZ1 indicated sediment reworking to a depth of 1 cm. A significant tracer concentration was visible within the exploratory core indicating tracer remained <i>in situ</i> following the initial tidal inundation.</p>
Post deployment of tracer at DZ2	Tracer observed south of deployment zone 1 and 2 through 100 m. Rapid drop in tracer concentration north of deployment zone 2. Exploratory trench in deployment zone 2 showed significant reworking to a depth of 4 cm.
Post deployment of tracer at DZ3	Tracer observed south of DZ1 and DZ2 through 100 m. Rapid drop in tracer concentration north of deployment zone 2. Tracer visible on beach surface in the vicinity of DZ3 with transport occurring both north and south over short distances (< 20 m).
Following the neap- spring tidal cycle	Tracer particles visible in low concentrations on beach surface across the majority of the beach face with increase in concentration in the upper foreshore.

The first wave event resulted in a mean wave height of 1.2 ± 0.5 m with a mean wave period of 4.4 ± 0.9 s, reaching a peak wave height of 2.4 m and

a peak wave period of 6 s, observed from a northerly direction (340 – 20 degrees re true north).

Both the magnetic susceptibility survey, and tracer mass derived from sediment samples, indicated that a significant load of tracer was mobilised by the first wave event. From the change in magnetic susceptibility (Equation 19), the quantity of sediment mobilised was estimated at 108, 21 and 101 kg from DZ1, DZ2 and DZ3 respectively. These data were reflected in the tracer content sampled from the deployment zones. Where the quantity of sediment mobilised from the deployment zone was estimated to be greatest, the quantity of tracer recovered from the respective sampling grid was least. The total tracer recovered from DZ1, DZ2 and DZ3 was 0.9, 3.1 and 0.4 g respectively.

Initial sampling of the sediment surface revealed that the first wave event mobilised and transported the tracer from the deployment zones bi-directionally (Figure 59). 48 hours after the first wave event, waves continued to be observed from a northerly direction at a mean wave height of 1.1 ± 0.5 m and mean wave period of 4.4 ± 0.8 s. The sediment samples collected from the beach face revealed continued, bi-directional transport, extending over 1 km (Figure 60).

Evaluation of the transport pathway over the remainder of the study indicated continued bi-directional transport away from the deployment zones (Figure 61, 62 and 63), with tracer sampled over the whole extent of the sandy foreshore (Figure 64). In total, 72 % of tracer was sampled from the upper beach, compared with 27 % from the mid beach, and 0.5 % from the lower beach. This demonstrates that the rate of cross - shore (i.e. offshore-directed) transport is much lower than the rate of alongshore transport (Figure 65).

As anticipated sampling of the beach face demonstrated a reduction in tracer content as distance from source (deployment zones) increased (Figure 66). Accumulation of sediment was observed in the upper foreshore and northern end of the beach (Figure 66). This demonstrated that once sediment was mobilised and transported to the north, it accumulated rapidly due to the protection of the harbour infrastructure. Comparatively, sediment transported

in the direction of the general sediment drift showed low residency times. The night time transects with blue light torches indicated sediment transport was observed to the south of the deployment zones (Table 12), yet tracer content data indicated rapidly depleting tracer concentration over time to the south of the deployment zones (Figure 60, 61, 63). Sediment transported south appears to not accumulate on the beach face with accumulation observed solely within the lee of sea wall infrastructure (Figure 60). These data have significant implications for shoreline and sediment management practices.

The system continued to be 'seeded' by each deployment zone throughout the neap-spring tidal cycle. Following 336 hours of exposure, the tracer signal decreased to the point where it was no longer possible to discern transport pathways, and the system was no longer being 'seeded' by the original deployment zones (Figure 64). Any remaining tracer had become admixed with the native beach sediment. The tracer remained identifiable within the environment up to 54 days following the initial wave event, demonstrating the potential to monitor dual-signature tracer over extended spatio-temporal scales, with subsequent re-seeding (i.e. the introduction of more tracer) to the deployment zones.



Figure 59: Geospatial distribution of tracer dry mass (g m^{-2}) 24 h after injection.

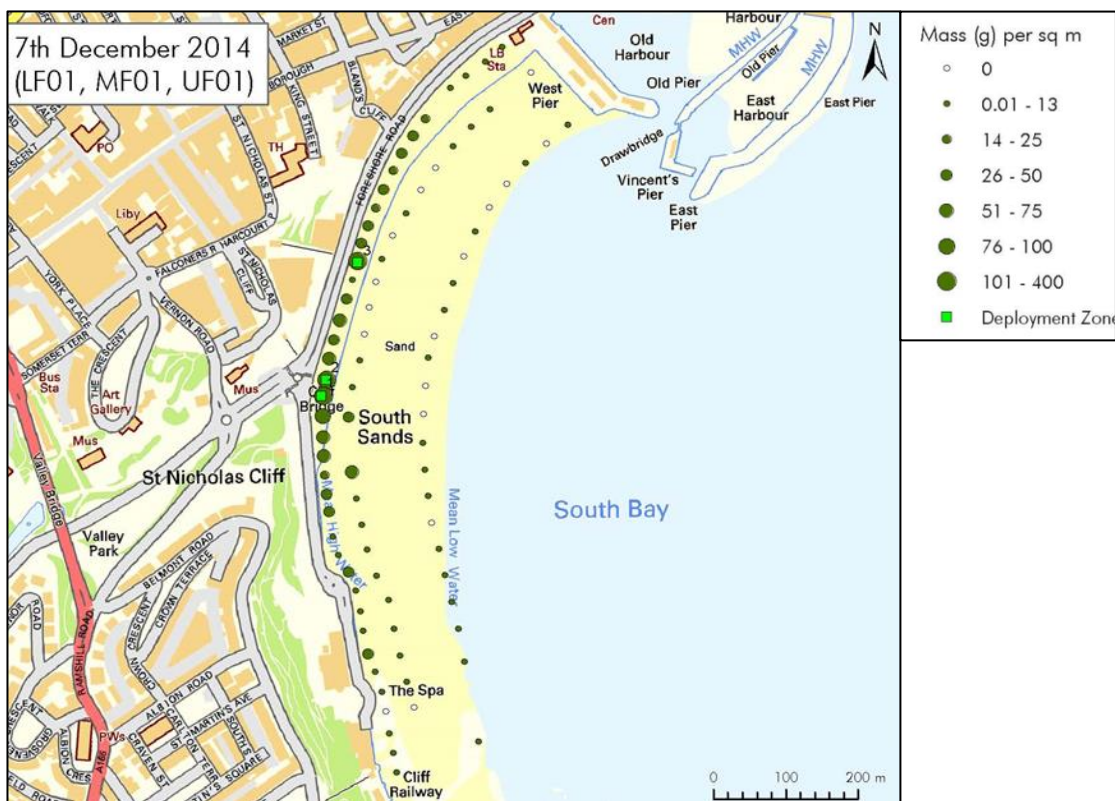


Figure 60: Geospatial distribution of tracer dry mass (g m^{-2}) 48 h after injection.

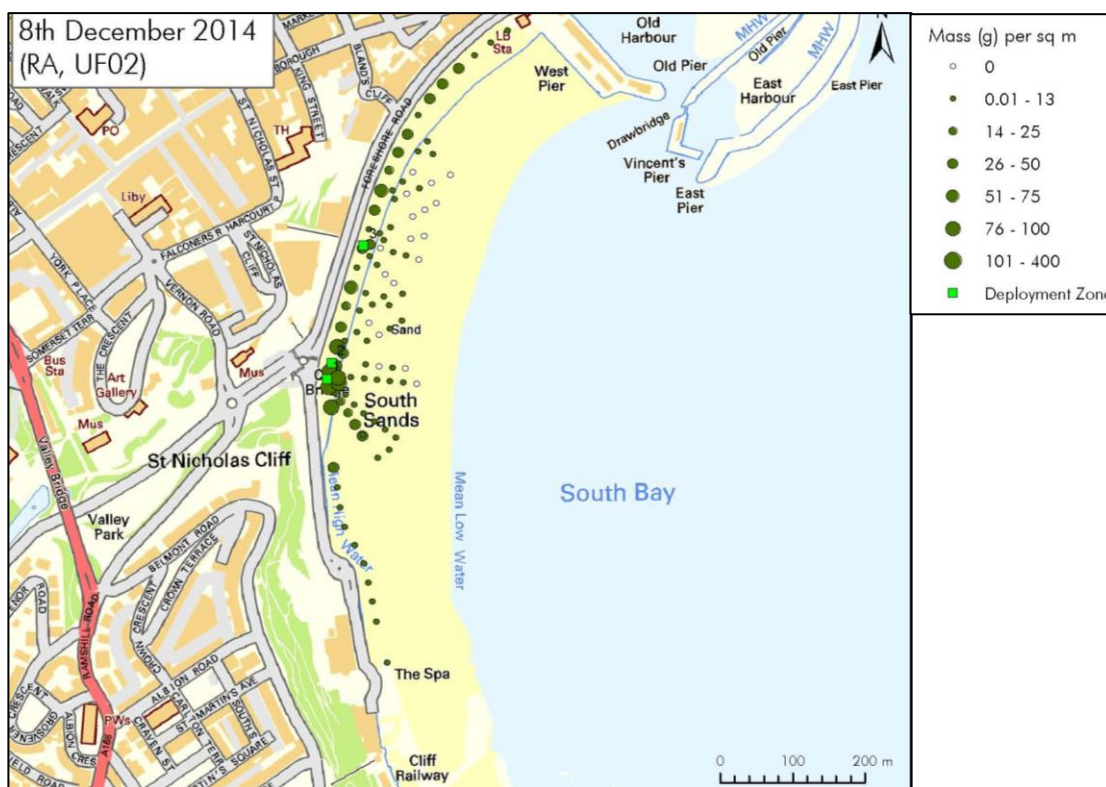


Figure 61: Geospatial distribution of tracer dry mass (g m^{-2}) 72 h after injection.

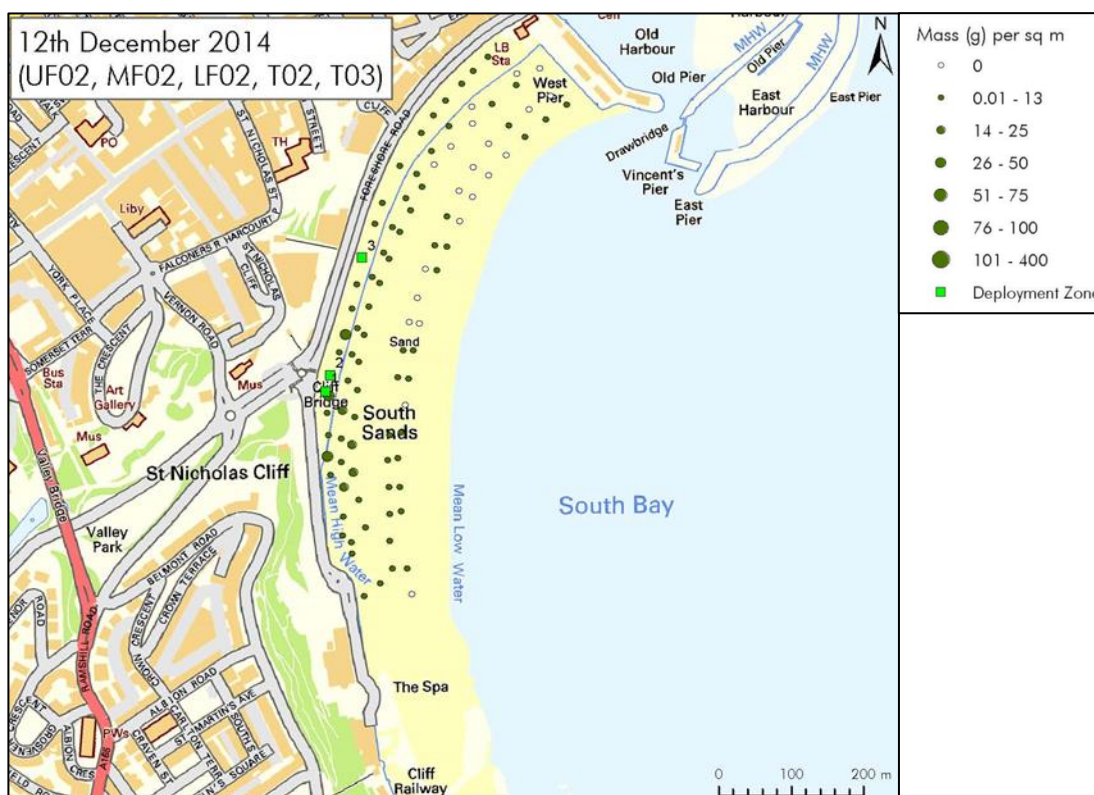


Figure 62: Geospatial distribution of tracer dry mass (g m^{-2}) 168 h after injection.

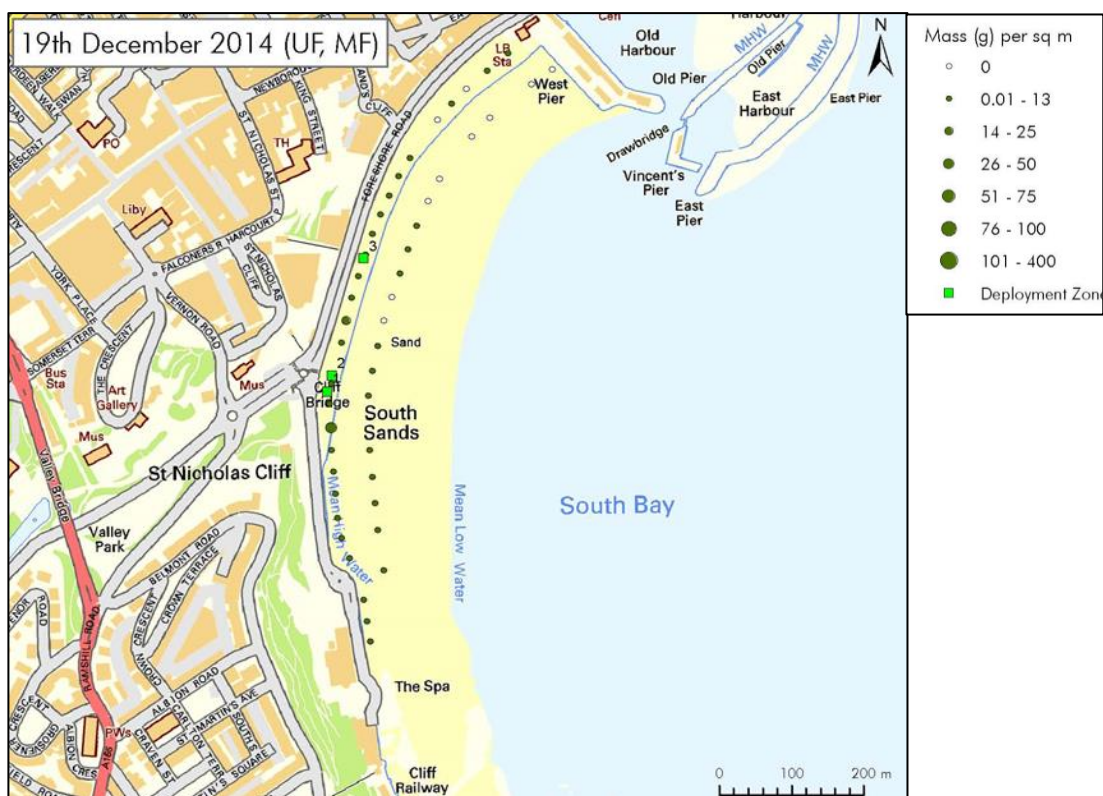


Figure 63: Geospatial distribution of tracer dry mass (g m^{-2}) 336 h after injection

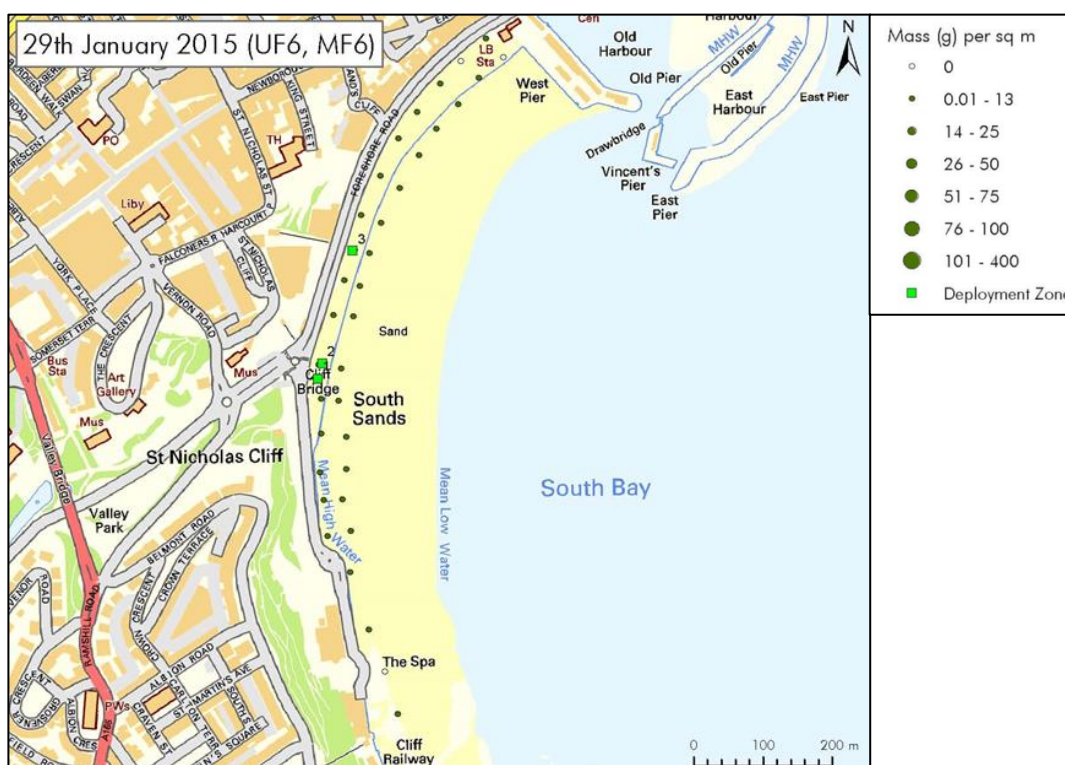


Figure 64: Geospatial distribution of tracer dry mass (g m^{-2}) 54 days after injection.

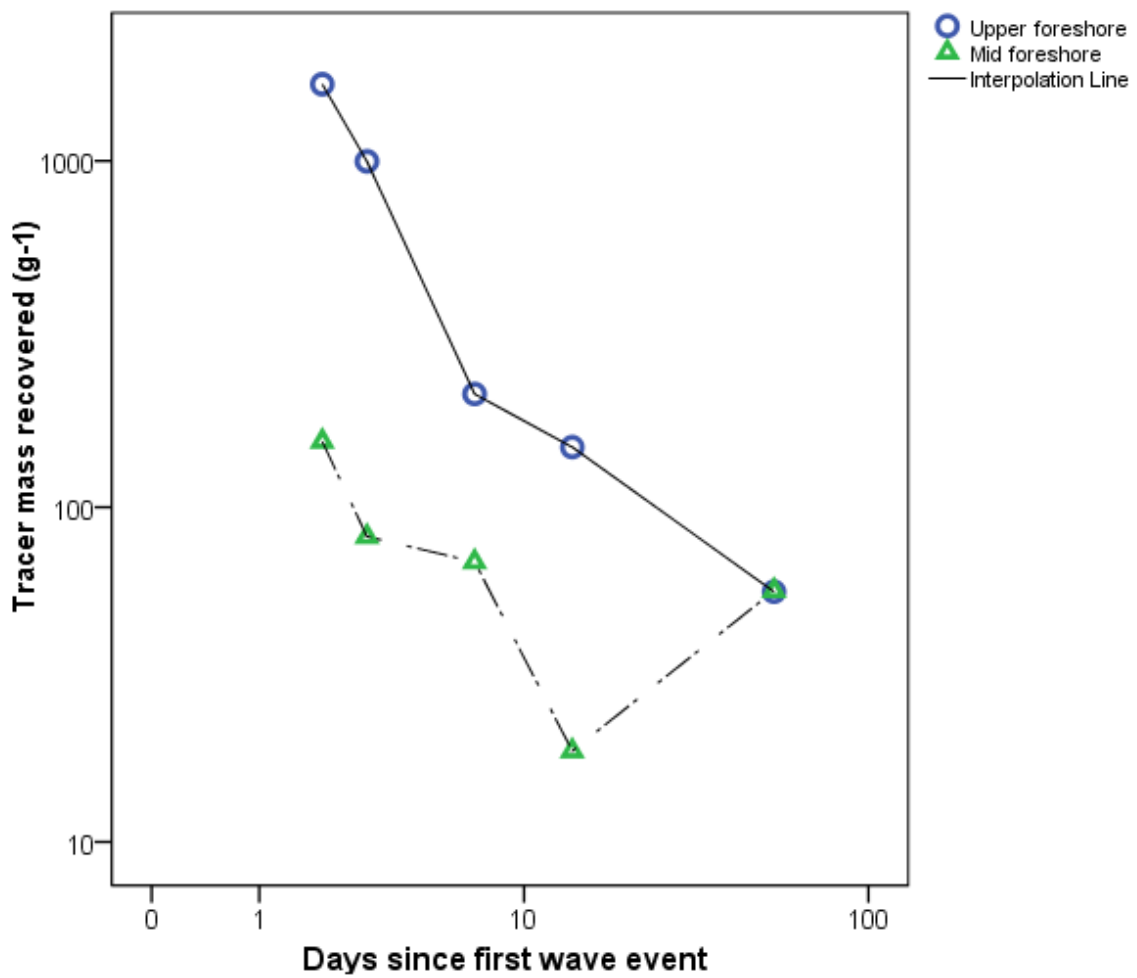


Figure 65: Tracer mass recovered (normalised to a unit area g m^2) from the upper and mid foreshore on the days following tracer deployment. The data graphically represented only reports the sampling campaigns where both the mid and upper foreshore were sampled at the same time, these being 2, 3, 7, 14 and 54 days following the first wave event.

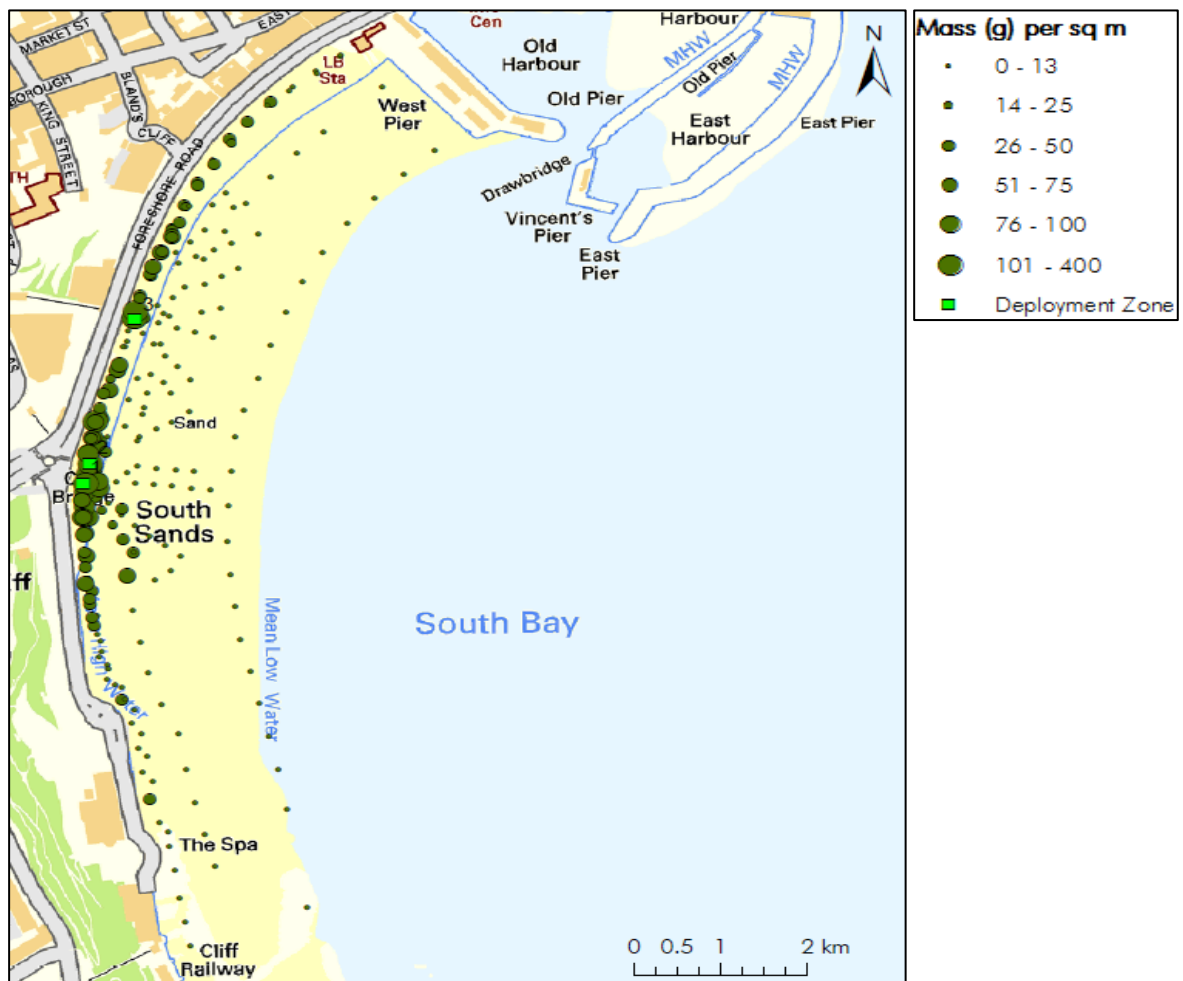


Figure 66: Total tracer mass recovered from the beach face during the sampling campaign.

7.6. Discussion

Through the use of a sediment tracing technique, the sediment transport pathways on the Scarborough South Bay beach face were identified. The data generated, demonstrated the potential benefits of the sediment tracing approach for validating both numerical and physical models of sediment transport. The study demonstrated the utility of the sediment tracing technique to shoreline management. The dual-signature tracer was successfully monitored across extensive spatial and temporal scales within a complex anthropogenically altered setting. In addition, a fluorescent–magnetic

tracing methodology to trace the movement of beach sediments was developed.

The tracing data highlighted the bi-directional transport of sediment in response to the dominant prevailing direction of waves that impact upon the shore, at any particular time. Transport of sediment contrary to the general sediment drift was driven by northerly directed waves being refracted to a southerly aspect as they enter the bay due to the location and morphology of the headland, and sub tidal bathymetry (Brown et al., 1999, Collins, 1972, Short and Wright, 2007). The data confirmed sediment accumulation in the northern end of the beach, due to trapping of the sediment in the lee of harbour infrastructure, as described by Royal Haskoning (2007). That southerly sand transport is also observed suggests that the middle sector of the foreshore may be a zone of sediment transport divergence, i.e. supplying sand (until depleted) in both directions (Bray et al., 1995, Cowell et al., 2001). If this is the case, this zone may move (north or south) in response to differing wave approach (Brown et al., 1999). These data have the potential to provide information useful to the calibration of established physical and numerical sediment transport models of the site (Wallingford, 2001, Wallingford, 2002), critical when sediment management decisions are based solely on modelling evidence (Schoones and Theron, 1995, Cromey et al., 2002).

Multiple tracer deployment zones enabled the transport pathways to be assessed over the entire beach face. This provided greater opportunity to assess wave driven transport where wave approach is variable. However, multiple deployment zones restricted the determination of the sediment transport rate e.g. Vila-Concejo et al. (2004), Ciavola et al. (1998), Ingle (1966), Carrasco et al. (2013), as the tracer source could not be determined. Fewer budgetary constraints would enable the use of two tracer colours to assess different source areas on the beach face. The use of two tracer colours would have improved the study enabling greater information regarding longshore sediment transport rates, to be garnered. Thus, the costs associated with the use of dual signature tracer must be considered a limiting factor (Pedocchi et al., 2008).

The dual-signature tracer proved to be an effective sediment tracer, which was easily deployed (logistically), and effectively monitored within and recovered from the environment. The tracer strongly matched the hydraulic properties (particle size distribution and specific gravity) of the native sediment, thus tracer movement could be considered representative of sand movement (Black et al., 2007, Dyer, 1986). Having two tracer signals proved beneficial and enabled a multifaceted sampling campaign focused on both the magnetic and fluorescent signals of the tracer to be conducted. This increased the volume of data garnered from the study, crucial as sediment tracing is fundamentally an empirical evidence-based approach.

A significant concern, when conducting tracing studies in high energy environments, is that the study is not defeated by the occurrence of a transport event sufficient to disperse the tracer to beyond/below the analytical limit (Ciavola et al., 1998, Crickmore and Lean, 1962). As it is not possible to know *a priori*, when the tracer will be mobilised nor where the tracer will be transported to, an adaptive sampling strategy must be devised (Black, 2012). The tracer was monitored over 54 days, indicating that the deployment, monitoring and recovery techniques were appropriate for the study area and environment.

The use of passive sampling techniques enabled the study to be adaptive rather than reactive. Night-time transects with blue light torches were particularly useful to evaluate the distribution of tracer on the sediment surface, and provided an insight into the dominant transport direction e.g. Russell (1960a), Ciavola et al. (1998), Silva et al. (2007), Carrasco et al. (2013), Vila-Concejo et al. (2004). Measuring the magnetic susceptibility of the deployment zones enabled rapid determination of tracer concentration in the surface sediments (Guzman et al., 2013, Van Der Post et al., 1995). These data used with the adapted conversion model (Equation 19), enabled estimation of the quantity of sediment mobilised prior to and during the first wave event. The use of magnetic susceptibility was limited to a single event as the susceptibility of the native sand was highly variable (mean value of $144 \pm 92 K_{LF}$). This is attributed to the industrial legacy of the surrounding area (Council, 2014, Schmidt et al., 2005). However, if this technique was applied

to an environment where the native sediment was closer in character to pure quartz sand (which display weak and negative susceptibilities of $-0.58 \times 10^{-8} \text{ m}^3 \text{ kg}^{-1}$ (Mullins, 1977)), susceptibility could potentially be used to assess the spatio-temporal distribution of the tracer, over multiple events (Van Der Post et al., 1995).

The spectrofluorimetric tracer enumeration methodology was able to process quickly, a large number of samples (Guzman et al., 2013). The methodology was less resource intensive than previous methods utilised within fluorescent tracing studies e.g. Carrasco et al. (2013), Ciavola et al. (1998), enabling high sampling frequency, critical to conducting tracing studies over large spatial and temporal scales (Guzman et al., 2013, Black et al., 2007). Further, the technique offered a means with which to obviate the additional mass due to the presence of magnetic but non-fluorescent particulates, simply and directly, and provided a high analytical resolution facilitating detection of low tracer mass. A conservative methodological bias of $\pm 20 \%$ was calculated from previous testing.

7.7. Conclusion

This study demonstrated the utility of sediment tracing within the sediment and coastal management arena. Tracing studies have the potential to improve upon the conceptual understanding of sediment transport regimes. They can be conducted to identify potential sediment source areas, transport pathways and specific areas of sediment deposition and accumulation. These data are critical to developing a robust shoreline management plan, and implementing informed, remedial strategies. This large-scale field study demonstrated the benefits of using a tracer with two signals. The large data base acquired, from a highly dynamic environment, provided a robust platform from which to draw evidence-based conclusions regarding sediment transport on the beach face. The potential of magnetic susceptibility as a sampling tool was highlighted, yet had limited use within this study. Further work regarding the relationship between the background material, particle size distribution and homogeneity of the tracer signal is required to quantify tracer content using susceptibility. The use of two tracer colours would have proved beneficial to this study, providing greater clarity of the source-sink relationship

and potentially enabling determination of two (bi-directional) sediment transport rates. Despite this, the study has demonstrated sediment tracers are a valuable tool. While sediment tracing is not a panacea for the management of sediment transport related problems, it should be considered, a useful tool in the box.

8. An Assessment of the Transport and Deposition of Sediments, Following a Simulated Disposal of Silt Sized Dredge Material Within a Near Shore Harbour Setting.

8.1. Summary

Dredge disposal at sea detrimentally impacts the marine environment, effecting fish species, benthic communities and marine and coastal ecosystems. Determining the transport pathway and sedimentation pattern of disposal of sediment, and particulates, from dredge vessels is critical to improve forecast models, assess risk, and implement mitigation strategies. Until now, the dispersion of fine sediment following the disposal of dredge material has primarily been investigated using numerical modelling techniques, yet there is a dearth of field - scale calibration data. This study utilised active sediment tracers to identify sediment transport pathways and capture deposition patterns following a simulated, silt-rich, dredge disposal event. A fluorescent–magnetic tracing method to monitor suspended sediment transport was developed. The simulated disposal event enabled the transport pathways and sedimentation pattern of dredged sediments to be monitored. Extensive sediment deposition in the area surrounding the dredge disposal site was observed. The timing of disposal events is critical. These results demonstrated the fundamental role of tide and current in the transport and subsequent deposition of discharged sediment. Assessment of the transport and dispersal of sediments following disposal of dredge materials has generated field data from which risk assessment and informed management practices can be developed. This study provides baseline data for future tracing studies, and modelling approaches.

8.2. Introduction

The contamination of the coastal zone, impacts upon marine habitats and coastal ecosystems (Islam and Tanaka, 2004 , Lotze et al., 2006, Gray, 1997). One source of nearshore contamination is the disposal of dredge material (Rees et al., 2003). The majority of disposed dredged material contains a significant load of fine (< 63 microns) sediment (Anon, 1996, CEFAS, 2003, Bolam et al., 2003). Due to the requirement for dredging operations to seek a beneficial use for dredge material disposal of material in

the nearshore coastal zone occurs more regularly to support habitat creation and enhancement (Bolam et al., 2003, Bolam and Whomersley, 2003, Bolam and Whomersley, 2005). The disposal of dredge material in the near shore zone effects both the water column and sea bed condition (Okado et al., 2009) detrimentally impacting the nearshore marine environment (USACE, 1983, Research, 1999) due to increased turbidity, nutrient loading and a reduction in water clarity potentially leading to anaerobic conditions within water bodies (Johnston, no date). These detrimental impacts are compounded in when material is deposited in the vicinity of sensitive receptors such as sea grass beds (Duarte, 2002), reef habitats (Zimmerman et al., 2003) or coral reefs (Erftemeijer et al., 2012) . Of particular concern, is the distribution of solids following a discharge event, as this contributes to the degradation of benthic habitats due to sediment accumulation (Birch and Taylor, 1999, Carr et al., 2000, Petrenko et al., 1997); and can result in sediments being enriched with heavy metals and anthropogenic contaminants (Hatch and Burton, 1999, Pitt et al., 1995, Marsalek et al., 1999, Schiff, 2000) or buried (Lindeman and Synder, 1999). Therefore, understanding the near shore transport of sediment disposed from a dredging vessel is important to develop effective mitigation strategies and assess risk (Okado et al., 2009).

Factors which affect the dispersion and deposition of sediment disposed from a vessel include: the receiving water flow characteristics; depth; current direction; and current velocity (Huang et al., 1994, Ludwig, 1988, Fischer, 1979). Critical entrainment thresholds depend on the disposal site characteristics and the sediment characteristics, including: water depth; particle size; material density; and material load (Guymer et al., 2010, Ludwig, 1988). Grains < 63 microns in size, travel as a suspended load (Droppo, 2001) within the water column, at the same velocity, supported by turbulence (Masselink and Hughes, 2003), and are deposited only once the flow velocity diminishes (Dyer, 1986). A dredge disposal characterised by a large (silt-rich) material load (Figure 57) will create a sediment-laden plume (Cardoso and Zarrebini, 2002) Theoretical modelling has been applied to investigate the particle fallout mechanisms of a sediment laden plume: investigating the fallout at the margins of plumes (Ernst et al., 1996); the effect of a radial

spreading surface gravity current (Sparks et al., 1991, Zarrebini and Cardoso, 2000, Cardoso and Zarrebini, 2001); and sediment depositional patterns in varying flow conditions (Cuthbertson and Davies, 2008, Cuthbertson et al., 2008a, Neves and Fernando, 1995). Particles are primarily deposited close to the source with a steady decrease in accumulation as distance from the source increases (Neves and Fernando, 1995, Kim et al., 2000). Currently though, insufficient field data exist for validation of these models (Akar and Jirka, 1994, Cuthbertson et al., 2008).

Previous studies utilised numerical modelling (Clarke et al., 1982, Gallacher and Hogan, 1998, Van den Eynde, 2004), grain size trend analysis (Friend et al., 2006, McLaren, 1981, McLaren and Bowles, 1985, Gao and Collins, 1992, Gao, 1996) and metal concentrations in sediments (Matthai and Birch, 2001, Rowlatt et al., 1991, Kress et al., 2004) to investigate the spatial distribution of the disposed material. It is difficult to monitor the transport dynamics of disposed sediment using native sediment as it is difficult to distinguish between the disposed sediment and the native sediment load. Therefore, in order to monitor the near shore transport and assess the deposition pattern of a sediment-laden plume, following a dredge disposal event, a material load that can be deployed, monitored and recovered from the environment is required; the optimal tool being a sediment tracer e.g. Guymer et al. (2010). Tracing is a field technique which uses sediment tracers to assess sediment transport pathways in fluvial, marine and aeolian systems (Kondolf and Piegay, 2005, Black et al., 2007, Black, 2012). Tracers are often particles that possess similar hydraulic properties to natural mineral sediments (silts; sands; gravels) but which are labelled or tagged to enable unequivocal identification in the ocean (Ciavola et al., 1997, Ciavola et al., 1998, Carrasco et al., 2013, Vila-Concejo et al., 2004), or other environmental settings. As it is a field method, the technique has potential to further the understanding of the transport of discharged sediments following a dredge disposal event (Black et al., 2013).

The majority of tracing studies conducted to date (aside from those which used radioactive signatures, which are now banned for safety reasons) have used fluorescent only, or mono-signature, tracers (see Black et al.

(2007)., op. cit., for a synthesis on the subject). This study aims to assess the near shore transport, and deposition of a particle-laden plume, disposed from a dredging vessel, focusing on the distribution and deposition of fine (silt sized) sediment (10-63 microns). To do this a high concentration discharge of lithogenic solids was simulated using a dual signature particulate tracer. The objectives of the study were to:

1. Simulate a dredge disposal event.
2. Assess the behaviour and transport pathway of the discharged particles.
3. Evaluate the depositional footprint of the discharged particles.

8.3. Method

The study area was located within Naval Base San Diego, California, USA. The coastal zone had been significantly altered through the years via extensive dredging of channels and in the area of deployment the dredged depth was fairly uniform (~10 m). The deployment site was positioned within a highly industrialised setting characterised by a permanent quay wall and two large floating piers (Figure 59).

8.3.1. Tracer characterisation

A chartreuse-coloured dual-signature tracer was used comprised of natural mineral kernels coated with two applied tracer signals, fluorescence and ferrimagnetism (Partrac Ltd, UK). The tracer was designed to replicate a silt-rich sediment population. Pre-deployment, the hydraulic characteristics of the tracer were determined. The specific gravity (particle density) was determined using an adapted pycnometer technique (Germaine and Germaine, 2009); the particle size distribution using a *Mastersizer 2000* laser diffraction device (Malvern Instruments Ltd, UK); and the settling (fall) velocity of the particles determined using an adapted settling column procedure (Wong and Piedrahita, 2000).

8.3.2. Tracer deployment

The tracer was deployed from the aft of a vessel, secured on an anchor line to the quay wall (Figure 67). On board the vessel a device was specially

designed to deploy tracer in suspension as a high concentration tracer / seawater slurry. Tracer was continually introduced to two drums where high powered water pumps, continually pumped seawater into the drums, creating an overflow system. The tracer / seawater slurry overflowed into two tubes. In total, 800 kg of tracer was deployed in suspension, subsurface (1 m) over a period of five hours beginning at high water. Two distinct deployment systems and the high flow rate of the pumped seawater ensured, sufficient turbulent mixing ensure disaggregation of any aggregated particles occurred.

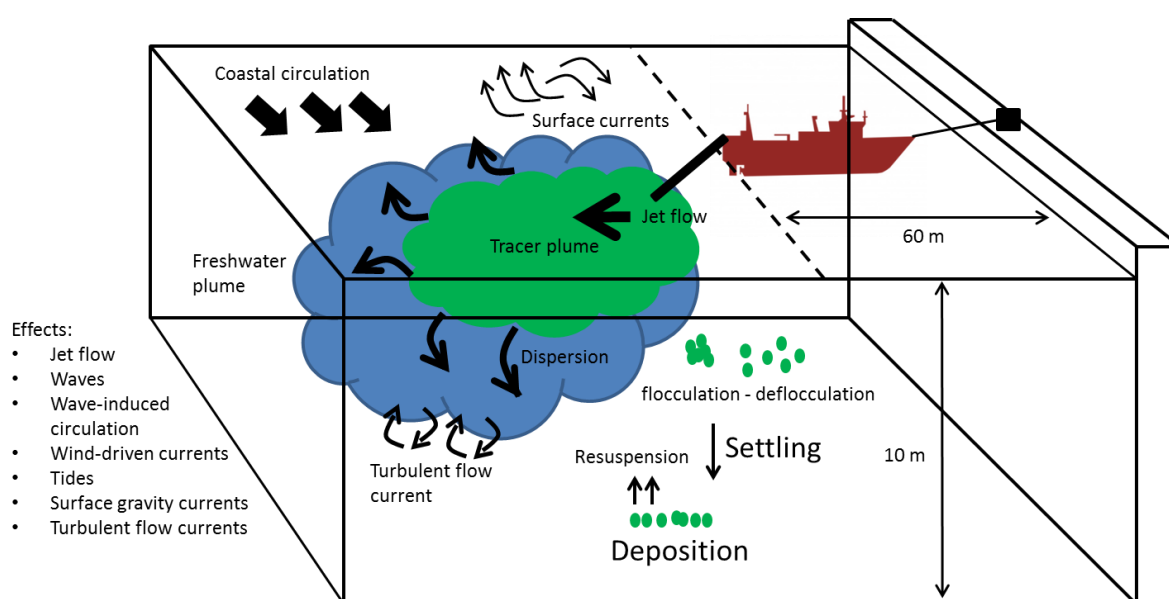


Figure 67: A schematic diagram to illustrate the deployment methodology and the transport processes of disposed sediment from a discharge vessel in the coastal zone. The boat is secured to the quay wall while tracer is being deployed subsurface from a pipe from the aft of the vessel. The diagram is not to scale.

8.3.3. Sampling

Following the introduction of the tracer to the environment, a multistage sampling campaign was conducted to sample the water column and the sea bed. *In situ* magnetic moorings were secured on the sea bed and sampled 24 h following tracer deployment. Each comprised a high – field, permanent magnet (11,000 Gauss, 0.3 m in length, sampling an area of 225 cm²), a ballast block, lines and a sub-surface float rig to locate the magnet 1 m above

the bed (Figure 68 and 69). Additional magnets were hung from floating piers, resulting in 44 magnet sampling stations in total (Figure 71). The quantity of background – non fluorescent, magnetic material was assessed by sampling the water column with a high – field, permanent magnet, 1 m and 5 m above the sea bed over a period of 24 hours. These magnets captured 0.105 and .159 g of iron or Fe-bearing material from 1m and 5m above the bed.

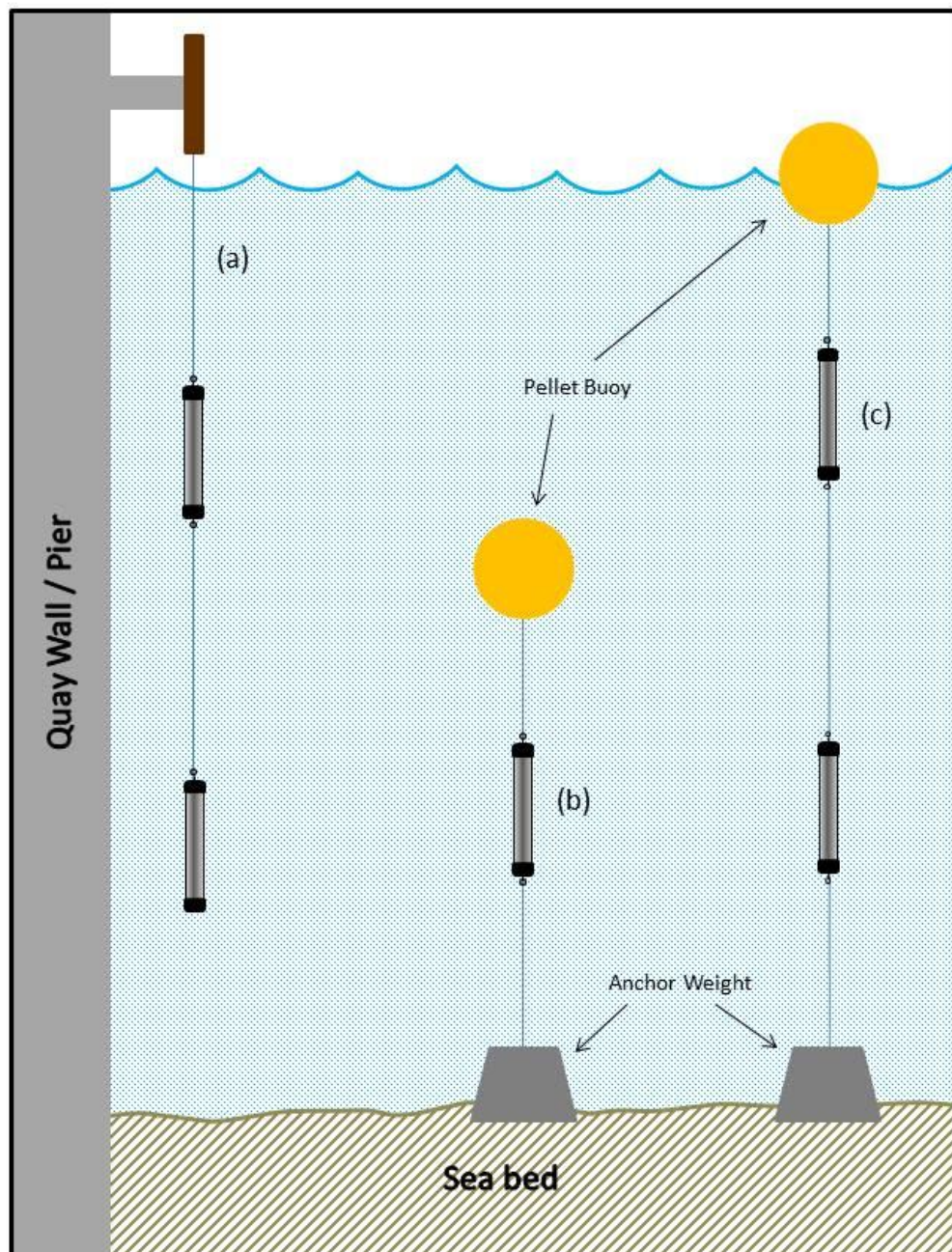


Figure 68: Schematic diagram showing how the magnets were deployed to sample tracer travelling in suspension.

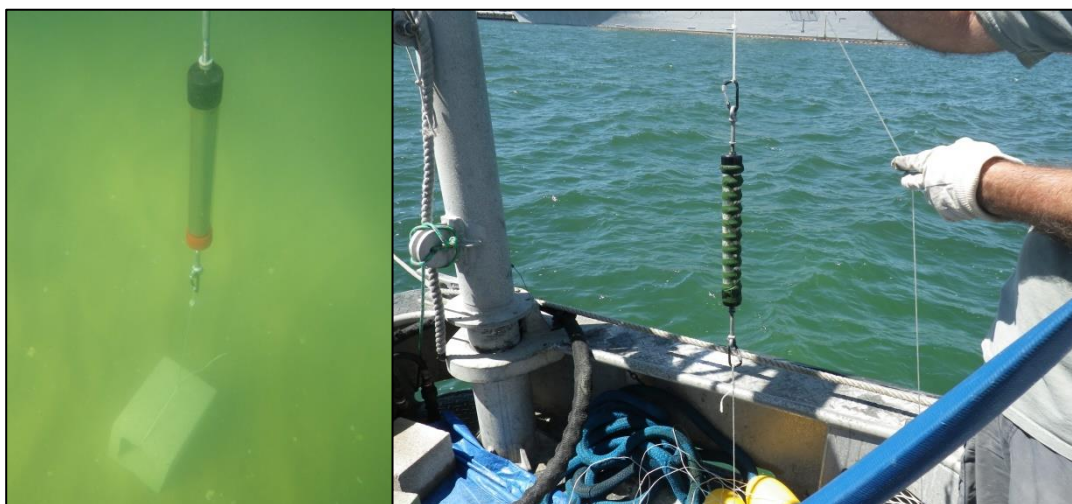


Figure 69: The magnets deployed *in situ* and recovered with tracer captured.

A laboratory calibrated (Figure 58) UniLux™ fluorescein fluorometer probe (Chelsea Technologies Ltd, UK), spectrally targeted to detect chartreuse tracer particles via a configuration to excite fluorescence at 470 nm and collect emission at 530 nm, was used *in situ* to monitor fluorescent material (tracer particles) in suspension. The probe was attached to an aluminium pole and secured to the starboard side of the vessel – mid ship, at a depth of 5 m. The fluorometer captured continuous data at a 1 Hz per second sampling rate during the deployment of tracer, and subsequent transects (Figure 70) of the discharge and sampling area conducted 24 and 48 h following tracer deployment.

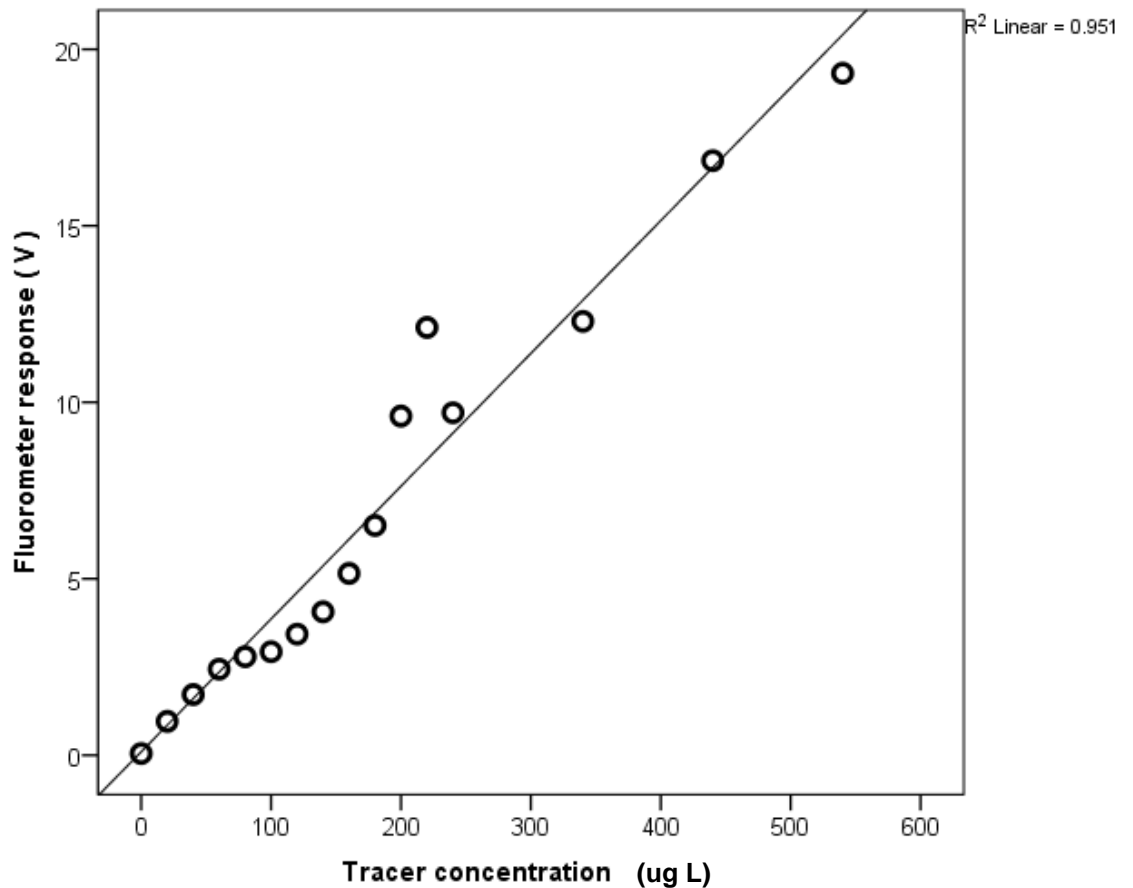


Figure 70: The laboratory calibration of the field fluorometer. The calibration shows the fluorometer response to increasing tracer concentration ($\mu\text{g l}^{-1}$).

The sea bed was sampled 48 hours following tracer deployment using a Van Veen sea bed grab, deployed from a davit and winch, from the bow of the vessel at 33 locations (Figure 71). Outlying sampling locations were positioned at ~600 m offshore: however, the majority of sampling resources were focused within the vicinity of the discharge zone up to ~300 m offshore, where six sampling transects (T_x) were conducted from the quay wall - offshore. T_1 and T_2 were positioned to the north of the discharge zone, T_3 was positioned directly in line with the discharge zone, and T_4 , T_5 and T_6 positioned to the south of the discharge zone (Figure 71). All samples were stored and labelled on the vessel and transported securely to the laboratory to determine the mass of tracer within each sample.

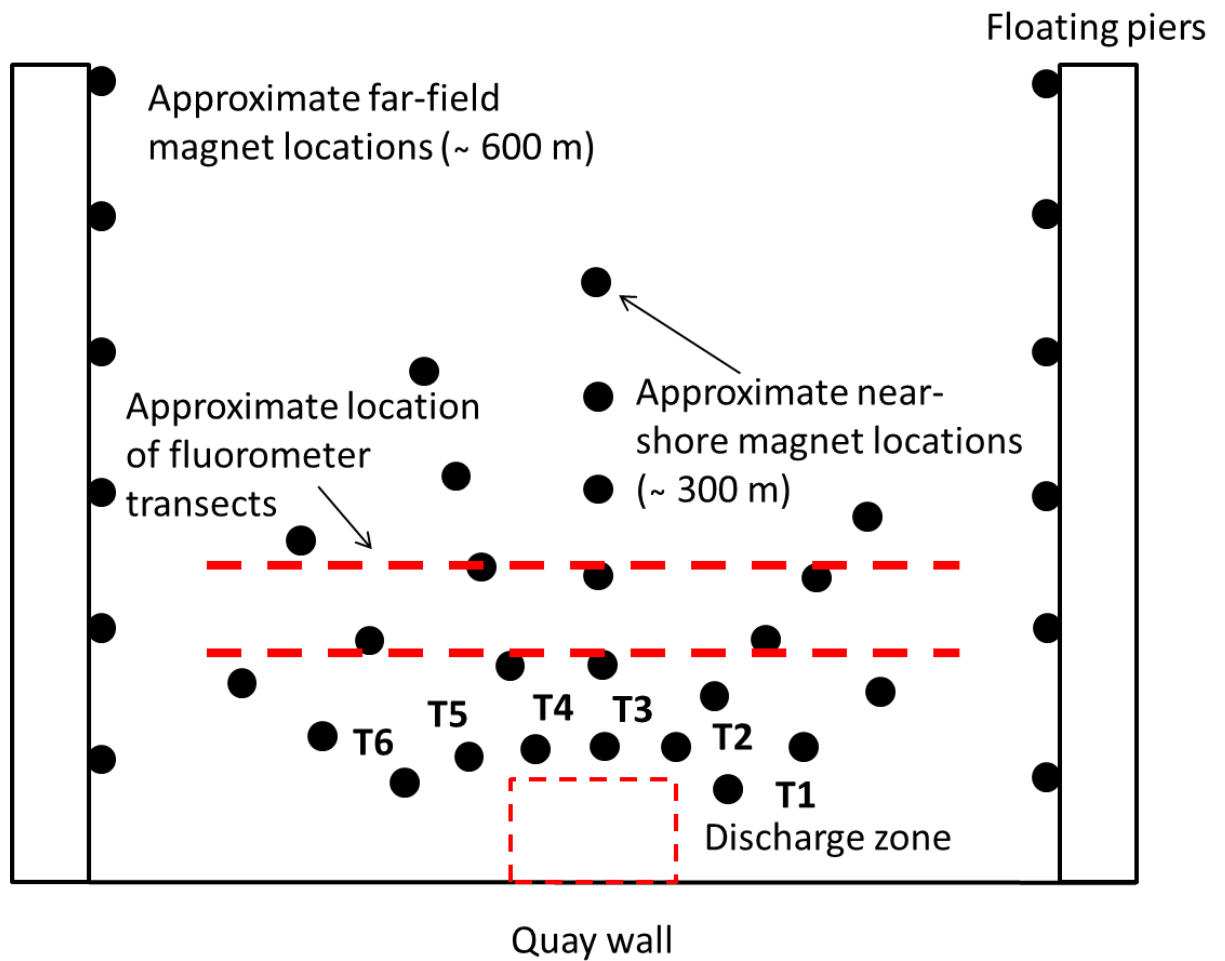


Figure 71: A schematic diagram showing the approximate near-shore and far-field sampling locations. The markers indicate the location of sample points where both the water column (1 m above the bed) and the sea bed were sampled. Each nearshore transect is marked (i.e. T1). The dashed red box indicates the discharge area and the red line indicate the approximate location of the fluorometer transects. The diagram is not to scale.

8.3.4. Tracer enumeration

To enumerate tracer content within each sample collected a spectrofluorimetric technique was used (Carey, 1989). Four 'dose response' curves (otherwise known as 'calibration curves'), consisting of a plot of fluorescence intensity vs. dye concentration, were developed to empirically relate fluorimetric measurements (probe reading in volts) to tracer dye concentration (Figure 72, 73). Eluted dye solutions for the chartreuse tracer are prepared by adding a known dry mass of tracer particles to a known volume of analytical grade acetone in an Eppendorf tube, mixing and then allowing the solution to equilibrate for 168 hours (7 days). This time period has been established as optimal for maximal extraction of the pigment into the solvent. Dose response curves were obtained by filling the calibration cell with 3 ml of analytical grade acetone, recording a baseline reading and then adding sequential 20 μ l aliquots of the dye solution, mixing and recording further readings. Due to the (significant) non-fluorescent magnetic background material present at the site, dose response curves were prepared with tracer and native material to account for the 'quenching' effects of the native material, which acts to reduce the fluorescent intensity of the sample (Lakowicz, 2006). The distinct difference between samples containing 'high' and 'low' magnetic material load resulted in four individually tailored dose response curves being prepared to enumerate the tracer mass from the samples collected, two dose response curves representing samples of 'high' material load (Figure 73) and two representing samples of 'low' material load (Figure 72) for both material collected using *in situ* magnets and sea bed grabs respectively (Table 13). The mass of background material added was derived from the mean background material concentration for samples with 'high' and 'low' material load. Least-squares regression analysis (Fowler et al., 1998) was performed on the data to generate calibration functions.

Table 13: Summary of the calibration (dose response) curves produced.

Sample type	Description	Dry tracer mass (g)	Native material mass (g)	Peak (assumed) dye concentration ($\mu\text{g L}^{-1}$)
<i>In situ</i> magnet	'Low material load'	0.1	1	166.6
<i>In situ</i> magnet	'High material load'	1	10	1666.6
Sea bed grab	'Low material load'	0.1	10	166.6
Sea bed grab	'High material load'	5	25	8333.3

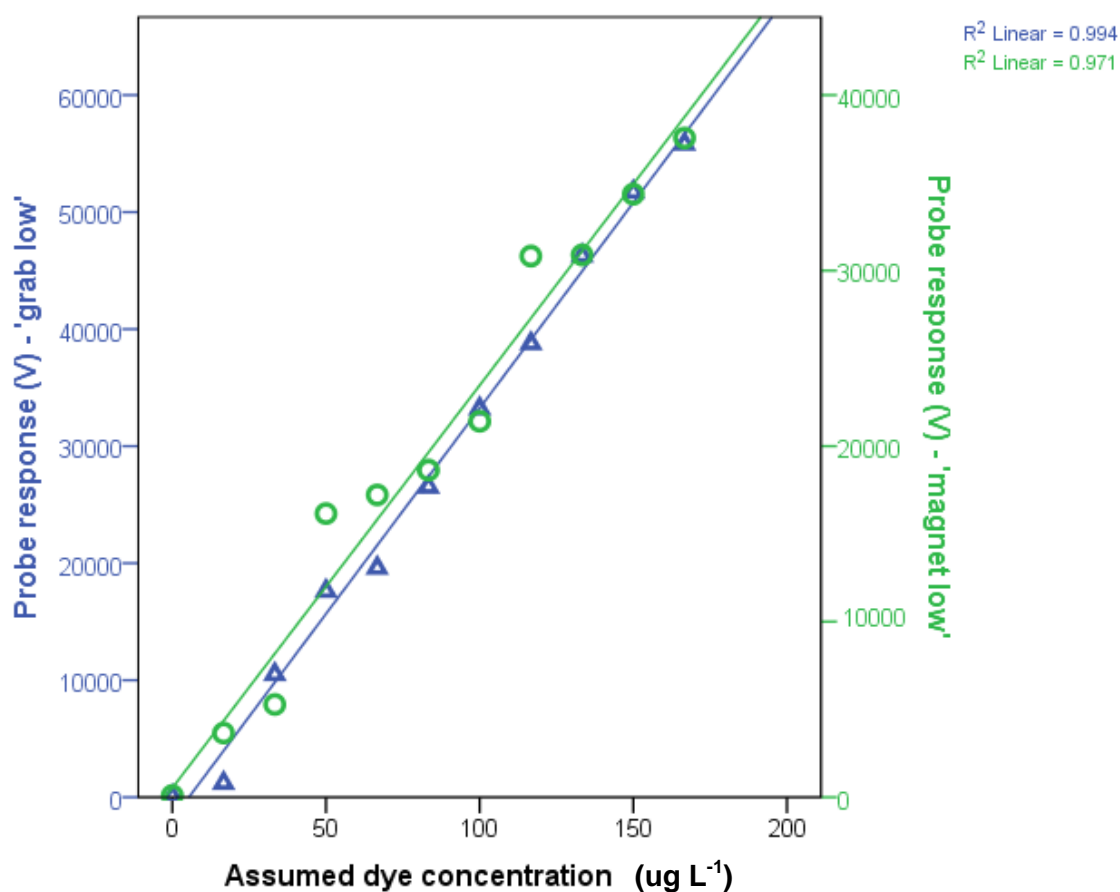


Figure 72: Calibration (dose response) curves prepared for low material loads for samples collected using the magnet rigs (e.g. magnet – low) and low material loads collected using a sea bed grab sampler (e.g. grab – low).

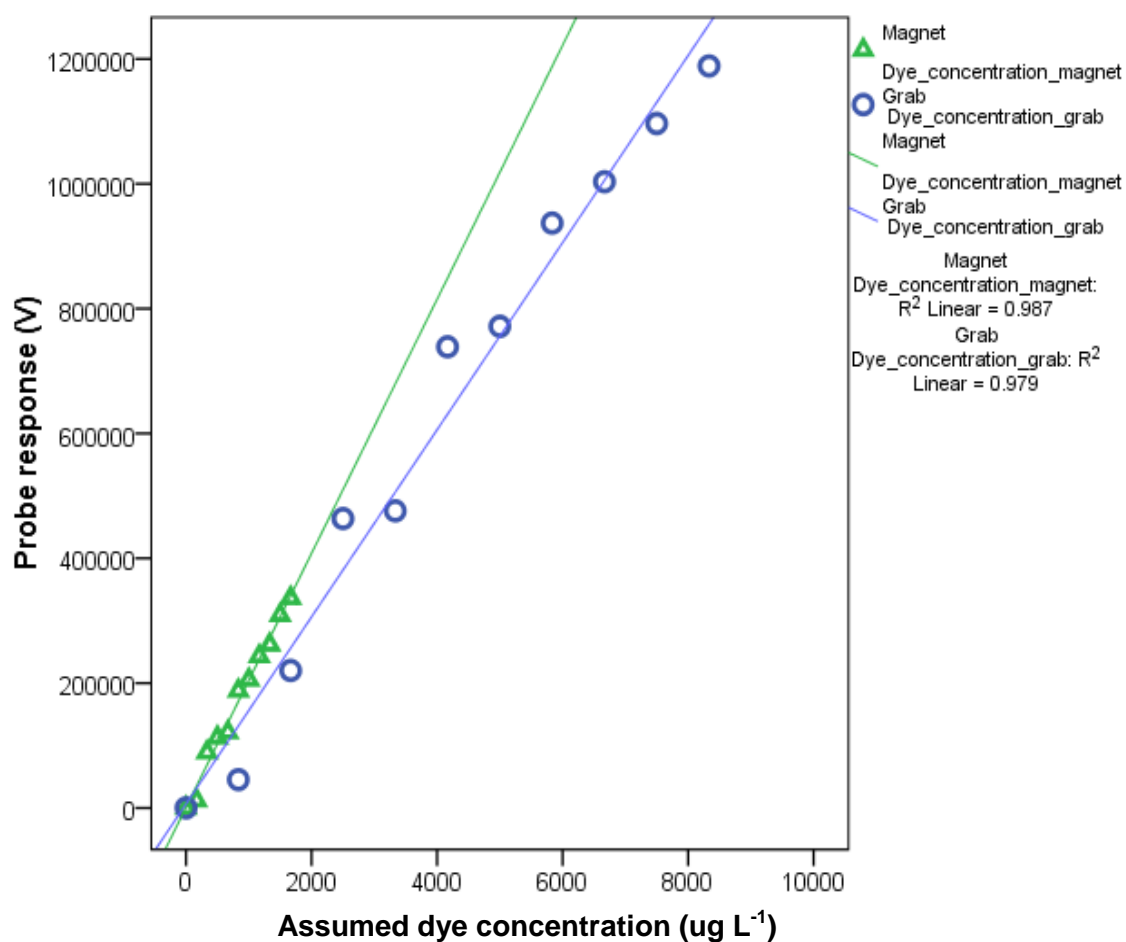


Figure 73: Calibration (dose response) curves prepared for high material loads for samples collected using the magnet rigs (i.e. magnet – high) and high material loads collected using a sea bed grab sampler (i.e.. grab – high).

The analyses were carried out using a FluorosensTM fluorometer (Gilden Photonics Ltd, UK). An emission scan was conducted at the tracer's peak excitation wavelength (485 nm) and the response recorded at the peak emission wavelength (530 nm). Each sample was run in triplicate and the mean value determined. To enumerate the dry mass of tracer the respective regression equation is used to determine dye concentration (D_C) from probe response. Tracer dry mass (T_{DM}) is then calculated using the following equation;

$$T_{DM} = \left(\frac{D_C}{C_{max}} \right) T_{DMmax} \quad (23)$$

Prior to analysis a magnetic separation method was used to reduce sample volume. Briefly, the sample was oven dried at 105 °C for 24 h, then transferred to a pestle and mortar and gently disaggregated. The sample was then smoothed to an approximately granular monolayer on a large white board and a permanent, 11,000 Gauss magnet was scanned across the sample at a distance of 2-3 mm, facilitating separation of magnetic particles. This procedure was repeated, with intermittent cleaning and recovery of the particles from the surface of the magnet, until no further magnetic particles were extracted. During sample preparation a tracer extraction efficiency of 70 % was calculated (determined through testing of spiked samples).

Where, C_{max} is the maximum assumed dye concentration ($\mu\text{g L}^{-1}$) and T_{DMmax} is the equivalent tracer dry mass value. Tracer content values (T_C) are derived from the tracer dry mass (T_{DM}) divided by the extraction efficiency (E).

$$T_C = \left(\frac{T_{DM}}{E} \right) 100 \quad (24)$$

A conservative methodological bias of ± 20 % was calculated from previous testing. Tracer content values derived from sea bed (grab) samples were normalised to relate to a unit area and hence reported as g m^2 ; tracer mass values derived from samples of the water column are reported as g l^3 , based on the assumption that tracer content from a sample is representative of tracer concentration within the surrounding area (White, 1998, Black et al., 2007b, Inman and Chamberlain, 1959a).

8.3.5. Oceanographic monitoring

Local current velocity data were collected during the study. An Acoustic Doppler Current Profiler (ADCP) (Teledyne RD instruments Ltd) was deployed 70 m offshore from the quay wall collecting one measurement every 5 minutes.

8.3.6. Theoretical assessment of the threshold of motion of deposited sediments

Following deposition to assess whether the sediments deposited would remain in situ a theoretical evaluation of the threshold of motion driven by tidal currents was conducted. The following equation derived from Soulsby (1997) was used the threshold depth-averaged current speed \bar{U}_{CR} required to mobilise sediments deposited on the bed.

$$\bar{U}_{CR} = 7 \left(\frac{h}{D_{50}} \right)^{1/7} [g (s - 1) D_{50} f(D_*)]^{1/2} \quad (24)$$

With

$$f(D) = \left(\frac{0.30}{1 + 1.2 D_*} \right) + 0.055 [1 - \exp(-0.020 D_*)] D_* \left[\frac{g(s-1)}{U^2} \right]^{1/3} D_{50} \quad (25)$$

Where s is the ratio of densities of grains and water, U is the kinematic viscosity of water, D_* is the dimensionless grain size, f is the Coriolis parameter, g is the acceleration due to gravity 9.81 ms^{-2} , h is water depth, and d is the sieve diameter of grains.

8.3.7. Statistical analyses

SPSS Statistics 20 software (IBM, 2015) was used for all analysis. Statistically significant values are reported at $p < 0.05$. A paired t test was used to assess for significant differences between the background fluorescent signal and the fluorescent signal following tracer deployment. In addition, a one-way analysis of variance (ANOVA) test was used to determine significant differences between tracer content values on different sampling transects.

8.4. Results

8.4.1. Tracer characterisation, tide and current data

The tracer was characterised as a silt-rich material load (Figure 74). The median grain size (D_{50}) of the tracer was observed at 30 microns with a specific gravity of $2182 \text{ kg / m}^3 \pm 115 \text{ kg / m}^3$. The settling velocity of the tracer particles < 100 microns in size was 0.009 cm s . There was no attempt to mimic local sediment properties as the principal aim of the study was to simulate a silt-rich, sediment-laden, plume (Figure 75).

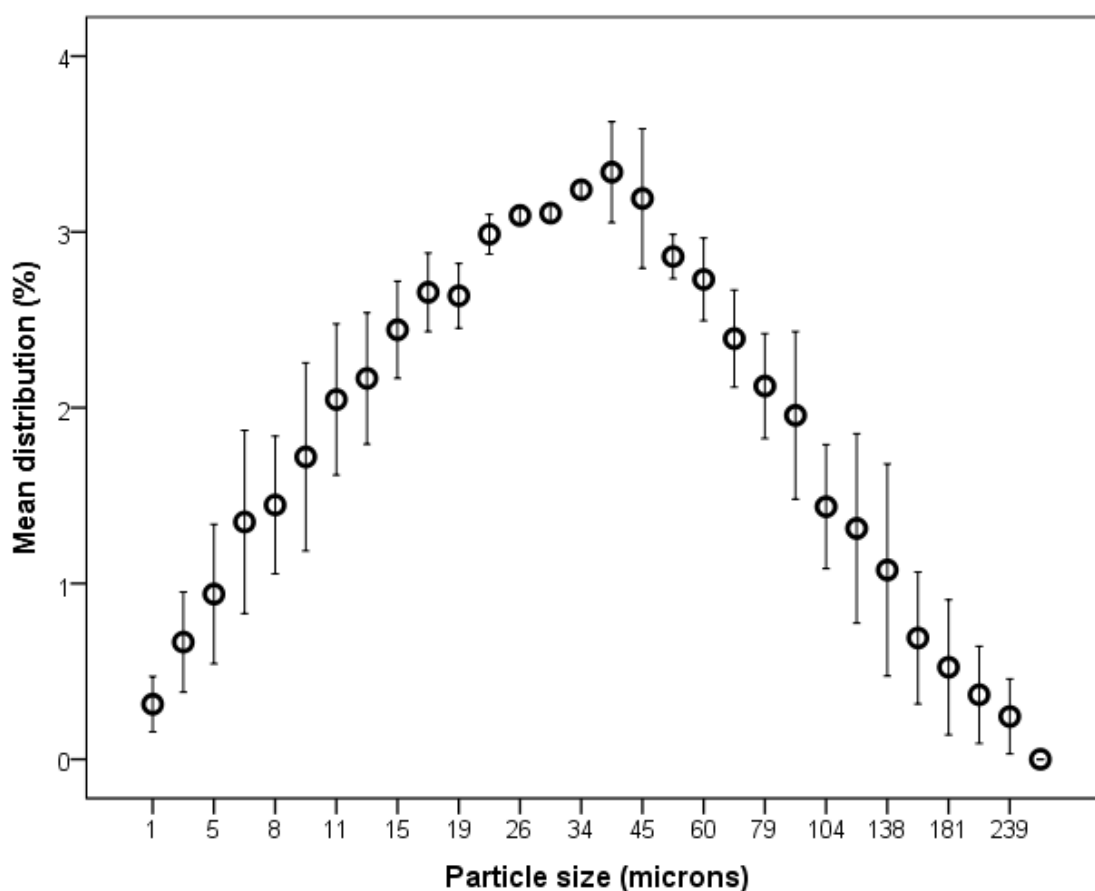


Figure 74: The particle size distribution of the tracer. The markers show the mean and the whiskers represent the standard error.



Figure 75: Tracer being deployed subsurface as a high concentration slurry. The plume of tracer dispersing is visible in the background.

During tracer deployment the tidal range was 4.4 m, increasing to 5.2 m by the end of the study period. Data collected using the ADCP indicated a mean current velocity of 33.8 mm s (Figure 76) which strongly correlated with modelled predictions of tidal current velocities at the site (Figure 77), and a mean current direction of 174 degrees re true north (Figure 78) showing a dominant tidal current in a southerly direction. Ebb current velocities were generally lower than flood current velocities and the net current was flood directed.

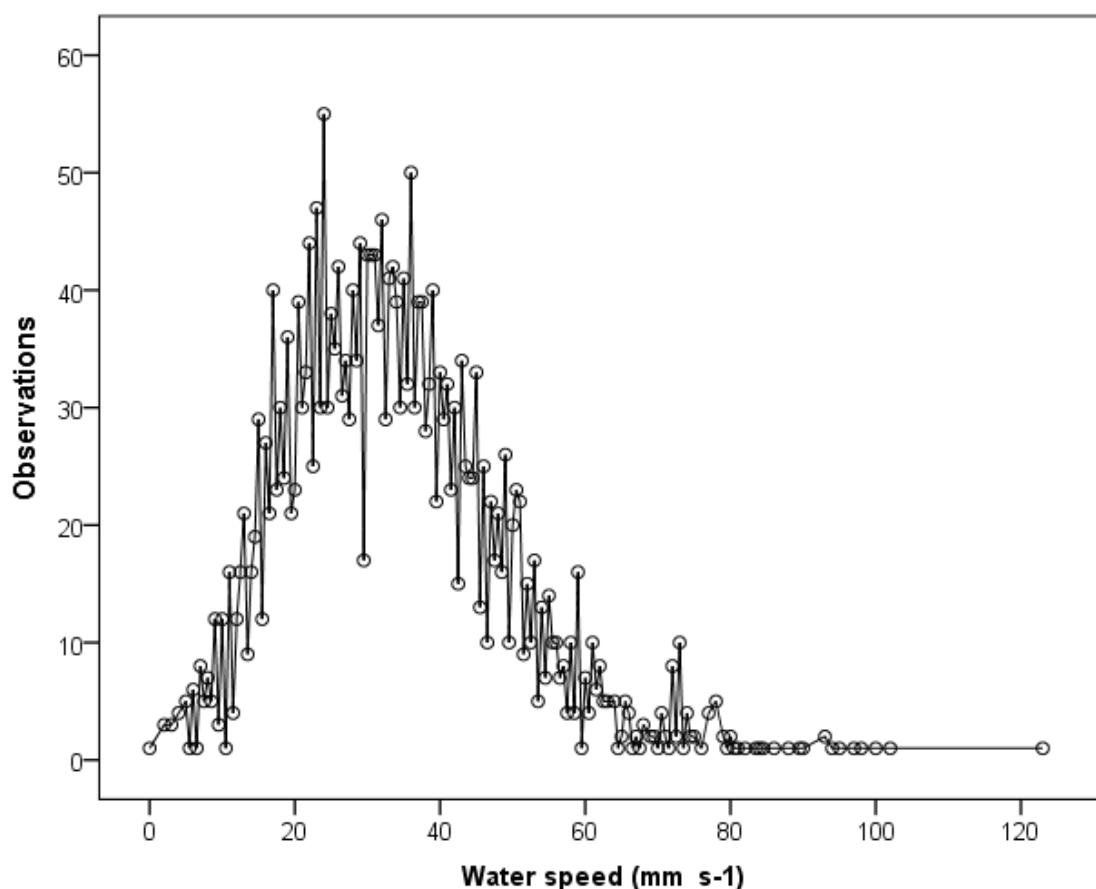
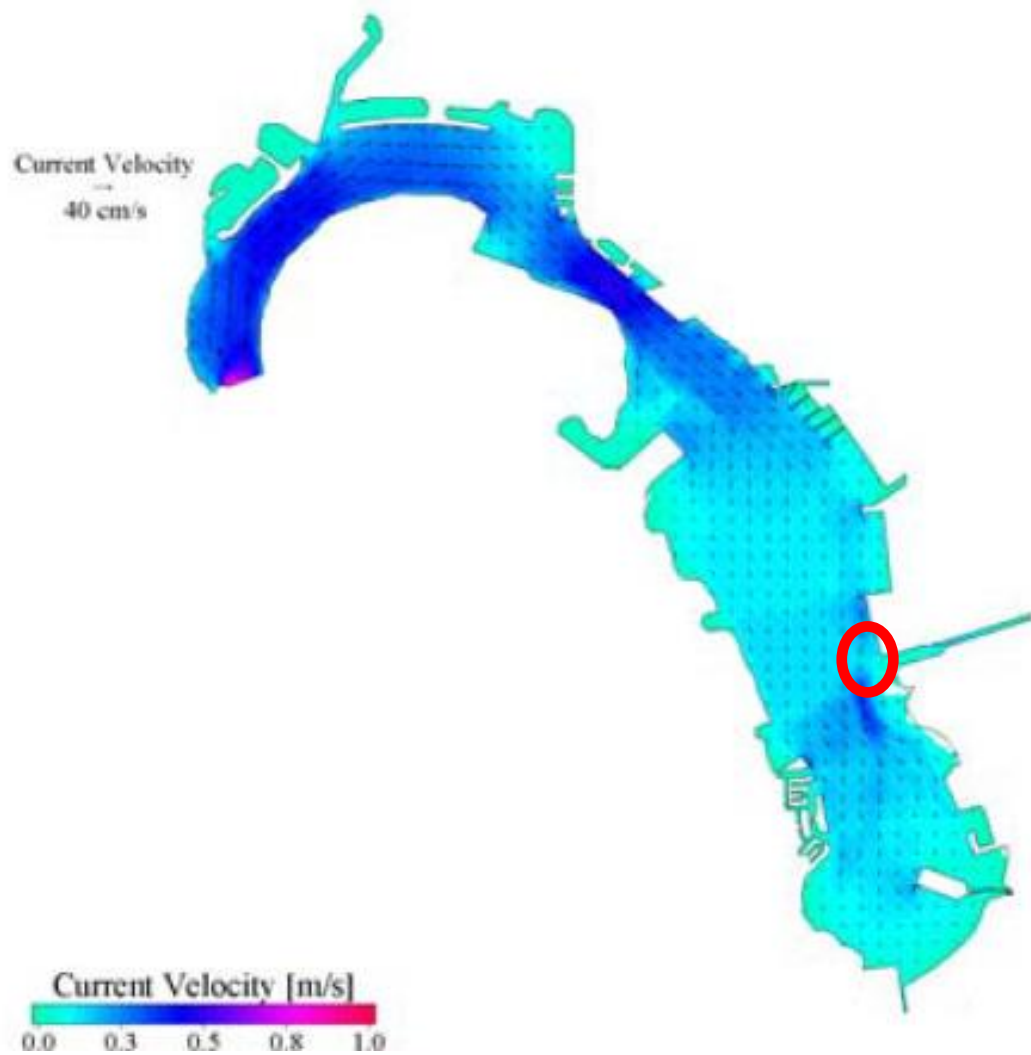


Figure 76: Observations of current magnitude derived from the data collected using the ADCP.



0 Study site location

Figure 77: Current velocities at flood tide derived from a hydrodynamic model of San Diego Harbour (Elawany, 2012). The location of the site is marked.

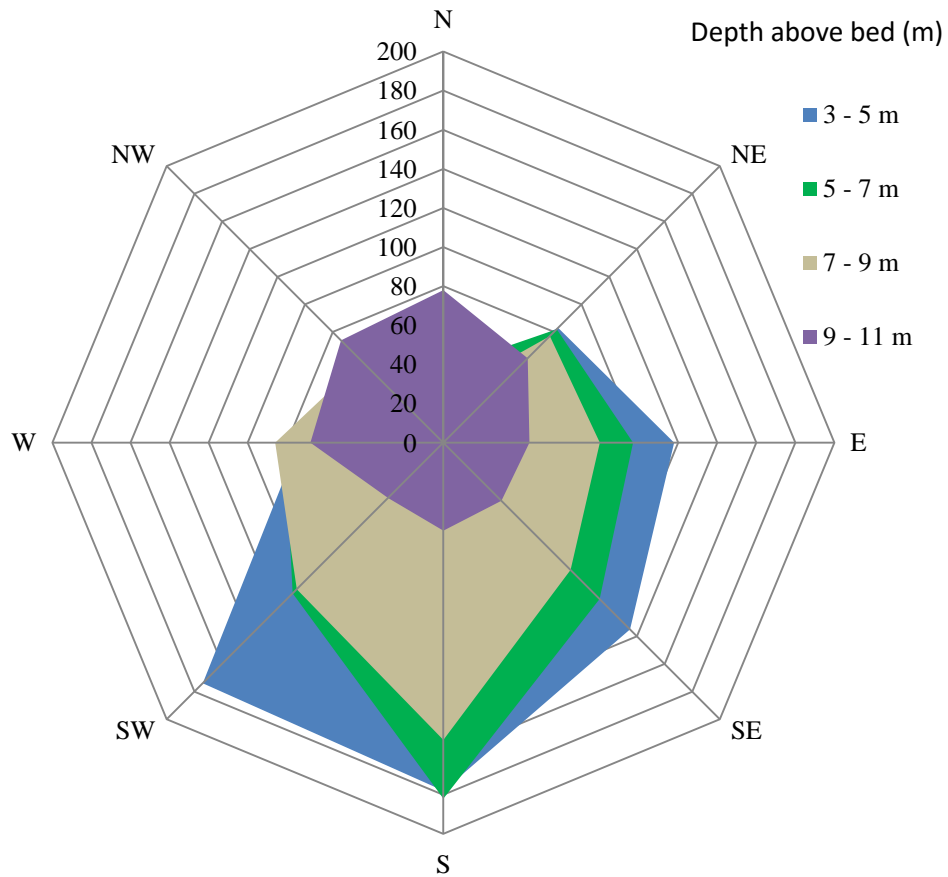


Figure 78: Observations of current direction degrees (re true north) derived from the data collected using the ADCP (the various colours indicate different depth intervals).

8.4.2. Sediment transport pathway

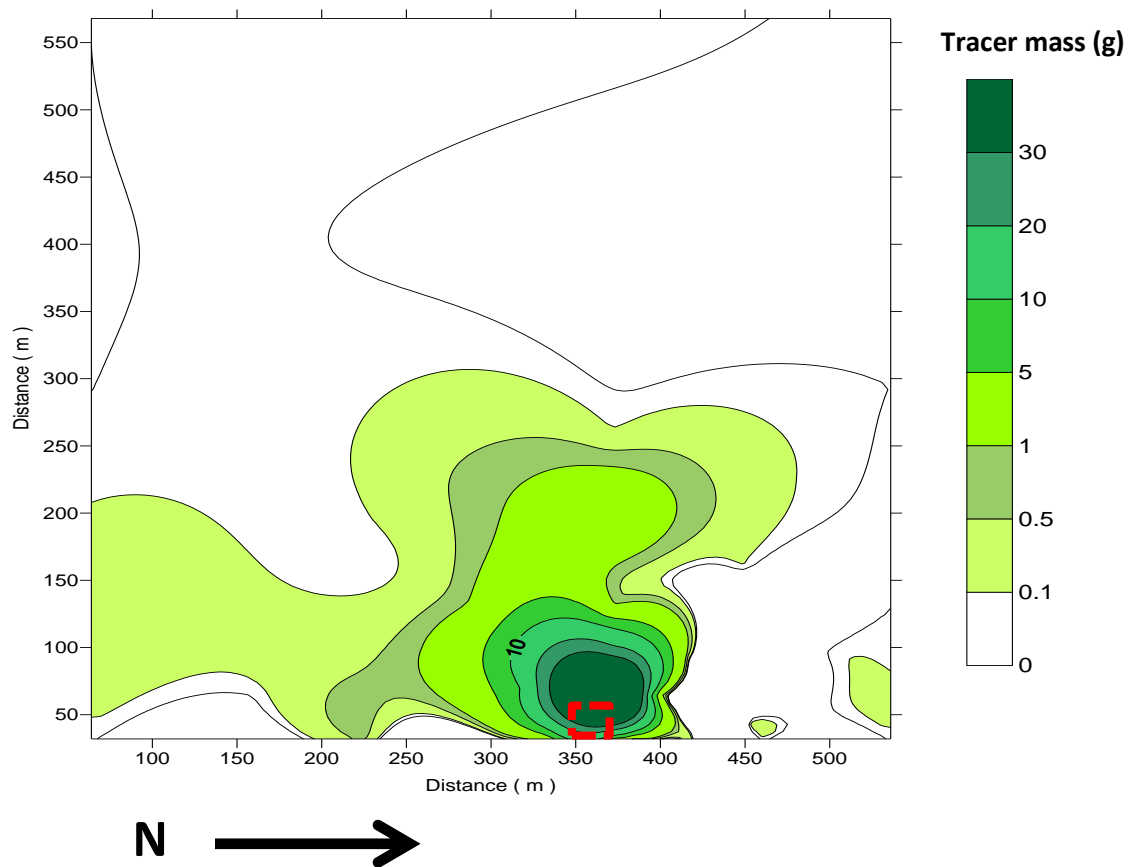
The transport pathway was determined from analysis of the data collected from sampling of the water column and the sea bed. Sampling of the water column through the use of *in situ* magnetic rigs resulted in the recovery of 189 g of tracer, 75 % from directly in line, 23 % from south, and 2 % from north of the discharge (Figure 66). Sampling transects conducted to the north of the discharge (T_1 and T_2) showed higher tracer concentrations nearer the shore. Comparatively, transects positioned to the south of the discharge (T_5 and T_6) showed higher tracer concentration offshore, with near shore locations recording no or low concentrations of tracer (Figure 79). On T_3 as the distance from source increased (offshore), tracer concentration within the water column decreased by $\sim 0.4 \text{ g} / \text{l}^3$ per metre offshore. Sampling of the sea bed resulted in the recovery of 238 g of tracer, 92 % was recovered from directly in line, 7 %

recovered from south and 1 % recovered from north of the discharge. These data indicate net transport of discharged particles in the dominant current direction (southerly direction).

Further evidence of the transport pathway was garnered from the data collected using the *in situ* fluorimeter. The fluorimeter position remained constant throughout, relative to the disposal, providing an indication of transport direction. Further, the fluorimeter provided a time series of data, critical to understanding the role of tide and current in the redistribution of discharged sediments. Transport was directly linked with tide state. Initial transport was observed in the direction of the net current flow, where tracer concentration values were observed at 934 ug l (Figure 80). With the commencement of slack high water, the observed tracer concentration, decreased to 15 ± 34 ug l, for a period of 79 minutes. This is indicative of transport in the direction contrary to the net current flow, driven by the discharge jet flow. Following the commencement of the flood tide, high tracer concentrations were observed for 50 minutes (Figure 80), attributed to the transport of a sediment-laden plume in the net current direction.

The plume, which developed during slack high water, was estimated to be 108 m in length, (assumed to be along the plume axis based on dominant current conditions). Within the plume, tracer concentrations ranged from 33 to 533 ug l, characterised by a high concentration front which decreased exponentially with time and thus length along the plume axis (Figure 80).

For the remainder of the discharge, tracer concentration levels observed by the fluorimeter remained higher than background levels. This indicated sustained transport of discharged particles in the net current direction (southerly direction) (Figure 80).



Discharge zone

Figure 79: An interpolated map of the spatial distribution and relative tracer mass 1m above the bed post simulated discharge event. Data collected using *in situ* magnetic sampling. The discharge zone and North is marked.

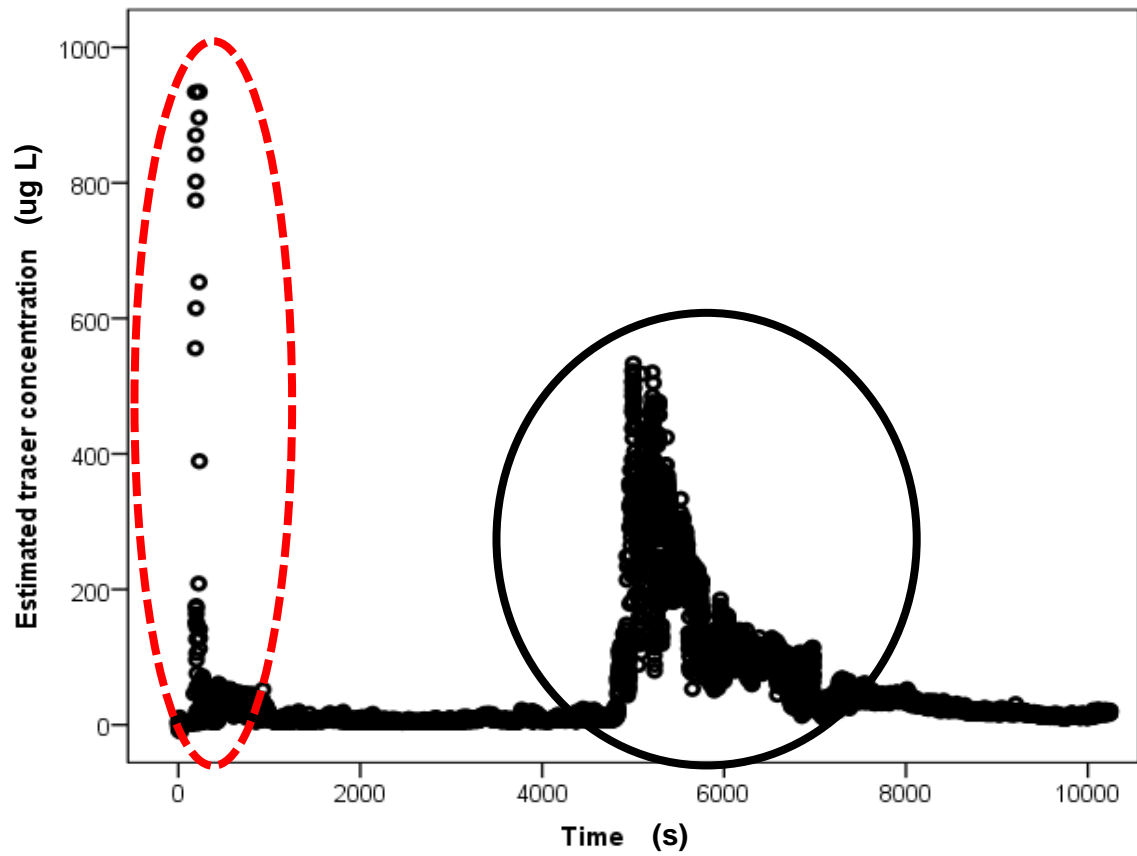


Figure 80: The fluorometer response during tracer deployment. The transport pathway is determined from the position of the fluorometer in relation to the discharge. The dashed red circle indicates initial transport to the south and the black circle indicates detection of significant tracer particles moving south, inferred to be a sediment laden plume.

8.4.3. Sedimentation pattern

The sedimentation pattern of the discharged particles shows an elongated, high-concentration area of sediment deposition, extending from within the discharge zone to 150 m offshore (Figure 81). On T_3 as the distance offshore increased, tracer concentration on the sea bed reduced at a rate of $\sim 0.98 \text{ g m}^{-2}$ per metre offshore. On T_3 , the tracer concentration reduced from a peak of 158 g m^{-2} at 64 m to 0.3 g m^{-2} at 224 m, offshore. Similarly, on T_4 , the tracer concentration reduced from a peak of 13 g m^{-2} at 64 m to 0.3 g m^{-2} at 224 m, offshore. Across T_1 , T_2 , T_5 and T_6 , no significant difference is observed between the tracer concentration on the sea bed, ranging from $0.28 - 0.48 \text{ g m}^{-2}$ ($n = 9$, $p = > 0.05$). This is indicative of consistent particle fallout at the bottom boundary layer (Figure 82).

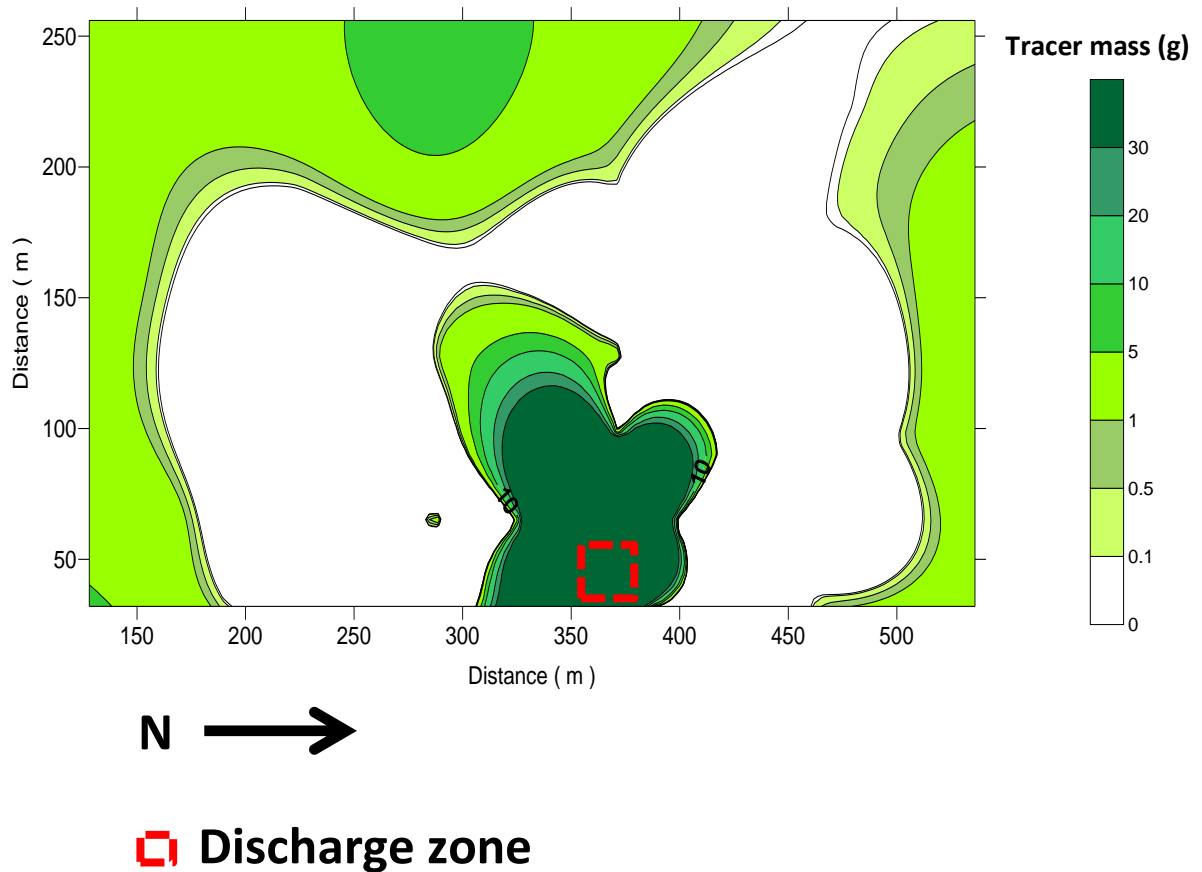


Figure 81: An interpolated map of the spatial distribution and relative tracer mass on the sea bed post simulated discharge event. Samples collected using a van veen sea bed grab sampler. The discharge zone and North is marked.

In total 94 and 98 % of the tracer sampled was recovered from within 100 m of the discharge zone from the water column and sea bed respectively. As expected, the data demonstrated as the distance offshore increased, the tracer concentration decreased (Figure 82). A mass balance calculation indicated that 450 kg of tracer remained within 100 m² of the discharge zone, with 150 kg remaining within the 600 m² area within the sampling boundary, accounting for approximately 75 % of the tracer deployed.

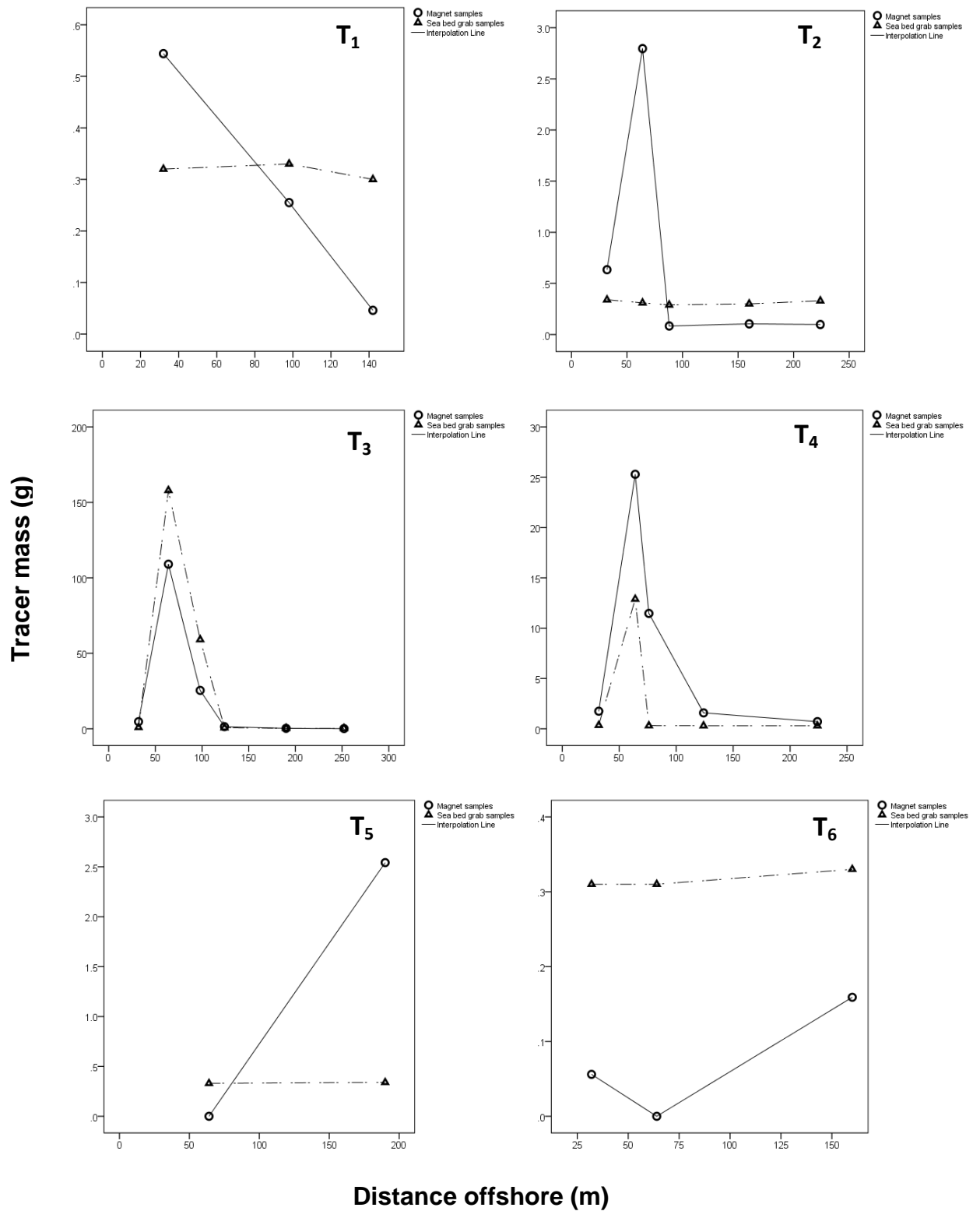


Figure 82: The tracer concentration on the sea bed (g m^{-2}) and in the water column (g l^{-3}) Vs distance offshore from the quay wall. T₁ and T₂ are located to the north of the discharge zone, T₃ is directly offshore from the centre of the discharge zone and T₄, T₅ and T₆ are located to the south of the discharge zone. Note: the offshore edge of the discharge zone is located at 60 m offshore from the quay wall.

As the current velocities observed at the site occasionally exceed the threshold of incipient motion of particles at rest on the sea bed (Figure 83) the theoretical data indicates where fine material is deposited on the seabed medium silt sized sediments ($< 0.04 \text{ mm}$) are likely to be mobilised by the tidal currents at the site. Consequently, the evidence suggests deposits at the site can be considered *highly mobile*.

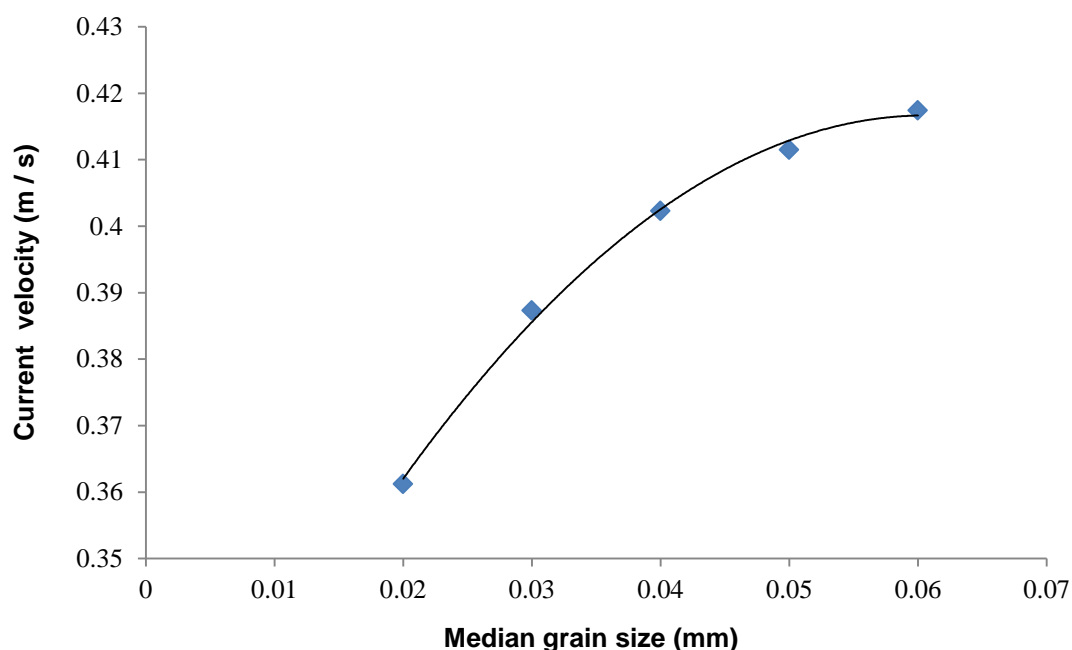


Figure 83: The threshold of incipient motion of deposited fine sediment at the site derived from the equation outlined by (Soulsby, 1997).

8.5. Discussion

This study simulated a field-scale, dredge disposal event from a small dredging vessel. This enabled the assessment of the spatio-temporal distribution of a silt-rich, sediment-laden discharge. Significant tracer deposition was observed within 100 m of the disposal zone. As the distance from source increased (offshore), tracer concentration both within the water column and on the sea bed decreased by $\sim 0.4 \text{ g / l}^3$ and $\sim 0.98 \text{ g / m}^2$ per metre offshore, respectively (derived from the data collected from sampling transect 3). Sediment transport was driven by the discharge jet flow and the receiving current. The mean current velocity was 33.8 mm s travelling in a mean current direction of 174 degrees, re true north, indicating a dominant tidal current in a

southerly direction. Sampling of the water column and sea bed indicated net transport of discharged particles in the dominant current direction. These data demonstrated that the pattern of sediment transport, and the subsequent sedimentation pattern, of discharged sediment will be controlled by the stage of the tide, and is therefore directly linked to the timing of discharge events (Akar and Jirka, 1995).

On a tidal scale, consistent current speed and direction were measured throughout the water column, resulting in tracer being transported in the direction of the net current flow (Brown et al., 1999b, van Rijn, 1993, Barua et al., 1994, Akar and Jirka, 1994, Akar and Jirka, 1995). During the high water slack, near field transport in a contrary direction to the net current flow was observed, driven by the jet flow (Akar and Jirka, 1994, Akar and Jirka, 1995). In total, 21% and 6% greater tracer mass was recovered from samples collected to the south of the discharge zone from the water column and sea bed, respectively, indicating net transport to the south. The observed sedimentation patterns show a high-concentration waste field region (Roberts et al., 1989, Kim et al., 2000), elongated significantly in the mean flow direction (Cuthbertson and Davies, 2008). Extensive deposition of tracer within 100 m of the discharge zone is attributed to reduced current velocity at high water slack (Brown et al., 1999), and the general low ambient current velocities observed at the site (Soulsby, 1997).

Monitoring of the discharged sediment utilising an *in situ* fluorimeter and *in situ* magnetic sampling rigs provided estimation of the length and in-plume tracer concentrations. Estimated in-plume concentrations reduced exponentially along the assumed plume axis, attributed to continuous particle fallout at the bottom boundary layer (Cardoso and Zarrebini, 2001), and the transition to a passive diffusion process (Akar and Jirka, 1994). Plume tracer concentrations peaked at 934 $\mu\text{g l}^{-1}$. Examination of the magnetic rigs indicated a cumulative, peak concentration, at the bottom boundary layer of the plume of 49 g l^{-3} at the edge of the discharge zone, reducing to 0.04 g l^{-3} at the edge of the sampling boundary. The magnetic rigs act as suspended *time integrated samplers* but with the benefit of only sampling iron rich or Fe-bearing material. The limitation of the magnetic rigs is that there is an upper

limit to the amount of sediment that can be retained on the magnet (Guymer et al., 2010). This was evident at the sampling station located directly in front of the discharge zone, where tracer concentrations on the sea bed, exceeded those observed in the water column. This limitation prevented the reliable determination of tracer concentration values.

The measured current velocity data captured using the ADCP deployed at the site corresponded well with modelled hydrodynamic data at the site. These data enabled a theoretical assessment of the stability of the deposited silt sized sediment following deposition. The measured data showed that current velocities at the site occasionally exceed (i.e. during the spring tidal regime) the threshold of motion i.e. the shear stress applied on the sea bed due to the tidal currents is great enough to mobilise the deposited sediment. This theoretical assessment provides a greater understanding of the sediment transport dynamics at the site despite field data not being available. That silt sized sediment deposited is highly likely to be re-mobilised and distributed around the site during spring tidal currents will result in increased water turbidity and decreased water quality. These data show the importance of appropriate management strategies to control the volume of sediment (particularly fine (< 63 micron) sized sediment) discharged within the nearshore marine environment because of the potentially significant environmental implications of increasing volumes of fine sediment in the water column. This study demonstrates the importance of sediment tracing to understand and inform upon the sediment transport pathway of silt sized sediments.

The dual-signature tracer provided a tool to simulate a discharge event from a storm water outfall. A tracer with multiple tracer signals was beneficial as it enabled a variety of sampling techniques to be employed to monitor the tracer once deployed to the environment. This is particularly beneficial when deploying silt sized tracer particles in a highly industrialised setting due to the likely presence of significant anthropogenic contamination - which can be considered background noise. The silt tracer was successfully deployed to create a sediment-laden plume, identifiable within the environment, enabling the transport and deposition patterns of the discharged sediments to be

assessed (Black et al., 2007b). The sampling campaign, which utilised, both the magnetic and fluorescent signatures of the tracer, incorporated active and passive sampling techniques, to determine the immediate transport pathway and depositional footprint of the discharged sediments. These pathways can be considered reflective of sediment transport processes in the environmental setting studied. Further, the spectrofluorimetric tracer enumeration technique provided an effective method of determining tracer content within samples where non-fluorescent, magnetic, background material was present. The strongly linear calibration lines, small variance of experimental points and consistently high coefficients of determination (R^2) indicated the potential for high accuracy of tracer enumeration.

8.6. Conclusion

This study demonstrated the critical role of tide and current in the near and far field transport of disposed dredged sediment. The use of a particulate, dual-signature tracer enabled monitoring of a simulated field-scale, fine sediment disposal event. Once deployed, the spatio-temporal distribution and sedimentation pattern of the discharged particles was assessed over a tidal scale. Due to study resources, data was only collected over 48 hours limiting the information provided by the study. Significant deposition was observed within 100 m of the discharge zone. These results highlight the requirement for informed mitigation strategies and risk assessment approaches to be developed, to reduce the detrimental impacts of environmentally irresponsible dredge disposal. This study provides baseline data useful for future field studies and validation of modelling approaches. Finally, the study outlined a sediment tracing methodology that can be used at the field-scale, within a complex, highly industrialised setting, to monitor the transport and deposition of silt sized sediments transported in suspension. The theoretical assessment of the stability of the deposited sediments under the native tidal current regime indicated that deposited sediment would be mobilised by tidal current velocities observed during the spring tidal regime. This highlights the requirement for effective management strategies to be developed to ensure the disposal of fine sediment in the near shore environment will not adversely affect the area in the future. This is clear evidence which shows the

importance of understanding sediment transport pathways and sediment transport regimes within the environment and thus demonstrates the utility of the active sediment tracing approach to investigate and inform on potential environmental impacts in the marine and coastal environment.

9. Thesis summary

Particle tracking, sometimes referred to as 'sediment' or 'particle' tracing is a direct field method that utilises 'marked' or 'tagged' particles to define the transport pathway, quantify the mass and rate of sediment / soil in transit and determine source-sink relationships within a broad range of environments. This novel technique has far-reaching applications and is able to provide information and quantitative data regarding sediment / soil dynamics over broad spatial and temporal scales. For these reasons interest in the use of particle tracking techniques has increased due to the additional information they provide. Recent technological developments have reignited interest in active sediment tracing techniques and approaches with government organisations, researchers and industry. These developments have led to innovative sampling strategies, refined analysis techniques and original application. Active sediment tracing does not provide a panacea for sediment investigations, but does provide a powerful tool for oceanographers, hydrologists, soil researchers and geologists. Effective, proven methodologies within the scope of active sediment tracing approaches, when utilised within the limitations of the technique can provide robust data and information of value to a multi-disciplined academic community, government organisations and industry.

This thesis was positioned on the nexus between industry and academia and has highlighted the benefits of working with commercial organisations to deliver research programmes. The commercial product, dual signature tracer, proved to be an effective tool to monitor and map sediment transport pathways useful to academic and research organisations alongside commercial clients. This thesis has demonstrated the utility of active sediment tracing as a practical field tool to investigate sediment transport dynamics. Further, it has demonstrated the significance of practical field tools able to further our understanding of earth surface processes to aid in the assessment and mitigation of environmental impacts. A practical fluorescent-magnetic tracing methodology and a standardised active sediment tracing methodological framework have been developed for robust active sediment tracing. The methodology is best utilised to: 1) improve our understanding of

sediment and soil transport processes; 2) provide field data to develop or validate existing sediment transport models; and 3) evaluate the effectiveness of sediment management techniques, preventive measures or management protocol to develop informed management or mitigation strategies. The development of a robust fluorescent-magnetic sediment tracing methodology, applied within the guidelines of the methodological framework, presents a versatile tool with which to investigate sediment transport dynamics.

The review of relevant literature revealed that there were two distinct trends within the field of active sediment tracing research; 1) the use of active sediment tracers as a methodological tool to investigate sediment transport processes; and, 2) studies striving to develop novel tracing materials, field methodologies and laboratory techniques. Further distinctions were apparent primarily driven by study context and environment and therefore methodological approach. Studies which utilised active sediment tracing approaches to monitor the movement of sediment in coastal and estuarine environments predominately still follow methodologies and tracing theory outlined by researchers in the 1960's who undertook a series of experiments utilising fluorescent or radioactive tracers e.g. Ingle (1966), Inman and Chamberlain (1959), Russell (1960) whereas the application of active sediment tracing approaches in terrestrial and agricultural settings began more recently following the work of authors such as Parsons et al. (1993), Plante et al. (1999). The ban on the use of radioactive tracers and the desire / requirement to design silt and clay sized tracers inspired a series of authors to seek new tracing materials (e.g. rare earth elements) and this wave of research inspired methodological developments both in terms of field and laboratory techniques. Zhang et al. (2001) first noted the characteristics required for the optimal active tracing material within this description it was noted that a tracer with multiple signals would be considered beneficial. The development of a dual signature sediment tracer therefore can be considered advancement within the field of active sediment tracing. This thesis explored the suitability and efficacy of the tracer material as a tracer of soils, mineral sands and silts and assessed the methodological benefits that the tracer provided through the application of the tracer to a series of real world

sediment management problems. This enabled a fluorescent-magnetic sediment tracing methodology to be developed applicable to a range of environments and study contexts, to inform applied sediment management research in both academic and commercial fields.

The review of relevant literature outlined the techniques currently available to monitor and evaluate sediment transport within the environment. The sediment tracing technique proved to be the only technique that is able to directly evaluate the geospatial distribution of sediment transport in the field. This is important as field data regarding sediment transport is often studied using point measurement sampling techniques. A geospatial sediment transport data set is beneficial and potentially could improve modelling approaches by providing checks and balances for model development. Further, as a tool to confirm the existence of sediment transport pathways and source – sink relationships, the active sediment tracing approach is able to unequivocally confirm the existence / presence of sediment transport pathway(s). Current active sediment tracing approaches based on the principles established by the pioneering studies conducted in the 1960's by authors such as Ingle (1966) and Inman and Chamberlain (1959) still utilise a mono-signature tracer. Having a single signature by which to differentiate the sediment tracer from the native sediment restricts the sampling techniques available to monitor the sediment tracer. This often increases the resource intensive nature of active sediment tracing approaches by increasing the volume of samples collected in the field as the use of non-intrusive sampling approaches is finite. Dual signature tracers increase the variety of sampling techniques and non-intrusive *in situ* monitoring techniques that can be utilised. Dual-signature tracer can replicate multiple tracer size fractions, from silts to cobbles, and marries the individual fields of fluorescent and magnetic sediment tracing. This improves the cost benefit ratio of sediment tracing studies. Thus, when deploying the same quantity (mass input) of tracer, studies which use the dual signature tracer are more likely to reap greater information. This is important as the cost of the tracing material often constitutes the principal cost within an active tracing study. Further, the presence of two tracer signals increases the flexibility of the technique and

enables studies to be conducted within complex, industrialised or anthropogenically altered settings. The passive and active sampling techniques described, detail a range of techniques available to monitor and recover silt and coarse sized tracer particles once deployed to the environment. In light of this research and analysis it is reasonable to conclude that the dual signature sediment tracer can be considered an advance over previously used mono-signature tracers.

The active sediment tracing approach does have inherent limitations that must be considered within each application of the active sediment tracing technique. It is critical to remember that sediment tracing studies only provide information regarding the forcing mechanisms observed during the study period and these conditions must be considered when interpreting the results. To improve any sediment tracing the availability or collection of longer term data regarding the forcing mechanisms at the site are beneficial (i.e. the collection of weather, metocean and hydrodynamic data). This improves the framing of any study and provides study context (i.e. framing a study provides greater understanding as to whether the conditions experienced during the study were 'typical' of the forcing experienced throughout the year / decade / century). Regardless of whether this data is collected active sediment tracing studies are best applied to monitor sediment transport from instantaneous and event based scales through to year scales. The data from this thesis indicates that the dual signature tracer will remain identifiable within the environment for > 1 year, yet without repeat nourishment of the tracer source (dependant on the initial tracer mass deployed and hydrodynamic conditions experienced at the site or during the observation period) it is highly unlikely that sediment transport pathways will continue to be able to be elucidated at this point as the likelihood is that the tracer concentration within the system will be significantly reduced. These findings indicate that as a tool to evaluate geomorphological change over decadal time scales active sediment tracers are not the appropriate tool to use. However, the technique does have a potentially key role to play within geoscience research and commercial studies within the future. The technique is particularly useful in answering direct sediment transport questions. As sampling resources are never finite specific objectives

need to be set and the limitation of the technique thoroughly understood at the study planning stage. Phrasing of appropriate research questions is key, questions phrased *where does the sediment go?* are far less likely to achieve successful results compared with a hypothesis; *does the sediment deposit within this area?* This provides a far greater opportunity for the technique to provide useful study results. In addition, when using active sediment tracer there is always the chance that a transport event of significance could occur that is able to transport the tracer beyond the study limits, destroying a tracing study. This is a recurrent problem in any tracing study and must be considered and where possible mitigated against. These limitations remain despite the technological advancements described in this thesis and should be considered a methodological limitation.

A tracer which strongly matches the native sediment will behave in a similar fashion (Black et al., 2007, Dyer, 1986). Here, the hydraulic properties (i.e. particle size distribution, specific gravity and settling velocity) of each tracer deployed closely matched those of the target sediment. Thus, it is reasonable to conclude that the movement of tracer reasonably simulated the movement of each native sediment traced (soils, silts and marine sands). Further, the Gaussian-type particle size distribution of each tracer batch facilitated the creation of composite tracers, characterised by a multimodal size distribution. A significant limitation of dual signature tracer is the inability to coat clay and fine silt sized particles. Understanding the transport behaviour of clay sized sediment is fundamental to the sustainable management of aquatic environments (Droppo and Ongley, 1992), yet the collection of field data relating to cohesive sediments presents a range of theoretical and practical difficulties, and significant challenges in terms of tracer design (Spencer et al., 2007, Spencer et al., 2010). There is a great need for field data relating to sediment transport trends of fine and cohesive sediments (Spanhoff and Suijlen, 1990). As effective clay tracers are not currently commercially available a pragmatic approach towards tracking the fine silts and clay fractions has been outlined. This practical field method is termed *floc tagging* yet further research is required to fully characterise the effectiveness of this technique. During the investigation of suspended sediment transport in

the near-shore coastal zone deployment, sampling and recovery techniques needed to be adapted in terms of practical approach and technology (Black et al., 2007). Silt - sized sediment (10 - 63 micron in size) transported in suspension can be distributed over great distances before being deposited (Dyer, 1986, Dyer, 1995, Droppo and Ongley, 1994). This has significant practical implications for the comparative success of silt tracing studies (Black et al., 2007). The field study to monitor the disposal of dredged sediments in the nearshore coastal zone demonstrated the critical role of tide and current in the near and far field transport of disposed dredged which creates a high density tracer plume. The study investigated the initial near field and far field dispersion of the sediment in an area where low current velocities were observed. Monitoring of sediment in suspension was required. The approach here utilised two approaches: 1) an *in situ* fluorimeter to monitor the cloud of tracer as it moved through the water column. The methodology described within this thesis highlights the potential of sensor based technologies to monitor tracer travelling in suspension, yet further development would be valuable (e.g. multi-sensor arrays); and, 2) *in situ* magnets which act as a time integrated sampler which samples only Fe or Fe bearing materials. This significantly reduces the volume of sediment collected, which is useful practically. These tracer sampling tools enabled silt sized sediments to be monitored and sampled whilst in suspension. Further research is required to evaluate the use of these techniques in more dynamic environments with greater current velocities and turbulence.

The other two field trials focused upon soil erosion within a fallow agricultural field and sediment transport on a beach face. The soil erosion study tested a dual signature tracer within controlled laboratory experiments and applied it in a fallow agricultural field. The laboratory studies suggested that the tracer showed strong potential in tracing a variety of soil types and particle sizes. The laboratory results indicated that the tracer performed optimally when deployed within coarser, sandier sediments in comparison to clay rich soils, highlighting the requirement for effective clay sized tracers to be developed. The study focused on developing a method to trace soil utilising the dual signature tracer and the effectiveness of the tracer as a tracer of

different soil types. A primary challenge was to develop a composite tracer that matched the multimodal size distributions of soils. The composite tracer developed performed well and the results indicated the composite tracer replicated the sediment transport processes of the native soil. The developed methodology enabled the quantification of a soil erosion rate and in future studies would enable soil loss to be monitored, evaluated and transport pathways elucidated. However, the results suggested that further work is required to improve the understanding of the behaviour of the tracer once deployed to the soil in terms of aggregation and disaggregation through time, and the effect of a multimodal tracer size distribution on the response to the magnetic parameter magnetic susceptibility which proved to be a simple, quick passive sampling methodology. The field trial based on the beach face demonstrated the utility of active sediment tracing approaches to monitor beach face sediment transport to provide useful information for shoreline management. This large-scale field study elucidated sediment transport pathways in a complex anthropogenically influenced shoreline environment. Again, the use of magnetic susceptibility proved a valuable tool, yet requires further work to fully understand the relationship between the background signal and the tracer, especially in areas of low tracer concentration. This study though it did provide valuable insight into the sediment transport pathways at the site, would have benefited from the use of two tracer colours as bidirectional transport was observed and therefore understanding the source area was compromised.

Given the high spatio-temporal variability of particle movement, sediment tracing studies involve the collection of a substantial number (up to 1000) of environmental samples (Guzman et al., 2013). This requires significant time and effort in the field and the laboratory (Badr and Lofty, 1998), and often involves expensive, resource intensive methods of sample analysis (White, 1998). These factors act to reduce both the number of samples able to be collected in the field, and the number that can reasonably be analysed in the laboratory. These limitations have formed a significant constraint on the tracing technique. Consequently, authors have placed strong emphasis on developing simple, rapid and reliable analytical methods for

enumeration of tracer (Black, 2012, Guzman et al., 2013). The analytical method developed within this thesis can be considered an advance on previously used fluorescent (and magnetic) enumeration methodologies e.g. Ciavola et al. (1997), Ciavola et al. (1998), Carrasco et al. (2013), Solan et al. (2004), Forsyth (2000) as it reduces analytical timescales and associated costs. This increases the number of samples that can be reasonably analysed within a tracing project. Simply, this increases the spatial and temporal resolution of active sediment tracing studies.

Having two signatures (fluorescence and ferrimagnetism) proved particularly beneficial during the analytical process. Magnetic separation provides a quick and simple technique to determine the tracer dry mass content (mass per unit mass) within environmental samples. However, in the majority of study contexts naturally occurring magnetic material is present (Pearce et al., 2014). This undesired additional mass is considered 'noise' within magnetic sediment tracing studies and in these cases magnetic separation cannot be used to determine tracer dry mass or tracer content within an environmental sample. Regardless however, magnetic separation remains useful practically, as it reduces sample volume eliminating the need for subsampling. If the tracer was solely magnetic this would be a significant constraint of the technique, but as the tracer has two signatures, fluorescence and ferrimagnetism a spectrofluorometric technique has been developed to obviate the problems associated with additional mass in samples following magnetic separation.

Spectrofluorometric detection of fluorescent tracer particles is a method of broad applicability in the study of particle dynamics within coastal, aquatic and terrestrial environments. The described analytical method provided a practical solution that was used to analyse a significant number of samples in a short period of time, at low cost. This is helpful within any tracing study (Guzman et al., 2013). The spectrofluorometric analytical procedure was adapted and developed to exploit the fluorescent attribute of the tracer particles, to provide directly, the dry tracer mass (M , g). The technique has sufficient spectral resolution to distinguish low concentrations (< 0.01 g) of two spectrally unique tracer colours. The fluorescent excitation and emission

wavelengths of fluorescent derivative are not common to materials commonly found in water (Stern et al., 2001, Wilson et al., 1986). This is strong evidence to suggest that this sample analysis technique will be applicable to analyse samples collected from a variety of environments and or study contexts. The dye concentration was proportioned to dry mass (M , g) of fluorescent tracer particles through the use of colour specific reference standards. A methodological bias of $\pm 20\%$ for single colour sample analysis, and $\pm 30\%$ for two tracer colour sample analysis, was quantified. A range of factors affect the specific coefficient of fluorescence intensity vs. tracer dry mass and potential sources of error include: 1) human error, which can be obviated by using an experienced technician with a practical and theoretical understanding of spectrofluorimetry (Gunn, 1963); and, 2) the empirical relationship between the assumed concentrations of a sample to tracer dry mass; the homogenous mixing of the particles and the native sediment; particle size distribution and surface area of the particles; the dye loading on the surface of the individual tracer particles; and the properties of the solvent and dye pigment. These potential sources of error can be significantly reduced if the coefficient is determined empirically for each combination of conditions (Carey, 1989, Gunn, 1963). The observed increased error associated with the analysis of two colour spiked samples in comparison to single coloured spiked samples, indicated where high precision is required, the use of a single tracer colour is preferable. However, the methodological bias is considered tolerable within the sediment tracing methodology, due to the error associated with other enumeration techniques (e.g. an error of 5 - 10 % attributed by Carrasco et al. (2013) to counting fluorescent tracer grains by eye) and the error related to models of sediment transport which are judged to be of the order of a factor of 10 (Eidsvik, 2004), reduced to a factor of 5 or better once validated (Soulsby, 1997) and due to the benefits it provides (e.g. reduction of analytical timescales and thus the resource intensive nature of sample analysis). This methodology provided a relatively simple, fast and non-resource intensive approach to tracer enumeration within fluorescent tracing studies, which will potentially contribute to improvement of the general utility of the technique. The three field deployments demonstrated the flexibility of the technique to monitor different sediment types. This is important as sediment tracers that

are applicable universally would be considered highly beneficial in the field of active sediment tracing. Soils and sediments differ greatly and tracing studies conducted within marine and coastal environments and terrestrial and fluvial environments present environment and site specific challenges.

This thesis provides baseline data for future studies that utilise the dual signature tracer within both academic research and industry based studies. Each field application highlighted the utility of sediment tracing studies to the wider scientific community providing information and data regarding real world, sediment management problems and the impact of sediment transport on the environment. Further, the field deployments of the tracer have demonstrated the effectiveness of the technique as the only direct field tool able to confirm the existence of sediment transport pathways and define source-sink relationships which provides important information to inform environmental management strategies. From this research three limitations of dual signature tracer have been identified: 1) clay sized tracers are not available; 2) the creation of a dust fraction with varied properties to the tracer batch; and, 3) the manufacturing cost. Limitations, 1 and 3 are unfortunately, not specific to dual signature tracers and at this moment the 'ideal' active tracer (i.e. a low cost tracer which can be designed / manufactured to mimic the properties of the entire sediment class range from clays to gravels) remains elusive. Limitation 2 can be addressed through methodological best practice (i.e. wet sieving of the tracer prior to deployment), and this should be considered by the manufacturer.

From the extensive theoretical and experimental work undertaken a number of areas where further research is required have been identified. The areas identified fall into three categories: 1) the development of new field methodologies; 2) specific experimental work to further our understanding of the behaviour of tracers once flocculated with native clays and silt size sediment; and 3) the theoretical challenge of interpreting high resolution, event scale field data. Future research should strive to develop passive sampling techniques that reduce the resource intensive nature of monitoring and sampling tracer in the field. Potentially fruitful fields of exploration include *in situ*, quantitative, image analysis e.g. Darvishan et al. (2014), the use of

sensor based techniques e.g. Guymer et al. (2010); and, the use of drone technology and Unmanned Aerial Vehicles (UAV's) with fluorescent detection capabilities. Developments of new passive monitoring techniques have the potential to increase the spatial and temporal resolution of tracing studies enabling successful tracer monitoring in increasingly dynamic environments. As clay and fine silt sized tracers are still primarily in the developmental stage this thesis has proposed a practical field methodology that provides information on the sediment transport pathways of fine silt and clay sized sediments. This technique tags a component (target size fraction) of the floc rather than the entire floc. Further research is required to better understand the sediment transport dynamics and behaviour of the tracer once flocculated to further our understanding of the efficacy of the proposed methodology. Finally, research should be conducted regarding the most appropriate methodology for interpreting and extrapolating event scale, high resolution field data to further the impact and utility of a sediment tracing study as a geomorphological tool. A multi-tool approach should be considered where long term field monitoring, active sediment tracing studies and a numerical modelling approach is utilised for applied sediment management research. The optimal tool to inform long term sediment transport assessments is a numerical modelling approach, yet these models need to be validated and calibrated using field data. The data generated through active sediment tracing studies can provide useful information to underpin model checks and balances yet future research should consider the most appropriate way to integrate this 'snapshot' data into a sediment transport model to optimise the use of the quantitative qualitative data garnered during an active sediment tracing study.

10. Thesis conclusion

Tracing studies have the potential to improve upon the conceptual understanding of sediment transport regimes. They can be conducted to identify potential sediment source areas, transport pathways and specific areas of sediment deposition, accumulation and erosion and when applied correctly can be used to determine the sediment transport rate. These data are critical to developing robust sediment management plans, and implementing informed, remedial strategies to maintain and improve the environment we reside within. The environment specific methodologies outlined, enabled a large volume of data to be collected during each study. This suggests that future studies could work at a greater spatial and temporal resolution, a factor important to improving our understanding of soil erosion and sediment transport across the earth's surface. Overall, the results suggest that dual signature tracer appears to be an effective tracer of soils and sediments. While active sediment tracing does not provide a panacea for the management of sediment transport related problems, it should be considered, a useful tool in the box.

This thesis has developed a fluorescent magnetic tracing methodology that has been successfully applied to investigate a range of real world, sediment problems. The method has demonstrated value and applicability across a range of contexts, encompassing soil erosion, and beach and near shore sediment transport in the coastal zone. The developed universal methodological framework provides an aid for future practitioners. The framework might act to provide consistency across academic fields and industry, within which each stage of the methodology can continue to be developed.

The findings of this thesis indicate dual signature tracer is an advance within the field of active sediment tracing. Having two signatures proved beneficial. This enabled unique monitoring, recovery and enumeration methodologies to be developed. The field methodology was adaptive and could be specifically tailored to suit both the receiving environment, and study context. The use of a multistage sampling campaign enabled a greater wealth of information to be garnered from each field application. Further, the

developed tracer enumeration methodology reduced analytical timescales, and associated costs, improving the benefit cost ratio of the technique. Dual signature tracing studies are now able to: employ two tracer colours in the same area concurrently; utilise *in situ* tracer monitoring techniques; increase sampling frequency in the field; and analyse a greater quantity of samples in the laboratory. These developments act to increase the scope of active sediment tracing studies and improve the validity of the technique as an environmental monitoring tool. Through the research conducted the limitations of dual signature tracer have been outlined and areas where further study is required, identified.

11. References

- ADAMS, E. E. 1998. Deposition of contaminated sediments in Boston Harbor studied using fluorescent dye and particle tracers. *Estuarine, Coastal and Shelf Science*, 46, 371-382.
- AKAMATSU, K. & MATSUO, M. 1973. Safety of optical whitening agents *Senryo To Yakuhin*, 18, 2-11.
- AKAR, P. J. & JIRKA, G. H. 1994. Buoyant spreading processes in pollutant transport and mixing Part1: Lateral spreading with ambient current advection *Journal of Hydraulic Research*, 32, 815-831.
- AKAR, P. J. & JIRKA, G. H. 1995. Buoyant spreading processes in pollutant transport and mixing Part 2: Upstream spreading in weak ambient current. *Journal of Hydraulic Research*, 33, 87-100.
- AL-MADANY, I. M., ABDALLA, M. A. & ABDU, A. S. E. 1991. Coastal Zone Management in Bahrain: an Analysis of Social, Economic and Environmental Impacts of Dredging and Reclamation. *Journal of Environmental Management*, 32, 335-348.
- ALBANI, J. R. 2008. Fluorescence Quenching. *Principles and Applications of Fluorescence Spectroscopy*.
- ALLEN, J. R. L. 1985. *Principles of physical sedimentology*, London, George Allen & unwin Ltd 159-170 Principles of physical sedimentology.
- AMBULATOV, N. A. & PATRIKEIEV, V. V. 1963. On the influence of luminophoric and agaroid films on the hydrodynamic properties of tracer sand. *Okeanologia*, 3, 921-924.
- AMORE, E., BANASIK, K., BELYAEV, V. R., BIDIN, K., BLAKE, W. H., CARRIGAN, E., CHAFER, C. J., CHAPPELL, N. A., CLARKE, M. A., COLLINS, A. J., CURRAN, K. J., DOERR, S. H., DOUGLAS, I., DROPPO, I. G., ELLIOT, W. J., EVANS, D. J., EVANS, R., FARGUELL, J., FOSTER, I. D. L., GIBSON, C. E., GOLOSOV, V. N., HANAPI, J., HEJDUK, L., HILL, R. D., HUMPHREYS, G. S., IRVINE, K. N., JARRITT, N. P., JASKOT, C., JETTEN, V., KINNELL, P. I. A., KUHN, N. J., LARENUS, J., LAWRENCE, D. S. L., LICCIARDELLO, F., MAYO, S., MCHUGH, M., MORGAN, R. P. C., MURRAY, A. S., NACHTERGAELE, J., NEARING, M. A., NIKORA, V., NUNNY, R. S. & OWENS, P. N. 2006. *Soil erosion and Sediment Redistribution in River*

Catchments, Measurement, Modelling and Management, Oxfordshire, UK, CABI.

- ANDERSON, W. P., ANTHONY, E. J., CONLEY, D. C., FITZGERALD, D., GEHRELS, R., GEORGIU, I., HETEREN, S. V., KENCH, P., KROON, A., LOVELOCK, C. E., MASSELINK, G., MILNE, G. A., MINER, M., NICHOLLS, R. J., NORDSTROM, K. F., RANASINGHE, R., ROGERS, K., RUESSINK, G., STEPHENSON, W., STIVE, M. J. F., SWWITZER, A. D., TOL, R. S. J. & WOODROFFE, C. D. 2014. *Coastal Environments and Global Change*, Chichester UK, John Wiley & Sons.
- ANGARITA-JAIMES, D., ORMSBY, M., CHENNAOUI, M., ANGARITA-JAIMES, N., TOWERS, C., JONES, A. & TOWERS, D. 2008. Optically efficient fluorescent tracers for multi-constituent PIV. *Exp. Fluid*, 45, 623-631.
- ANON 1996. Monitoring and assesment of the marine benthos at UK dredged material disposal sites. . *Scottish Fisheries Information Pamphlet* 21, 35.
- ARAUJO, M. F., JOUANNEAU, J. M., VALERIO, P., BARBOSA, T., GOUVEIA, A., WEBER, O., OLIVEIRA, A., RODRIGUES, A. & DIAS, J. M. A. 2002. Geochemical tracers of northern Portuguese estuarine sediments on the shelf. *Progress in Oceanography*: elsevier.
- ARIK, M., CELEBI, N. & ONGANER, Y. 2005. Fluorescence quenching of fluorescein with molecular oxygen in solution. *Journal of Photochemistry and Photobiology*, 170, 105-111.
- ARMSTRONG, A., QUINTON, J. N., HENG, B. C. P. & CHANDLER, J. H. 2011. Variability of interrill erosion at low slopes. *Earth Surface Processes and Landforms*, 36, 97-106.
- ARMSTRONG, A., QUINTON, J. N. & MAHER, B. A. 2012. Thermal enhancement of natural magnetism as a tool for tracing eroded soil. *Earth Surface Processes and Landforms*, 37, 1567-1572.
- ARMSTRONG, J. D., KEMP, P. S., KENNEDY, G. J. A., LADLE, M. & MILNER, N. J. 2003. Habitat requirements of Atlantic salmon and brown trout in rivers and streams. *Fisheries Research*, 143-170.

- ASPILA, K. I., AGEMIAN, H. & CHAU, A. S. Y. 1976. A semi-automated method for the determination of inorganic, organic and total phosphate in sediments. *Analyst*, 101, 187-197.
- ASSOULINE, S. & BEN-HUR, M. 2006. Effects of rainfall intensity and slope gradient on the dynamics of interrill erosion during soil surface sealing. *Catena*, 66, 211-220.
- ATHANASIOS, N., ELHAKEEM, M., KRALLIS, G., PRAKASH, S. & EDINGER, J. 2008. Sediment Transport Modeling Review - Current and Future Developments. *Journal of Hydraulic Engineering*.
- BACON, M. P. & RUTGERS VAN DER LOEFF, M. M. 1989. Removal of ^{234}Th by scavenging in the bottom nepheloid layer of the ocean. *Earth and Planetary Science Letters*, 92, 157-164.
- BADR, A. A. & LOFTY, M. F. 1998. Tracing beach sand movement using fluorescent quartz along the Nile delta promontorie. *Journal of Coastal Research*, 15, 261-265.
- BAGARELLO, V. & FERRO, V. 1998. Calibrating storage tanks for soil erosion measurement from plots. *Earth Surface Processes and Landforms*, 23, 1151-1170.
- BAI, X., ZHANG, X., LONG, Y., LIU, X. & ZHANG, S. 2013. Use of ^{137}Cs and ^{210}Pb measurements on deposits in a karst depression to study the erosional response of a small karst catchment in Southwest China to land-use change. *Hydrological Processes*, 27, 822-829.
- BALCERZAK, W. 2006. The Protection of Reservoir Water against the Eutrophication Process. *Polish Journal of Environmental Studies* 15, 837-844.
- BALLANTINE, D. J., WALLING, D. E., COLLINS, A. L. & LEEKS, G. J. L. 2009. The content and storage of phosphorus in fine-grained channel bed sediment in contrasting lowland agricultural catchments in the UK. *Geoderma*, 141-149.
- BANDT, H. J. 1957. Giftig oder ungiftig fur Fische? *Deut. Fisch. Rundsch*, 4, 170-171.
- BARUA, D. P., KUEHL, S. A., MILLER, R. L. & MOORE, W. S. 1994. Suspended sediment distribution and residual transport in the coastal

- ocean off the Ganges - Brahmaputra river mouth. *Marine geology*, 120, 41-61.
- BATELAAN, O. & DE SMEDT, F. 2007. GIS-based recharge estimation by coupling surface–subsurface water balances. *Journal of Hydrology*, 337, 337-355.
- BAUER, N., WALLNER, A. & HUNZIKER, M. 2009. The change of European landscapes: Human-nature relationships, public attitudes towards rewilding, and the implications for landscape management in Switzerland. *Journal of Environmental Management*, 90, 2910-2920.
- BAXTER, C. V. & HAUER, F. R. 2000. Geomorphology, hyporheic exchange and selection of spawning habitat by bull trout (*salvelinus confluentus*). *Canadian Journal of Fisheries and Aquatic Science*, 57, 1470-1481.
- BEASLEY, R. P. 1972. *Erosion and sediment pollution control*, Iowa, Ames.
- BEEKEY, M. A., MCCABE, D. J. & MARSDEN, J. E. 2004. Zebra mussels affect benthic predator foraging success and habitat choice on soft sediments. *Behavioural Ecology*, 141, 164-170.
- BELYAEV, V. R., GOLOSOV, V. N., MARKELOV, M. V., EVRARD, O., IVANOVA, N. N., PARAMONOVA, T. A. & SHAMSHURINA, E. N. 2013. Using Chernobyl-derived ¹³⁷Cs to document recent sediment deposition rates on the River Plava floodplain (Central European Russia). *Hydrological Processes*, 27, 807-821.
- BENAMAN, J., SHOEMAKER, C. & HAITH, D. 2005. Calibration and Validation of Soil and Water Assessment Tool on an Agricultural Watershed in Upstate New York. *journal of Hydraulic Engineering*, 10, 363-374.
- BENEVENTE, J., GRACIA, F., ANFUNSO, G. & LOPEZ-AGUAYO, F. 2005. Temporal assessment of sediment transport from beach nourishments by using foraminifera as natural tracers. *Coastal Engineering: Elsevier*.
- BERNACCHI, S. & MELY, Y. 2001. Exciton interaction in molecular beacons: a sensitive sensor for short range modifications of the nucleic acid structure. *Nucleic acids Research*, 29, 62.
- BERTIN, X., DESHOULIERES, A., ALLARD, J. & CHAUMILLON, E. 2007. A new fluorescent tracers experiment improves understanding of

- sediment dynamics along the Arcay Sandspit (France). *Geo Marine Letters*, 27, 63-69.
- BERTIN, X., OLIVIERA, A. & FORTUNATO, A. B. 2009. Simulating morphodynamics with unstructured grids: Description and validation of a modeling system for coastal applications. *Ocean Modelling*, 28, 75-87.
- BERTRAND-KRAJEWSKI, J. L., CHEBBO, G. & SAGET, A. 1998. Distribution of pollutant mass vs volume in stormwater discharges and the first flush phenomenon. *Water Research*, 32, 2341-2356.
- BIANCHI, T. S. 2007. *Biogeochemistry of estuaries*, New York, Oxford University Press.
- BILLOTTA, G. S. & BRAZIER, R. E. 2008. Understanding the influence of suspended solids on water quality and aquatic biota. *Water Research*, 42, 2849-2861.
- BIRCH, G. & TAYLOR, S. 1999. Source of heavy metals in sediments of the Port Jackson estuary, Australia. *Science of the Total Environment*, 227, 123-138.
- BISWAS, T. D. & MUKHERJEE, S. K. 1994. *Soil Science*, Delhi, Tata McGraw-Hill Publishing Company Ltd.
- BLACK, K., ATHEY, S., WILSON, P. & EVANS, D. Direct assessment of dredging impact in sensitive environments using particle tracking technology. World Organisation of Dredging Organisations, 2004a Hamburg.
- BLACK, K., ATHEY, S., WILSON, P. & EVANS, D. Particle Tracking: A new tool for coastal zone sediment management. the 4th International Conference. Littoral'04, 2004b Aberdeen. 525-530.
- BLACK, K., ATHEY, S., WILSON, P. & EVANS, D. 2007. The Use of Particle tracking in sediment transport studies: A Review. *Geological Society of London. Special Publications*, 274, 73-91. The Use of Particle tracking in sediment transport studies: A Review.
- BLACK, K., SLOAN, J. & GRIES, T. Everything Goes Somewhere; Tracking the Movement of Contaminated Sediments in an Industrialised Estuary Using Dual Signature Sediment Tracers. Tracer 6 – Sixth International Conference on Tracers and Tracing Methods, 2013.

- BLACK, K. S. 2012. Using Sediment Tracers to Map Sediment Transport Pathways.
- BLAKE, W. H., WALLBRINK, P. J., DOERR, S. H., SHAKESBY, R. & HUMPHREYS, A. 2006. Magnetic enhancement in wildfire-affected soil and its potential for sediment-source ascription. *Earth Surface Processes and Landforms*, 31, 249-264.
- BLAKE, W. H. & WALLING, D. E. 1999. Fallout beryllium-7 as a tracer in soil erosion investigations. *Applied Radiation and Isotopes*, 51, 599-605.
- BOARDMAN, J. 1993. The sensitivity of downland arable land to erosion by water. In: THOMAS, D. S. G. & ALLISON, R. J. (eds.) *Landscape sensitivity* Chichester John Wiley and Sons.
- BOARDMAN, J. & FAVIS-MORTLOCK, D. T. 1992. Soil erosion and sediment loading of water course *SEESOIL*, 7, 5-29.
- BOARDMAN, J., SHEPHEARD, M. L., WALKER, E. & FOSTER, I. D. L. 2009. Soil erosion and risk - assessment for on - and off -farm impacts: A test case using the Midhurst area, West Sussex, UK. *Journal of Environmental Management*, 1-11.
- BOLAM, S. G., REES, H., MURRAY, L. A. & WALDOCK, R. Intertidal placement of fine-grained dredged material. International Conference of Coastal Engineers, 2003 Cardiff. American Society of Coastal Engineers, 3606-3615.
- BOLAM, S. G. & WHOMERSLEY, P. 2003. Invertebrate recolonisation of fine-grained beneficial use schemes: an example from the south east coast of England *Journal of Coastal Conservation*, 9, 159-169.
- BOLAM, S. G. & WHOMERSLEY, P. 2005. Development of macrofaunal communities on dredged material used for mudflat enhancement: a comparison of three beneficial use schemes after one year. *Marine pollution bulletin*, 50, 40-47.
- BOOTH, D. B. & JACKSON, C. R. 1997. Urbanization of aquatic systems: degradation thresholds, stormwater detection, and the limits of mitigation. *Journal of the American Water Resources Association*, 33, 1077-1090.

- BRASSINGTON, J., LANGHAM, J. & RUMSBY, B. 2003. Methodological sensitivity of morphometric estimates of coarse fluvial sediment transport. *Geomorphology*, 53, 299-316.
- BRAY, M. J., CARTER, D. J. & HOOKE, J. M. 1995. Littoral Cell Definition and Budgets for Central Southern England *Journal of Coastal Research*, 11, 381-400.
- BRILLS, J. 2008. Sediment monitoring and the European Water Framework Directive. *Super Sanita*, 44, 218-223.
- BROWN, E., COLLING, A., PARK, D., PHILLIPS, J., ROTHERY, D. & WRIGHT, J. 1999. *Waves, Tides and Shallow-water processes*, Oxford, Reed Elsevier.
- BRUQUE, S., MOZAS, T. & RODRIGUEZ, A. 1980. Factors influencing retention of lanthanide ions by montmorillonite. *Clay Minerals*, 15, 413-420.
- BRYAN, R. B. 2000. Soil erodibility and processes of water erosion on hillslope. *Geomorphology*, 32, 385-415.
- CABRERA, L. & ALONSO, I. 2010. Correlation of aeolian sediment transport measured by sand traps and fluorescent tracers. *Journal of Marine Systems: Elsevier*.
- CADWALADER, G. O., RENSHAW, C. E., JACKSON, B. P., MAGILLIGAN, F. J., LANDIS, J. D. & BOSTICK, B. C. 2011. Erosion and physical transport via overland flow of arsenic and lead bound to silt sized particles. *Geomorphology*, 128.
- CAITCHEON, G. G. 1993. APPLYING ENVIRONMENTAL MAGNETISM TO SEDIMENT TRACING. *Tracers in Hydrology*, 215, 1-8.
- CALDWELL, N. E. 1981. Relationship between tracers and background beach material. *Journal of Sedimentary Petrology*, 51, 1163-1168.
- CAMPBELL, J. B. & WYNNE, R. H. 2011. *Introduction to Remote Sensing*, New York, The Guilford Press.
- CARDOSO, S. S. S. & ZARREBINI, M. 2001. Sedimentation of polydispersed particles from a turbulent plume. *Chemical Engineering Scientific*, 56, 4725-4736.

- CARDOSO, S. S. S. & ZARREBINI, M. 2002. Convection driven by particle settling surrounding a turbulent plume. *Chemical Engineering Scientific*, 56, 3365-3375.
- CAREY, D. A. 1989. Fluorometric detection of tracer particles used to study animal-particle dynamics. *Limnology and Oceanography*, 34, 630-635.
- CARR, R. S., MONTAGNA, P. A., BIEDENBACH, J. M., KALKE, R., KENNICUTT, M. C., HOOTEN, R. & CRIPE, G. 2000. Impact of storm-water outfalls on sediment quality in Corpus Christi Bay, Texas, USA. *Environmental Toxicology and Chemistry*, 19, 561-574.
- CARRASCO, A. R., FERREIRA, O. & DIAS, J. A. 2013. Sediment transport measurements with tracers in very low-energy beaches. *Earth Surface Processes and Landforms*, 38, 561-569.
- CARVALHO, F. P. 1995. ²¹⁰Pb and ²¹⁰PO in sediments and suspended matter in the Tagus Estuary, Portugal. Local enhancement of natural levels by wastes from phosphate ore processing industry. *Science of the Total Environment*, 159, 201-214.
- CASTILLO, C., PEREZ, R., JAMES, M. R., QUINTON, J. N., TAGUAS, E. V. & GOMEZ, J. A. 2012. Comparing the accuracy of several field methods for measuring gully erosion *Soil Science Society of America Journal*, 76, 1319-1332.
- CATT, J. A., HOWSE, K. R., FARINA, R., BROCKIE, D., TODD, A., CHAMBERS, B. J., HODGKINSON, R., HARRIS, G. L. & QUINTON, J. N. 1998. Phosphorus losses from arable land in England. *Soil Use and Management*, 168-174.
- CEFAS 2003. Monitoring the quality of the marine environment. *In*: CEFAS (ed.). Sci. Ser. Aqua. Environ. Monit. Rep.
- CHEN, J. & ADAMS, B. J. 2007. A derived probability distribution approach to stormwater quality modeling. *Advances in Water Resources*, 30, 80-100.
- CHEONG, H. N., SHANKAR, O. R., RADHAKRISHNAN, R. & TOH, A. 1993. Estimation of sand transport by use of tracers along a reclaimed shoreline at Singapore Changi Airport. *Coastal Engineering*, 19, 311-325.

- CHRISTOPHER, D. G., HARLEY, A., HUGHES, R., HULTGREN, K. M., MINER, B. G., CASCADE, J., SORTE, B., THORNBUR, C. S., RODRIGUEZ, L. F., TOMANEK, L. & WILLIAMS, S. L. 2006. The impacts of climate change in coastal marine systems. *Ecology Letters*, 9, 228-241.
- CHURCH, J. A., CLARK, P. U., CAZENAVE, A., GREGORY, J. M., JEVREJEVA, S., LEVERMANN, A., MERRIFIELD, M. A., MILNE, G. A., NEREM, R. S., NUNN, P. D., PAYNE, A. J., PFEFFER, W. T., STAMMER, D. & UNNIKRISSNAN, A. S. 2013. Sea Level Change. *In*: STOCKER, T. F., QIN, D., PLATTNER, G. K., TIGNOR, M., ALLEN, S. K., BOSCHUNG, J., NAUELS, A., XIA, Y., BEX, V. & MIDGLEY, P. M. (eds.) *Climate Change 2013: The Physical Science Basis, Contribution of Working Group I to the Fifth Assessment Report of the Intergovernmental Panel on Climate Change*. Cambridge, United Kingdom and New York, USA: Cambridge University Press.
- CIAVOLA, P., DIAS, N., TABORDA, R. & FERREIRA, Ó. D. 1998. Fluorescent sands for measurements of longshore transport rates: a case study from Praia de Faro in southern Portugal. *Geo Marine Letters*, 18, 49-57.
- CIAVOLA, P., TABORDA, R., FERREIRA, O. & DIAS, J. A. 1997. Field measurements of longshore sand transport and control processes on a steep meso-tidal beach in Portugal. *Journal of Coastal Research*, 13, 1119-1129.
- CLARK, E. H., HAVERKAMP, J. A. & CHAPMAN, W. 1985. Eroding soils: the Off-farm Impacts. *In*: FOUNDATION, T. C. (ed.). Washington DC.
- CLARKE, T. I., SWIFT, D. J. P. & YOUNG, R. A. 1982. A numerical model of fine sediment transport on continental shelf. *Environmental Geology*, 4, 117-129.
- COCHRAN, W. G. 1977. *Sampling techniques*, New York,, Wiley.
- COLLINS, A. L., WALLING, D. E. & LEEKS, G. J. L. 1997. Source type ascription for fluvial suspended sediment based on a quantitative composite fingerprinting technique. *Catena*, 29, 1997.

- COLLINS, A. L., ZHANG, Y., MCCHESENEY, D., WALLING, D. E., HALEY, S. M. & SMITH, P. 2012. Sediment source tracing in a lowland agricultural catchment in southern England using a modified procedure combining statistical analysis and numerical modelling. *Sci Total Environ*, 414, 301-17.
- COLLINS, A. L., ZHANG, Y. S., DUETHMANN, D., WALLING, D. E. & BLACK, K. S. 2013. Using a novel tracing-tracking framework to source fine-grained sediment loss to watercourses at sub-catchment scale. *Hydrological Processes*, 959-974.
- COLLINS, I. J. 1972. Prediction of shallow-water spectra. *Journal of Geophysical Research*, 77, 2693-2707.
- COLLINS, M. B., SHIMWELL, S. J., GAO, S., POWELL, H., HEWITSON, C. & TAYLOR, J. A. 1995. Water and sediment movement in the vicinity of linear sandbanks: the Norfolk Banks, southern North Sea. *Marine Geology*, 123, 125-142.
- CORBAU, C., HOWA, H., TESSIER, B., RESSEGUIER, A. & CHAMLEY, H. 1994. Evaluation du transport sédimentaire sur une plage macrotidale par tracage fluorescent, Dunkerque, Est, France. *Compte Rendu Acad. Sci*, 319, 1503-1509.
- CORDOVA-KREYLOS, A. L., CAO, Y., GREEN, P. G., HWANG, H., KUIVILA, K. M., LAMONTAGNE, M. G., VAN DE WERFHORST, L., HOLDEN, P. A. & SCOW, K. M. 2006. Diversity, Composition, and Geographical Distribution of Microbial Communities in California Salt Marsh Sediments. *Applied and Environmental Microbiology*, 72, 3357-3366.
- COSTANZA, R., SKLAR, F. H. & WHITE, M. L. 1990. Modelling Coastal Landscape Dynamics. *BioScience*, 40, 91-107.
- COUNCIL, S. 2014. Contaminated Land Strategy - Scarborough Borough Council.
- COURTOIS, G. & MONACO, A. 1968. Radioactive methods for the quantitative determination of coastal drift rate. *Marine Geology*, 187-211.
- COVICH, A. P., PALMER, M. A. & CROWL, T. A. 1999. The role of benthic invertebrate species in freshwater ecosystems. *BioScience*, 49, 119-127.

- COWELL, P. J., STIVE, M. J. F., ROY, P. S., KAMINSKY, G. M., BUIJSMAN, M. C., THOM, B. G. & WRIGHT, D. L. 2001. Shoreface Sand Supply to Beaches *Coastal Engineering*, 2495-2508.
- CRABILL, C., DONALD, R., SNELLING, J., FOURST, R. & SOUTHAM, G. 1999. The impact of sediment fecal coliform reservoirs on seasonal water quality in Oak Creek, Arizona. *Water Research*, 33, 2163 - 2171.
- CRICKMORE, M. J. 1967. Measurement of sand transport in rivers with special reference to tracer methods. *Sedimentology*, 8, 175-228.
- CRICKMORE, M. J. & LEAN, G. H. 1962. The Measurement of Sand Transport by the Time-Integration Method with Radioactive Tracers. *Proceedings of the Royal Society A: Mathematical, Physical and Engineering Sciences*, 270, 27-47.
- CROMEY, C. J., NICKEL, T. D., BLACK, K. D., PROVOST, P. G. & GRIFFITHS, C. R. 2002. Validation of a Fish Farm Waste Resuspension Model by Use of a Particulate Tracer Discharged from a Point Source in a Coastal Environment. *Estuaries*, 25, 916-929.
- CRONIN, K., DEVOY, R. J. D. & MONTSERRAT, F. 2011. Validation of modelled intertidal flat bed sediment transport using a simple tracer method. *Journal of Coastal Research*, 64, 741-745.
- CURTIS, B., KELLNER, M. I. & OVER, J. 1992. Process modelling. *Magazine communications of the ACM - Special issue on analysis and modelling in software development*, 35, 75-90.
- CURZIO, S. L. & MAGLIULO, P. 2009. Soil erosion assessment using geomorphological remote sensing techniques: an example from southern Italy. *Earth Surface Processes and Landforms*, 35, 262-271.
- CUTHBERTSON, A. J. S., APSLEY, D. D., DAVIES, P. A., LIPARI, G. & STANSBY, P. K. 2008a. Deposition from Particle-Laden, Plane, Turbulent, Buoyant Jets. *Journal of Hydraulic Engineering*, 1110-1122.
- CUTHBERTSON, A. J. S. & DAVIES, P. A. 2008. Deposition from Particle-Laden, Round, Turbulent, Horizontal, Buoyant Jets in Stationary and Coflowing Receiving Fluids. *Journal of Hydraulic Engineering*, 134, 390-402.
- DAN, R. 2001. Use of mineral magnetic measurements to investigate soil erosion and sediment delivery in a small agricultural catchment in

- limestone terrain. *Catena*, 46, 15-34 %! Use of mineral magnetic measurements to investigate soil erosion and sediment delivery in a small agricultural catchment in limestone terrain.
- DANIEL, T. C., SHARPLEY, A. N. & LEMUNYON, J. L. 1997. Agricultural Phosphorus and Eutrophication: A Symposium Overview. *Journal of Environmental Quality*, 27, 251-257.
- DARVISHAN, A. K., SADEGHI, S. H., HOMAEI, M. & ARABKHEDRI, M. 2014. Measuring sheet erosion using synthetic color-contrast aggregates. *Hydrological Processes*, 28, 4463-4471.
- DAVIDSON, J. 1958. Investigations of sand movement using radioactive sand. *Lund University, studies in physical geography*, A12, 69-126 %! Investigations of sand movement using radioactive sand.
- DAVIES, A. G., VAN RIJN, L. C., DAMGAARD, J. S., VAN DE GRAAFF, J. & RIBBERINK, J. S. 2002. Intercomparison of research and practical sand transport models. *Coastal Engineering*, 46, 1-23.
- DAWDY, D. R. & VANONI, V. A. 1986. Modelling alluvial channels. *Water Resources Research*, 22, 77-81.
- DEARING, J. A. 1992. Sediment yields and sources in a Welsh upland lake catchment during the past 800 years. *Earth Surface Processes and Landforms*, 17, 1-22 %! Sediment yields and sources in a Welsh upland lake catchment during the past 800 years.
- DEASY, C. & QUINTON, J. N. 2010. Use of rare earth oxides as tracers to identify sediment source areas for agricultural hillslopes. *Solid Earth*, 1, 111-118.
- DEFERSHA, M. B. & MELESSE, A. M. 2012. Effect of rainfall intensity, slope and antecedent moisture content on sediment concentration and sediment enrichment ratio. *Catena* 90, 47-52.
- DEVOY, R. J. N. 1992. Questions of coastal protection and the human response to sea-level rise in Ireland and Britain. *Ir. Geogr.*, 25, 1-22.
- DEY, S. 2014. Sediment Threshold. *Fluvial Hydrodynamics. Hydrodynamics and Sediment Transport Phenomena*. Springer Ltd.
- DIGIACOMO, P. M., WASHBURN, L., B, H. & JONES, B. H. 2004. Coastal pollution hazards in southern California observed by SAR imagery:

- stormwater plumes, wastewater plumes, and natural hydrocarbon seeps. *Marine Pollution Bulletin*, 49, 1013-1024.
- DOBBS, P. H. 1958. Effects of wave action on the shape of beach gravel. *Compass*, 35, 269-275.
- DOLPHIN, T. J., HUME, T. M. & PARNELL, K. E. 1995. Oceanographic processes and sediment mixing on a sand flat in an enclosed sea, Manukau Harbour, New Zealand. *Marine geology*, 42, 19-34.
- DONAHUE, R. L., SHICKLUNA, J. C. & ROBERTSON, L. S. 1971. *Soils: An introduction to soils and plant growth*, USA, Prentice Hall.
- DONG, Y. J., MA, Y. Z., SHI, Y. X. & CHEN, W. F. 2007. Developing a man-made magnetic tracer to study soil erosion. *Journal of soil and water conservation*. *Journal of soil and water conservation*, 21, 46-49.
- DONG, Y. J., SHI, Y. X., KONG, F. M. & CHEN, W. F. 2009. Magnetic-measurement-based spatial distribution of soil erosion on slope. *Acta Pedol Sini*, 46, 144-48.
- DOWNING, J. P., STERNBERG, R. W. & LISTER, C. R. B. 1981. New instrumentation for the investigation of sediment suspension processes in the shallow marine environment. *Marine Geology*, 42, 19 - 34.
- DRAAIJER, A., TADEMA WIELANDT, R. & HOUP, P. M. 1984. Investigation on the applicability of fluorescent synthetic particles for the tracing of silt. *Netherlands organisation for applied scientific research*.
- DRAPEAU, G., LONG, B. & KAMPHIUS, W. Evaluation of radioactive sand tracers to measure longshore sediment transport rates. *Proceeding of the 22nd International Conference on Coastal Engineering ASCE*, 1991 New York. 2710-2723.
- DROPPO, I., LEPPARD, G., FLANNIGAN, D. & LISS, S. 1997. The freshwater flock: A functional relationship of water and organic and inorganic flock constituents affecting suspended sediment properties. *Water*, 99, 43-54.
- DROPPO, I. G. 2001. Rethinking what constitutes suspended sediment. *Hydrological Processes*, 15, 1551-1564.
- DROPPO, I. G. & ONGLEY, E. D. 1992. The state of suspended sediment in the fresh-water fluvial environment - a method of analysis. *Water Research*, 26, 65-72.

- DROPPO, I. G. & ONGLEY, E. D. 1994. Flocculation of suspended sediment in rivers of south eastern Canada. *Water Research*, 28, 1799-1809.
- DUARTE, C. M. 2002. The future of seagrass meadows *Environmental Conservation* 29, 192-206.
- DYER, K. R. 1986. *Coastal and Estuarine Sediment Dynamics*, Chichester, John Wiley and Sons.
- DYER, K. R. 1995. Sediment transport processes in Estuaries. In: PERILLO, G. M. E. (ed.) *Geomorphology and Sedimentology of Estuaries. Developments in Sedimentology*. Elsevier Science.
- EFTINK, M. R. & GHIRON, C. A. 1976. Fluorescence quenching of indole and model micelle systems. *The Journal of Physical Chemistry*, 80, 486-493.
- EFTINKA, M. R. & GHIRON, C. A. 1981. Fluorescence quenching studies with proteins. *Analytical Biochemistry*, 114, 199-227.
- EIDSVIK, K. J. 2004. Some contributions to the uncertainty of sediment transport predictions. *Continental Shelf Research*, 24, 739-754.
- EISMA, D. 1993. *Suspended matter in the aquatic environment*, Berlin Heidelberg, Springer.
- EL-ASMAR, H. M. & WHITE, K. 2002. Changes in coastal sediment transport processes due to construction of New Damietta Harbour, Nile Delta, Egypt. *Coastal Engineering*, 46, 127-138.
- EL KATEB, H., ZHANG, H., ZHANG, P. & MOSANDL, R. 2013. Soil erosion and surface runoff on different vegetation covers and slope gradients: a field experiment in Southern Shaanxi Province, China. *Catena*, 105, 1-10.
- ELAWANY, H. 2012. Proposal Environmental Projects Benefitting San Diego Bay: A Finite Element Model For San Diego Bay To Address Sea Level Rise Environmental Changes and Challenges Coastal Environments, Inc.
- ERFTEMEIJER, P. L. A., RIEGL, B., HOEKSEMA, B. W & TODD, P. A. 2012. Environmental impacts of dredging and other sediment disturbances on corals: A review. *Marine Pollution Bulletin*, 64, 1737-1765.

- ERFTMEIJER, P. L. A. & ROBIN LEWIS III, R. R. 2006. Environmental impacts of dredging on seagrasses: A review. *Marine Pollution Bulletin*, 52, 1553-1572.
- ERNST, G. G. J., SPARKS, R. S. J., CAREY, S. N. & BURSİK, M. I. 1996. Sedimentation from turbulent jets and plumes. *Journal of Geophysical Research*, 101, 5575–5589.
- EVANS, R. 1996. *Soil erosion and its impacts in England and Wales*, London, Friends of the Earth Trust.
- EYRE, B., HOSSAIN, S. & MCKEE, L. 1998. A Suspended Sediment Budget for the Modified Subtropical Brisbane River Estuary, Australia. *Estuarine coastal and shelf science*, 47, 513-522.
- FALKOWSKI, R., SCHOLLES, R. J., BOYLE, E., CANADELL, J., CANFIELD, D., ELSE, J., GRUBER, N., HIBBARD, K., HÖGBERG, P., LINDER, S., MACKENZIE, F. T., MOORE, B., PEDERSEN, T., ROSENTHAL, Y., SEITZINGER, S., SMETACEK, V. & STEFFEN, W. 2000. The Global Carbon Cycle: A Test of Our Knowledge of Earth as a System. *Science*, 290, 291-296.
- FARINATO, R. S. & KRAUS, N. C. 1980. Spectrofluorometric determination of sand tracer concentrations. *Journal of Sedimentary Petrology*, 51, 663-665.
- FERGUSON, R. I. 2002. Mobility of river tracer pebbles over different timescales. *Water Resources Research*, 38.
- FERREIRA, O., FACHIN, S., BRAGA COLI, A., TABORDA, R., ALVEIRINHO, G. & LONTRA, G. 2002. Study of harbour infilling using sand tracer experiment. *Journal of Coastal Research*, 36, 283-289.
- FISCHER, H. B. 1979. *Mixing in Inland and Coastal Waters*, Academic Press Inc.
- FOLEY, J. A., DEFRIES, R., ASNER, G. P., BARFORD, C., BONAN, G., CARPENTER, S. R., CHAPIN, S. F., COE, M. T., DAILY, G. C., GIBBS, H. K., HELKOWSKI, J. H., HOLLOWAY, T., HOWARD, E. A., KUCHARIK, C. J., MONFREDA, C., PATZ, J. A., PRENTICE, I. C., RAMANKUTTY, N. & SNYDER, P. K. 2005. Global Consequences of Land Use. *Science*, 309, 570-574.

- FORSTNER, U. & SALOMONS, W. 2008. Trends and challenges in sediment research 2008: the role of sediments in river basin management. *Journal of Soils and Sediments*, 8, 281-283.
- FORSYTH, S. H. 2000 *New developments in artificial fluorescent tracer counting techniques applied to sand transport studies*. MSc. Thesis, University of Waikato.
- FOSTER, I. D. L. 2000. *Tracers in Geomorphology*, Chichester, Wiley.
- FOWLER, J., COHEN, L. & JARVIS, P. 1998. *Practical statistics for field biology*, Chichester, John Wiley & Sons.
- FOX, D. M. & BRYAN, R. B. 1999. The relationship of soil loss by interrill erosion to slope gradient. *Catena*, 38, 211-222.
- FOX, D. M., BRYAN, R. B. & PRICE, A. G. 1997. The influence of slope angle on final infiltration rate for interrill conditions. *Geoderma*, 80, 181-194.
- FRANCIS, C. Soil erosion and organic matter losses on fallow land: a case study from south-east Spain. *In*: BOARDMAN, J., FOSTER, I. D. L. & DEARING, J. A., eds. Soil erosion on agricultural land. Proceedings of a workshop sponsored by the British Geomorphological Research Group, 1990 Coventry, UK.
- FRIEND, P. L., VELEGRAKIS, A. F., WEATHERSTON, P. D. & COLLINS, M. B. 2006. Sediment transport pathways in a dredged ria system, southwest England. *Estuarine, Coastal and Shelf Science*, 67, 491-502.
- GALLACHER, P. C. & HOGAN, P. J. 1998. Hydrodynamical dispersion of dredged materials sequestered on the abyssal seafloor. *Journal of Marine System*, 14, 305-318.
- GALLAGHER, E. L., SEYMOUR, R. J. & KING, J., D 1991. Bedload transport measurement by imaging of tracers. *Coastal Sediments*, 91, 717-725.
- GALLAWAY, E. 2012. *Magnetic mineral transport and sorting in the swash-zone: Northern Lake Erie*.
- GANZ, C. R. J. & STENSBY, P. S. 1975. Accumulation and elimination studies of four detergent fluorescent whitening agents in bluegill (*Lepomis macrochirus*). *Environmental Science and Technology*, 9, 738-744.

- GAO, S. 1996. A Fortran program for grain-size trend analysis to define net sediment transport pathways *Computers and Geosciences*, 22.
- GAO, S. & COLLINS, M. 1992. Net sediment transport patterns inferred from grain-size trend, based upon definition of 'transport vectors'. *Sedimentary Geology*, 80, 47-60.
- GARCIA- RUIZ, J. M. 2010. The effects of land uses on soil erosion in Spain: A review. *Catena*, 81, 1-11.
- GEDDES, C. D. 2001. Optical halide sensing using fluorescence quenching: theory, simulations and applications - a review. *Measurement Science and Technology*, 12, 53-88.
- GEHLEN, M. H. & DE SCHRIVER, F. C. 1993. Fluorescence quenching in micelles in the presence of a probe-quencher ground-state charge-transfer complex. *The Journal of Physical Chemistry*, 97, 11242-11248.
- GERLACH, T. 1967. Hillslope troughs for measuring sediment movement *REv. Geomorph. Dyn*, 4, 173-175.
- GERMAINE, J. T. & GERMAINE, A. V. 2009. *Geotechnical Laboratory Measurements for Engineers*, Hoboken, New Jersey, John Wiley & Sons.
- GHIDEY, F. & ALBERTS, E. E. 1998. Runoff and soil losses as affected by corn and soybean tillage systems. *Journal of Soil and Water conservation*, 53, 64-70.
- GIBSON, S., HEATH, R., ABRAHAM, D. & SCHOELLHAMER, D. 2011. Visualization and analysis of temporal trends of sand infiltration into a gravel bed. *Water Resources Research*, 47.
- GILLAN, D. C., DANIS, B., PERNET, P., JOLY, G. & DUBOIS, P. 2005. Structure of Sediment - Associated Microbial Communities along a Heavy - Metal Contamination Gradient in the Marine Environment. *Applied Environmental Microbiology*, 71, 679-690.
- GILMOUR, J. 1999. Experimental investigation into the effects of suspended sediment on fertilisation, larval survival and settlement in a scleractinian coral. *Marine Biology*, 135, 451-462.
- GILVEAR, D. J., SPRAY, C. J. & CASAS-MULET, R. 2013. River rehabilitation for the delivery of multiple ecosystem services at the river network scale. *Journal of Environmental Management*, 126, 30-43.

- GOBIN, A., GOVERS, G., JONES, R., KIRKBY, M. & KOSMAS, C. 2003. Assessment and reporting on soil erosion - Background and workshop report. Copenhagen, Denmark: European Environment Agency.
- GÓMEZ, J. A., GIRÁLDEZ, J. V. & VANWALLEGHEM, T. 2008. *RE: Comments on "Is soil erosion in olive groves as bad as often claimed?"*. Type to FLESKEND, L. & STROOSNIJDER, L.
- GONENC, I. E. & WOLFLIN, J. P. 2005. *Coastal Lagoons: Ecosystem Processes and Modelling for Sustainable Use and Development*, Florida, CRC Press.
- GRABOWSKI, R. C., DROPPO, I. G. & WHARTON, G. 2011. Erodibility of cohesive sediment: The importance of sediment properties. *Earth Science Reviews*, 105, 101–120.
- GRAY, J. S. 1981. *The Ecology of Marine Sediments*, Cambridge, Cambridge University Press.
- GRAY, J. S. 1997. Marine biodiversity: patterns, threats and conservation needs. *Biodiversity & Conservation*, 6, 153-175.
- GRUSZOWSKI, K. E., FOSTER, I. D. L., LEES, J. A. & CHARLESWORTH, S. M. 2003. Sediment sources and transport pathways in a rural catchment, Herefordshire, UK. *Hydrological Processes*, 17, 2665-2681.
- GUNN, A. H. 1963. *Introduction To Fluorimetry*, Richmond, Surrey, Electronic Instruments Limited.
- GUYMER, I., STOVIN, V., GASKELL, P., MALTBY, L. & PEARSON, J. 2010. Predicting the deposition of highway-derived sediments in a receiving river reach. *School of Engineering*, 1, 1-10.
- GUZMAN, G., BARRON, V. & GOMEZ, J. A. 2010. Evaluation of magnetic iron oxides as sediment tracers in water erosion experiments. *Catena*, 82, 126-133.
- GUZMAN, G., QUINTON, J. N., NEARING, M. A., MABIT, L. & GOMEZ, J. A. 2013. Sediment tracers in water erosion studies: current approaches and challenges. *Journal of Soils and Sediments*, 13, 816-833.
- HABERSACK, H. & KREISLER, A. 2012. Sediment Transport Processes. *Dating Torrential Processes of Fans and Cones*, 47, 51-73.
- HABOUDANE, D., BONN, F., ROYER, A., SOMMERS, S. & MEHL, W. 2002. Land degradation and erosion risk mapping by fusion of spectrally-

- based information and digital geomorphometric attributes. *International Journal of Remote Sensing*, 23, 3795-3820.
- HAIYAN, F., LIYING, S. & ZHENGHONG, T. 2015. Effects of rainfall and slope on runoff, soil erosion and rill development: an experimental study using two loess soils *Hydrological Processes*, 29, 2649-2658.
- HAMM, L., CAPOBIANCO, M., DETTE, H., H, LECHUGA, A., SPANHOFF, R. & STIVE, M. J. F. 2002. A summary of European experience with shore nourishment. *Coastal Engineering*, 47.
- HAMYLTON, S. M., LEON, J. X., SAUNDERS, M. I. & WOODROFFE, C. D. 2014. Simulating reef response to sea-level rise at Lizard Island: A geospatial approach. *Geomorphology*, 222, 151-161.
- HANSON, H., BRAMPTON, A., CAPOBIANCO, M., DETTE, H., HAMM, L., LAUSTRUP, A., LECHUGA, A. & SPANHOFF, R. 2002. Beach nourishment project, practices and objectives: An European overview. *Coastal Engineering*, 47, 237-264.
- HAO, Y., QING, C., MINGYUAN, D., KATSUYUKI, M. & TAMAO, H. 1998. Quantitative model of soil erosion rates using ¹³⁷ Cs for uncultivated soil. *Soil Science*, 163, 248-257.
- HARVEY, R. W., GEORGE, L. H., SMITH, R. L. & LE BLANC, D. R. 1989. Transport of microspheres and indigenous bacteria through a sandy aquifer: Results of natural and forced-gradient tracer experiments. *Environmental Science and Technology*, 23, 51-56.
- HASKONING, R. 2007. River Tyne to Flamborough Head Shoreline Management Plan
- HATCH, A. C. & BURTON, J. A. G. 1999. Sediment toxicity and stormwater runoff in a contaminated receiving system: consideration of different bioassays in the laboratory and field. *Chemosphere*, 39, 1001-1017.
- HAYGARTH, P. M. & JARVIS, S. C. 1999. Transfer of phosphorus from agricultural soils. *Adv. Agron*, 66, 195-249.
- HEIMSATH, A. M., CHAPPELL, J., SPOONER, N. A. & QUESTIAUX, D. G. 2002. Creeping soil *Geology*, 30, 111-114.

- HESHAM M. EL-ASMAR , K. W. 2002. Changes in coastal sediment transport processes due to construction of New Damietta Harbour, Nile Delta, Egypt. *Coastal Engineering*, 46, 127-138.
- HORN, D. P. & MASON, T. 1994. Swash zone sediment transport modes. *Marine Geology*, 120, 309-325.
- HORN, R., TAUBNER, H., WUTTKE, M. & BAUMGARTL, T. 1994. Soil physical properties related to soil structure *Soil and Tillage Research*, 30, 187-216.
- HORNG, C.-S. & HUH, C.-A. 2011. Magnetic properties as tracers for source-to-sink dispersal of sediments: A case study in the Taiwan Strait. *Earth and Planetary Science Letters*.
- HOSSAIN, S., EYRE, B. D. & MCKEE, L. J. 2004. Impacts of dredging on dry season suspended sediment concentration in the Brisbane River estuary, Queensland, Australia. *Estuarine coastal and shelf science*, 61.
- HU, G.-Q., DONG, Y.-J., WANG, H., QIU, X.-K. & WANG, Y.-H. 2011. Laboratory Testing of Magnetic Tracers for Soil Erosion Measurement. *Pedosphere*, 21, 328-338.
- HUANG, H., PRONI, J. R. & TSAI, J. J. 1994. Probabilistic Approach to Initial Dilution of Ocean Outfalls. *Water Environment Research*, 66, 787-793.
- HUBER, C., FAHNRICH, K., KRAUSE, C. & WERNER, T. 1999. Synthesis and characterisation of new chloride-sensitive indicator dyes based on dynamic fluorescence quenching. *Journal of Photochemistry and Photobiology*, 128, 111-120.
- HUGHES, M., MASSELINK, G., HANSLOW, D. & MITCHELL, D. 1997. Toward a better understanding of swash zone sediment transport *Proceeding Coastal Dynamics*, 804-823.
- HUNTLEY, D. A., DAVIDSON, M. A., RUSSELL, P. E., FOOTE, Y. & HARDISTY, J. 1993. Long waves and sediment movement on beaches: recent observations and implications for modelling. *Journal of Coastal Research*, 215-229.
- HUTCHINGS, P. 1998. Biodiversity and functioning of polychaetes in benthic sediments. *Biodiversity & Conservation*, 7, 1133-1145.

- HUTCHINSON, S. E., SKLAR, F. H. & ROBERTS, C. 1995. Short Term Sediment Dynamics in a Southeastern U.S.A *Spartina* Marsh. *Journal of Coastal Research*, 11.
- IHALAINEN, J. A., CROCE, R., MOROSINOTTO, T., VAN STOKKUM, I. H. M., BASSI, R., DEKKER, J. P. & GRONDELLE, R. V. 2005. Excitation Decay Pathways of Lhca Proteins: A Time-Resolved Fluorescence Study. *Journal of Physical Chemistry*, 109, 21150-21158.
- INGLE, J. C. 1966. *The movement of beach sand, an analysis using fluorescent grains*, Amsterdam, Elsevier.
- INMAN, D. L. & CHAMBERLAIN, T. K. 1959. Tracing beach sand movement with irradiated quartz. 64, 41-47.
- INMAN, D. L., ZAMPOL, J. A., WHITE, T. E., HANES, D. M., WALDORF, B. W. & KASTENS, K. A. 1980. Field measurements of sand motion in the surf zone. *Coastal Engineering*, 1215-1235.
- INTHORN, M., RUTGERS VAN DER LOEFF, M. & ZABEL, M. 2006. A study of particle exchange at the sediment-water interface in the Benguela upwelling area based upon $^{234}\text{Th}/^{238}\text{U}$ disequilibrium. *Deep sea Research*, 53.
- ISENSEEE, A. R. & SADEGHI, A. M. 1993. Impact of tillage practice on run-off and pesticide transport. *Journal of soil and water conservation*, 48, 523-527.
- ISLAM, S. & TANAKA, M. 2004 Impacts of pollution on coastal and marine ecosystems including coastal and marine fisheries and approach for management: a review and synthesis. *Marine pollution bulletin*, 48.
- JARVIS, K. E. 1989. Determination of rare earth elements in geological samples by inductively coupled plasma mass spectrometry. *Analytical atom spectrometry*, 4, 563-570 %! Determination of rare earth elements in geological samples by inductively coupled plasma mass spectrometry.
- JARVIS, N. J. 2007. A review of non-equilibrium water flow and solute transport in soil macropores: principles, controlling factors and consequences for water quality *European Journal of Soil Science*, 58, 523-546.

- JENNINGS, S. 2004. Coastal tourism and shoreline management. . *Annals of Tourism Research*, 31, 899-922.
- JEVREJEVA, S., GRINSTED, A. & MOORE, J. C. 2014. Upper limit for sea level projections by 2100. *Environmental Research Letters* 9.
- JIMOH, H. I. 2001. Erosion studies in a Nigerian city: A methodological approach. *The Environmentalist*, 21, 97.
- JOHANSSON, M. K. 2006. *Methods in Molecular Biology*, Totowa, New Jersey, Humana Press Inc.
- JOHNSTON, S. A. no date. Estuarine Dredge and Fill Activities: A review of Impacts Florida Department of Environmental Regulation.
- JOLIFFE, I. P. 1963. A study of sand movement on the Lowestoft sandbank using fluorescent tracers. *Geographical Journal*, 129, 480-493.
- JORDAN, T. E. & VALIELA, I. 1983. Sedimentation and resuspension in a New England salt marsh. *Hydrobiologia*, 98, 179-174.
- KAMPHUIS, J. W. 1991. Alongshore sediment transport rate distribution *Proceeding Coastal Sediments*, 170-183.
- KARYDAS, C. G., PANAGOS, P. & GITAS, I. Z. 2014. A classification of water erosion models according to their geospatial characteristics. *International Journal of Digital Earth*, 7 229-250.
- KAWATA, Y., YOSHIOKA, H. & TSUCHIYA, Y. 1990. The in-situ measurements of sediment transport and bottom topography changes. *Proceeding 22nd International Conference Coastal Engineering*.
- KENNETH, R., ANTHONY, N. & RIDD, P. V. 2004. Temporal variation of light availability in coastal benthic habitats: Effects of clouds, turbidity and tides. *Limnology and Oceanography*, 49, 2201-2211.
- KEPLINGER, M. L., FANCHER, O. E., LYMAN, F. L. & CALANDRA, J. C. 1974. Toxicological studies of four fluorescent whitening agents. *Toxicology and Applied Pharmacology*, 27, 494-506.
- KIDSON, C. & CARR, A. P. Beach drift experiments at Bridgewater Bay, Somerset. *Proceeding of the Bristol Nature Society*, 1961. 163-180.
- KIM, Y. D., KANG, S. W., W, S. I. & OH, B. C. 2000. Far-field transport of effluent plumes discharged from Masan Sea Outfalls. *Ocean and Polar Research*, 22, 69-80.

- KIMOTO, A., NEARING, M. A., SHIPITALO, M. J. & POLYAKOV, V. O. 2006a. Multiyear tracking of sediment sources in a small agricultural watershed using rare earth elements. *Earth Surface Processes and Landforms*, 31, 1763-1774.
- KIMOTO, A., NEARING, M. A., ZHANG, X. C. & POWELL, D. M. 2006b. Applicability of rare earth element oxides as a sediment tracer for coarse-textured soils. *Catena*, 65, 214-221.
- KING, C. 1951. Depth of disturbance of sand on sea beaches by waves. *Journal of Sedimentary Petrology*, 21, 121-140.
- KING, C., BAGHDADI, N., LECOMTE, V. & CERDAN, O. 2005. The application of remote-sensing data to monitoring and modelling of soil erosion. *Catena*, 62, 79-93.
- KINNELL, P. I. A. 2005. Raindrop impact induced erosion processes and prediction: a review. *Hydrological Processes*, 19, 2815–2844.
- KINNELL, P. I. A. 2009. The influence of raindrop induced saltation on particle size distributions in sediment discharged by rain-impacted flow on planar surfaces. *Catena*, 78, 2-11.
- KINNELL, P. I. A. 2010. Event soil loss, runoff and the universal soil loss equation family of models: a review. *Journal of Hydrology*, 385, 384-397.
- KNAUS, R. M. & VAN GENT, D. L. 1989. Accretion and canal impacts in a rapidly subsiding wetland. III. A new soil horizon marker method for measuring recent accretion. *Estuaries*, 12, 269-283.
- KOCH, G. R., HAGERTHEY, S., CHILDERS, D. L. & GAISER, E. 2013. Examining seasonally pulsed detrital transport in the coastal everglades using a sediment tracing technique. *Hydrologic Restoration*.
- KOMAR, P. D. 1969. *The Longshore Transport of Sand on Beaches*. Ph.D. Thesis University of California.
- KONDOLF, G. M. & PIEGAY, H. 2003. Sediment Budgets as an Organising Framework in Fluvial Geomorphology. In: REID, L. M. & DUNNE, T. (eds.) *Tools in Fluvial Geomorphology*. John Wiley and Sons.
- KONDOLF, G. M. & PIEGAY, H. 2005. Use of Tracers in Fluvial Geomorphology. In: HASSAN, M. A. & ERGENZINGER, P. (eds.) *Tools in Fluvial Geomorphology*.

- KOSMAS, C., DANALATOS, N., CAMMERAAT, L. H., CHABART, M., DIAMANTOPOULOS, J., FARAND, R., GUTIERREZ, L., JACOB, A., MARQUES, H., MARTINEZ-FERNANDEZ, J., MIZARA, A., MOUTAKAS, N., NICOLAU, J. M., OLIVEROS, C., PINNA, G., PUDDU, R., PUIGDEFABREGAS, J., ROXO, M., SIMAO, A., STAMOU, G., TOMASI, N., USAI, D. & VACCA, A. 1997. The effect of land use on runoff and soil erosion rates under Mediterranean conditions *Catena*, 29.
- KOULOURI, M. & GIOURGA, C. H. R. 2007. Land abandonment and slope gradient as key factors of soil erosion in Mediterranean teraced lands. *Catena*, 69, 274-281.
- KOZERSKI, H. P. & LEUSCHNER, K. 1999. Plate sediment traps for slowly moving waters. *Water Research*, 33, 2913-2922.
- KRAUS, N. C. & DEAN, J. L. 1987. Longshore sediment transport rate distribution measured by trap. *Society of Civil Engineering*, 881-896.
- KRESS, N., HERUT, B. & GALIL, B. S. 2004. Sewage sludge impact on sediment quality and benthic assemblages off the Mediterranean coast of Israel - a long-term study. *Marine Environmental Research*, 57, 213-233.
- KREZOSKI, J. R. Particle reworking in Lake Michigan sediments: in-situ tracer measurements using a rare earth element. 28th Conference Great Lakes Research International Association of Great Lakes Research,, 1985 Milwaukee.
- KREZOSKI, J. R. 1989. SEDIMENT REWORKING AND TRANSPORT IN EASTERN LAKE SUPERIOR: IN SITU RARE EARTH ELEMENT TRACER STUDIES. *Great Lakes Research*, 15, 26-33.
- LAKOWICZ, J. R. 2006. *Principles of Fluorescence spectroscopy*, Springer Science and Business Media.
- LAL, R. 1994. *Soil Erosion Research Methods*, Ankeny, IA, Soil and Water Conservation Society.
- LAL, R. 2001. Soil degradation by erosion. *Land Degradation and Development*, 12, 519-539.

- LAMB, H., H & FRYDENDAHL, K. 1991. *Historic Storms of the North Sea, British Isles and Northwest Europe*, Great Britain, Cambridge University Press.
- LANE, S. N., REID, S. C., TAYEFI, V., YU, D. & HARDY, R. J. 2007. Interactions between sediment delivery, channel change, climate change and flood risk in a temperate upland environment. *Earth Surface Processes and Landforms*, 32, 429-446.
- LARCOMBE, P., RIDD, P. V., PRYTZ, A. & WILSON, B. 1995. Factors controlling suspended sediment on inner-shelf coral reefs, Townsville, Australia. *Coral Reefs*, 14, 163-171.
- LARSEN, M. C., GELLIS, A. C., GLYSSON, G. D., GRAY, J. R. & HOROWITZ, A. J. Fluvial sediment in the environment: A national problem. 2nd joint Federal intraagency Conference, 2010 Las Vegas, Nevada.
- LAUBEL, A., KRONVANG, B., FJORBACK, C. & LARSEN, S. E. Time-integrated sediment sampling from a small lowland stream. International Association of Theoretical and Applied Limnology, 2003. 1420-1424.
- LAWLER, D. M. 2005. The importance of high-resolution monitoring in erosion and deposition dynamics studies: examples from estuarine and fluvial systems. *Geomorphology*, 64, 1-23.
- LE BISSONNAIS, Y. 1990. Experimental study and modelling of soil crusting processes. In: BRYAN, R. B. (ed.) *Soil erosion: Experiment and Models* Cremlin-Destedt, Germany: Catena-verlag.
- LEAFE, R., PETHICK, J. & TOWNEND, I. 1998. Realising the Benefits of Shoreline Management. *The Geographical Journal*, 163, 282-290.
- LEE, H., LAU, S., KAYHANIAN, M. & STENSTROM, M. K. 2004. Seasonal first flush phenomenon of urban stormwater discharges. *Water Research*, 38, 4153-4163.
- LEE, H., SWAMIKANNUB, X., RADULESCUB, D., KIMC, S. & STENSTROMD, M. K. 2007. Design of stormwater monitoring programs. *Water Research*, 41, 4186-4196.
- LEE, M. W. E., SEAR, D. A., ATKINSON, P. M., COLLINS, M. B. & OAKLEY, R. J. 2007b. Number of tracers required for the measurement of

- longshore transport distance on a shingle beach. *Marine Geology*, 240, 57-63.
- LESSER, G., ROELVINK, J. A., VAN KESTER, J. A. T. M. & STELLING, G. S. 2004. Development and validation of a three-dimensional morphological model. *Coastal Engineering*, 51, 883-915.
- LETCHER, R. A., JAKEMAN, A. J., CALFAS, M., LINFORTH, S., BAGINSKA, B. & LAWRENCE, I. 2002. A comparison of catchment water quality models and direct estimation techniques. *Environmental Modelling & Software*, 17, 77-85.
- LINDEMAN, K. C. & SYNDER, D. B. 1999. Nearshore hardbottom fishes of southeast Florida and effects of habitat burial caused by dredging. *Fishery Bulletin*, 97, 508-525.
- LIU, P.-L., TIAN, J.-L., ZHOU, P.-H., YANG, M.-Y. & SHI, H. 2004. Stable rare earth element tracers to evaluate soil erosion. *Soil and Tillage Research*, 76, 147-155.
- LONG, W., KIRBY, J. T. & SHAO, Z. 2008. A numerical scheme for morphological bed level calculations. *Coastal Engineering*, 55, 167-180.
- LOTZE, H. K., LENIHAN, H. S., BOURQUE, B. J., BRADBURY, R. H., COOKE, R. G., KAY, M. C., KIDWELL, S. M., KIRBY, M. X., PETERSON, C. H. & JACKSON, J. B. C. 2006. Depletion, degradation, and recovery potential of estuaries and coastal seas. *Science Magazine*, 312, 1806-1809.
- LOUISSE, C. J., AKKERMAN, R. J. & SUYLEN, J. M. A fluorescent tracer for cohesive sediment. International Conference on Measuring Techniques of Hydraulics Phenomena in Offshore, Coastal and Inland Waters,, 1986. 367-391.
- LTD, M. I. 2015. Mastersizer 200 user manual. <http://www.malvern.com/en/support/resource-center/user-manuals/MAN0384EN.aspx>.
- LU, X. X. & HIGGITT, D. L. 2000. Estimating erosion rates on sloping agricultural land in Yangtze Three Gorges, China, from caesium-137 measurements. *Catena*, 39, 33-51.

- LUBCZYNSKI, M. W. & GURWIN, J. 2005. Integration of various data sources for transient groundwater modeling with spatio-temporally variable fluxes: Sardon study case, Spain. *Journal of Hydrology*, 306, 22.
- LUDWIG, R. G. 1988. Siting and design of submarine outfalls. *EIA guidance document*. Monitoring and Assessment Research Centre, Kings College London, University of London World Health Organisation.
- LUHMANN, A. J., COVINGTON, M. D., ALEXANDER, S. C., CHAI, S. Y., SCHWARTZ, B. F., GROTEN, J. T. & ALEXANDER, E. C. 2012. Comparing conservative and nonconservative tracers in karst and using them to estimate flow path geometry. *Journal of Hydrology*, 448-449, 201-211.
- LUNEBERG, H. 1960. Sediment transport, sedimentation and erosion on the outer sands of the Weser estuary. In; *List International Geological Congress, Copenhagen*, 247-258. 1960. Sediment transport, sedimentation and erosion on the outer sands of the Weser estuary.
- MABIT, L., BENMANSOUR, M. & WALLING, D. E. 2008. Comparative advantages and limitations of the fallout radionuclides ¹³⁷Cs, ²¹⁰Pbex and ⁷Be for assessing soil erosion and sedimentation. *Journal of Environmental Radioactivity*, 99, 1799-1807.
- MADSEN, O. S. 1987. Use of tracers in sediment transport studies. *Coastal Sediments*, 87, 424-435.
- MAGAL, E., WEISBROD, N., YAKIREVICH, A. & YECHIELI, Y. 2008. The use of fluorescent dyes as tracers in highly saline groundwater. *Journal of Hydrology*, 358, 124-133.
- MAHAUT, M. L. & GRAF, G. 1987. A luminophore tracer technique for bioturbation studies. *Oceanol Acta*, 10, 323-328.
- MAHER, B. A., WATKINS, S. J., BRUNSKILL, G., ALEXANDER, J. & FIELDING, C. R. 2009. Sediment provenance in a tropical fluvial and marine context by magnetic 'fingerprinting' of transportable sand fractions. *Sedimentology*, 56, 841-861.
- MAHLER, B. J., BENNETT, P. C., HILLIS, D. M. & WINKLER, M. 1998a. DNA-labeled clay: a sensitive new method for tracing particle transport. *Geology*, 26, 831-834.

- MAHLER, B. J., BENNETT, P. C. & ZIMMERMAN, M. 1998b. Lanthanide-labelled clay: a new method for tracing sediment transport in karst. *Groundwater*, 36, 835-843.
- MALLIARIS, A. 1987. Static fluorescence quenching in the study of micellar systems. *Progress in Colloid and Polymer Science*, 73, 161-166.
- MALTBY, E. 1991. Wetland management goals: wise use and conservation. *Landscape and Urban Planning*, 20, 9-18.
- MALTBY, E. 2009. *Functional assessment of wetlands: Towards evaluation of ecosystem services*, Cambridge, Woodhead Publishing.
- MALTBY, E. & ACREMAN, M. C. 2011. Ecosystem services of wetlands: pathfinder for a new paradigm. *Hydrological Sciences Journal*, 56, 1341-1359.
- MARKING, L. L. 1969. Toxicity of rhodamine B and fluorescein sodium to fish and their compatibility with antimycin. *Progress in fish cultivation*, 31, 139-142.
- MARSALEK, J., ROCHFORD, Q., BROWNLIE, B., MAYER, T. & SERVOS, M. 1999. An exploratory study of urban runoff toxicity. *Water Science and Technology*, 39, 33-39.
- MARTÍNEZ-CARRERAS, N., UDELHOVEN, T., KREIN, A., GALLART, F., IFFLY, J. F., ZIEBEL, J., HOFFMANN, L., PFISTER, L. & WALLING, D. E. 2010. The use of sediment colour measured by diffuse reflectance spectrometry to determine sediment sources: Application to the Attert River catchment (Luxembourg). *Journal of Hydrology*, 382, 49-63.
- MASON, T. & COATES, T. T. 2001. Sediment Transport Processes on Mixed Beaches: A review for Shoreline Management. *Journal of Coastal Research*, 17, 645-657.
- MASSELINK, G. & HUGHES, M. 1998. Field investigation of sediment transport in the swash zone *Continental Shelf Research*, 18, 1179-1199.
- MASSELINK, G. & HUGHES, M. G. 2003. *Introduction to Coastal Processes and Geomorphology*, London, Hodder Arnold.
- MASSELINK, G. & PULEO, J. A. 2006. Swash-zone morphodynamics. *Continental Shelf Research*, 26, 661-680.

- MATTHAI, C. & BRIRCH, G. 2001. Detection of anthropogenic Cu, Pb and Zn in continental shelf sediments off Sydney, Australia - a new approach using normalisation with cobalt. *Marine pollution bulletin*, 42, 1055-1063.
- MAYES, M. A., JARDINE, P. M., MEHLHORN, T. L., BJORNSTAD, B. N., LADD, J. L. & ZACHARA, J. M. 2003. Transport of multiple tracers in variably saturated humid region structured soils and semi-arid region laminated sediments. *Journal of Hydrology*, 275, 141-161.
- MCDOWELL, R. W. & WILCOCK, R. J. 2004. Particulate phosphorus transport within stream flow of an agricultural catchment. *Journal of Environmental Quality*, 33, 2111-2121.
- MCHUGH, M., WOOD, G., WALLING, D., MORGAN, R., ZHANG, Y., ANTHONY, S. & HUTCHINS, M. 2002. Prediction of Sediment Delivery to Watercourses from Land Phase II. Environment Agency.
- MCLAREN, P. 1981. An interpretation of trends in grain size measures *Journal of Sedimentary Petrology*, 55, 457-470.
- MCLAREN, P. & BOWLES, D. 1985. The effects of sediment transport on grain-size distributions. *Journal of Sedimentary Petrology*, 55, 457-470.
- MCOMB, P. J. & BLACK, K. P. 2005. Detailed observations of littoral transport using artificial sediment tracer in a high-energy, rocky-reef and iron sand environment. *Journal of Coastal Research*, 21, 358-373.
- MEAD, C., HERCKES, P., MAJESTIC, B. J. & ANBAR, A. D. 2013. Source apportionment of aerosol iron in the marine environment using iron isotope analysis *Geophysical Research Letters*, 40, 5722-5727.
- MEHTA, A. J. 2012. On estuarine cohesive sediment suspension behaviour. *Journal of Geophysical Research*, 94, 14303-14314.
- MERRITT, W. S., LETCHER, R. A. & JAKEMAN, A. J. 2003. A review of erosion and sediment transport models. *Environmental Modelling & Software*, 18, 761-799.
- MESELHE, E. A., PEEVA, T. & MUSTE, M. V. I. 2004. Large scale particle image velocimetry low velocity and shallow water flows. *Journal of hydrological engineering*, 130, 937-940.

- MEYBECK, M., LAROCHE, L., DURR, H. H. & SYVITSKI, J. P. M. 2003. Global variability of daily total suspended solids and their fluxes in rivers. *Global and Planetary Change*, 39, 65-93.
- MEYER, V. F., REDENTE, E. F., BARBARICK, K. A. & BROBST, R. 2000. Biosolids Applications Affect Runoff Water Quality following Forest Fire. *Journal of Environmental Quality*, 30, 1528-1532.
- MICHAELIDES, K., IBRAIM, I., NORD, G. & ESTEVES, M. 2010. Tracing sediment redistribution across a break in slope using rare earth elements. *Earth Surface Processes and Landforms*, 35, 575-587.
- MILLER, I. M. & WARRICK, J. A. 2012. Measuring sediment transport and bed disturbance with tracers on a mixed beach. *Marine Geology*, 299-302, 1-17.
- MILLER, M. C., MCCAVE, I. N. & KOMAR, P. D. 1977. Threshold of sediment motion under unidirectional currents. *Sedimentology*, 24, 507-527.
- MILLINGTON, A. C. & TOWNSHEND, J. R. G. 1987. The potential of satellite remote sensing for geomorphological investigations, an overview. In: GARDINER, V. (ed.) *International Geomorphology*. Chichester: Wiley.
- MILNER, N. J., ELLIOTT, J. M., ARMSTRONG, J. D., GARDINER, R., WELTON, J. S. & LADLE, M. 2003. The natural control of salmon and trout populations in streams. *Fisheries Research*, 111-125.
- MITSCH, W. J., DORGE, C. L. & WIEMHOFF, J. R. 1979. Ecosystem dynamics and a phosphorus budget of an alluvial cypress swamp in Southern Illinois. *Ecology*, 60, 1116-1124.
- MITSCH, W. J. & GOSSELINK, J. G. 1983. *Wetlands*, New York, Van Nostrand Reinhold.
- MOLLER, I. 2006. Quantifying saltmarsh vegetation and its effect on wave height dissipation: results from a UK East coast saltmarsh. *Estuarine coastal and shelf science*, 69, 337-351.
- MONTGOMERY, D. R. Soil erosion and agricultural sustainability. Proceedings of the National Academy of Sciences, 2007. 268-272.
- MORGAN, R. P. C. 2005. *Soil Erosion and Conservation*, Victoria, Australia, Blackwell Publishing.
- MORGAN, R. P. C., QUINTON, J. N., SMITH, R. E., GOVERS, G., POESEN, J. W. A., AUERSWALD, K., CHISCI, G., TORRI, D. & STYCZEN, M. E.

1998. The European soil erosion model (EUROSEM): A dynamic approach for predicting sediment transport from fields and small catchments. *Earth Surface Processes and Landforms*, 23, 527-544.
- MORIN, J., BENYAMINI, Y. & MICHAELI, A. 1981. The effect of rain drop impact on the dynamics of soil surface crusting and water movement in the profile. *Journal of Hydrological processes*, 52, 321-335.
- MULLINS, C. E. 1977. Magnetic susceptibility of the soil and its significance in soil science - A review. *Journal of Soil Science*, 28, 223-246.
- NEARING, M. A., FOSTER, G. R., LANE, L. J. & FINKNER, S. C. 1989. A process-based soil erosion model for USDA-water erosion prediction project technology. *Trans. ASAE*, 32, 1587-1593.
- NEVES, M. J. & FERNANDO, H. J. S. 1995. Sedimentation of particles from jets discharged by ocean outfalls — a theoretical and laboratory study. *Water Science and Technology*, 32, 133.
- NEWELL, R. I. E., MARSHALL, N., SASEKUMAR, A. & CHONG, V. C. 1995. Relative importance of benthic microalgae, phytoplankton, and mangroves as sources of nutrition for penaeid prawns and other coastal invertebrates from Malaysia. *Marine Biology*, 123, 595-606.
- NIELSEN, P. 2009. Coastal and estuarine processes. *World Scientific: Advanced Series on Ocean Engineering*, 29, 343. Coastal and estuarine processes.
- NINO, Y. & GARCIA, M. H. 1996. Experiments on particle-turbulence interactions in the near-wall region of an open channel flow: Implications for sediment transport. *Journal of Fluid Mechanics*, 326, 285-319.
- NORTCLIFF, S., HULPKE, H., BANNICK, C. G., TERYTZE, K., KNOOP, G., BREDEMEIER, M. & SCHULTE-BISPING, H. 2012. Soil, 1. Definition, Function and Utilisation of Soil. *Encyclopedia of Industrial Chemistry*, 33.
- NOVARA, A., GRISTINA, L., SALADINO, S. S., SANTORO, A. & CERDA, A. 2011. Soil erosion assessment on tillage and alternative soil managements in a sicilian vineyard. *Soil and Tillage Research*, 117, 140-147.

- OGAWA, Y. & SHUTO, N. Field measurements of hydraulics and sediment movements in a swash zone Proc. 28th Japanese Conference Coastal Engineering, 1981. 212-216.
- OKADO, T., LARCOMBE, P. & MASON, C. 2009. Estimating the spatial distribution of dredged material disposed of at sea using particle - size distributions and metal concentrations *Marine pollution bulletin*, 58, 1164-1177.
- OLDFIELD, F., THOMPSON, R. & DICKSON, D. P. E. 1981. Artificial magnetic enhancement of stream bedload; a hydrological application of superparamagnetism. *Physics of the earth and planetary interiors*, 26, 107-124.
- OLDFIELD, F., WALDEN, J. & SMITH, J. 1999. *Environmental Magnetism: a practical guide*, Great Britain, Quaternary Research Association
- OLFF, H., DE LEEUW, J., BAKKER, J. P., PLATERINK, R. J., VAN WIJNEN, H. J. & DE MUNCK, W. 1997. Vegetation succession and herbivory in a salt marsh: changes induced by sea level rise and silt deposition along an elevational gradient. *Journal of Ecology*, 85, 799-814.
- OLMEZ, I., PINK, F. X. & WHEATCROFT, R. A. 1994. New particle-labeling technique for use in biological and physical sediment transport methods. *Environmental Science and Technology*, 29, 1487-1490.
- OLSON, K. R., GENNADIYEV, A. N., ZHIDKIN, A. P., MARKELOV, M. V., GOLOSOV, V. N. & LANG, J. M. 2013. Use of magnetic tracer and radio-caesium methods to determine past cropland soil erosion amounts and rates. *Catena*, 104, 108-110.
- ORVINI, E., E, SPEXIALI, M., SALVINI, A., A & HERBORG, C. 2000. Rare Earth Elements determination in environmental matrices by INAA. *Journal of Microchemistry*, 67, 97-104.
- OVERTON, D. C. & MEADOWS, M. E. 1976. *Storm water modeling*, New York, Academic.
- OWENS, P. N. 2009. Adaptive management frameworks for natural resource management at the landscape scale: implications and applications for sediment resources. *Journal of Soils and Sediments*, 9, 578-593.
- OWENS, P. N., BATALLA, R. J., COLLINS, A. J., GOMEZ, B., HICKS, D. M., HOROWITZ, A. J., KONDOLF, G. M., MARDEN, M., PAGE, M. J.,

- PEACOCK, D. H., PETTICREW, E. L., SALOMONS, W. & TRUSTRUM, N. A. 2005. Fine-grained sediment in river systems: Environmental significance and management issues. *Applied River Research*, 21, 693-717.
- OWENS, P. N. & WALLING, D. E. 1996. Spatial variability of caesium - 137 inventories at reference sites: an example from two contrasting sites in England and Zimbabwe. *Applied Radiation and Isotopes*, 47, 699-707.
- OWENS, P. N., WALLING, D. E. & LEEKS, G. J. L. 2000. Tracing fluvial suspended sediment sources in the catchment of the River Tweed, Scotland, using composite fingerprints and a numerical mixing model. Chichester: Wiley.
- PALMER, M. A., COVICH, A. P., LAKE, S., BIRO, P., JACQUI, J., COLE, B. J., DAHM, C., GIBERT, J., GOEDKOOP, W., MARTENS, K., VERHOEVEN, J. & VAN DE BUND, W. J. 2000. Linkages between Aquatic Sediment Biota and Life Above Sediments as Potential Drivers of Biodiversity and Ecological Processes A disruption or intensification of the direct and indirect chemical, physical and biological interactions between aquatic sediment biota and biota living above the sediments may accelerate biodiversity loss and contribute to the degradation of aquatic and riparian habitats. *BioScience*, 50, 1062-1075.
- PANTIN, H. 1961a. Magnetic concrete as an artificial tracer material. *New Zealand Journal of Geology and Geophysics*, 4, 424-433 %! Magnetic concrete as an artificial tracer material.
- PANTIN, H. 1961b. Magnetic concrete as an artificial tracer material. *New Zealand Journal of Geology and Geophysics*, 4, 424-433.
- PAPADOPOULOU, A., GREEN, R. J. & FRAZIER, R. A. 2005. Interaction of flavonoids with bovine serum albumin: A fluorescence quenching study. *Journal of Agricultural Food Chemistry*, 53, 158-163.
- PARCHURE, T. & MEHTA, A. 1985. Erosion of Soft Cohesive Sediment Deposits. *Journal of Hydraulic Engineering*, 111, 1308-1326.
- PARKER, G. G. 1973. Tests of Rhodamine WT dye for toxicity to oysters and fish. *Journal of Research U.S Geological Survey*, 1, 499.
- PARKIN, T. B. 1993. Spatial variability of microbial processes in soil - a review. *Journal of Environmental Quality*, 22, 409-417.

- PARSONS, A. J., WAINWRIGHT, J. & ABRAHAM, B. 1993. Tracing sediment movement in inter rill overland flow on a semi-arid grassland hill slope using magnetic susceptibility. *Earth Surface Processes and Landforms*, 18, 721-732.
- PEARCE, C. I., LIU, J., BAER, D. R., QAFOKU, O., HEALD, S. M., ARENHOLZ, E., GROSZ, A. E., MCKINLEY, J. P., RESCH, C. T., BOWDEN, M. E., ENGELHARD, M. H. & ROSSO, K. M. 2014. Characterisation of natural titanomagnetites (Fe₃-xTi_xO₄) for studying heterogenous electron transfer to Tc (VII) in the Hanford subsurface. *Geochimica et Cosmochimica Acta*, 128, 114-127.
- PEDOCCHI, F., MARTIN, J. & GARCIA, M., H 2008. Inexpensive fluorescent particles for large scale experiments using particle image velocimetry. *Exp. Fluid*, 45, 183-186.
- PEETERS, I., VAN OOST, K., GOVERS, G., VERSTRAETEN, G., ROMMENS, T. & POESEN, J. 2008. The compatability of erosion data at different temporal scales. *Earth and Planetary Science Letters*, 265, 138-152.
- PEINE, F., TURNEWITSCH, R., MOHN, C., REICHELT, T., SPRINGER, B. & KAUFMANN, M. 2009. The importance of tides for sediment dynamics in the deep sea—Evidence from the particulate-matter tracer ²³⁴Th in deep-sea environments with different tidal forcing. *Deep Sea Research Part I: Oceanographic Research Papers*, 56, 1182-1202.
- PETRENKO, A. A., JONES, B. H., DICKEY, T. D., LEHAITRE, M. & MOORE, M., 1997. Effects of a sewage plume on the biology, optical characteristics and particle size distributions of coastal waters. *Journal of Geophysical Research*, 102, 25061–25071.
- PETTICREW, E. L., OWENS, P. N. & GILES, T. R. 2006. Wildfire effects on the quantity and composition of suspended and gravel-stored sediments. *Water Air Soil Pollution*, 6, 647-656.
- PFITZNER, J., BRUNSKILL, G. & ZAGORSKIS, I. 2004. ¹³⁷Cs and excess ²¹⁰Pb deposition patterns in estuarine and marine sediment in the central region of the Great Barrier Reef Lagoon, north-eastern Australia. *Journal of Environmental Radioactivity*, 81-102.

- PICADO, A., SILVA, P. A., FORTUNATO, A. B. & DIAS, J. M. 2011. Particle tracking-modeling of morphologic changes in the Ria de Aveiro. *Journal of Coastal Research*, 64, 1560-1564.
- PIMENTAL, D., ALLEN, J., BEERS, A., GUINAND, L., LINDER, R., MCLAUGHLIN, P., MEER, B., MUSONDA, D., PERDUE, D., POISSON, S., SIEBERT, S., STONER, K., SALAZAR, R. & HAWKINS, A. 1987. World Agriculture and Soil Erosion. *BioScience*, 4, 277-283.
- PIMENTAL, D. & BURGESS, M. 2013. Soil erosion threatens food production. *Agriculture*, 3, 443-463.
- PIMENTAL, D. & SPARKS, D. L. 2000. Soil as an endangered ecosystem. *BioScience*, 50, 947.
- PINTO, J. C. R., DIAS, J. M. A., FERNANDEZ, S. P., FERREIRA, O., SILVA, A. V. & TABORDA, R. 1994. Automated system for tagged sand detection. *Gaia*, 8, 161-164.
- PITT, R., FIELD, R., LALOR, M. & BROWN, M. 1995. Urban stormwater toxic pollutants: assessment, sources, and treatability. *Water Environment Research*, 67, 260-275.
- PLANTE, A. F., DUKE, M. J. M. & MCGILL, W. B. 1999. A tracer sphere detectable by Neutron Activation for soil aggregation and translocation studies. *Soil Science Society American Journal*, 63, 1284-1290.
- POESEN, J., NACHTERGAELE, J., VERSTRAETEN, G. & VALENTIN, C. 2003. Gully erosion and environmental change: importance and research needs. *Catena*, 50, 91-133.
- POLYAKOV, V. O. & NEARING, M. A. 2004. Rare earth element oxides for tracing sediment movement. *Catena*, 55, 255-276.
- PONTEE, N. I. & PARSONS, A. 2009. A review of coastal risk management in the UK. *Proceedings of the Institution of Civil Engineers Maritime Engineering* 163, 31-42.
- PORTO, P., WALLING, D. E. & CALLEGARI, G. 2013. Using ¹³⁷Cs and ²¹⁰Pbex measurements to investigate the sediment budget of a small forested catchment in southern Italy. *Hydrological Processes*, 27, 795-806.

- PORTO, P., WALLING, D. E. & FERRO, V. 2001. Validating the use of caesium-137 measurements to estimate soil erosion rates in a small drainage basin in Calabria, Southern Italy. *Journal of Hydrology*, 248, 93-108.
- PULEO, J. A., BEACH, R. A., HOLMAN, R. A. & ALLEN, J. S. 2000. Swash zone sediment suspension and transport and the importance of bore-generated turbulence. *Journal of Geophysical Research*, 105, 17021-17044.
- QUINE, T. A., WALLING, D. E., CHAKELA, Q. K., MANDIRINGANA, O. T. & ZHANG, X. 1999. Rates and patterns of tillage and water erosion on terraces and contour strips: evidence from caesium-137 measurements. *Catena*, 36, 115-142.
- QUINTON, J. N. & CATT, J. A. 2007. Enrichment of heavy metals in sediment resulting from soil erosion on agricultural fields. *Environment Science and Technology*, 41, 3495–3500.
- RABEK, J. F. 2012. *Polymer Photodegradation: Mechanisms and experimental methods*, Springer Science and Business Media.
- READING, H. G. 1996. *Sedimentary Environments: Processes, Facies and Stratigraphy*, Oxford, Blackwell Publishing Company.
- REES, H., WALDOCK, R., MURRAY, L. A. & BOLAM, S. G. The disposal of fine-grained dredged material; a case study 28th International Conference of Coastal Engineers, 2003 Cardiff. American Society of Coastal Engineers, World Scientific Inc, 3616-3629.
- REGANOLD, J. P., ELLIOT, L. F. & UNGER, Y. L. 1987. Long term effects of organic and conventional farming on soil erosion. *Nature*, 330.
- RENSCHLER, C. S. & HARBOR, J. 2002. Soil erosion assessment tools from point to regional scales - the role of geomorphologists in land management research and implementation. *Geomorphology*, 47, 189-209.
- RENSCHLER, C. S., MANNAERTS, C. & DIEKKRUGER, B. 1999. Evaluating spatial and temporal variability in soil erosion risk-rainfall erosivity and soil loss ratios in Andalusia, Spain. *Catena*, 34.

- RESEARCH, A. 1999 Good practice guidelines for ports and harbours operating within or near UK European marine sites. *English Nature, UK Marine SACs Project*
- RICHARDSON, N. M. 1902. An experiment on the movements of a load of brickbats deposited on Chesil Beach. *Proceedings of the Dorset Natural History Field Club*, 23, 123-133 %! An experiment on the movements of a load of brickbats deposited on Chesil Beach.
- RICKSON, R. J. 2014. Can control of soil erosion mitigate water pollution by sediments? *Science of the Total Environment*, 468-469, 1187-1197.
- RIEBE, B. 1995. Monitoring the translocation of soil particles using a neutron activated tracer. *In: HARTGE, K. H. & STEWART, B. A. (eds.) Soil structure: Its development and function*. Boca Raton, FL: CRC Press.
- ROBERTS, P. J. W., SNYDER, W. H. & BAUMGARTNER, D. J. 1989. Ocean Outfalls: Submerged Wastefield Formation. *Journal of Hydraulic Engineering*, 115, 1-25.
- ROBINSON, D. A., HOCKLEY, N., COOPER, D. M., EMMETT, B. A., KEITH, A. M. & LEBRON, I. 2013. Natural capital and ecosystem services, developing an appropriate soils framework as a basis for valuation. *Soil Biology and Biochemistry*, 57, 1023-1033.
- ROMKENS, M. J. M., PRASAD, S. N. & WHISLER, F. D. 1990. Surface sealing and infiltration. *In: ANDERSON, M. G. & BURT, T. P. (eds.) Process studies in Hillslope Hydrology*. John Wiley.
- ROWLATT, S. M., REES, H. L., VIVIAN, C. M. G. & PARKER, M. M. 1991. The monitoring of UK sewage sludge disposal sites *Chemistry and ecology*, 5, 17-33.
- ROYALL, D. 2001. Use of mineral magnetic measurements to investigate soil erosion and sediment delivery in a small agricultural catchment in limestone terrain. *Catena*, 46, 15-34 %! Use of mineral magnetic measurements to investigate soil erosion and sediment delivery in a small agricultural catchment in limestone terrain.
- RUSHTON, K. R., EILERS, V. H. M. & CARTER, R. C. 2006. Improved soil moisture balance methodology for recharge estimation. *Journal of Hydrology*, 318, 379-399.

- RUSSELL, R. C. H. 1960a. The use of fluorescent tracers for the measurement of littoral drift *Coastal Engineering* 418-445.
- RUSSELL, R. C. H. The use of fluorescent tracers for the measurement of littoral drift. 77th Conference on Coastal Engineering, 1960b University of California, Berkeley. 418-444.
- RUTGERS VAN DER LOEFF, M., MEYER, R., RUDELS, B. & RACHOR, E. 2002. Resuspension and particle transport in the benthic nepheloid layer in and near Fram Strait in relation to faunal abundances and 234Th depletion. *Deep sea Research*, 49, 1941-1958.
- SANCHEZ-ARCILLA, A., GARCIA-LEON, M., GRACIA, V., DEVOY, R., STANICA, A. & GAULT, J. 2016. Managing coastal environments under climate change: Pathways to adaption. *Science of the Total Environment*.
- SARMA, T. P. & IYA, K. K. 1960. Preparation of artificial silt for tracer studies near Bombay Harbour. *Journal Scientific Indeed Research India astrinli*, 19, 99-101.
- SCHIFF, K. C. 2000. Sediment chemistry on the mainland shelf of the southern California Bight. *Marine pollution bulletin*, 40, 268-276.
- SCHINDLER, D. E. & SCHEUERELL, M. D. 2002. Habitat coupling in lake ecosystems. *OIKOS*, 98, 177-189.
- SCHMIDT, A., YARNOLD, R., HILL, M. & ASHMORE, M. 2005. Magnetic susceptibility as proxy for heavy metal pollution: a site study. *Journal of Geochemical Exploration*, 85, 109-117.
- SCHOONES, J. S. & THERON, A. K. 1995. Evaluation of 10 cross-shore sediment transport/morphological models. *Coastal Engineering*, 25, 1-41.
- SCHULLER, P., ELLIES, A., CASTILLO, A. & SALAZAR, I. 2003. Use of ¹³⁷Cs to estimate tillage- and water-induced soil redistribution rates on agricultural land under different use and management in central-south Chile. *Soil and Tillage Research*, 69, 69-83.
- SEBENS, K. P. 1991. Habitat structure and community dynamics in marine benthic systems. In: BELL, S. S., MCCOY, E. D. & MUSHINSKY, H. R. (eds.) *Habitat Structure*. Netherlands: Springer.

- SHARMA, B. K. & SHARMA, P. 1994. *Water Pollution*, Meerut, India, Goel Publishing House.
- SHARMA, P. P. & GUPTA, S. C. 1989. Sand detachment by single raindrops of varying kinetic energy and momentum. *Soil Science Society American Journal*, 53, 1005-1010.
- SHARMA, P. P., GUPTA, S. C. & RAWLS, W. J. 1991. Soil detachment by single raindrops of varying kinetic energy. *Soil Science Society American Journal*, 55, 301-307.
- SHERER, B. M., MINER, J. R., MOORE, J. A. & BUCKHOUSE, J. C. 1991. Indicator Bacterial Survival in Stream Sediments. *Journal of Environmental Quality*, 21, 591-595.
- SHINOHARA, K., TSUBAKI, T., YOSHITAKA, M. & AGEMORI, C. 1958. Sand transport along a model sandy beach by waves. *Coastal Engineering*, 1, 111-129.
- SHORT, A. D. & WRIGHT, L. D. 2007. Beach systems of the Sydney region. *Australian Geographer*, 15, 1981.
- SIGBJORNSSON, B. Use of Nuclear techniques in Food, Agriculture and Pest Control. National Seminar on Nuclear Energy in Everyday Life, 1994 Cairo.
- SILVA, A., TABORDA, R., RODRIGUES, A., DUARTE, J. & CASCALHO, J. 2007. Longshore drift estimation using fluorescent tracers: New insights from an experiment at Comporta Beach, Portugal. *Marine Geology*, 240, 137-150.
- SIMONS, R. K. & SIMONS, D. B. 1996. Modeling contaminated sediments. *Civil Engineering*, 66, 73-75.
- SMART, P. L. & LAIDLAW, I. M. S. 1977. An Evaluation of Some Fluorescent Dyes for Water Tracing. *Water Resources Research*, 13.
- SMITH, E., WANG, P. & ZHANG, J. 2003. Evaluation of the CERC formula using large-scale model data. *Proceeding Coastal Sediments*, 1-13.
- SMITH, H. G. & BLAKE, W. H. 2014. Sediment fingerprinting in agricultural catchments: A critical re-examination of source discrimination and data corrections. *Geomorphology*, 204, 177-191.

- SMITH, H. G., BLAKE, W. H. & OWENS, P. N. 2013. Discriminating fine sediment sources and the application of sediment tracers in burned catchments: a review. *Hydrological Processes*, 27, 943-958.
- SMITH, J. S. & FRIEDRICHS, C. T. 2011. Size and settling velocities of cohesive flocs and suspended sediment aggregates in a trailing suction hopper dredge plume. *Continental Shelf Research*, 31, 50-63.
- SMITH, S. J., MARSH, J. & PUCKETTE, T. Analysis of fluorescent sediment tracer for evaluating nearshore placement of dredged material. Proceedings of the Eighteenth World Dredging Congress, 2007 Florida.
- SNELGROVE, P. V. R. 1999. Getting to the Bottom of Marine Biodiversity: Sedimentary Habitats *BioScience*, 49, 129-138.
- SOLAN, M., D, B, WIGHAM, I. R., HUDSON, R. K., COULON, C. H., NORLING, K., NILSSON, H. C. & ROSENBERG, R. 2004. In situ quantification of bioturbation using time-lapse fluorescent sediment profile imaging (f-SPI), luminophore tracers and model simulation. *Marine ecology progress series*, 271, 1-12.
- SOULSBY, R. L. 1997. *Dynamics of Marine Sands*, London, Thomas Telford.
- SOWARDS, C. L. 1958. Sodium fluorescein and the toxicity of Pronoxfish. *Progress of Fish Cultivation* 20, 20.
- SPANHOFF, R. & SUIJLEN, J. M. 1990. Feasibility of tracer studies of large scale cohesive-sediment transport. In: MICHAELIS, W. (ed.) *Estuarine Water Quality Management*. Berlin: Springer-Verlag.
- SPARKS, R. S. J., CAREY, S. N. & SIGURDSON, H. 1991. Sedimentation from gravity currents generated by turbulent plumes. *Sedimentology*, 38, 856.
- SPENCER, K. L., DROPPO, I. G., HE, C., GRAPENTINE, L. & EXALL, K. 2011a. A novel tracer technique for the assessment of fine sediment dynamics in urban water management systems. *Water Res*, 45, 2595-606.
- SPENCER, K. L., JAMES, S. L., TAYLOR, J. A. & KEARTON-GEE, T. 2007a. Sorption of La³⁺ onto clay minerals: a potential tracer for fine sediment transport in the coastal marine environment? *British Geological Society, Special Publication*, 274, 17-24.

- SPENCER, K. L., MANNING, A. J., DROPPO, I. G., LEPPARD, G. G. & BENSON, T. 2010. Dynamic interactions between cohesive sediment tracers and natural mud. *Journals of Soils and Sediments*, 10, 1401-1414.
- SPENCER, K. L., SUZUKI, K., BENSON, T., TAYLOR, J. A., MANNING, A. & DEARNALEY, M. 2007b. The potential use of geochemically labelled minerals as tracers for cohesive sediments. *In: WESTRICH, B. & FORSTNER, U. (eds.) Sediment dynamics and pollutant mobility in rivers—interdisciplinary approach*. Berlin: Springer.
- SPENCER, K. L., SUZUKI, K. & HILLIER, S. 2011b. The development of rare earth element-labelled potassium-depleted clays for use as cohesive sediment tracers in aquatic environments. *Journal of Soils and Sediments*, 11, 1052-1061.
- STEILA, D. & POND, T. E. 1989. *The Geography of Soils: Formation, Distribution and Management*, Maryland, USA, Rowman & Littlefield Publishers INC.
- STEINER, R. F. & KUBOTA, Y. 1983. Fluorescent dye - Nucleic Acid Complexes. *Excited States of Biopolymers*, 203-254.
- STERN, D. A., KHANBILVARDI, R., C., J. & RICHARDSON, W. 2001. Description of flow through a natural wetland using dye tracer tests. *Ecological Engineering*, 18, 173-184.
- STEVENS, C. J. & QUINTON, J. N. 2008. Investigating source areas of eroded sediments transported in concentrated overland flow using rare earth element tracers. *Catena*, 74, 31-36.
- STURN, P. W. & WILLIAMS, K. E. 1975. Fluorescent whitening agents: Acute fish toxicity and accumulation studies. *Water Research*, 9, 211-219.
- SUH, S. W. 2006. A hybrid approach to particle and Eulerian-Lagrangian models in the simulation of coastal dispersion. *Environmental Modelling and Software*, 21, 234-242.
- SUTHERLAND, R. A. 1996. Caesium-137 soil sampling and inventory variability in reference locations: A literature survey. *Hydrological Processes*, 10, 43-52.
- SZMYTKIEWICZ, M., BIEGOWSKI, J., KACZMAREK, L. M., OKROJ, T., OSTROWSKI, R., PRUSZAK, Z., ROZYNSKY, G. & SKAJA, M. 2000.

- Coastline changes nearby harbour structures: comparative analysis of one-line models versus field data. *Coastal Engineering*, 40, 119-139.
- TANAKA, S., YAMAMOTO, K., ITO, H., ARISAWA, T. & TAGAKI, T. 1998. Field investigation on sediment transport into the submarine canyon in the Fuji coast with new type tracers. *Coastal Engineering*, 20, 3151-3164.
- TAURO, F., AURELI, M., PORFIRI, M. & GRIMALDI, S. 2010. Characterization of buoyant fluorescent particles for field observations of water flows. *Sensors (Basel)*, 10, 11512-29.
- TAZIOLI, A. 2009. Evaluation of erosion in equipped basins: preliminary results of a comparison between the Gavrilovic model and direct measurements of sediment transport. *Environmental Geology*, 56, 825-831.
- TELEKI, P. G. 1966. Fluorescent sand tracers. *Journal of sedimentary petrology*, 36, 468-485.
- TETZLAFF, D. & LAUDON, H. 2010. Dissolved Organic Carbon in Northern Catchments and Understanding Hydroclimatic Controls. *EOS*, 91, 200.
- THEURING, P., RODE, M., BEHRENS, S., KIRCHNER, G. & JHA, A. 2013. Identification of fluvial sediment sources in the Kharaa River catchment, Northern Mongolia. *Hydrological Processes*, 27, 845-856.
- THOMPSON, R. C., OLSEN, Y., MITCHELL, R. P., DAVIS, A., ROWLAND, S. J., JOHN, A. W. G., MCGONIGLE, D. & RUSSEL, A. E. 2004. Lost at sea: Where does all the plastic go? . *Science*, 304, 838.
- THORNES, J. B. 1990. The interaction of erosional and vegetational dynamics in land degradation: spatial outcomes. In: THORNES, J. B. (ed.) *Vegetation and Erosion. Processes and Environments*. Chichester: Wiley.
- THRUSH, S. F. & DAYTON, P. K. 2002. Disturbance to Marine Benthic Habitats by Trawling and Dredging: Implications for Marine Biodiversity. *Annual Review of Ecology and Systematics*, 33, 449-473.
- THRUSH, S. F., HEWITT, J. E., CUMMINGS, V. J., ELLIS, J. L., HATTON, C., LOHRER, A. & NORKKO, A. 2004. Muddy Waters: elevating sediment input to coastal and estuarine habitats. *Frontiers in Ecology and the Environment*, 2, 299-306.

- TIAN, J., ZHOU, P. & LIU, P. 1994. REE tracer method for studies on soil erosion. *International Journal of Sediment Research*, 9, 39-46.
- TONG, J., TIAN, F., LI, Q., LI, L., XIANG, C., LIU, Y., DAI, J. & JIANG, F. 2012. Probing the adverse temperature dependence in the static fluorescence quenching of BSA induced by a novel anticancer hydrazone. *Photochemical and Photobiological Sciences* 11, 1868-1879.
- TRESS, B. & TRESS, G. 2009. Environmental and landscape change: Addressing an interdisciplinary agenda. *Journal of Environmental Management*, 90, 2849-2850.
- TRUMAN, C. C. & BRADFORD, J. M. 1990. Effect of antecedent soil moisture on splash detachment under simulated rainfall. *Soil Science*, 150, 787-798.
- TUDHORPE, A. W. & SCOFFIN, T. P. 1987. A device to deposit tracer sediment evenly on the deep sea bed. *Journal of sedimentary petrology*, 57.
- TURNWITSCH, R. & SPRINGER, B. 2001. Do bottom mixed layer influence ²³⁴Th dynamics in the abyssal near-bottom water column? *Deep sea Research*, 48, 1279-1307.
- TYAGI, S., BRATU, D. P. & KRAMER, F. R. 1998. Multicolour molecular beacons for allele discrimination. *National Biotechnology*, 16, 49-53.
- ULLEN, B., BECHMANN, M., FOLSTER, J., JARVIE, H. P. & TUNNEY, H. 2007. Agriculture as a phosphorous source for eutrophication in the north-west European countries, Norway, Sweden, United Kingdom and Ireland: a review. *Soil use and Management*, 23, 5-15.
- USACE 1983. Dredging and dredged material disposal, Engineering and Design. *U.S Army Corps of Engineers, Engineer Manual*, 1110-25025.
- USSEGLIO-POLATERA, J. M. & CUNGE, J. A. Modeling of pollutant and suspended-sediment transport with Argos Modeling System. International Conference on Numerical and Hydraulic Modeling of Ports and Harbours, 1985 Birmingham.
- VALEUR, B. & BERBERAN-SANTOS, M. N. 2012. *Molecular Fluorescence: Principles and Applications*, Wiley - VCH.

- VAN DEN EYNDE, D. 2004. Interpretation of tracer experiments with fine-grained dredging material at the Belgian Continental Shelf by the use of numerical models. *Journal of Marine Systems*, 48, 171-189.
- VAN DER POST, K. D., OLDFIELD, F. & VOULGARIS, G. 1995. Magnetic tracing of beach sand: Preliminary results. *Coastal Dynamics*, 323-334.
- VAN RIJN, L. C. 1984. Sediment transport, Part 1: Bed Load Transport. *Journal of Hydraulic Engineering*, 110, 1431-1456.
- VAN RIJN, L. C. 1993. *Principles of sediment transport in rivers, estuaries and coastal seas*, Amsterdam, Aqua Publications.
- VENTERINK, H. O., VERMAAT, J. E., PRONK, M., WIEGMAN, F., VAN DER LEE, G. E. M., VAN DEN HOORN, M. W., HIGLER, L. W. G. & VERHOEVEN, J. T. A. 2006. Importance of sediment deposition and denitrification for nutrient retention in floodplain wetlands. *Applied Vegetation Science*, 9, 163-174.
- VENTURA, E., NEARING, M. A., AMORE, E. & NORTON, L. D. 2002. The study of detachment and deposition on a hillslope using a magnetic tracer. *Catena*, 48, 149-161.
- VENTURA, E. J., NEARING, M. A. & NORTON, D. L. 2001. Developing a magnetic tracer to study soil erosion. *Catena*, 43, 277-291.
- VERNON, J. 1963. *Fluorescent sand tracer tests, Zuniga Shoal, San Diego, California*. University of Southern California.
- VILA-CONCEJO, A., FERREIRA, O., CIAVOLA, P., MATIAS, A. & DIAS, J. 2004. Tracer studies on the updrift margin of a complex inlet system. *Marine Geology*: Elsevier.
- VINCENT, C. E., HANES, D. M., BOWEN, A. J. & 1991. Acoustic measurements of suspended sand on the shoreface and the control of concentration by bed roughness. *Marine Geology*, 96, 1-18.
- VRIELING, A. 2006. Satellite remote sensing for water erosion assessment: a review. *Catena*, 65, 2-18.
- WAINWRIGHT, J. & THORNES, J. B. 2004. *Environmental Issues in the Mediterranean. Processes and Perspectives from the Past and Present*, London, Routledge.
- WALLBRINK, P. J. & MURRAY, A. S. 1996. Distribution and Variability of ⁷Be in soils under different surface cover conditions and its potential for

- describing soil redistribution processes. *Water Resources Research*, 32, 467-476.
- WALLBRINK, P. J., OLLEY, J. M. & MURRAY, A. S. Measuring soil movement using ^{137}Cs : implications of reference site variability. Variability in Stream Erosion and Sediment Transport, Proceedings of the Canberra Symposium, 1994 Canberra.
- WALLBRINK, P. J., RODDY, B. P. & OLLEY, J. M. 2002. A tracer budget quantifying soil redistribution on hillslopes after forest harvesting. *Catena*, 47, 179-201.
- WALLING, D. E. Use of ^{137}Cs in the study of soil erosion and sedimentation. Joint FAO/IAEA Division of Nuclear Techniques in Food and Agriculture, 1995 Vienna.
- WALLING, D. E. 2013. Beryllium-7: The Cinderella of fallout radionuclide sediment tracers? *Hydrological Processes*, 27, 830-844.
- WALLING, D. E. & COLLINS, A. L. Suspended sediment sources in British Rivers. Symposium held during the Seventh IAHS Scientific Assembly 2005 Foz do Iguacu, Brazil. IAHS.
- WALLING, D. E., COLLINS, A. L., JONES, P. A., LEEKS, G. J. L. & OLD, G. 2006. Establishing fine-grained sediment budgets for the Pang and Lambourn LOCAR catchments, UK. *Journal of Hydrology*, 330, 126-141.
- WALLING, D. E., GOLOSOV, V. & OLLEY, J. 2013. Introduction to the special issue 'Tracer Applications in Sediment Research'. *Hydrological Processes*, 27, 775-780.
- WALLING, D. E. & HE, Q. 1999. Improved models for estimating soil erosion rates from caesium-137 measurements. *Journal of Environmental Quality*, 28, 611-622.
- WALLING, D. E., HE, Q. & BLAKE, W. H. 2000. Use of ^7Be and ^{137}Cs measurements to document short- and medium-term rates of water-induced soil erosion on agricultural land. *Water Resources Research*, 35, 3865-3874.
- WALLING, D. E. & QUINE, T. A. 2006. Calibration of caesium - ^{137}Cs measurements to provide quantitative erosion rate data. *Land Degradation and Development*, 2, 161.

- WALLINGFORD, H. 2001. Scarborough Coastal Defence Strategy Study – Site Investigation and Numerical Modelling Studies.
- WALLINGFORD, H. 2002. Scarborough Coastal Defence Strategy Physical Model Study – Overtopping Discharges and Beach Response in South Bay.
- WANG, J.-F., STEIN, A., GAO, B.-B. & GE, Y. 2012. A review of spatial sampling. *Spatial Statistics*, 2, 1-14.
- WANG, Z. B., LOUTERS, T. & DE VRIEND, H. J. 1995. Morphodynamic modelling for a tidal inlet in the Wadden Sea. *Marine Geology*, 126, 289-300.
- WATSON, D. A. & LAFLEN, J. M. 1986. Soil strength, slope, and rainfall intensity effects on interrill erosion. *Trans. ASAE*, 29, 98-102.
- WEBSTER, R. 1999. Sampling, estimating and understanding soil pollution. In: GOMEZ-HERNÁNDEZ, J., SOARES, A. & FROIDEVAUX, R. (eds.) *Geostatistics for Environmental Applications. Quantitative Geology and Geostatistics*. Dordrecht: Kluwer Academic Publishers.
- WENDT, R. C., ALBERTS, E. E. & HJELMFELT, A. T. 1986. Variability of runoff and soil loss from fallow experimental plots. *Soil Science Society of America Journal* 50, 730–736.
- WEST, P. J. 1949. Transportation of cubical bricks in a cobble beach environment. *California report*. Department Geology University Society.
- WHITE, R. E. 2006. *Principles and Practice of Soil Science: The soil as a Natural Resource*, Oxford, Blackwell Publishing Company.
- WHITE, T. E. 1987. *Nearshore sand transport*. PhD, University of California.
- WHITE, T. E. 1998. Status of measurement techniques for coastal sediment transport. *Coastal Engineering*, 35, 17-45.
- WHITE, T. E. & INMAN, D. L. 1989. *Measuring longshore transport with tracers*, New York, Plenum.
- WHITEHOUSE, R. J. S., COOPER, N., PETHICK, J., SPEARMAN, J., TOWNEND, I. H. & FOX, D. Dealing with geomorphological concepts and broad scale approaches for estuaries. 40th Defra Flood and Coastal Management Conference, 5 - 7 July 2005 York UK.
- WHITLATCH, R. B. 1981. Animal-sediment relationships in intertidal marine benthic habitats: Some determinants of deposit-feeding species

- diversity. *Journal of Experimental Marine Biology and Ecology*, 53, 31-45.
- WILBER, D. H. & CLARKE, D. G. 2001. Biological Effects of Suspended Sediments: A Review of Suspended Sediment Impacts on Fish and Shellfish with relation to Dredging Activities in Estuaries. *North American Journal of Fisheries Management*, 21.
- WILCOX, B. P., NEWMAN, B. D., ALLEN, C. D., REID, K. D., BRANDES, D., PITLICK, J. & DAVENPORT, D. W. Runoff and erosion on the pajarito plateau: observations from the field. New Mexico Geological Society Guidebook, 47th Field Conference 1996 Jemez Mountains Region.
- WILSON, J. F., COBB, E. D. & KILPATRICK, F. A. 1986. Fluorometric Procedures for Dye Tracing. In: SURVEY, U. S. G. (ed.). Denver.
- WINN, P. J. S., YOUNG, R. M. & EDWARDS, A. M. C. 2003. Planning for the rising tides: the Humber Estuary Shoreline Management Plan. *Science of the Total Environment*, 314-316, 13-30.
- WONG, K. B. & PIEDRAHITA, R. H. 2000. Settling velocity characterization of aquacultural solids. *Aquacultural Engineering*, 21, 233-246.
- WOOD, P. J. & ARMITAGE, P. D. 1997. Biological effects of fine sediment in the lotic environment. *Environmental Management* 21, 203-217.
- WYATT, W. A., BRIGHT, F. V. & HIEFTJE, G. M. 1987. Characterisation and comparison of three fiber-optic sensors for iodide determination based on dynamic fluorescence quenching of Rhodamine 6G. *Analytical Chemistry*, 59, 2272-2276.
- YANG, B., WANG, Y. & LIU, J. 2011. PIV measurements of two phase velocity fields in aeolian sediment transport using fluorescent tracer particles. *Measurement*, 44, 708-716.
- YIN, Y., CHANG, N., ZHONG, W., SUN, S., ZHANG, Y., CUI, H., CHEN, S., FENG, Y. & SUN, L. 1993. A study of neutron activation tracer sediment technique. *Sci China Ser A*, 36, 243-248.
- YU, L. & OLDFIELD, F. 1989. A multivariate mixing model for identifying sediment source from magnetic measurements. *Quatern Research*, 32, 168-181.

- ZARREBINI, M. & CARDOSO, S. S. S. 2000. Patterns of sedimentation from surface currents generated by turbulent plumes. *AIChE J*, 46, 1947-1956.
- ZHANG, X., QUINE, T. A. & WALLING, D. E. 1998. Soil erosion rates on sloping cultivated land on the Loess Plateau near Ansai, Shaanxi province, China: an investigation using ¹³⁷Cs and rill measurements. *Hydrological Processes*, 12, 171-189.
- ZHANG, X. C., FRIEDRICH, J. M., NEARING, M. A. & NORTON, L. D. 2001. Potential use of rare earth oxides as tracers for soil erosion and aggregation studies. *Soil Science Society American Journal*, 65, 1508-1515.
- ZHANG, X. C., NEARING, M. A., POLYAKOV, V. O. & FRIEDRICH, J. M. 2003. Using rare earth oxide tracers for studying soil erosion dynamics. *Soil Science Society American Journal*, 67, 279-288.
- ZIMMERMAN, L. E., JUTTE, P. C. & VAN DOLAH, R. F. 2003. An environmental assessment of the Charleston Ocean Dredged Material Disposal Site and surrounding areas after partial completion of the Charleston Harbor Deepening Project *Marine pollution bulletin*, 46, 1408-1419.
- ZOBECK, T. M., STERK, G., FUNK, R., RAJOT, J. L., STOUT, J. E. & SCOTT VAN PELT, R. 2003. Measurement and Data Analysis Methods for Field-Scale Wind Erosion Studies and Model Validation. *Earth Surface Processes and Landforms*, 28, 1163-1188.